Inamuddin
Tauseef Ahmad Rangreez
Abdullah M. Asiri   *Editors*

Applications of Ion Exchange Materials in Chemical and Food Industries

Springer

Applications of Ion Exchange Materials in Chemical and Food Industries

Inamuddin · Tauseef Ahmad Rangreez ·
Abdullah M. Asiri
Editors

Applications of Ion Exchange Materials in Chemical and Food Industries

Springer

Editors
Inamuddin
Department of Chemistry,
Faculty of Science
King Abdulaziz University
Jeddah, Saudi Arabia

Tauseef Ahmad Rangreez
Department of Chemistry
National Institute of Technology Srinagar
Srinagar, India

Abdullah M. Asiri
Department of Chemistry,
Faculty of Science
King Abdulaziz University
Jeddah, Saudi Arabia

Preface

Amid the most recent decade, the chemical industry has understood that ion-exchange resins have the enormous potential for uses other than customary water softening. In this manner, industrial water softening by ion-exchange processes is currently applied to countless applications including deionization, dealkalization, dehydration, hydrogenation, esterification, reactive separations, synthesis and separation, and purification of industrial products. Ion-exchange materials used in chromatographic applications have various other applications beyond water softening. A large group of new applications are currently being used in the laboratory, pilot plant, and at the plant stage, including chemical synthesis. It is conceivable that some fine chemicals could be synthesized utilizing ion-exchange metathesis. Thus, the engineering disciplines are now using ion-exchange materials.

This edition will cover applications of ion-exchange materials in the area of chemical and food industries. It includes topics related to the application of ion-exchange materials in dehydration, hydrogenation, alkylation and esterification reactions, reactive separations, and the separation and purification of beverages and precious and noble metals.

It provides an in-depth knowledge of ion-exchange materials and their applications suitable for postgraduate students and researchers, as well as industrial research and development specialists in chemistry, chemical and biochemical technology, food chemistry, synthetic chemistry, and industrial chemistry. Additionally, this book provides an overview of ion-exchange columns and operation suitable for engineers and industrialists. This book is divided into the following nine chapters.

Chapter 1 reviews the main uses of ion-exchange resins as catalysts for dehydration processes. The main catalytic processes are described by providing detailed information about the catalytic performance and underlying advantages and drawbacks of ion-exchange resins for each catalytic process.

Chapter 2 summarizes some selected applications of hydrogenation reactions using ion-exchange resins as catalyst support materials. Some of the applications of ion-exchange resins including hydrodesulphurization, hydrodenitrification, and hydrodechlorination are reviewed.

Chapter 3 presents a review of the use of ion-exchange resins in alkylation reactions on different substrates, highlighting the particularities of each case. First, definitions and classical industrial processes followed by an illustration of alkylation reactions in terms of mechanism, activity, and selectivity are discussed. Finally, the use of biomass derivatives in catalysed alkylation reactions with ion-exchange resins is presented.

Chapter 4 deals with the esterification reactions catalysed by strong acidic ion-exchange resins. Industrially important esterification reactions in the petrochemical and oleochemical industries are discussed.

Chapter 5 discusses the methods for the synthesis and control of silver aggregates in ion-exchanged silicate glass by thermal annealing and gamma irradiation.

Chapter 6 introduces the conceptual understanding of reactive separation processes such as reactive distillation, reactive extraction, reactive chromatography, and reactive absorption in different areas and the use of ion-exchange resin in these processes.

Chapter 7 reviews the salient features and industrial applications of reactive separations using ion-exchange resins.

Chapter 8 reviews about the applications of ion-exchange chromatography in the separation and purification of beverages including softening of water as well as nonalcoholic and alcoholic beverages.

Chapter 9 explores the present uses and future developments of ion-exchange resins used in the extraction and recovery of precious and noble metals including gold, silver, copper, uranium, and iron. A comprehensive overview of the effectiveness of surface modified resins and the major limitations of the resin adsorption techniques are pointed out.

Jeddah, Saudi Arabia   Inamuddin
Srinagar, India   Tauseef Ahmad Rangreez
Jeddah, Saudi Arabia   Abdullah M. Asiri

Contents

Contents

Chapter 1
Use of Ion-Exchange Resins
in Dehydration Reactions

**María José Ginés-Molina, Juan A. Cecilia, Cristina García-Sancho,
Ramón Moreno-Tost and Pedro Maireles-Torres**

Abstract This chapter reviews the main uses of ion-exchange resins as catalysts for dehydration processes. In this regard, the dehydration of alcohols to alkenes is dealt with, and mainly to ethers, since these latter processes require a lower reaction temperature. Moreover, the large variety of ethers (linear, branched, cyclic), which can be synthesized in the presence of ion-exchange resins, has attracted the interest of many research groups, and important industrial applications have been envisaged. Another group of hydroxylated compounds, that is, bearing OH groups susceptible to be dehydrated, are carbohydrates. Monosaccharides such as glucose, fructose and xylose, mainly present in the lignocellulosic biomass, can be transformed, in the presence of ion-exchange resins, into platform molecules. Among them, furfural and 5-hydroxymethylfurfural possess a great potential as they can be utilized as building blocks for the production of high value-added chemicals and materials. The main catalytic processes will be described, providing detailed information about the catalytic performance, and underlining advantages and drawbacks of ion-exchange resins for each catalytic process.

1.1 Introduction

Dehydration processes encapsulated in this chapter involve the removal of water from an organic molecule, which is transformed in another one with lower oxygen content. In this sense, there is a large spectrum of organic reactions where the participation of strong acid catalysts favours the elimination of water, such as the 1,2-elimination of alcohols to produce alkenes, condensation of alcohols to ethers, conversion of carboxylic acids to acid anhydride, amides to nitriles, among others.

In organic chemistry and biochemistry, there are many other examples of dehydration reactions such as peptide formation from two amino acids with the elimination of

M. J. Ginés-Molina · J. A. Cecilia · C. García-Sancho · R. Moreno-Tost · P. Maireles-Torres (✉)
Departamento de Química Inorgánica, Cristalografía y Mineralogía (Unidad Asociada al ICP-CSIC), Facultad de Ciencias, Universidad de Málaga, Campus de Teatinos, 29071 Málaga, Spain
e-mail: maireles@uma.es

one water molecule at each step, by condensation of an amine group with a carboxylic group to form an amide bond. Disaccharides can be formed from monosaccharides by the formation of a glycosidic linkage between two monomeric carbohydrates with the elimination of water molecule (e.g. glucose combines with fructose to form sucrose with removing of a water molecule). Many synthetic polymers, like, for instance, polyethylene terephthalate, are produced by a dehydration reaction between ethylene glycol and terephthalic acid with the elimination of water molecules at each step of polymerization. Moreover, monomeric carbohydrates can be dehydrated to form furanic compounds, such as furfural and 5-hydroxymethylfurfural, which are considered as platform molecules derived from lignocellulosic biomass for the production of biofuels and high value-added chemicals [1, 2].

In industry, most of the dehydration reactions are accomplished under homogeneous conditions, where reactants, products and catalyst are in liquid phase. However, heterogeneous catalysis allows to develop more sustainable and greener catalytic processes, avoiding neutralization and washing steps, and the recovery of the solid catalyst facilitates its reutilization. Moreover, strong liquid acid catalysts are corrosive, toxic and difficult to separate from the reaction mixture, also requiring reactor and equipment resistant to corrosion, thus increasing the cost of the target chemical. For a long time, in the field of heterogeneous catalysis, ion-exchange resins have been used as catalysts of a large variety of organic reactions, and among them, dehydration of alcohols occupies a prevalent position [3].

1.2 Catalytic Processes of Dehydration

1.2.1 Dehydration of Alcohols to Alkenes

Usually, intramolecular dehydration of alcohols to alkenes requires reaction temperatures above 180 °C, whereas their intermolecular dehydration to ethers can be carried out at lower temperatures. This fact, in some cases, limits the application of ion-exchange resins to the intermolecular dehydration of alcohols to ethers.

The formation of alkenes from alcohols is performed by heating the alcohol in the presence of liquid acids, mainly Brönsted acid catalysts (H_2SO_4, H_3PO_4) to facilitate the –OH group to quit the alcohol molecule because $-OH_2^+$ is a better leaving group. The reaction usually proceeds by an E1 mechanism, via a carbocation intermediate, which can undergo rearrangement, whereas for a primary alcohol, due to the fact that a primary carbocation is unfavourable, the process proceeds via an E2 mechanism.

Concerning about the mechanism of dehydration reaction, the first step involves the protonation of the hydroxyl group of an alcohol to form an alkyl oxonium ion, which, after subsequent elimination of a water molecule, generates a carbocation intermediate. Depending on the type of carbocation, it can be rearranged by H or alkyl group shifting, and finally, the proton loss leads to the regeneration of the Brönsted acid catalyst in the presence of the conjugated base, with the formation of the alkene.

The reactivity of alcohols follows the stability order: tertiary > secondary > primary, in such a way that the principal reaction product is the more highly substituted alkene (Zaitsev's rule), whereas stereoselectivity is also controlled (trans- > cis-). Thus, higher reaction temperatures are required for the dehydration of primary alcohols, in comparison with secondary and tertiary ones.

Dehydration of alcohols to alkenes by using ion-exchange resins dates back to 1972, where the kinetics of t-butyl alcohol dehydration to isobutylene was studied in a semi-batch reactor, with two resins: Dowex 50W and Amberlyst 15 [4]. This work highlighted the difficulty of anhydrous t-butyl alcohol to penetrate the shrunken network of the resin, whereas the water produced in the dehydration process can go into the macroporous network and swelled it, thus facilitating the access of alcohol molecules to the inner acid sites. This fact increases the reaction rate, which then decreases as the water molecules competed with the reactant for catalytic sites. Other tertiary alcohols can give selectively the most stable alkene in good yield in the presence of Amberlyst-15 [5], avoiding the formation of rearrangement and polymerization products. Moreover, this ion-exchange resin can be recovered and used at least during five catalytic cycles, preserving the catalytic efficiency. A large variety of tertiary alcohols have been studied in CH_2Cl_2, as a solvent, with a substrate/Amberlyst 15 weight ratio of 1:1.2, at room temperature or under reflux conditions. In most cases, isolated yields of the corresponding olefins were higher than 80%.

Liquid-phase dehydration of propylene glycol has been evaluated in the presence of Amberlyst 36 Dry and its catalytic performance was compared with different MFI-framework zeolite catalysts [6]. Propylene glycol dehydration proceeded by three pathways: (i) dehydration of the secondary hydroxyl group leading to the formation of propionaldehyde, which can subsequently react with propylene glycol to give rise to 2-ethyl-4-methyl-1,3-dioxolane (EMD) and water; (ii) dehydration of the primary hydroxyl group producing acetone, which further reacts with propylene glycol to form 2,2,4-trimethyl-1,3-dioxolane (TMD) and water; and (iii) etherification reaction producing dipropylene glycol (DPG). The ion-exchange resins, at 130 °C after 5 h of reaction, were the most selective towards EMD (78%), a cyclic acetal, with a 13% of dipropylene glycol and the remaining 9% of acetone and TMD formed from acetone. Zeolites were found more prone to form DPG and propionaldehyde.

1.2.2 Dehydration of Alcohols to Ethers

The acid-catalysed intermolecular dehydration of primary alcohols to synthesize ethers has attracted the interest of many research groups. Thus, for instance, dimethyl ether (DME), obtained via methanol dehydration, has found uses as substitute propellant for the ozone-depleting chlorofluorocarbons (presently being phased out), clean diesel fuel, a key intermediate for producing important chemicals such as methyl acetate, dimethyl sulphate and light olefins [7, 8]. DME has a cetane number and ignition temperature close to that of diesel fuel and generates low NO_x, SO_x and par-

ticulate matter emissions compared to conventional diesel engines. The synthesis of DME is accomplished using solid acid catalysts, in a fixed-bed reactor at 250–400 °C, high pressure (up to 10 bar) and several ordinary distillation columns [7]. However, under these experimental conditions, methanol dehydration is limited because it is an equilibrium–controlled reaction. For overcoming this drawback, different technologies have been proposed, and among them, single catalytic distillation is one of those offering more advantages [9].

Hosseininejad et al. evaluated the catalytic behaviour, in DME production via methanol dehydration, of different ion-exchange resins (Amberlyst 15, 35, 36 and 70), at moderate temperature and pressure (110–135 °C and 0.9 MPa) [10]. Amberlysts 35 and 36 demonstrated suitable activity and the kinetic data fitted well with a Langmuir–Hinshelwood kinetic mechanism, for which the surface reaction was the rate determining step. The methanol concentration did not have any effect on the reaction rate, and the proposed mechanism suggested that two molecules of methanol occupy two adjacent acid sites, and the reaction occurred between those molecules. However, the presence of water exerted an inhibiting effect on the reaction rate by competing with methanol molecules over acid sites.

Besides DME, other oxygenated additives can be incorporated into gasoline and diesel fuels for enhancing the combustion efficiency in internal combustion engines and reducing the consumption of non-renewable fossil fuels. Depending on the chemical structure (short or long alkyl chain, branched or linear), they can be suitably used in gasoline (short and branched such as methyl and ethyl tert-butyl ethers) or diesel (linear with a relatively long chain) blends. Industrial production of linear symmetrical ethers is carried out by using sulphuric acid as catalyst, with a quite high selectivity. However, strong liquid acids are very corrosive and heavy products are mostly generated. In order to overcome these drawbacks, the use of solid acid catalysts has been proposed, due to the advantages of easier separation of the catalyst from the reaction medium.

During last three decades, an exhaustive research activity focused on the evaluation of the catalytic performance of many different types of resins has been carried out by the Cunill and Tejero research group [11–17]. Thus, sulfonated polystyrene–divinylbenzene resins, with a high concentration of acid sites with similar acid strength and homogeneously distributed, showed a thermal stability below 200 °C (150 °C, typically), which limited the maximum working temperature. However, they demonstrated that the incorporation of electron-attracting groups (for instance, halogen atoms) to the sulfonated phenyl rings improved the acid strength and thermal resistance to desulfonation. Moreover, water release in many reactions was an additional drawback, since it impeded the reaction to proceed. These resins were capable to catalyse a wide spectrum of catalytic processes, i.e. alkylation, hydration, etherification and dehydration.

There are many examples revealing the use of ion-exchange resins for the dehydration of alcohols. Thus, di-n-pentyl ether (DNPE) has a blending cetane number as high as 109, and it behaves as a light diesel fuel due to its density and viscosity [13]. The production of DNPE by 1-pentanol dehydration in liquid phase has been realized at 110–180 °C and 1 MPa, in the presence of different types of sulfonic styrene—

divinylbenzene copolymers (Amberlyst-type, CT-x, Dowex, among others) and a perfluoroalkanesulfonic resin (Nafion NR50). These resins exhibited macroreticular and gel-type structures and were both sulfonated conventionally and oversulfonated. The catalytic data pointed out that gel-type S/DVB resins that swelled moderately in the reaction medium, as CT-224, were found more suitable catalysts, considering 1-pentanol conversion, selectivity to DNPE and initial reaction rates at 150 °C. The most selective catalyst (95% at 180 °C) was Nafion NR50, which is thermally stable up to 200 °C, but it is very expensive for industrial use. Selectivity to DNPE decreases as temperature increases showing that side reaction of dehydration to 1-pentene is favoured at a higher temperature.

Different reaction pathways can be followed in the dehydration of 1-pentanol to DNPE (Fig. 1.1). Thus, dehydration of 1-pentanol to 1-pentene leads through isomerization to cis- and trans-2-pentenes, as well as to 2-methyl-1-butene. The addition of water to pentene gives rise to amyl alcohols. The intermolecular dehydration of different alcohol pair combinations opens the way of branched ethers production, which can be also formed by the reaction between an alcohol and a particular olefin.

Following the dehydration of 1-pentanol to yield DNPE, Bildea et al. have carried out an optimization design of this catalytic process for a plant capacity of 26.5 kton DNPE per year [18]. In comparison to membrane reactor, a reaction–separation–recycle system based on an adiabatic tubular reactor as well as catalytic distillation process has been two suitable options in terms of easy implementation, investment costs and plantwide control. In both systems, an Amberlyst-70 was used as a solid acid catalyst.

As regards to the production of di-n-butyl ether (DNBE) by dehydration of 1-butanol [12] at 150 °C and 4 MPa, it was found that the macroreticular thermostable Amberlyst 70 resin was the most selective, together with gel-type resins (with easy swelling), whereas oversulfonated resins (Amberlyst 35 and 36) were the most active. In this work, the influence of different impurities on the dehydration was also examined. The catalytic behaviour of these ion-exchange resins was compared with those of γ-alumina and zeolites [19], at 130–300 °C and 0.1–7 MPa, in a fixed-bed flow reactor. The optimization of several operating parameters (T, P, weight hourly space velocity (WHSV)) revealed that Amberlyst ion-exchange resins were suitable acid catalysts for DNBE production. Thus, a conversion of 79% of 1-butanol conversion and a yield of 65% of DNBE were achieved with Amberlyst 36, at 130 °C, 0.1 MPa and 0.3 h^{-1} WHSV.

The research group of Cunill and Tejero has also studied the bimolecular dehydration of other primary alcohols, such as 1-hexanol and 1-octanol [11], to the corresponding di-n-ethers (DNHE and DNOE, respectively), at 150 °C and 2 MPa of pressure, in a batch reactor with ion-exchange resins. Again, different types of resins were evaluated as solid acid catalysts: macroporous (with high, medium and low medium crosslinking degrees) and gel type, together an ion-exchange resin sulfonated only at the polymer surface and Nafion. The catalytic data revealed that the yields of linear symmetrical ethers, derived from 1-pentanol, 1-hexanol and 1-octanol, were strongly depended on the resin structure. Again, the most swollen resins in reaction medium gave the best results (Amberlyst-121, Amberlyst-31 and
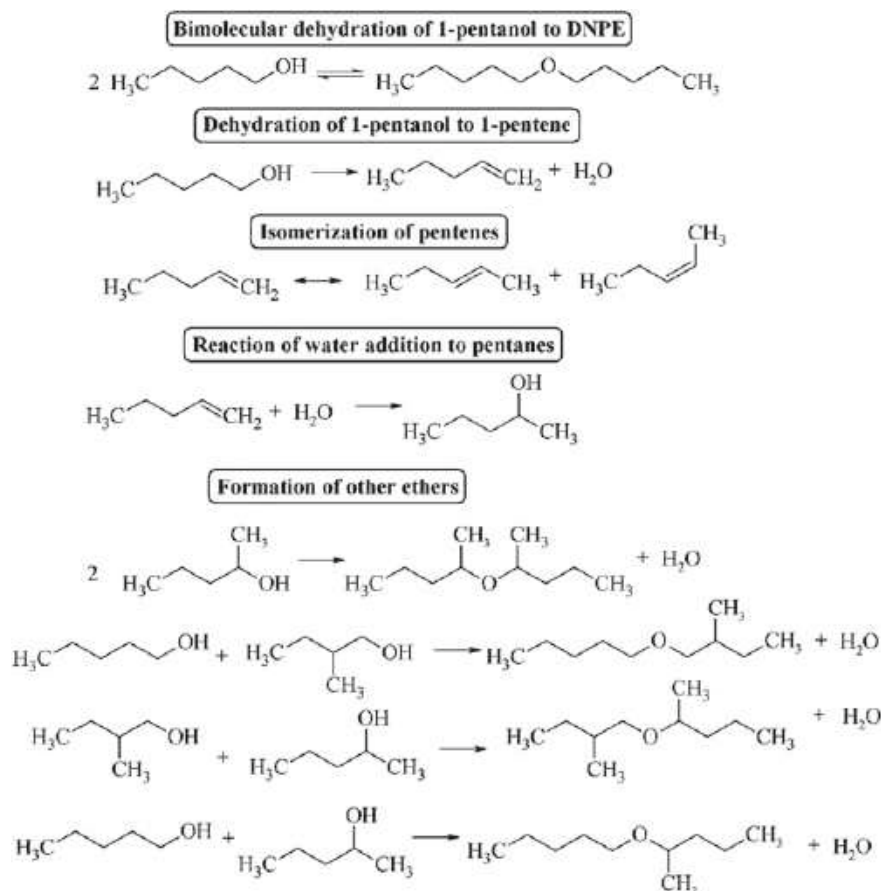
Fig. 1.1 Reaction routes for the formation of different products coming from 1-pentanol dehydration. Adapted from [13]

Dowex 50WX4-50), thus corroborating that swelling is a key factor to attain high selectivity to linear ethers. It was also observed that oversulfonated resins did not improve the activity in comparison with their conventionally sulfonated analogues. Moreover, a high acid capacity and V_{sp} (specific volume) values favoured the dehydration process. They concluded that high ether yields were due to the high alcohol conversions and especially to the very high selectivity to ethers ($\geq 94\%$). The highest initial turnover frequency (TOF_0) values were obtained with NR50, due to higher acid strength, whereas, among PS-DVB resins, the best performance in terms of TOF_0 value was obtained with Amberlyst-46, a special resin with all sulfonic groups at the polymer surface, and so fully accessible to alcohol molecules. However, lower TOF_0 values observed for the rest of PS-DVB resins could be explained that only a fraction of active acid sites was available for reaction, and hence the ether formation

was hindered in less swollen polymers. Linear ether formation was influenced by resin swelling level. It is generally observed that initial rates followed the order r_0 DNPE > r_0 DNHE > r_0DNOE.

The incorporation of ethyl groups to ethers has been a sustainable strategy for the preparation of oxygenated compounds since the source of the ethyl group can be bioethanol derived from lignocellulosic biomass. The liquid-phase dehydration of ethanol to diethyl ether (DEE) has been studied over the Amberlyst-type catalysts previously mentioned [20]. Similar catalytic activities were found at 160 °C, with an internal pressure up to 1.5 MPa, in a stirred batch reactor. The lower acid capacity of Amberlyst-70 has been compensated by a higher specific activity. Reaction rates greatly depended on ethanol concentration, as well as on the reaction mixture polarity, as inferred from the comparison of ethanol conversion as a function of reaction mixture composition. The swelling of the used resins did not explain the observed variations of initial reaction rate since this effect was also observed with homogeneous catalyst (*p*-toluenesulfonic acid). However, DEE has a low flash point, and its addition to diesel can change considerably the initial diesel properties, so the addition of large quantities of DEE must be avoided. An option for overcoming this limitation is the incorporation of longer chain alcohols to the ether molecule, together with the ethyl group. Thus, for instance, ethyl hexyl ether (EHE) provides a suitable compromise between cold flow properties and blending cetane number. The main catalytic route is the ethylation of 1-hexanol, and diethyl carbonate has demonstrated to be the most suitable ethylating agent [15]. The process was carried out in the liquid phase at a temperature between 130 and 190 °C and 2.5 MPa, in the presence of ion-exchange resins. The formation of EHE involved the thermal decomposition of ethyl hexyl carbonate and subsequent intermolecular dehydration of 1-hexanol with ethanol, requiring the previous transesterification of diethyl carbonate and 1-hexanol. From the evaluation of the catalytic performance of several acidic ion-exchange resins, it could be inferred that the formation of ether favoured in zones of 0.4 nm nm^{-3} polymer density (2.6 nm of pore diameter), which are present in Dowex 50WX2 and Amberlyst 70, and a low temperature minimizes the formation of by-products (mainly, di-*n*-hexyl ether).

Ethyl octyl ether (EOE) has been synthesized from ethanol and 1-octanol over Amberlyst 70 [14]. However, the formation of DEE has been the main competitive process, with similar activation energies (105 ± 4 and 100 ± 5 kJ mol^{-1} for EOE and DEE, respectively), whereas, DNOE was barely formed. The catalytic process was studied in a fixed-bed and batch reactors at 150–190 °C and 2.5 MPa. A negative effect of generated water was observed since water molecules compete with alcohol reactants for the surface active sites.

The dehydration of 1,4-butanediol produced tetrahydrofuran (Fig. 1.2), which is a five-membered cyclic ether with important industrial applications [21], such as the manufacture of poly(tetramethylene ether) glycol (PTMEG) and polytetrahydrofuran (PTHF), important in the production of thermoplastic polyurethanes, moulded elastomers, elastic fibres and copolyesters or copolyamides. It has also been used as a versatile solvent for adhesives, vinyl films and cellophane, industrial resins, elastomers, coatings and printing inks, pharmaceutical synthesis, component of cleaning
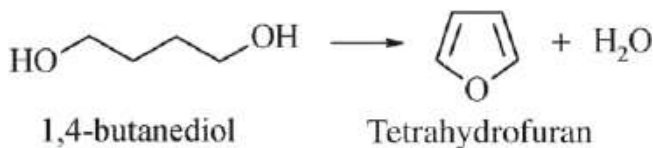
Fig. 1.2 Dehydration of 1,4-butanediol to tetrahydrofuran

fluids, paint removers and stripping fluids, as well as extracting agent and medium for organometallic synthesis.

The dehydration–cyclization of 1,4-butanediol has been accomplished in the presence of strong liquid acids (H_2SO_4), but different heterogeneous catalysts have been reported to overcome drawbacks associated with the homogeneous process. In this sense, ion-exchange resins have been reported to be active catalysts for this reaction. Thus, Vaidya et al. studied the kinetics of dehydration of 1,4-butanediol using a strongly acidic cation-exchange resin, Indion-130 [22]. In comparison to alumina and silica gel, this ion-exchange resin has shown a much better catalytic performance under batch conditions at a lower temperature (125 °C). The dehydration rate seems to depend on the catalyst loading in all the temperature range, confirming the absence of diffusional resistance. They observed that 1,4-dioxane, as a solvent, allowed higher conversion than in the presence of ethanol and water. The initial rate varied more than one order for substrate concentration, is strongly inhibited by the initial water present in the system. This was explained by the competitive adsorption of water on $-SO_3H$ groups of resin, thus decreasing the number of available active sites. The intrinsic kinetics was well fitted to a Langmuir–Hinshelwood kinetic model.

The negative effect of water was corroborated by using a macroreticular ion-exchange resin like Amberlyst-15 [23]. Aiming at the process intensification, batch reactive distillation was proposed, showing that the removing of water from the reaction medium helped to overcome this drawback.

1.2.3 Dehydration of Carbohydrates

Currently, there is a great interest in developing sustainable and integrated catalytic processes for the vaporization of lignocellulosic biomass, by transforming its main structural components (cellulose, hemicellulose and lignin) into biofuels and carbon-based chemicals [24, 25]. In this context, the dehydration of C_6 and C_5 sugars gave rise to 5-hydroxymethylfurfural (HMF) and furfural (FUR), respectively (Fig. 1.3), which have been identified as platform molecules due to their versatility for the synthesis of alternative fuels and a very large spectrum of chemicals.

On the one hand FUR is industrially produced from renewable agricultural sources such as food crop residues and wood wastes. Under homogeneous conditions, H_2SO_4 is employed as an acid catalyst, FUR recovered from the liquid phase by steam strip-

ping to minimize further degradation, and purified by double distillation [2, 26, 27]. Currently, its most relevant application is as feedstock mainly for the production of furfuryl alcohol, though furanic compounds, such as furan, 2-methylfuran, furfurylamine and furoic acid, among others, can be also obtained. Moreover, different transformation pathways can be used to transform FUR in fine and commodity chemicals and fuels. FUR is also used as a solvent and in the manufacturing of phenol-FUR resins as well as nylon-6,6.

On the other hand, 5-HMF is also a versatile platform molecule, being an important intermediate in the industrial production of resins, plastics (2,5-furandicarboxylic acid proposed as a replacement for terephthalic acid in the production of polyesters), additives, biofuels like 2,5-dimethylfuran, among others [28, 29].

As previously indicated, the dehydration of C_5 carbohydrates has been carried out industrially in the presence of liquid mineral acids (homogeneous catalysis), although much efforts are being paid to the development of heterogeneous catalysis for a sustainable production of these important furanic molecules. However, the main drawbacks associated with these dehydration processes lie in their low yields due to the secondary reactions, such as resinification and condensation leading to the formation of humins. In order to improve HMF and FUR yields, several strategies have been proposed: (i) use of biphasic solvents to continuously extract these molecules with an organic phase, sometimes in the presence of inorganic salts to ameliorate
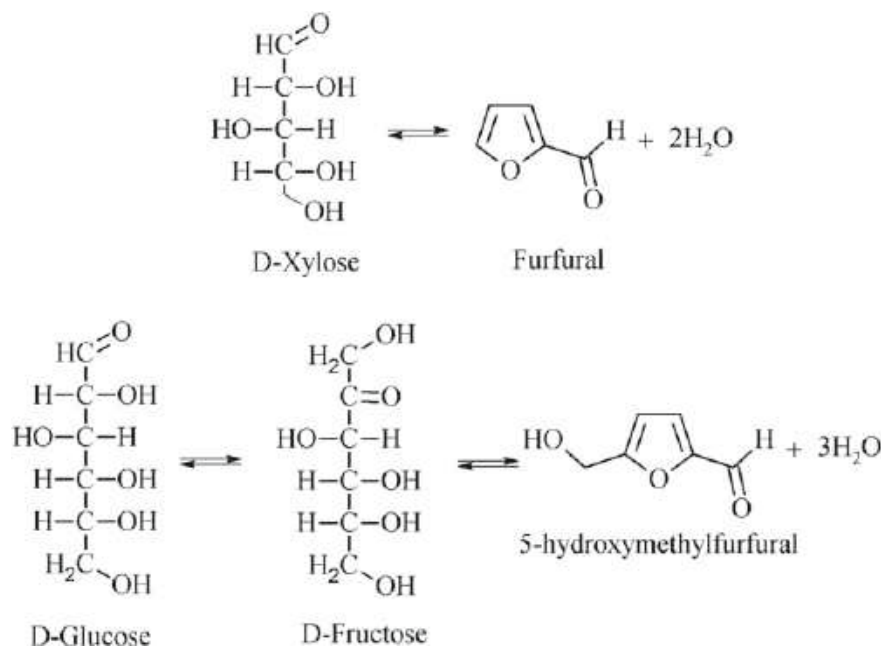
Fig. 1.3 Dehydration of D-xylose and D-glucose to furfural and 5-hydroxymethylfurfural, respectively

the partition coefficients, thus minimizing their degradation which occurs mainly in water and (ii) removal employing steam or inert gas by stripping.

Different types of ion-exchange resins have been assayed for the dehydration of carbohydrates. In this regard, furfural production from xylose has been carried out in the presence of Amberlyst 70, followed by using stripping with N_2 under semi-batch conditions to ameliorate FUR yield [30]. This methodology allowed an average xylose conversion of 55%, at 175 °C, with almost 100% selectivity to FUR in the condensate, thus reducing considerably purification costs for obtaining high-quality FUR. The formation of water–furfural immiscible phases for high xylose loading in the reactor was observed. This study demonstrated the reduction in energy requirements in comparison to steam-stripping or biphasic systems. This research group compared the FUR production by feeding a mixture of xylose and glucose with conventional batchwise (biphasic water/toluene and water as solvents) and simultaneous N_2 stripping (solvent: water), also in the presence of Amberlyst 70 [31]. Their study concluded that, by continuous feeding of xylose/glucose solutions with a molar ratio similar to the real pentosan-rich biomass, FUR yield of 75% was achieved at 200 °C by using N_2 stripping.

Recently, Mittal et al. have reported the use of Purolite CT275 and Nafion NR50 as heterogeneous acid catalysts for the production of FUR from pentose rich corn stover hydrolysates [32]. The xylose conversion reached to a value of 96% when 8 wt% pentose concentration was used in the presence of Purolite CT275, in a biphasic water/methyl isobutyl ketone batch system, with a FUR yield of 80%, at 170 °C for 20 min, with 125 mg catalyst per gram of pentose. The better catalytic performance of Purolite was due to its greater H^+ concentration, and the FUR yield was similar to that obtained with the homogeneous H_2SO_4 catalyst. However, recycling studies demonstrated the loss of catalytic activity, which was attributed to the strong adsorption of reaction products on the active catalytic sites. Usually, these adsorbed products can be removed by calcination but the thermal stability of ion-exchange resins impedes this regeneration treatment.

Another approach for improving furfural yield consisted in a continuous-flow biphasic fixed-bed reactor over a catalytic bed formed by a physical mixture of a Lewis acid gallium-containing USY zeolite for xylose isomerization and a Brönsted acid ion-exchange resin (Amberlyst-36) for hemicellulose hydrolysis and xylulose dehydration [33]. The optimization of different experimental variables (catalyst loading, nature of the extracting phase, contact time and feed concentration) enabled to achieve furfural yields of 69 and 72% from xylan and xylose, respectively. A biphasic water/methyl isobutyl ketone system, a 2.5 wt% xylan in water, 0.36 g of zeolite and 0.72 g of resin, at 130 °C, with a contact time of 6.8 min were employed as optimal conditions. The intimate physical mixing of the two catalysts maximized FUR production and made possible to extend this technology to the conversion of more complex xylan hemicellulose substrate to FUR.

On the other hand, Dowex 50WX8-200, an acidic ion-exchange resin, suspended in an ionic liquid (1-*n*-butyl-3-methylimidazolium chloride, [C4mim]Cl), has demonstrated to be active in the dehydration of different carbohydrates [34]. A FUR yield of 90% was attained at 100 °C, after 6 h, under batch conditions, from ribose,

decreasing the reactivity order as ribose > arabinose > lyxose > xylose. This trend could be explained by considering an open chain mechanism, in which ribose and arabinose showed the same ketose form (ribulose), although much research efforts are needed to clarify the mechanism. Concerning glucose dehydration, Amberlyst-15 attained an HMF yield of 61 and 34% from glucose and fructose, respectively. By using Dowex 50WX8-200, a higher yield from fructose was achieved (44%). During the study of catalyst utilization, after washing the used catalyst with acetone and air dried, a drastic drop of the HMF yield (90%) was observed in a second catalytic cycle. However, the regeneration of the ion-exchange resin, by washing with 10% H_2SO_4 and brought to pH 6 with distilled water, only allowed to use the resin once more with a drop of 16%, being non-feasible to repeat the regeneration for additional cycles without important loss of activity.

Regarding the production of HMF from C_6 carbohydrates, a key step is an isomerization of glucose to fructose, catalysed by basic or Lewis acid catalysts, which is subsequently dehydrated to HMF (Fig. 1.3). Different ion-exchange resins (Amberlite IRA-743, IRA-400 and IRA-900, Amberlyst A-26 and 15) were evaluated for the isomerization of glucose into fructose [35]. The best catalytic result, among these anion-exchange resins, was obtained with Amberlyst A-26, with a glucose conversion of 53% and superior selectivity (94%) to fructose, using ethanol, at 80 °C for 3 h. This is an anion-exchange resin with a 3.2 mmol basic functional groups per gram of resin, with a macroreticular polymeric structure based on cross-linked styrene-divinylbenzene copolymer containing tertiary amine terminal groups. This unique structure and pore size distribution provided Amberlyst A-26 superior resistance to mechanical and osmotic shocks. It was concluded that protic solvents were more suitable than aprotic ones, as well as that macroporous (IRA-743) and macroreticular (A-26 and IRA-900) resins allowed to reach higher yields of fructose (30–45 than gel-type resins (IRA-400) and tertiary amine functionalities were better compared to tetraalkylammonium ones. Moreover, these resins roughly maintained their catalytic activity for five catalytic cycles. This isomerization process seems to proceed via a proton transfer mechanism (Lobry de Bruyn–van Ekenstein transformation) in aqueous basic conditions, although in organic solvents, the Meerwein–Ponndorf–Verley process via intramolecular transfer of hydride can also play an important role. In order to accomplish the conversion of glucose into HMF, a combination of anion-exchange (IRA-743) and cation-exchange (Amberlyst-15) resins were used, in N,N-dimethylformamide (DMF), at 100 °C for 5 h, which led to an HMF yield of 34%. However, in dimethyl sulfoxide (DMSO), values were lower than 30%, and, in ethanol as solvent, HMF and 5-ethoxymethyl-2-furfural were produced with 23 and 11% yields, respectively, at 80 °C.

The ion-exchange resin, PK-216, was used by Dumesic's group in the production of HMF from fructose [36]. By using high fructose concentration (30 wt%), in a two-phase reactor system (water/MIBK), by adding polar aprotic molecules such as DMSO and poly(1-vinyl-2-pyrrolidinone) to water in order to suppress undesired side reactions, HMF yield close to 55% was achieved, at 90 °C, after 8 h of reaction time. However, the absolute HMF selectivities were lower for the resin in comparison with HCl. This study demonstrated that HMF can be efficiently separated from the

extracting solvent (MIBK) by vacuum distillation, and low-boiling point solvents were a better choice than other like pure DMSO.

Another strategy to improve the HMF yield from fructose consisted of modifying a mesocellular silica foam (MCF) by incorporation of a Nafion perfluorosulfonic acid resin, which exhibited an acid strength comparable to that of pure sulphuric acid. The impregnation led to Nafion resin highly dispersed in the ultra-large pores of the MCFs. In the presence of DMSO, as a solvent, at 90 °C after 2 h, 89% HMF yield with 95% selectivity was attained. Moreover, the catalyst could be regenerated, maintaining the catalytic performance for five catalytic cycles.

The mixture of a sulfonic acid ion-exchange resin (Amberlyst-15) and ionic liquid (1-butyl 3-methyl imidazolium tetrafluoroborate, [Bmim]Cl) has also allowed obtaining HMF yield up to 87%, at 80 °C, after 32 h, with DMSO as co-solvent [37]. Later, similar HMF yields (95–100%) were attained by using this Amberlyst-15 and a Dowex 50WX8, after 10 min at 80 °C, with the same ionic liquid [38]. It was also observed that water content higher than 5 wt% in the ionic liquid led to lower conversions and yields. Li et al. also found that macroporous strong acid resins (D001-cc, D072) exhibited higher catalytic performance in fructose dehydration than gel strong acid resins (001×1, 001×7, 001×14.5), due to the easier accessibility of fructose to active acid sites located in the large pores of macroporous resins [39]. An HMF yield of 93% was obtained at 75 °C for 20 min with D001-cc resin in [Bmim]Cl. Moreover, this catalytic system can be reused, with an 86.2% HMF yield after seven recycles.

Most of the publications on HMF production related to the use of fructose as feedstock, which can be readily dehydrated to HMF using Brönsted acid sites. Though glucose is more difficult to be dehydrated, it has been preferred as raw material because it is more abundant and less expensive than fructose. Nevertheless, HMF can also be produced from sucrose (a disaccharide formed by glucose and fructose). It has been proposed a four steps sequential process: (a) hydrolysis, (b) dehydration, (c) glucose/fructose isomerization and (d) dehydration in the presence of different ion-exchange resins [40]. For accomplishing this process, an Amberlite IR-120(H$^+$) resin was used for steps a, b and d, and an Amberlite IRA-400 for the isomerization of glucose to fructose. After each step, the resin was filtered off, and the contents were concentrated to dryness, and then dissolved in the corresponding reaction medium. Each step was performed under specific experimental conditions (solvents, reaction temperature and time, catalyst), and an overall HMF yield of 50% was attained from sucrose.

Bifunctional Cr^{3+} modified ion-exchange resins have demonstrated to be efficient catalysts for the production of HMF from glucose [41, 42]. Cr^{3+} (2.4–5.24 w/w) was incorporated to different ion-exchange resins (Amberlyst 15, 36 and IRC86, Amberlite IRC748I and 120), in methanol, at 80 °C in a pressure glass rector, under stirring overnight [41]. The best catalytic performance was achieved with Amberlyst-type resins, in particular with the Amberlyst 15/Cr^{3+} catalyst, with the highest HMF yield (70%) with outstanding purity of 98% at 120 °C, 100% w/w, glucose/catalyst, in tetraethylammonium bromide/water, after 60 min. Without Cr^{3+}, under similar experimental conditions, the HMF yield was only 24%. The catalytic results pointed

out that there was no correlation between Cr^{3+} loadings and HMF yields, although a suitable balance between Cr^{3+} loading and acidity seemed to be important for attaining high catalytic activity. The introduction of Lewis acid sites, associated with metal cations, favoured the glucose/fructose isomerization. In the reutilization study, high HMF yield values were only maintained until the third cycle. The leaching of chromium was only important (16%) in the first cycle, which decreased for subsequent cycles. However, the catalytic activity was only partially recovered (50%) after treatment with 10% HCl_{aq}. This strategy was also employed with different cation-exchange resins, which were modified with $CrCl_3$ [42], but in the [Bmim]Cl ionic liquid. The nature of the metal ion was studied, and the highest yield was obtained with Cr^{3+}, and among resins (001 × 1, 001 × 7, NKC-9, D072, D001-cc and D152), D001-cc was the most active. Several experimental variables were optimized and the highest HMF yield of 61.3% was attained at 110 °C, after 30 min, in the presence of D001-cc cation-exchange resin, with 0.1 g glucose, 1.5 g of ionic liquid, and 0.1 g catalyst. This behaviour could be explained by the macroporosity and strong acidity of the D001-cc resin. A relatively stable HMF yield was observed in the first four catalytic cycles, in the reutilization study. The increase in HMF yield in the second and third runs was justified by the presence of Cr^{3+} leached in solution.

This combination of acid ion-exchange resin (NKC-9) and metal oxides in ionic liquids has been also evaluated under microwave heating [43]. It was found that the binary catalyst (NKC-9 and Al_2O_3) caused an HMF yield of 62% at 140 °C, after 20 min, with only a slight decrease in activity after five reuses. However, in the absence of metal oxide, a very low HMF yield was attained (4%). The presence of basic sites on alumina catalysed the isomerization of glucose to fructose, which was subsequently dehydrated on the acid resin.

1.2.4 Other Dehydration Processes

The hydrolysis/hydrogenation of lignocellulosic biomass or hydrogenation of glucose led to sorbitol, which is one of the most important platform molecules derived from biomass [25, 44]. Sorbitol finds many applications in food, pharmaceutical and cosmetic industries, as well as additives in many end products. Thus, for instance, it is used as a key intermediate in the industrial synthesis of ascorbic acid (vitamin C), and its fatty acid esters can be employed as surfactants [45]. However, a new interest arose from the double dehydration of sorbitol giving rise to isosorbide (1,4:3,6-dianhydro-D-glucitol), with important applications in pharmaceutical and personal care products, for the synthesis of polymers, dimethyl isosorbide (DMI) or other mono- or di-alkylethers, and isosorbide esters [46, 47]. Among its derivatives, isosorbide mononitrate is a drug used principally as a vasodilator for angina and congestive heart failure, and dimethyl isosorbide is used in cosmetic formulations and as fuel or fuel additives due to its high energy content. The dehydration of sorbitol to isosorbide occurs through two consecutive steps: the loss of a water molecule, and subsequent cyclization, can lead to different chemical intermediates: (a) 2,5- and
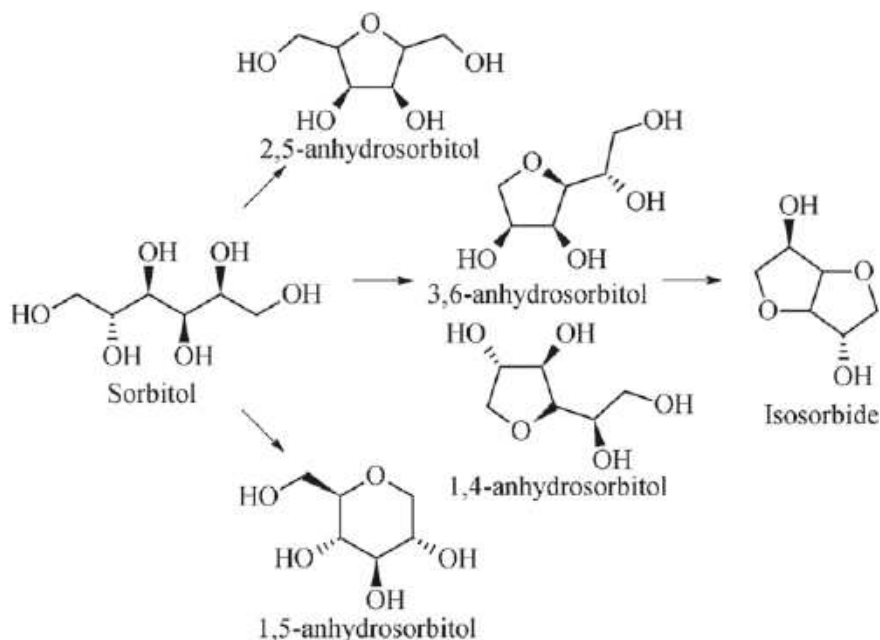
Fig. 1.4 Reaction pathways in sorbitol dehydration

1,5-anhydrosorbitols, considered as by-products since they do not evolve towards isosorbide, and (b) 1,4- and 3,6-anhydrosorbitols. These latter can lose a second water molecule, and after a new cyclization, give rise to isosorbide (Fig. 1.4). Nevertheless, 1,4-anhydrosorbitol is an important chemical for emulsifiers, surfactants, cosmetics, synthetic resins and pesticides, among many applications [48].

The most accepted mechanism for dehydration/cyclization involves SN2 substitution reactions with a protonated hydroxyl group ($-OH_2^+$) as the leaving group, a similar mechanism to that operating in the dehydration of 1,4-butanediol to form tetrahydrofuran (vide supra).

Mineral acids (H_2SO_4, HCl) have been used for years for the synthesis of isosorbide, under homogeneous conditions, and the relative performance of mineral and organic acids has been compared by Dabbawala et al., concluding that p-toluene sulfonic acid (PTSA) and trifluoromethane sulfonic acid provided turnover frequencies similar to that of sulphuric acid [49].

As previously noted, the recycling of the catalyst offers to heterogeneous catalysis a key advantage in comparison to homogeneous processes. Among the acid solid catalysts proposed for the production of isosorbide by dehydration of sorbitol, commercial sulfonic acid resins occupied a privileged position. Goodwin et al. performed a spectroscopy study by using FTIR and ^{13}C NMR techniques to study the nature of products obtained in the dehydration of sorbitol in the presence of commercial ion-exchange resins: Amberlite IR-120 and AG 5OW-X4 [50]. After distillation of

formed isosorbide, a 39% yield was attained after 24 h, under reflux conditions using dioxane/ethyl acetate as solvent. In the patent filed by Moore and Sanborn [51], different ion-exchange resins (Amberlyst 35, 15, Dowex 50WX4 and RXP21H) were evaluated at 135 °C, by using sorbitol in a solvent-free system, at a reduced pressure of 1–10 mm Hg. After 2 h of reaction, a 74% yield of isosorbide was obtained with Amberlyst 35. By using microwave irradiation, the dehydration rate was accelerated in comparison with conventional electric heating, working at the same temperature. Thus, the reaction temperature can be also lowered for attaining similar isosorbide yields, by using melt sorbitol and Amberlyst 15 [52] and Amberlyst 35 [53], as solid acid catalysts. As regards to the kinetic study of this dehydration process, Polaert et al. concluded, by using Amberlyst 35, that the reaction kinetics can be adjusted by a Langmuir–Hinshelwood type model, that includes the adsorption–desorption equilibrium on the catalyst surface [53]. Amberlyst 36 has been also used in a fixed-bed quartz reactor, in a continuous process, with a feed of 70% sorbitol solution at a flow rate of 0.021 ml/min, at 125 °C. After 1000 h of reaction, the catalyst was found stable for incomplete conversion of sorbitol (80%).

Recently, different Amberlyst and Purolite resins have been also evaluated in the dehydration of sorbitol under solvent-free conditions, by melting sorbitol [54]. At shorter reaction duration, different anhydrosorbitols (monodehydration products) were detected, whose dehydration and subsequent cyclization led to the formation of isosorbide. A maximum yield of 75% was attained, at 140 °C after 12 h, by using a 5 wt% of Purolite CT269, at atmospheric pressure. The stability of this resin was inferred from the maintenance of its catalytic activity after four runs, and corroborated by the negligible presence of sulphur species (coming from sulfonic acid leaching) in the reaction medium. This suitable catalytic performance can be explained by its high acid capacity (5.2 meq g^{-1}) as well as mechanical and thermal stabilities associated to the macroreticular structure, in comparison with the rest of ion-exchange resins.

1.3 Conclusion

The use of ion-exchange resins in dehydration reactions has been reported for a long time, mainly for transforming alcohols to ethers. The requirements associated to each catalytic process were fulfilled by the availability of many different types of ion-exchange resins, with different chemical nature as well as thermal and mechanical stabilities. Their physicochemical properties have facilitated the choice of the most suitable ion-exchange resin. Recently, due to the increasing attention paid to the development of new catalytic processes for biomass conversion for the production of biofuels and chemicals as an alternative to the use of fossil-based feedstock, new applications for ion-exchange resins are emerging. This is the case of dehydration of carbohydrates (C5 and C6 sugars) to platform molecules such as furfural and 5-hydroxymethylfurfural, or the dehydration of sorbitol to isosorbide, where high yields of target product have been attained in the presence of ion-exchange resins,

at moderate temperatures. However, it is still necessary to improve the chemical and thermal resistances of ion-exchange resins for their use in catalytic processes requiring high reaction temperatures, typically higher than 200 °C, where ion-exchange resins lack stability.

References

1. Serrano-Ruiz JC, West RM, Dumesic JA (2010) Catalytic conversion of renewable biomass resources to fuels and chemicals. Annu Rev Chem Biomol Eng 1:79–100. https://doi.org/10.1146/annurev-chembioeng-073009-100935
2. Alonso DM, Bond JQ, Dumesic JA (2010) Catalytic conversion of biomass to biofuels. Green Chem 12:1493–1513. https://doi.org/10.1039/c004654j
3. Polyanskii NG, Sapozhnikov VK (1977) New advances in catalysis by Ion-exchange resins. Russ Chem Rev 46:226–245
4. Heath HW, Gates BC (1972) Mass transport and reaction in sulfonic acid resin catalyst: the dehydration of t -butyl alcohol. AIChE J 18:321–326
5. Frija LMT, Afonso CAM (2012) Amberlyst -15: a reusable heterogeneous catalyst for the dehydration of tertiary alcohols. Tetrahedron 68:7414–7421. https://doi.org/10.1016/j.tet.2012.06.083
6. Courtney TD, Nikolakis V, Mpourmpakis G, Chen JG, Vlachos DG (2012) Applied catalysis a: general liquid-phase dehydration of propylene glycol using solid-acid catalysts. Applied Catal A Gen 449:59–68. https://doi.org/10.1016/j.apcata.2012.09.034
7. Kaneko T, Derbyshire F, Makino E, Gray D, Tamura M (2005) Coal liquefaction. In: ULLMANN'S encyclopedia of industrial chemistry, Wiley-VCH Verlag GmbH & Co. KGaA, Weinheim
8. Lei Z, Zou Z, Dai C, Li Q, Chen B (2011) Synthesis of dimethyl ether (DME) by catalytic distillation. Chem Eng Sci 66:3195–3203. https://doi.org/10.1016/j.ces.2011.02.034
9. Azizi Z, Rezaeimanesh M, Tohidian T, Rahimpour MR (2014) Dimethyl ether: a review of technologies and production challenges. Chem Eng Process Process Intensif 82:150–172. https://doi.org/10.1016/j.cep.2014.06.007
10. Hosseininejad S, Afacan A, Hayes RE (2012) Catalytic and kinetic study of methanol dehydration to dimethyl ether. Chem Eng Res Des 90:825–833. https://doi.org/10.1016/j.cherd.2011.10.007
11. Casas C, Bringué R, Ramírez E, Iborra M, Tejero J (2011) Liquid-phase dehydration of 1-octanol, 1-hexanol and 1-pentanol to linear symmetrical ethers over ion exchange resins. Appl Catal A Gen 396:129–139. https://doi.org/10.1016/j.apcata.2011.02.006
12. Pérez MA, Bringué R, Iborra M, Tejero J, Cunill F (2014) Ion exchange resins as catalysts for the liquid-phase dehydration of 1-butanol to di-n-butyl ether. Appl Catal A Gen 482:38–48. https://doi.org/10.1016/j.apcata.2014.05.017
13. Tejero J, Cunill F, Iborra M, Izquierdo JF, Fité C (2002) Dehydration of 1-pentanol to di- n -pentyl ether over ion-exchange resin catalysts. J Mol Catal A Chem 183:541–554
14. Guilera J, Bringué R, Ramírez E, Fité C, Tejero J (2014) Kinetic study of ethyl octyl ether formation from ethanol and 1-octanol on amberlyst 70. AIChE J 60:2918–2928. https://doi.org/10.1002/aic
15. Guilera J, Ramírez E, Fité C, Tejero J, Cunill F (2015) Synthesis of ethyl hexyl ether over acidic ion-exchange resins for cleaner diesel fuel. Catal Sci Technol 5:2238–2250. https://doi.org/10.1039/C4CY01548G
16. Tejero J, Cunill F, Iborra M (1987) Molecular mechanisms of MTBE synthesis on a sulphonic acid ion exchange resin. J Mol Catal 42:257–268

17. Soto R, Fité C, Ramírez E, Iborra M, Tejero J (2018) Catalytic activity dependence on morphological properties of acidic ion-exchange resins for the simultaneous ETBE and TAEE liquid-phase synthesis. React Chem Eng 3:195–205. https://doi.org/10.1039/C7RE00177K

18. Bildea CS, Gyorgy R, Sánchez-Ramírez E, Quiroz-Ramírez JJ, Segovia-Hernandez JG, Kiss AA (2015) Optimal design and plantwide control of novel processes for di-n-pentyl ether production. J Chem Technol Biotechnol 90:992–1001. https://doi.org/10.1002/jctb.4683

19. Samoilov VO, Ramazanov DN, Nekhaev AI, Egazar SV, Maximov AL (2015) Flow reactor synthesis of cetane-enhancing fuel additive from 1-butanol. Fuel Process Technol 140:312–323. https://doi.org/10.1016/j.fuproc.2015.08.021

20. Vanoye L, Zanota M, Desgranges A, Favre-reguillon A, De Bellefon C (2011) Solvent effects in liquid-phase dehydration reaction of ethanol to diethylether catalysed by sulfonic-acid catalyst. Appl Catal A Gen 394:276–280. https://doi.org/10.1016/j.apcata.2011.01.012

21. Müller H (2005) Tetrahydrofuran. In: ULLMANN'S encyclopedia of industrial chemistry, Wiley-VCH Verlag GmbH & Co. KGaA,Weinheim

22. Vaidya SH, Bhandari VM, Chaudhari RV (2003) Reaction kinetics studies on catalytic dehydration of 1, 4-butanediol using cation exchange resin. Appl Catal A Gen 242:321–328

23. Shinde VM, Patil GN, Katariya A, Mahajan YS (2015) Chemical engineering and processing: process intensification production of tetrahydrofuran by dehydration of 1, 4-butanediol using amberlyst-15: batch kinetics and batch reactive distillation. Chem Eng Process Process Intensif 95:241–248. https://doi.org/10.1016/j.cep.2015.06.016

24. Corma Canos A, Iborra S, Velty A (2007) Chemical routes for the transformation of biomass into chemicals. Chem Rev 107:2411–2502. https://doi.org/10.1021/cr050989d

25. Gallezot P (2012) Conversion of biomass to selected chemical products. Chem Soc Rev 41:1538–1558. https://doi.org/10.1039/c1cs15147a

26. Mariscal R, Maireles-Torres P, Ojeda M, Sádaba I, Granados ML (2016) Furfural: a renewable and versatile platform molecule for the synthesis of chemicals and fuels. Energy Environ Sci 9:1144–1189. https://doi.org/10.1039/c5ee02666k

27. Lange JP, Van Der Heide E, Van Buijtenen J, Price R (2012) Furfural-a promising platform for lignocellulosic biofuels. Chem Sus Chem 5:150–166. https://doi.org/10.1002/cssc.201100648

28. Wang T, Nolte MW, Shanks BH (2014) Catalytic dehydration of C 6 carbohydrates for the production of hydroxymethylfurfural (HMF) as a versatile platform chemical. Green Chem 16:548–572. https://doi.org/10.1039/c3gc41365a

29. Van Putten R, Van Der Waal JC, De Jong E, Rasrendra CB, Heeres HJ, De Vries JG (2013) Hydroxymethylfurfural, a versatile platform chemical made from renewable resources. Chem Rev 113:1499–1597

30. Agirrezabal-Telleria I, Larreategui A, Requies J, Güemez MB, Arias PL, Guemez MB, Arias PL (2011) Furfural production from xylose using sulfonic ion-exchange resins (Amberlyst) and simultaneous stripping with nitrogen. Bioresour Technol 102:7478–7485. https://doi.org/10.1016/j.biortech.2011.05.015

31. Agirrezabal-Telleria I, Requies J, Güemez MB, Arias PL (2012) Furfural production from xylose + glucose feedings and simultaneous. Green Chem 14:3132–3140. https://doi.org/10.1039/c2gc36092f

32. Mittal A, Black SK, Vinzant TB, Brien O, Tucker MP, Johnson DK (2017) Production of furfural from process-relevant biomass- derived pentoses in a biphasic reaction system. ACS Sustain Chem Eng 5:5694–5701

33. Aellig C, Scholz D, Dapsens PY, Mondelli C, Pérez-Ramírez J (2015) When catalyst meets reactor: continuous biphasic processing of xylan to furfural over GaUSY/Amberlyst-36. Catal Sci Technol 5:142–149. https://doi.org/10.1039/C4CY00973H

34. Heguaburu V, Franco J, Reina L, Tabarez C, Moyna G, Moyna P (2012) Dehydration of carbohydrates to 2-furaldehydes in ionic liquids by catalysis with ion exchange resins. Catal Commun 27:88–91. https://doi.org/10.1016/j.catcom.2012.07.002

35. Mun D, Thanh N, Huynh T, Shin S, Kim YJ, Kim S, Shul Y-G, Cho JK (2017) Facile isomerization of glucose into fructose using anion-exchange resins in organic solvents and application to direct conversion of glucose into furan compounds. Res Chem Intermed 43:5495–5506. https://doi.org/10.1007/s11164-017-2942-3

36. Román-leshkov Y, Chheda JN, Dumesic JA (2012) Phase modifiers promote efficient production of hydroxymethylfurfural from fructose. Science (80): 1933–1937. https://doi.org/10.1126/science.1126337

37. Lansalot-Matras C, Moreau C (2003) Dehydration of fructose into 5-hydroxymethylfurfural in the presence of ionic liquids. Catal Commun 4:517–520. https://doi.org/10.1016/S1566-7367(03)00133-X

38. Qi X, Watanabe M, Aida TM, Smith RL Jr (2009) Efficient process for conversion of fructose to 5-hydroxymethylfurfural with ionic liquids. Green Chem 11:1327–1331. https://doi.org/10.1039/b905975j

39. Li Y, Liu H, Song C, Gu X, Li H, Zhu W, Yin S (2013) The dehydration of fructose to 5-hydroxymethylfurfural efficiently catalyzed by acidic ion-exchange resin in ionic liquid. Bioresour Technol 133:347–353. https://doi.org/10.1016/j.biortech.2013.01.038

40. Pérez-Maqueda J, Arenas-Ligioiz I, López Ó, Fernández-Bolaños JG (2014) Eco-friendly preparation of 5-hydroxymethylfurfural from sucrose using ion-exchange resins. Chem Eng Sci 109:244–250. https://doi.org/10.1016/j.ces.2014.01.037

41. Ravasco JMJM, Coelho JAS, Simeonov SP, Afonso CAM (2017) Bifunctional Cr3 + modified ion exchange resins as efficient reusable catalysts for the production and isolation of 5- hydroxymethylfurfural from glucose. RSC Adv 7:7555–7559. https://doi.org/10.1039/C6RA22539J

42. Liu H, Wang H, Li Y, Yang W, Song C, Li H, Zhu W, Jiang W (2015) Glucose dehydration to 5-hydroxymethylfurfural in ionic liquid over Cr3 + -modified ion exchange resin. RSC Adv 5:9290–9297. https://doi.org/10.1039/C4RA09131K

43. Wang P, Ren L, Lu Q, Huang Y (2016) Dehydration of glucose to 5- hydroxymethylfurfural using combined catalysts in ionic liquid by microwave heating. Chem Eng J 203:1507–1514. https://doi.org/10.1080/00986445.2016.1213724

44. Werpy T, Petersen G (2004) Top value added chemicals from biomass. U.S. Dep. Energy. 1:76. https://doi.org/10.2172/926125

45. Vilcocq L, Cabiac A, Especel C, Guillon E, Duprez D (2013) Transformation of sorbitol to biofuels by heterogeneous catalysis: chemical and industrial considerations. Oil Gas Sci Technol Rev d'IFP Energies Nouv. 68: 841–860. https://doi.org/10.2516/ogst/2012073

46. Rose M, Palkovits R (2012) Isosorbide as a renewable platform chemical for versatile applications-quo vadis? Chem Sus Chem 5:167–176. https://doi.org/10.1002/cssc.201100580

47. Dussenne C, Delaunay T, Wiatz V, Wyart H, Suisse I, Sauthier M (2017) Synthesis of isosorbide: overview of challenging reactions. Green Chem 19:5332–5344. https://doi.org/10.1039/C7GC01912B

48. Morita Y, Furusato S, Takagaki A, Hayashi S, Kikuchi R (2014) Intercalation-controlled cyclodehydration of sorbitol in water over layered-niobium-molybdate solid acid. Chem Sus Chem 8565:748–752. https://doi.org/10.1002/cssc.201300946

49. Dabbawala AA, Mishra DK, Huber GW, Hwang JS (2015) Role of acid sites and selectivity correlation in solvent free liquid phase dehydration of sorbitol to isosorbide. Appl Catal A Gen 492:252–261. https://doi.org/10.1016/j.apcata.2014.12.014

50. Goodwin JC, Hodge JE, Weisleder D (1980) Preparation of bicyclic hexitol anhydrides by using acidic cation-exchange resin in a binary solvent. p 13C-N.m.r. spectroscopy confirms configurational inversion in chloride displacement of methanesulfonate in isomannide and isosorbide derivatives. Carbohydr Res. 79: 133–141. https://doi.org/10.1016/s0008-6215(00)85138-1

51. Moore KV, Sanborn AJ (2005) Process for the production of anhydrosugar alcohols. US 6,849,748 B2.

52. Khan NA, Mishra DK, Hwang JS, Kwak YW, Jhung SH (2011) Liquid-phase dehydration of sorbitol under microwave irradiation in the presence of acidic resin catalysts. Res Chem Intermed 37:1231–1238. https://doi.org/10.1007/s11164-011-0389-5

53. Polaert I, Felix MC, Fornasero M, Marcotte S, Buvat JC, Estel L (2013) A greener process for isosorbide production: Kinetic study of the catalytic dehydration of pure sorbitol under microwave. Chem Eng J 222:228–239. https://doi.org/10.1016/j.cej.2013.02.043

54. Ginés-Molina MJ, Moreno-Tost R, Santamaría-González J, Maireles-Torres P (2017) Dehydration of sorbitol to isosorbide over sulfonic acid resins under solvent-free conditions, Appl. Catal. A Gen. 537: 66–73. https://doi.org/10.1016/j.apcata.2017.03.006

Chapter 2
The Application of Ion-Exchange Resins in Hydrogenation Reactions

Osarieme Uyi Osazuwa and Sumaiya Zainal Abidin

Abstract Reaction processes with minimal energy consumption and potentials to generate renewable energy, alongside dynamism in catalyst functionality, are the driving force behind the use of ion-exchange resins and more specifically, heterogeneous ion-exchange resins over homogeneous catalysts. For hydrogenation reactions, ion-exchange resins have mainly been employed as a catalyst support. The synthesis entails implanting/impregnating metallic ions into the ion-exchange resin matrix. The major disadvantage of the ion-exchange resin is its low thermal stability which makes the resin disadvantageous for some specific types of reactions. Research is still ongoing toward obtaining resins able to withstand extreme temperature (above 200 °C). This chapter summarizes some selected applications of hydrogenation reactions using ion-exchange resins as catalyst support material. Some of its applications include hydrodesulphurization, hydrodenitrification, and hydrodechlorination which have been reviewed in this chapter.

2.1 Introduction

Ion exchange can be defined as a process where mobilized ions obtained from a liquid phase are replaced with ions bound to a functional ion present in a solid. Ion-exchange resin entails the existence of covalent and non-covalent bonds in relation to interactions as a result of ionic and electrostatic relationships between the chemicals [1]. Generally, ion-exchange resins can readily be applied as catalyst sup-

S. Z. Abidin (✉)
Faculty of Chemical and Natural Resources Engineering, Universiti Malaysia Pahang, Lebuhraya Tun Razak, 26300 Gambang, Pahang, Malaysia
e-mail: sumaiya@ump.edu.my

O. U. Osazuwa
Department of Chemical Engineering, University of Benin, PMB 1154, Benin City, Edo State, Nigeria

S. Z. Abidin
Centre of Excellence for Advanced Research in Fluid Flow (CARIFF), Universiti Malaysia Pahang, Lebuhraya Tun Razak, 26300 Gambang, Pahang, Malaysia

port in catalysis studies and commercially for industrial use. The chemical buildup of conventional ion-exchange resin generally consists of styrene–divinylbenzene cross-linked copolymer with a charged ion exchanging group which could either be a strong or weak cationic group (sulfonate or carboxylate groups) or a strong or weak anionic group in nature (ammonium groups) [2].

Ion-exchange resins (IER) possess evenly dispersed functional groups and undergo post-adsorption which causes a reduction in the metallic ion species, thereby resulting in a uniform dispersion of the nanoparticles. The flexibility of the IER ionic structure allows for the modification of the resins sites, and hence, creates the possibility of exchanging other ions with metallic ions or other ionic species to enhance its activity. Ion-exchange resin selectivity is affected by pore size and particle distribution due to the degree of ionic sites accessibility. Important resin factors that must be duly considered include the resin type, porosity/polymeric framework of the resin, suitability of the reaction, regeneration/recyclability, economic/commercial effects of employing resins, type of reactor, and reaction operating conditions.

2.2 Ion-exchange resin as a catalyst and support in reaction processes

The acidity and basicity of ion-exchange resins which refer to their functionality are responsible for their ability to be successfully applied as catalysts for several chemical reactions. Acidic cation resins have been applied in reactions such as amidation, carbonylation, condensation, cyclization, dehydration, esterification, hydrogenation, and hydrolysis reactions. On the other hand, basic resins have been applied to acylation, condensation, cyclization, dehalogenation, esterification, hydration, and hydrolysis reactions. For acidic cationic resins, the main functional groups are sulphonic and carboxylic acid groups which are the active sites for strong and weak acid resins, respectively. These functional groups operate on the basis of dissociation of the acid; H^+ species have been employed in catalytic esterification and alkylation reactions. The functional thermal stability of the commercial acid cation-exchange resins is about 120 °C [1]. The degradation of the cation-exchange resins is in the form of desulphonation and continual exposure to an extreme temperature which leads to catalytic loss of activity. For the strong basic resins, the active functional groups are the hydroxyl groups, while the amine groups and N_2 form the weak base resins. The functionality of N_2 is such that the lone pair electron acts as a free base group.

Basic resins have been used for condensation and ester hydrolysis reactions. Bhandari et al. [1] reported the commercial use of ion-exchange resins as a catalyst in the production of alcohols, esters, ketones, and solvents such as methyl tert-butyl ether. The functional thermal stability of the basic anion-exchange resins is about 60 °C [1]. For catalytic reactions, acidic and basic resins have been applied in separation and purification processes. Functionalized resins as support materials doped with active

metallic particles for catalytically driven reactions have been studied by Corain et al. [3]. The study analyzed the prospect of applying functionalized resins as support materials to the metal catalyst and as complementary supports to the conventional catalyst.

2.2.1 Hydrogenation reactions and catalysis

Hydrogenation is the process where atoms of hydrogen are moved to unsaturated compounds from other hydrogen sources or gaseous hydrogen [4]. Other researchers have defined hydrogenation reaction as the addition of H_2 to C=C or C=O bond. In order to obtain the best outcomes, hydrogenation reactions are often catalyzed with either homogeneous or heterogeneous catalyst. For homogeneous catalyst, they exist in the same physical phase as the reactants to be used in the reaction, while heterogeneous catalysts exist in different physical phases from the reactants. Homogeneous catalysts often proceed with very good catalytic activity due to the ease of the reactants to access their active sites. However, a major drawback is the difficulty in separating the catalyst from the reactants or products stream [4].

In comparison with a homogeneous catalyst, heterogeneous catalysts have shown greater efficiency for hydrogenation reactions. This is as a result of their active sites and large surface area. However, their inability to obtain a stable state due to undesired particle growth and particles agglomeration are the major drawbacks [5]. Researchers have tried to minimize these disadvantages by developing a well-structured catalyst/catalyst support known as the ion-exchange resin. Ion-exchange resins possess acidic or basic polymeric structure which can be used to catalyze reactions by providing acidic or basic sites in a heterogeneous environment, hence, resulting in catalyst recovery.

The heterogeneous or homogeneous catalyst must fulfill certain requirements which include availability in varieties, low cost, reduced treatment before use, compatibility with a solvent to be used, thermal and mechanical stabilities, resistant to chemical attack, high quality, easy to decant or filter, and a defined number of the single active site [2]. Wang et al. [6] analyzed homogeneous and heterogeneous catalysts such as sulphuric acid, p-toluenesulfonic acid, Y-zeolite, ZSM-5, and polyoxymethylene dimethyl ethers. It was found that the ion-exchange resins were better in terms of activity and selectivity. Sharma [7] carried out the industrial applications of resin catalysts and homogeneous catalysts for the etherification of phenols/naphthols with isobutylene/isoamylene. It was observed that the resin catalyst was more favorable when compared with the homogeneous catalyst. In a study conducted by Barbaro [2], heterogenized catalysts for hydrogenation reactions have to possess certain qualities comparable to original homogeneous catalyst such as ability to undergo synthetic modifications prior to embedding in the support, ease of material synthesis, and good turnover frequencies (TOF) which can be compared to the original homogeneous catalyst. Barbaro [2] further stated that the number of cross-linking agent ranged 2–16% controls the porosity (gel, microporous, or macroporous resins) of the resin parti-

cles, thereby affecting the resin bulk properties (capacity, equilibrium rate, swelling, physical stability selectivity, etc.).

Hydrogenation reactions are favorable with the use of a catalyst which may be homogeneous or heterogeneous in terms of catalytic buildup. Catalysts that exist in the same physical phase with the reactants are called homogeneous catalyst, while heterogeneous catalysts exist in different phases with the reactants. Su and Chen [4] explained that even though homogeneous catalyst shows high activity due to the availability of the excess active site, the difficulty in separating reactants from catalyst remains a major drawback when applying this kind of catalyst for reaction systems. Large surface area and highly active channels are responsible for the application of hydrogenation industrially. Nevertheless, its main limitation is the unstable nature of the catalyst due to undesired particle growth and agglomeration of particles resulting from high surface energy [5].

Researchers have attempted to minimize this drawback by introducing a specific type catalyst: ion-exchange resin. Ion-exchange resins employed as support materials in catalytic hydrogenation reactions are strong sulfonated cation-exchange resins such as Nafion NR-50 polymer. Very recently, the use of ion-exchange resin as catalyst support with a functional metallic catalyst for hydrogenation reactions has gained a lot of interest. After reduction of the catalyst, the metal migrates from the polymer surface to the pores. However, this is dependent on the pre-surface area and the bulk structure of the ion-exchange resin. In liquid-phase hydrogenation reactions, the supply of H_2 in the liquid phase has over time being a major challenge. Alemán-Vázquez et al. [8] suggested that this setback could be limited industrially using H_2 with high partial pressures which comes at a high cost. Generally, substrates containing C=C bonds are hydrogenated with Rh- or Ru-based organometallic complexes as homogeneous catalysts. Researchers have focused attention on the immobilization of these complexes. For example, the immobilization of metals on polystyrene support structures has numerous advantages. Although often referred to as being electronegative, H_2 can be used as a proton, an atom, or a hybrid depending on the reactants and the reaction conditions. Cobzaru and Inglezakis [9] suggested that negative functional ions attract cations, while positive charged functional ion attracts anions. Hydrogenation spreads into various industrial applications such as fine chemicals, agrochemicals, and pharmaceuticals. As a result of vast applications, various types of hydrogenation processes exist which include hydrodechlorination, hydrogenation of cyclohexane, nitrates reduction, and hydrodesuphurization.

In recent times, ion-exchange resins have been employed as catalyst supports for hydrogenation reactions. This is carried out by embedding a metal catalyst in the structure of the resin. In situ reaction, during reduction of the catalyst in a swelling medium, there is a provision for movement of the metal from the bulk of resin to the outer pores. The pore surface area and resin structure are responsible for the ease of migration of reactants through the metal surface and pores. Inglezakis and Poulopoulos [10] reported that ion exchange is the repositioning of ions present in two phases making use of diffusional methods with less chemical influence. Nevertheless, they reported that neutralization reaction is one of few exceptions existing where ion exchange takes place with a chemical reaction. Post [11] suggested four

aspects centered on ion exchange and its applications which include ion-exchange equilibrium, kinetics of ion exchange, ion-exchange capacity, and selectivity of ion-exchange ions for certain anions/cations as the case may be. Ion-exchange reaction is shown as in equation

$$Z_A B^{z_B^+} + Z_B A_{(s)}^{z_A^+} \rightarrow Z_A B_{(s)}^{z_B^+} + Z_B A_{(Z)}^{z_A^+} \tag{2.1}$$
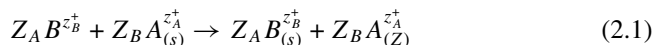
where Z_A^+ and Z_B^+ are the charges of the cations to be exchanged, A and B, respectively, (Z) is the ion-exchange material, and (S) is the ion-exchange solution. Another important function of the ion-exchange resin is its ability to release cationic hydrogen into a solution and removing another ion in the process. This ion-exchange reaction can be described in equation

$$A - H + B^+ \leftrightarrow A - B + H^+ \tag{2.2}$$
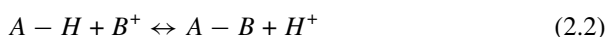
where A is the insoluble structure of the ion-exchange resin and B is the solution ion. Various applications of this functionality have been reviewed in this chapter. The effectiveness of the ion-exchange resin is dependent on the number of exchange sites per unit weight of the dry resin (mmol g^{-1}). Various chemical reactions such as alkylation, condensation, esterification, etherification, hydration, and hydrogenation reactions involve the use of commercial resins such as Amberlyst, Nafion, and indion ion-exchange resins. Chemical processes such as wastewater treatment, separation processes, chemical synthesis, medical research, food processing, mining, agriculture, etc., utilize the ion-exchange resins.

2.3   Ion-Exchange Resins as Catalyst and Support for Hydrogenation Reactions

Commercially, ion-exchange resins have been employed industrially in esterification and hydrogenation reactions. The different types of hydrogen reactions include hydrodesulphurization, hydrodechlorination, reduction of nitrates, hydrogenation of cyclohexene, etc. Hydrodesulphurization is a catalytic chemical reaction which is often employed for the removal of sulfur from organic compounds. Hydrodechlorination is the catalytic removal of chlorine from chlorinated compounds. Nitrate reduction entails the partial reduction of nitrates to nitrites, reduction of nitrites to ammonia, and finally to nitrogen. Hydrogenation of cyclohexene is the addition of H$_2$ to cyclohexene (unsaturated hydrocarbon) to yield cyclohexane which is saturated. In this chapter, several applications of hydrogenation reactions using ion-exchange resins already established have been reviewed.

2.3.1 Hydrogenation of Unsaturated Hydrocarbon Compounds Using Ion-Exchange Resins

The catalytic hydrogenation of cyclohexene using polymers as H_2 donors over Pt/Al$_2$O$_3$ catalyst has been studied by Alemán-Vázquez et al. [8]. The effects of catalytically adding H_2 donor to cyclohexene in the form of organic polymer or polymer supported on an inorganic structure have been explained. It was found that there was a 10% rise in the zero-order kinetic coefficients when the solid H_2 donor was used, whereas a 40% rise was observed when using the unsupported polymer. For the liquid-phase hydrogenation of cyclohexene when using Pt/Al$_2$O$_3$ catalyst supported on a polymer, 83% conversion was observed in the zero-order reaction, while when the reaction was first order, the conversion was above 83%. Goszewska et al. [12] investigated a novel nanopalladium catalyst for a continuous-flow chemo-selective hydrogenation reaction. They immobilized palladium nanoparticles on polymeric resin and tested it for the hydrogenation of 2-heptene and 6-methyl-5-heptene-2-one. It was found that the catalyst exhibited high activity and 100% selectivity toward hydrogenation of C=C double bond. Chemo-selective continuous-flow hydrogenation of aldehydes catalyzed by platinum nanoparticles immobilized on an amphiphilic resin has been investigated by Osako et al. [13]. Aromatic and aliphatic aldehydes with various functional groups such as keto, ester, or amide groups were able to undergo hydrogenation in aqueous solutions in a continuous-flow system containing an amphiphilic polymer to produce primary benzylic or aliphatic alcohols yield of about 99% and very good selectivity. It was found that the hydrogenation of benzaldehyde for 8 days was achieved with total turnover catalyst number of 997.

A chelate resin-supported palladium catalyst for chemo-selective hydrogenation has been reported by Monguchi [14]. Dual species of palladium catalysts supported on a chelate resin-bearing diiminoacetate or polyamine moieties on the polystyrene divinylbenzene polymer were synthesized by the adsorption of Pd (II) ions on the resins and subsequent reduction to metallic Pd with hydrazine monohydrate. It was found that both catalysts were similar in terms of activity for hydrogenation. The author(s) stated that apart from benzylic alcohol, alkyl benzyl ether, and epoxide, all other variety of reducible functionalities could be reduced under the hydrogenation conditions using any of the synthesized catalysts. Amine-functionalized nanoporous polymer supported (AFPS) Ru nanoparticles based catalysts were used in the selective hydrogenation of D-glucose to produce D-sorbitol by Dabbawala [15]. The catalyst was synthesized using impregnation–chemical reduction method to impregnate Ru nanoparticle on amine-functionalized nanoporous polymer. It was found that there was a direct relationship between the composition of Ru in Ru/AFPS catalyst and the product formation. Specifically, 5Ru/AFPS catalyst (5 wt% of Ru) had a better conversion rate and 98% selectivity toward the product (D-sorbitol). A comparison was made with the 5Ru/AFPS and the non-functionalized polymer supported Ru catalyst (5Ru/PS). It was found that the 5Ru/AFPS exhibited higher catalytic performance with up to 2.5 times turnover frequency (TOF) of 5Ru/PS. The better performance

was attributed to the catalyst high specific surface area, larger pores, and availability of functional groups on the catalyst surface.

The Pd nanoparticles supported on hyper-cross-linked polystyrene have been used to catalyze the selective hydrogenation of 2-methyl-3-butyn-2-ol (MBY) to 2-methyl-3-butene-2-ol (MBE) and the effects of the solvent were studied by Nikoshvili et al. [16]. The authors determined the effects of polar and nonpolar solvents on the selective hydrogenation of 2-methyl-3-butyn-2-ol. From their study, it was found that, although solvent polarity was inadequate to analyze the performance and selectivity, the solvent properties such as dipole moment and dielectric constant remained significant. Enantioselective hydrogenation of olefins in water using chiral Rh phosphine–phosphite catalysts immobilized on ionic resins was reported by Kleman et al. [17]. In MeOH, increased enantioselectivities were observed in the hydrogenation of methyl α-N-acetamido acrylate (4a), while a decrease was observed for less reactive methyl α-N-acetamido cinnamate (4b). The high modular structure of P-OP ligands led to catalyst optimization for the hydrogenation of 4a and 4b in water with enantioselectivities over 95% ee and S/C values up to 2300 and 500, respectively. In order to assess the potential of the catalyst, the hydrogenation of a set of β-aryl α-dehydro amino acids (4c–4j) in water has been investigated with good activity and high enantioselectivity (87–97% ee) obtained. Continuous-flow synthesis of Rh and Pd nanoparticles onto ion-exchange borate monoliths with the application of selective catalytic hydrogenation of unsaturated carbonyl compounds has been investigated by Liguori and Barbaro [18]. It was found that borate monolith is an effective support material for Rh and PdNP catalysts under ambient conditions. In comparison to other systems, superior performance was observed by the synthesized catalyst in the continuous-flow selective hydrogenation reactions of unsaturated carbonyl compounds in terms of durability, energy saving, and the selectivity at total conversion.

Facile heterogeneous catalytic hydrogenations of C=N and C=O bonds in neat water using water-soluble metal complexes onto ion-exchange resins have been reported by Barbaro et al. [19]. The authors synthesized a novel Ir (I) complex incorporated with water-soluble monodentate cage phosphine PTA (PTA = 1,3,5-triaza-7-phosphaadamantane) immobilized on commercial ion-exchange resin by a heterogenization method. The catalyst which showed good activity and selectivity was used to hydrogenate cyclic imines and α-keto esters employing water as the green reaction solvent, thereby eradicating the use of toxic solvents. The catalytic activity decreased in the following order: alcohols > cyclohexane > water/ethanol mixture > octane ≥ hexane ≥ xylene > toluene > heptane. A process for the production of γ-valerolactone (GVL) by hydrogenation of biomass-derived levulinic acid (LA) has been investigated by Maria et al. [20]. In their study, GVL was obtained by the hydrogenation of an aqueous solution of levulinic acid over commercial ruthenium supported on ion-exchange resins such as Amberlyst A70 or A15, niobium phosphate or oxide. The operating conditions of the process were at 50–70 °C and 0.5–3.0 MPa. It was found that the most efficient support was Amberlyst A70, with a yield of GVL of 99 mol% and an activity of 558 h^{-1} after 3 h at 0.5 MPa and 70 °C. The physicochemical and catalytic properties of Pd catalyst supported on amine groups functionalized gel-type resin tested in the hydrogenation of alkynes

(2-butyne-1,4-diol and phenylacetylene) have been investigated by Drelinkiewicz et al. [21]. In their study, the synthesis procedure followed two routes: the first was the immobilization of Pd precursor in the pre-swollen resin from THF solution of Pd(OAc)$_2$, and the second was chemical reduction of the Pd centers. The second route was the deposition of Pd species on dry resin beads by employing an aqueous solution of PdCl$_2$. It was found that using catalysts prepared by both routes showed over 90% selectivity toward alkenes. However, the catalyst prepared via the first route showed better activity and selectivity than the second.

Hydrogenation and isomerization of diisobutylenes over Pd-doped ion-exchange resin catalyst have been investigated by Talwalkar et al. [22]. The authors evaluated the possibility of applying a bifunctional ion-exchange resin catalyst (Amberlyst CH28) for the hydrogenation of 2,4, 4 trimethylpent-1-ene and 2, 4, 4-trimethylpent-2-ene (diisobutylene). It was found that the catalyst showed good performance, by increasing the reaction rates in terms of hydrogenation and isomerization of the reactants. Furthermore, the author(s) evaluated various parameters in order to predict the kinetic model to explain the enhanced reaction rates. The effects of the polymer properties on the hydrogenation of C=C bond of maleic, fumaric acids, and isomers of dicarboxylic acids have been studied over a functional gel-type palladium catalyst by Drelinkiewicz et al. [23]. The gel resin which was used as support for the palladium catalysts comprised of two hydroxyethyl methacrylate (HEMA, 20 mol%), styrene (60–77 mol%), and diethylene glycol dimethacrylate with DEGDMA, and 3–20 mol% used as the cross-linking reagent. The effects of polymer mass expansion on the activity of Pd/OFP catalyst in the hydrogenation of cis- and trans-isomers of unsaturated dicarboxylic acids, maleic (MA), and fumaric (FA) were examined. During the hydrogenation test, operating conditions such as Pd loading, catalysts concentration, cross-linking degree of polymer, and the size of catalyst grains were varied. The test showed that swelling of polymer mass during hydrogenation was the major factor for the activity of Pd/OFP catalyst. Differences were observed only when the catalysts were in the swollen state. Higher reaction rates were observed for MA (*cis*-isomer) than FA (trans-isomer). This was as a result of the ease of penetration of *cis*-isomer (MA) in the bulk of the polymer mass, leading to more efficient consumption of the substrate. The effects of the substrate were connected to the link between the functional groups in the reduced catalysts and the hydrogenated reagents, maleic or fumaric acids.

Hydrogenolysis of glycerol to 1, 2-propanediol over a heat-resistant ion-exchange resin combined with Ru/C was studied by Miyazawa et al. [24]. In their study, Ru/C, combined with Amberlyst ion-exchange resins, was effective in the hydrogenolysis of glycerol to 1, 2 propanediol. It was found that increase in temperature increased the difference in performance between Amberlyst 15 and 70. This was a result of the poisoning of Ru/C with sulfur compounds obtained from the thermal decomposition of the resins. Doping of heat-resistant Amberlyst 70 in Ru/C at 453 K resulted in a higher conversion, better selectivity to the product, and stability at optimum temperature (463 K). Synthesis and characterization of spherical nickel-doped carbonized resin as a catalyst for hydrogenation have been reported by Li [25]. The resins were decomposed thermally followed by doping with the metal catalyst of different nickel

loadings. In order to obtain a proper understanding of the pyrolysis mechanism, characterization of Ni-Ca/D152, GC, DTA, TGA, XRD, and elemental analysis was employed to analyze the carbonization process and Ni–Ca/C properties. It was found that nickel and calcium in D152 enhanced the carbonization process and the steam activating process of the carbonized resin. The thermal decomposition temperature was in the range 380–520 °C.

The reaction mechanism and the conversion of glycerol in an aqueous solution under H_2 over Ru/C, Rh/C, Pt/C, and Pd/C supported on an ion-exchange resin; Amberlyst, H_2SO_4 (aq) and HCl (aq) have been studied by Miyazawa et al. [26]. In their study, Ru/C with Amberlyst was seen to be an effective catalyst in the dehydration and hydrogenation of glycerol under reaction operating conditions: 393 K, 8.0 MPa. Acid catalysts were used to dehydrate glycerol to acetol before hydrogenation of acetol on the metallic catalysts yielded 1, 2 -propanediol. With reference to the acid catalysts, H_2SO_4 (aq) was inferior in terms of glycerol dehydration activity than Amberlyst. Also, HCL (aq) showed decreased activity of acetol hydrogenation on Ru/C. The reports also showed that the OH group on Ru/C increases the dehydration of glycerol to 3-hydroxypropionaldehyde which in turn gives 1, 3-propanediol through hydrogenation and degradation. Ru/C was combined with Amberlyst for the dehydration and hydrogenation of glycerol under controlled reaction by Miyazawa et al. [26]. They dehydrated glycerol using an acid catalyst to obtain acetol before the acetol was transformed to 1, 2-propanediol over the metallic catalyst. The activities of other catalysts, such as H_2SO_4 (aq) and HCl (aq), were also tested in the reaction process. It was observed that the acid catalyst H_2SO_4 (aq) showed lower glycerol dehydration activity than the Amberlyst. The HCL (aq) showed decreased activity for the acetol hydrogenation on Ru/C. In situ generation of Pd nanoparticles supported on resin under mild catalytic conditions via a green route to highly efficient, reusable hydrogenation catalyst has been investigated by Marrodan and Berti [27]. In their study, a single-pot strategy for the preparation of solid-supported Pd nanoparticles based on ion-exchange resins, palladium nitrate, and in situ formed metal particles under mild conditions were investigated. In comparison to the conventional methods for synthesizing supported metal nanoparticles, the process employed in their study was more convenient, had better activity and was more eco-friendly.

2.3.2 Reduction, Removal, and Hydrogenation of Nitrates Using Ion-Exchange Resin

The reduction of nitrate in water applying bimetallic Pd–Cu catalyst supported on ion-exchange resin has been used as a new process by Mendow et al. [28]. It was found that increasing the flow rate of H_2 had no significant effect on the removal of nitrate, while the selectivity of N_2 decreased. Also, nitrate removal reduced as a result of ion competition between sulfate bicarbonate and chloride. In other to regenerate the catalyst, H_2 was bubbled through the catalyst bed to eliminate the

nitrate present in the resin. An alternative process where the ion exchange of nitrate was carried out simultaneously with the regeneration of the catalyst gave 36.7% removal of nitrate from the resin. A process for removing nitrites contaminants from water using ion-exchange and catalytic reduction has been reported by Mendow et al. [29]. In another report, P-nitrophenol flow hydrogenation with nano-Cu_2O grafted on polymeric resin was carried out by Paun et al. [30]. In their study, the novel continuous-flow hydrogenation of P-nitrophenol to P-aminophenol with molecular hydrogen and heterogeneous nano-Cu_2O employed as reducing agent and catalyst, respectively, was reported. The catalyst was synthesized by the one-pot synthesis methodology and the reaction involved the conversion of a pollutant into a high-value product with water as solvent and by-product. It was found that the catalyst reactivity was related to the differences in density-of-states between the bulk sites and the surface sites, and the size of the active catalyst. Abdullaev and Gebekova [31] investigated the hydrogenation of aromatic nitro compounds on palladium-containing anion-exchange resins under mild reaction conditions. Observations from their study showed that stericity has a major effect on the performance of the hydrogenation reaction. The palladium-containing anion-exchange resins were very effective for hydrogenation of aromatic nitro compounds. Halonitrobenzenes were dehalogenated to obtain a low yield of amine.

Kim et al. [32] used an integrated batch process comprising of catalytic reduction and ion exchange of nitrates. In their study, an anionic resin containing 1% Pd and 1% Cu was used for adsorption of nitrates. Furthermore, nitrates were reduced in the presence of CO_2/H_2 at 1:1 ratio. Their results showed 100% conversion to N_2 without the formation of toxic NH_4^+. The removal of nitrate from water using bimetallic catalysts supported on cation-exchange resins has been investigated by Barbosa et al. [33]. Impregnation and catalytic reduction were employed to synthesize the palladium–tin and palladium–indium catalysts from sulfonated polystyrene divinylbenzene (sty-DVB). Findings from their study showed that the selectivity toward N_2 was increased by the acidity of the support as compared to the alumina-supported catalyst. Indium-based catalysts showed better activity for nitrate reduction and reduced selectivity toward N_2 when compared to tin-based catalysts. Their results showed that with respect to performance, the best catalyst was 5% Pd 2.6% Sn/Sty-DVB. The performance of the support was attributed to its buffering properties which decreased the resulting pH.

Bimetallic Pd–Cu catalyst supported on anionic and cationic ion-exchange resins was employed for nitrate reduction by Gašparovičová et al. [34]. It was found that the activity of anionic resins was fourfold better than cationic resins. In comparison to Pd–Cu supported on Al_2O_3, the activity was reduced with an increased selectivity toward N_2. Imchuen et al. [35] used cation-exchange resin (Purolite C160H) for ammonium removal as part of the sequential process for nitrate reduction by nanoiron (nZVI). Prior to their study, the pH (4–10) was optimized for the nitrate removal by nZVI (0.25 g L^{-1}). The optimized conditions resulted in 77% nitrate removal at pH 4. Also, the maximum NH_4^+–N formation of 60% occurred at pH 4. The pseudo-second-order reaction was applied for the various nitrate concentrations (50–250 mg L^{-1}) and initial pHs (4–10) with the rate constants (0.058–2.1) $\times$ 10^{-3} M^{-1} min^{-1} and

$(0.24–0.56) \times 10^{-3}$ M^{-1} min^{-1}, respectively. For the ammonium in the nZVI during the initial study, dual successive runs were carried out to ascertain the effects of competitive ions (Fe^{2+}/Fe^{3+}, NO_2^-/NO_3^-) and initial pH on the removal process. It was found that the equilibrium time required for the removal of ammonium was 10 min for an initial pH of 4, 7, and 9. The ammonium removal efficiency was reduced by about 40% by Fe^{2+} and Fe^{3+}, while NO_3^- and NO_2^- have no effect on the removal.

Hydrogenation in aqueous media via asymmetric transfer and catalyzed by a resin-supported peptide having a polyleucine tether has been investigated by Akagawa et al. [36]. The catalyst was a resin-supported N-terminal prolyl peptide having a β-turn motif and a polyleucine tether that was developed for the organocatalytic asymmetric transfer hydrogenation in an aqueous medium. It was found that polyleucine increased the rate of reaction by allowing a hydrophobic microenvironment around the prolyl residue. Catalyst characterization showed that the L-form of polyleucine is required for the enantioselectivity and efficiency of the reaction process. A resin-supported peptide comprising a polyleucine tether has been applied for organocatalytic asymmetric transfer hydrogenation in aqueous media by Akagawa et al. [37]. In their study, a resin-supported N-terminal prolyl peptide with a β-turn motif and hydrophobic polyleucine chain was used as a catalyst for the asymmetric transfer hydrogenation in an aqueous medium. It was seen that the polyleucine tether generated a hydrophobic hole in the aqueous solution which was responsible to increase the rate of reaction. Interestingly, they observed that the polyleucine chain turned out to be a key factor for high enantioselectivity.

Hydroamination of vinylpyrindines with aliphatic/aromatic amines over cation-exchange resins has been reported by Bhanushali et al. [38]. The authors developed an effective process for the hydroamination of vinylpyridines catalyzed by a recyclable and heterogeneous catalyst employing mild reaction conditions. Several gel-type cation-exchange resins were tested, and Amberlyst-15/Nafion NR-50 gave a yield of about 90%. The process was also applied for pyridylethylation of various aryl/alkyl amines with varying steric and electronic properties. Supported Pd/Cu catalyst was employed for denitrification of water by Palomares et al. [39]. In their study, the influence of support on the liquid-phase catalytic hydrogenation of nitrates was investigated. In addition, hydrotalcite and Pd/Cu supported on alumina catalysts were used as a means of comparison to test the activities and selectivities of the catalysts. Better activity and lesser ammonium production were observed for metals supported on hydrotalcite as compared to metals supported on alumina.

2.3.3 Hydrodechlorination Reaction Using Ion-Exchange Resin

Pd and Pt catalysts supported on cationic resins have been applied for the hydrogenation of chloronitrobenzenes by Králik et al. [40]. In their study, chloronitrobenzene

isomers (κ-CNB, κ = 2, 3, 4) were hydrogenated to chloroanilines (κ = CAN) over palladium and platinum catalysts supported on trimethylammonium functionalized poly(styrene-co-divinylbenzene) (Dowex-D). It was found that the selectivities to κ = CAN over Pd/D-Cl and Pd/D-OH catalysts were 72 and 42%, respectively, at 80% conversion of κ-CNB. Average selectivities of 81 and 84% were obtained using Pt/D-Cl and Pt/D-OH, respectively, at a 90% conversion of κ-CNB. Palladium (Pd) catalyst has shown very good activity in hydrodechlorination reactions under ambient conditions. Chen et al. [41] suggested that the presence of Pd was responsible for the formation and cleavage of reactive atomic hydrogen and C–Cl bond. Bacik et al. [42] reported that in order to improve the Pd catalyst, support materials can be utilized.

A new palladium catalyst supported on anion-exchange resin has been used for the hydrodechlorination of triclosan in water by Han et al. [43]. Two anion-exchange resins (IRA-900 and IRA-958) with polystyrene and polyacrylic structures were employed as a support for catalyst synthesized using the uptake of PDCL42 followed by subsequent reduction of Pd (II). Employing a pseudo-first-order rate equation with 2.0 wt% loading, the rate constants were 1.25 ± 0.06 and 1.6 ± 0.1 L g^{-1} min^{-1} for Pd@IRA-900 and Pd@IRA-958, respectively. The catalysts were compared with other supported Pd catalysts and results showed that resin-supported catalyst was resistant to CL$^-$ contamination and fouling. The addition of 10 mM NaCl dropped the kobs' value by 31 and 23% for Pd@IRA-900 and Pd@IRA-958, respectively. In addition, the presence of humic acid at 30 mg L^{-1} reduced the rates by 28 and 27%, respectively. Pd@IRA-958 gave better results which were attributed to the Pd particle size and polymeric properties of the catalyst.

In an attempt to convert halogenated compounds to less toxic compounds, palladium–resin composites for the catalytic hydrogenation of 4-chlorophenol have been studied by Jadbabaei et al. [44]. MN200, MN100, XAD4 (neutral resins), IRA910, and IRA96 (anion-exchange resins) were used as supports for palladium catalyst for the hydrogenation of 4-chlorophenol. The process was to test the catalyst activity in the reaction and to remove the halogen compounds. Consequently, a Langmuir–Hinshelwood kinetic model was employed to obtain the rate-determining step. It was found that there was an improved effect of adsorption on the catalytic reactivity. When the adsorption was fixed and the pH varied, the reactivity of the catalysts increased because the increase in pH reduced the impact of the products containing halogens on the catalytic reaction. Furthermore, after eight reaction cycles, when constantly charging feed (4-CP) to the reactor system, there was activity loss of the resin, which was subsequently regenerated.

2.4 Conclusions

Studies have shown that ion-exchange resins have often been applied as metallic catalyst support for hydrogenation reactions. This chapter discusses the application of functionalized ion-exchange resins as catalyst support for hydrogenation

reactions. Several applications on hydrogenation reactions have been reviewed with cases where production has been enhanced and outlined in this chapter. In reaction processes, specifically for hydrogenation reactions, ion-exchange resins have several advantages when applied as a catalyst support. Moreover, the resin structure can be modified to a bifunctional catalytic system which can be used for multiple-step reaction. Furthermore, the chapter has discussed ion-exchange resins as support materials for various applications of hydrogenation reactions such as hydrogenation of unsaturated hydrocarbons, hydrogenation of nitrates, and hydrodechlorination.

References

1. Bhandari VM, Sorokhaibam LG, Ranade VV (2016) Ion exchange resin catalyzed reactions—an overview. Elsevier Inc. https://doi.org/10.1016/b978-0-12-801457-8.00009-4
2. Barbaro P. Recycling asymmetric hydrogenation catalysts by their immobilization onto ion-exchange resins 2006:5666–5675. https://doi.org/10.1002/chem.200501133
3. Corain B, Centomo P, Lora S, Kralik M (2003) Functional resins as innovative supports for catalytically active metal nanoclusters. J Mol Catal A Chem 204–205:755–762. https://doi.org/10.1016/S1381-1169(03)00361-3
4. Su J, Chen JS (2017) Synthetic porous materials applied in hydrogenation reactions. Microporous Mesoporous Mater 237:246–259. https://doi.org/10.1016/j.micromeso.2016.09.039
5. White RJ, Luque R, Budarin VL, Clark JH, Macquarrie DJ (2009) Supported metal nanoparticles on porous materials. Methods and applications. Chem Soc Rev 38:481–494. https://doi.org/10.1039/B802654H
6. Wang L, Wu WT, Chen T, Chen Q, He MY (2014) Ion-exchange resin-catalyzed synthesis of polyoxymethylene dimethyl ethers: a practical and environmentally friendly way to diesel additive. Chem Eng Commun 201:709–717. https://doi.org/10.1080/00986445.2013.778835
7. Sharma MM (1995) Some novel aspects of cationic ion-exchange resins as catalysts. React Funct Polym 26:3–23. https://doi.org/10.1016/1381-5148(95)00029-F
8. Alemán-Vázquez LO, Cano-Domínguez JL, Torres-Mancera P, Ancheyta J (2017) Organic polymers as solid hydrogen donors in the hydrogenation of cyclohexene. Catal Today https://doi.org/10.1016/j.cattod.2017.08.039
9. Cobzaru C, Inglezakis V (2015) Ion exchange, Elsevier Ltd. https://doi.org/10.1016/b978-0-12-384746-1.00010-0
10. Inglezakis VJ, Poulopoulos SG (2006) Adsorption, ion exchange and catalysis: design of operations and environmental applications, Elsevier Sci B V, p 602 https://doi.org/10.1016/b978-044452783-7/50003
11. Post MFM (1991) Diffusion in zeolite molecular sieves. Stud Surf Sci Catal 58:391–443 (Chapter 11). https://doi.org/10.1016/s0167-2991(08)63609-5
12. Goszewska I, Giziński D, Zienkiewicz-Machnik M, Lisovytskiy D, Nikiforov K, Masternak J et al (2017) A novel nano-palladium catalyst for continuous-flow chemoselective hydrogenation reactions. Catal Commun 94:65–68. https://doi.org/10.1016/j.catcom.2017.02.014
13. Osako T, Torii K, Hirata S, Uozumi Y (2017) Chemoselective continuous-flow hydrogenation of aldehydes catalyzed by platinum nanoparticles dispersed in an amphiphilic resin. https://doi.org/10.1021/acscatal.7b02604
14. Monguchi Y, Ichikawa T, Nozaki K, Kihara K (2015) Development of chelate resin-supported palladium catalysts for chemoselective hydrogenation. Tetrahedron 71:6499–6505. https://doi.org/10.1016/j.tet.2015.03.086
15. Dabbawala AA, Mishra DK, Hwang JS (2016) Selective hydrogenation of D-glucose using amine functionalized nanoporous polymer supported Ru nanoparticles based catalyst. Catal Today 265:163–173. https://doi.org/10.1016/j.cattod.2015.09.045

16. Nikoshvili L, Shimanskaya E, Bykov A, Yuranov I, Kiwi-Minsker L, Sulman E (2015) Selective hydrogenation of 2-methyl-3-butyn-2-ol over Pd-nanoparticles stabilized in hypercrosslinked polystyrene: solvent effect. Catal Today 241:179–188. https://doi.org/10.1016/j.cattod.2014.01.045

17. Kleman P, Barbaro P, Pizzano A (2015) Chiral Rh phosphine-phosphite catalysts immobilized on ionic resins for the enantioselective hydrogenation of olefins in water. Green Chem 17:1–54. https://doi.org/10.1039/C5GC00485C

18. Liguori F, Barbaro P (2014) Continuous flow synthesis of Rh and Pd nanoparticles onto ion-exchange borate monoliths: Application to selective catalytic hydrogenation of unsaturated carbonyl compounds under flow conditions. Catal Sci Technol 4:3835–3839. https://doi.org/10.1039/C4CY01050G

19. Barbaro P, Gonsalvi L, Guerriero A, Liguori F (2012) Facile heterogeneous catalytic hydrogenations of C=N and C=O bonds in neat water : anchoring of water-soluble metal complexes onto ion-exchange. Green Chem 3211–3219. https://doi.org/10.1039/c2gc36144b

20. Maria A, Galletti R, Antonetti C, Luise V. De, Martinelli M (2012) A sustainable process for the production of γ-valerolactone by hydrogenation of biomass-derived levulinic acid. Green Chem 688–694. https://doi.org/10.1039/c2gc15872h

21. Drelinkiewicz A, Stanuch W, Knapik A, Ghanem A, Kosydar R, Bukowska A et al (2009) Amine groups functionalized gel-type resin supported Pd catalysts: physicochemical and catalytic properties in hydrogenation of alkynes. J Mol Catal A: Chem 300:8–18. https://doi.org/10.1016/j.molcata.2008.10.035

22. Talwalkar S, Thotla S, Sundmacher K, Mahajani S (2009) Simultaneous hydrogenation and isomerization of diisobutylenes over pd-doped ion-exchange resin catalyst. Ind Eng Chem Res 10857–10863

23. Drelinkiewicz A, Knapik A, Waksmundzka-Góra A, Bukowska A, Bukowski W, Noworól J (2008) Functional gel-type resin based palladium catalysts: the role of polymer properties in the hydrogenation of the C=C bond of maleic and fumaric acids, the isomers of dicarboxylic acids. React Funct Polym 68:1059–1071. https://doi.org/10.1016/j.reactfunctpolym.2008.02.008

24. Miyazawa T, Koso S, Kunimori K, Tomishige K (2007) Glycerol hydrogenolysis to 1, 2-propanediol catalyzed by a heat-resistant ion-exchange resin combined with Ru/C, 329:30–35. https://doi.org/10.1016/j.apcata.2007.06.019

25. Li B (2007) Preparation and characterization of spherical nickel-doped carbonized resin as hydrogenation catalysts II. Thermal decomposition of resin and preparation of metal-doped catalysts with different nickel loadings. Carbon 45:1219–1225. https://doi.org/10.1016/j.carbon.2007.02.002

26. Miyazawa T, Kusunoki Y, Kunimori K, Tomishige K (2006) Glycerol conversion in the aqueous solution under hydrogen over Ru/C + an ion-exchange resin and its reaction mechanism. J Catal 240:213–221. https://doi.org/10.1016/j.jcat.2006.03.023

27. Marrodan CM, Berti D (2012). In situ generation of resin-supported Pd nanoparticles under mild catalytic conditions : a green route to highly efficient, reusable hydrogenation catalysts. Catal Sci Technol 2279–2290. https://doi.org/10.1039/c2cy20205k

28. Mendow G, Sánchez A, Grosso C, Querini CA (2017) A novel process for nitrate reduction in water using bimetallic Pd-Cu catalysts supported on ion exchange resin. J Environ Chem Eng 5:1404–1414. https://doi.org/10.1016/j.jece.2017.01.033

29. Mendow G, Grosso CI, Sánchez A, Querini CA (2017) Hybrid process for the purification of water contaminated with nitrites: Ion exchange plus catalytic reduction. Chem Eng Res Des 125:348–360. https://doi.org/10.1016/j.cherd.2017.07.019

30. Paun C, Giziński D, Zienkiewicz M (2017) p-Nitrophenol flow hydrogenation with nano-Cu2O grafted on polymeric resin. Catal Commun https://doi.org/10.1016/j.catcom.2017.01.003

31. Abdullaev MG, Gebekova ZG (2016) Hydrogenation of aromatic nitro compounds on palladium-containing anion-exchange resins. Pet Chem 56:146–150. https://doi.org/10.1134/S096554411602002X

32. Kim YN, Kim MY, Choi M (2016) Synergistic integration of catalysis and ion-exchange for highly selective reduction of nitrate into N2. Chem Eng J 289:423–432. https://doi.org/10.1016/j.cej.2016.01.002

33. Barbosa DP, Tchiéta P, Rangel MDC, Epron F (2013) The use of a cation exchange resin for palladium-tin and palladium-indium catalysts for nitrate removal in water. J Mol Catal A Chem 366:294–302. https://doi.org/10.1016/j.molcata.2012.10.008

34. Gašparovičová D, Králik M, Hronec M, Vallušová Z, Vinek H, Corain B (2007) Supported Pd-Cu catalysts in the water phase reduction of nitrates: functional resin versus alumina. J Mol Catal A Chem 264:93–102. https://doi.org/10.1016/j.molcata.2006.08.081

35. Imchuen N, Lubphoo Y, Chyan JM, Padungthon S, Liao CH (2016) Using cation exchange resin for ammonium removal as part of sequential process for nitrate reduction by nanoiron. Sustain Environ Res 26:156–160. https://doi.org/10.1016/j.serj.2016.01.002

36. Akagawa K, Akabane H, Sakamoto S, Kudo K (2009) Asymmetric transfer hydrogenation in aqueous media catalyzed by resin-supported peptide having a polyleucine tether. Tetrahedron Asymmetry 20:461–466. https://doi.org/10.1016/j.tetasy.2009.02.036

37. Akagawa K, Akabane H, Sakamoto S, Kudo K. (2008) Organocatalytic asymmetric transfer hydrogenation in aqueous media using resin-supported peptide having a polyleucine tether. https://doi.org/10.1021/ol800031p

38. Bhanushali MJ, Nandurkar NS, Bhor MD, Bhanage BM (2008) Cation exchange resin catalyzed hydroamination of vinylpyridines with aliphatic/aromatic amines. Catal Commun 9:425–430. https://doi.org/10.1016/j.catcom.2007.07.025

39. Palomares AE, Prato JG, Márquez F, Corma A (2003) Denitrification of natural water on supported Pd/Cu catalysts. Appl Catal B Environ 41:3–13. https://doi.org/10.1016/S0926-3373(02)00203-5

40. Králik M, Vallušová Z, Major P, Takáčová A, Hronec M, Gašparovičová D (2014) Hydrogenation of chloronitrobenzenes over Pd and Pt catalysts supported on cationic resins. Chem Pap 68:1690–1700. https://doi.org/10.2478/s11696-014-0565-3

41. Chen N, Rioux RM, Ribeiro FH (2002) Investigation of reaction steps for the hydrodechlorination of chlorine-containing organic compounds on Pd catalysts. J Catal 211:192–197. https://doi.org/10.1016/S0021-9517(02)93717-6

42. Bacik DB, Zhang M, Zhao D, Roberts CB, Seehra MS, Singh V et al (2012) Synthesis and characterization of supported polysugar-stabilized palladium nanoparticle catalysts for enhanced hydrodechlorination of trichloroethylene. Nanotechnology 23:294004. https://doi.org/10.1088/0957-4484/23/29/294004

43. Han B, Liu W, Li J, Wang J, Zhao D, Xu R et al (2017) Catalytic hydrodechlorination of triclosan using a new class of anion-exchange-resin supported palladium catalysts. Water Res 120:199–210. https://doi.org/10.1016/j.watres.2017.04.059

44. Jadbabaei N, Ye T, Shuai D, Zhang H (2017) Development of palladium-resin composites for catalytic hydrodechlorination of 4-chlorophenol. Appl Catal B Environ 205:576–586. https://doi.org/10.1016/j.apcatb.2016.12.068

Chapter 3
Use of Ion-Exchange Resins in Alkylation Reactions

Elizabeth Roditi Lachter, Jorge Almeida Rodrigues, Viviane Gomes Teixeira, Roberta Helena Mendonça, Paula Salino Ribeiro and Santiago Villabona-Estupiñan

Abstract Important organic reactions require the use of catalysts in order to be industrially or academically applicable. Heterogeneous catalysts, in this context, show significant advantages over conventional homogeneous catalysts, especially with regard to separation of products from the reaction medium, recycling, and reuse. Ion-exchange resins are solid acid heterogeneous catalysts that play a key role in many useful reactions such as alkylation, esterification, etherification of olefins with alcohols, dehydration of alcohols to olefins or ethers, olefin hydration, and ester hydrolysis. Alkylation is the transfer of an alkyl group from one molecule to another, and is one of the most important catalytic processes of the chemical industries since it is widely applied in different areas such as fuels, cleaning products, and pharmacological products. This chapter presents a review of the use of ion-exchange resins in alkylation reactions on different substrates, highlighting the particularities of each case. First, definitions and classical industrial processes are discussed followed by an illustration of alkylation reactions in terms of mechanism, activity, and selectivity. Finally, the use of biomass derivatives in catalyzed alkylation reactions with ion-exchange resins is presented.

3.1 Introduction

The alkylation reaction is a very important process in the synthesis of high octane motor fuel, alkyl phenols, and alkyl aromatic compounds both in the laboratory and industries [1–6].

In the fuel market, the alkylation of isobutene with light olefins produce branched alkanes. These alkylate improve gasoline properties such as octane number (RON) and motor octane number (MON). The RON and MON can be increased after the proper selection of the feedstock, catalysts, and operating conditions [7]. Other

E. R. Lachter (✉) · J. A. Rodrigues · V. G. Teixeira · P. S. Ribeiro · S. Villabona-Estupiñan
Instituto de Química, Universidade Federal do Rio de Janeiro, Rio de Janeiro, Brazil
e-mail: lachter@iq.ufrj.br

R. H. Mendonça
Instituto de Tecnologia, Universidade Federal Rural do Rio de Janeiro, Rio de Janeiro, Brazil

important examples of industrial applications are the alkylation of benzene with ethylene and propylene to produce ethylbenzene and cumene, respectively. Cumene is an important intermediate mainly used for the production of phenol and acetone while ethylbenzene is the intermediate for styrene production. Linear alkylbenzenes (LAB) are obtained from the alkylation of benzene with olefins and are the starting material for the manufacture of alkylbenzene sulfonates, an important detergent [3, 8]. The alkylation of phenols is another important process in preparing butyl, octyl, nonyl, and dodecyl phenol, used in the production of nonionic surfactants, oil-soluble resins, lubricant additives, and antioxidants [9, 10]. Benzylation reactions of aromatic compounds using benzylating agents such as benzyl alcohol and benzyl chloride for production of benzylated aromatic compounds are very important in the pharmaceutical and fine chemical industries [1, 11, 12].

Recently, the use of biomass as a raw material to produce chemicals and renewable fuels has been an alternative source of fossil feedstock. The general C–C coupling reaction pathways have been recently developed for increasing the carbon-chain length of biomass-derived oxygenate fuels and/or other relevant reactions to value-added chemicals. For example, the alkylation of aromatic compounds with C_2–C_4 olefins derived from bio-oil or lignin to produce biofuels, and the alkylation of phenols and its derivatives obtained from lignin [13]. Liquid catalysts such as HF and H_2SO_4, have been applied in the alkylation processes. However, due to environmental concerns and problems related to equipment corrosion due to the use of these acids, the development of safer and non-waste producing alternatives for applications in catalysis has been considered [2, 5, 6, 14]. Efforts have been devoted to finding heterogeneous catalysts which are considered more selective, safe, environmentally friendly, and reusable. On the other hand, the development of alternative processes using solid catalysts has a great impact on a large number of industrial processes, with the objective always to improve these processes economically and environmentally. Solid catalysts are considered to be as green catalysts and have been applied in alkylation study since the 1960s due to the fact that the catalysts separation from reactants and products can be performed easily using a unit operation as, for example, filtration [5, 15, 16].

Among the solid acids, special attention has been on ion-exchange resins. The anion- and cation-exchange resins have been widely used as catalysts for organic reactions and are important for petrochemical reactions and biomass transformation [3, 17–19]. The interest in ion-exchange resins is due to their highly selective properties, environmentally benign character, and commercial availability.

Our intention in this chapter is to present briefly the alkylation reactions catalyzed by ion-exchange resins with emphasis on the alkylation of light olefins, aromatics hydrocarbons, phenols, and biomass derivatives such as indol and furans.

3.2 Aspects of Ion-Exchange Resins for the Alkylation Reaction

Ion-exchange resins introduced in the 1960s have wide applications as catalysts till now [12, 17, 18, 20, 21]. These materials can be defined as a cross-linked polymer network containing reactive groups with Brønsted and/or Lewis acid or basic character [20]. The most commonly used precursor materials of ion-exchange resins are styrene-divinylbenzene copolymers with different kinds of porous structure. These copolymers are very attractive because of their low cost and ease of porous structure control. These are suitable for all sorts of reactions that can be carried out in aromatic rings, leading to the introduction of a variety of functional groups in the polymer matrix [22].

The first synthesized ion-exchange polymer resins had a continuous microscopic structure with high mechanical stability and swelling capacity. These so-called gel-type resins had a narrow variety of application due to their poor surface characteristics. In 1962, Kunin et al. [23] reported the synthesis of styrene-divinylbenzene copolymer beads with fixed porosity by suspension polymerization. In this technique, the organic suspended phase contained the monomers and an inert solvent with high solvation power for the liquid monomers but low solvation power for the growing copolymer. The macroporous structure of the copolymers obtained by this method was formed by channels between agglomerates of microspheres. After this report, many efforts were made to elucidate the mechanism of pore formation in such kind of polymers [24–29].

The thermodynamic process of polymer chain solvation during the synthesis reaction is the factor mainly responsible for determining the kind of porosity in divinylbenzene cross-linked copolymers. The effectiveness of solvation is a function of polymer–solvent interaction, which can be predicted by the solubility parameter theory, first proposed by Hildebrand [30]. The Hildebrand solubility parameter (δ) is defined as the square root of cohesive energy density and is related to the amount of energy necessary to overcome intermolecular forces and promote liquid vaporization. The molecular interaction forces that occur in the liquid phase determine this energy, and thus also define the energy associated with solvation since solvation is a process of overcoming intermolecular forces [31]. In this sense, two solvents are miscible if they have similar solubility parameters because the intermolecular forces that are present in both liquids are similar in nature and intensity. When the solubility of solid materials such as divinylbenzene copolymers are considered, their solubility parameters or cohesive parameters are estimated by their degree of swelling in solvents with different and known values of solubility parameters. By comparing the difference between solvent and polymer solubility parameters ($\Delta\delta$), solvents can be classified as good, if $\Delta\delta$ is less than 1.5 MPa$^{1/2}$, intermediary, for $\Delta\delta$ between 1.5 and 3.0 MPa$^{1/2}$ and poor if $\Delta\delta$ is higher than 3.0 MPa$^{1/2}$ [29]. Although Hildebrand solubility parameters are very useful for predicting polymer–solvent interactions, these take into account only Van der Waals interactions. Hansen, therefore, proposed a three-dimensional solubility parameter composed of three vectors, each one corre-

sponding to dispersive, polar, and hydrogen-bond interactions [32]. Hansen solubility parameters are more versatile in predicting polymer–solvent interaction in a polar medium, but Hildebrand is a good choice when styrene-divinylbenzene copolymers are studied.

The process of pore formation of styrene-divinylbenzene copolymers synthesized in the presence of a solvent begins with the formation of low molecular weight chains that are soluble in the reaction medium, which is composed of monomers and solvent. Even if the solvent does not have a high solvation power for the copolymers chains, their solvation is still efficient because of the high concentration of non-polymerized monomers. As polymerization occurs, the reaction medium becomes poor in monomers and the solvent begins to play a significant role in polymer solvation. If a poor solvent is present, the cross-linked polymer chains precipitate sooner from the solution in comparison to a system composed of a good solvent. Due to the low interaction with the solvent, the polymer chains precipitate in a more entangled and less swelled way. The nuclei formed in this step agglomerate and become covalently bounded by the reaction between growing linear chains, which results in the formation of microspheres. In the presence of poor solvents, the microspheres become more compact resulting in a final copolymer with pores of high diameters. If the proportion of the solvent in the reaction medium is high, phase separation occurs sooner with the formation of more separated microspheres, and thus a more porous material is obtained. Good solvents impart better solvation power to the reaction medium and the rate of phase separation becomes lower. In this condition, more extended polymer chains precipitate, leading to the formation of a continuous surface with low porosity. High dilution degrees with good solvents promote the formation of higher amounts of pores but still with low diameters. Although the solvent plays a definite role in phase separation, the degree of cross-linking also influences this process since it determines the molecular weight and the solubility of the copolymer. Chains formed with high contents of divinylbenzene are more entangled and form a material with high volumes of pores. Consequently, the phase separation process determines each step of the pore formation mechanism and this process is governed by the solvating power and amount of the solvent that constitutes the reaction medium as well as by the proportion of the cross-linker in the monomers mixture [22, 30, 33–37].

The association of these parameters has been used to obtain ion-exchange resins with different porous structures, which vary from microporous to macroporous, and with a large spectrum of swelling properties [38, 39]. The catalytic process in the presence of ion-exchange resins is based on diffusion of the reactants through the polymer matrix, as well as adsorption and desorption of the final product [40]. Considering these steps, porosity and swelling are two properties responsible for the performance of these materials in catalysis as these determine the specific surface area of the material in its dry and solvated states [41]. The efficiency of the polymer matrix solvation by the reaction medium and the cross-linking degree regulate the swelling extension of the ion-exchange resin and define the type of catalysis that undergoes in a specific condition. Heterogeneous catalysis assumes no swelling of the solid catalyst but, even in a very low extension, this phenomenon always occurs

for ion-exchange resins. Therefore, in a reaction medium with low solvating power for these materials, the catalysis process is called as quasi-heterogeneous. In solvating systems, where the surface and inner ionic groups of the swelled resin are efficiently solvated and ionized, catalysis is classified as quasi-homogeneous since the ionic polymer matrix still interacts with the catalytic species [42].

As resumed by Chakrabarti and Sharma [40], reactions catalyzed by ion-exchange resins are classified as Type A or Type B, depending on whether water is present or not in the reaction medium. Alkylation reactions fall into the Type B since water is absent at the beginning of the process. The undissociated ionic group catalyzes this type of reaction and the presence of water compromises the catalytic activity of the ion-exchange resin. Due to the absence of polar solvents, the reaction mixture is not able to promote a good swelling of the polymer and the quasi-heterogeneous catalysis occurs. Considering these characteristics of alkylation reactions catalyzed by ion-exchange resins, macroporous copolymers synthesized with high degrees of divinylbenzene, also called macroreticular copolymers, are the most common precursors of ion-exchange resins for this application. In macroreticular resins, the groups available for catalysis are located on the surface of the polymer matrix because its low swelling ability prevents internal groups to interact with the reaction mixture in a high extension and it imparts low catalytic activities for this material when compared to gel-type ones. Because of this limitation, the specific surface area of the precursor copolymers must be as high as possible, but it should be considered that the improvement in the area is attained in detriment to pore size [41], although macroporosity is desired for alkylation reactions because of the nonpolar medium where these reactions occur. The gel regions present in the polymer with swelling ability contribute to the selectivity of the catalyst since it is determined by the steric hindrances imposed by the polymer network to the substrates [18]. The control of the location of the catalytic sites in the copolymer network enhances the selectivity of ion-exchange resins. Besides the steric hindrance, the porous structure of the catalyst also imparts selectivity by its action as a molecular sieve, determining the size of molecules that can reach the active sites [40].

Another sulfonic resin used in alkylation reaction is the Nafion-H, which presents strong acid sites and the Hammett acidity is around $H_0 \sim -10$ to -12. This perfluorinated ion-exchange polymer resin is prepared by the copolymerization of tetrafluoroethylene and perfluoro-2-(fluorosulfonylethoxy)propylvinyl ether developed by Dupont [43]. Examples of ion-exchange resins applied to alkylation are shown in Table 3.1.

3.3 Alkylation Process Using Ion-Exchange Resins

The importance of industrial processes using heterogeneous catalysts such as ion-exchange resins has increased significantly in the last decades. Amid an enormous range of reactions in which these materials can be applied stand out dehydration, isomerization, esterification, oil cracking, and alkylation reactions [2, 4].

Table 3.1 Examples of ion-exchange resins applied to alkylation

	Purolite® CT169[a]	Ambertlist™ 16 WET[b]	Lewatit® 2640[c]	Nafion
Polymer structure	Macroporous polystyrene cross-linked with divinylbenzene	Macroreticular structure	Cross-linked polystyrene	Perfluorinated ion-exchange polymer
Appearance	Beads	Beads	Beads	Membrane
Functional group	Sulfonic acid	Sulfonic acid	Sulfonic acid	Sulfonic acid
Ionic form	H^+	H^+	H^+	H^+
Moisture retention	51–57%	52–58%	–	
Particle size range	425–1200 μm	0.025 μ	400–1250 μm	
Surface area	35–50 $m^2\ g^{-1}$	30 $m^2\ g^{-1}$	33 $m^2\ g^{-1}$	0.02 $m^2\ g^{-1}$
Pore volume	0.3–0.5 $cm^3\ g^{-1}$	0.2 $cm^3\ g^{-1}$	0.45 $cm^3\ g^{-1}$	–
Shipping weight	755–790 g/L	780 g/L	–	–
Temperature limit	130 °C	130 °C	140 °C	175 °C
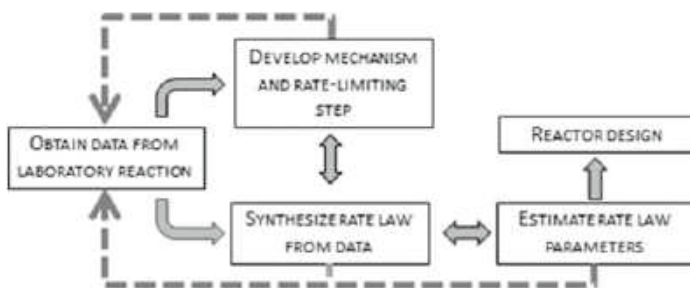
Fig. 3.1 Algorithm to project a heterogeneous reactor

3.3.1 Reactors and Heterogeneous Catalysis

The choice of the appropriate reactor is quite important for the success of catalytic processes as a whole. Alkylation reactions using ion-exchange resins as catalysts are heterogeneous processes since reactants and catalyst are in different phases. Thus, reactor selection and catalyst development, simultaneously, can provide advantages to the catalytic process. Figure 3.1 shows an algorithm to project a heterogeneous reactor. In this context, it is evident that understanding the thermodynamics and the chemical mechanism is necessary to design adequate processes. According to Thomas and Thomas [44], this new paradigm of simultaneous catalyst and reactor development for new processes is becoming prevalent in modern chemical engineering.

The catalytic reactions can be carried out in batch or continuous processes. In the case of solid resins as a catalyst, the batch operation can be performed in a slurry reactor. This reactor is one of the most commonly employed industries [45]. Important process parameters such as stirring to promote the right catalyst distribution in the reactor, catalyst loading, and transport phenomena such as mass heat and mass transfer have to be controlled. After the reaction in the slurry reactor, the catalyst can be easily separated from the reaction mass by the filtration unit operation.

Continuous processes have the advantage of producing large amounts of products in shorter periods. Generally, in these processes, fixed-bed reactors are employed and two important parameters (catalyst particle size and temperature) have to be considered. The resin is packed in the form of the catalyst bed and the pressure drop across the reactor is directly affected by the resin particle size, increasing as the particle size decreases. Therefore, it is very important to control this parameter. The heat removal on a fixed bed, for example, is facilitated using a multitubular design [46].

In order to improve the alkylation process, innovations on catalysts and reactors have been performed. For example, an alkylation apparatus using solid catalyst particles suspended in the reactor was developed by Radcliffe and coworkers in 2004 [47]. This invention finds use in the production of motor fuels by the alkylation of liquid hydrocarbons in the presence of solid catalyst particles. According to authors, this method and apparatus allowed uniform or symmetric flow of catalysts from the effluent of the transport reactor to the bottom of the transport reactor ensuring uniform or symmetric flow of alkylation substrate, and thus provide better heat exchange.

3.3.2 Alkylation Process

In the chemical industry, many aspects have to be taken into account to make the process economically viable. For example, the application of continuous processes requires rapid reaction rates. In alkylation processes, more rapid reaction rates are achieved by the use of pressure in the reaction vessel, which results in an increase in heat production during the reaction. Therefore, it is quite important to control the temperature due to the reaction's exothermicity. In this case, where ion-exchange resins are employed as catalysts, the temperature control is fundamental to avoid resin damages. Being thus, it is important to control the temperature of the reaction zone. Different configurations and equipment may be used for the purpose of favoring the alkylation reaction and removing the heat satisfactorily [48]. A generic representation of an alkylation unit is shown in Fig. 3.2.

The main aspects of alkylation processes using ion-exchange resins are maintained until today, but the processes are not in the open literature. In order to illustrate this, two old processes are described below.
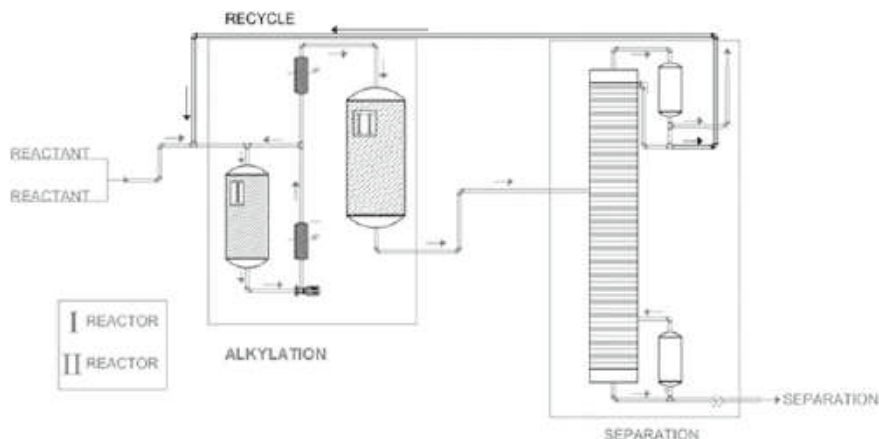
Fig. 3.2 Alkylation process

3.3.3   A Process for Continuous Alkylation of Phenol Using Ion-Exchange Resin

A process for continuous alkylation of phenol, with olefins using ion-exchange resins, was developed by Alfs et al. [14]. The catalysts employed in this process were sulfonic ion-exchange resins, in H-ion form mounted in a fixed bed, for example, polystyrene based or those based on phenol-formaldehyde resins. Olefins used contained from 6 to 12 carbon atoms. In this process, phenol and olefins were passed in a first stage at temperatures from about 80 to 120 °C, over the ion-exchange resin catalyst having an exchange capacity from 50 to 96 m Val per 100 mL of catalyst and then passed in a second stage at temperatures from 110 to 130 °C, over another ion-exchange resin catalyst having an exchange capacity from 100 to 180 m Val per 100 mL of catalyst. According to the literature, the use of ion-exchange resins with an exchange capacity of about 50 to 95 m Val per 100 mL of catalyst in the first stage prevented the local overheating [14].

Phenol alkylation using nonene was described in the US 4,168,390 patent [44] and is summarized as follows. In this process, two fixed-bed reactors containing ion-exchange resin was used. The first reactor was filled with 120 kg of sulfonated polystyrene ion-exchange resin Lewatit® SC 102H or SC104 deactivated with $Al_2(SO_4)_3$ as manufactured by Bayer, with an activity of approximately 80 m Val per 100 mL of the catalyst. The second was filled with 120 kg of ion-exchange resin Lewatit (R) SC104H with an activity of 140 m Val per 100 mL of the catalyst. A heat exchanger was used to heat 1.7 tons of nonene and 2.2 tons of phenol to 70 °C, which in the sequence were supplied within 1 hour to the first reactor. The exhaust temperature at the first reactor was about 120 °C. Before being fed into the second reactor, the reaction mixture was cooled to about 100 °C using a heat exchanger. In the second reactor, the temperature of the reaction mixture raised to approximately

125 °C. Taking contact filling into account, the entire dwell time was about 4 min. Following distillation recovery and recycling of the dinonylphenol formed and of the non-converted nonene and phenol, the yield in nonylphenol was 99%; and the color coefficient or dye number of the nonylphenol was 10 APHA.

3.3.4   Process for Alkylating Benzene with Tri- and Tetra-substituted Olefins with a Sulfonic Acid Type Ion-Exchanger Resin

The process for alkylating aromatic hydrocarbons using a sulfonated ion-exchange resin as a catalyst was described in the USA patent in 1966 [49]. They provided a process for alkylating benzene with tri- and tetra-substituted olefins using a sulfonic acid type ion-exchange resin catalyst. Their process may be employed to alkylate mononuclear aromatic compounds such as benzene, toluene, xylene, etc. A brief description of the process is presented as follows.

The alkylation was performed using a 1-in. I.D., a 10.7-ft long bed reactor filled with 574 g of the ion-exchange resin (poly(styrene-divinylbenzene) type in bead form). Propylene tetramer boiling in the range of 171–215.5 °C was blended with nitration grade benzene at a ratio of 20:1 benzene to tetramer, and passed downwardly through the reactor, which was kept completely full of liquid. The liquid hourly space velocity was maintained at 0.125 and the mass velocity at 0.5 gal/min-ft. The reaction mixture was maintained at a temperature of 121 °C. The products from the reaction were charged to a batch still and topped to 176 °C to remove excess benzene. The yield of detergent alkylate product was 69.7 mol percent of detergent alkylate based on the tetramer in the feed.

3.4   Alkylation of Alkenes with Isoalkanes

The alkylation reaction of saturated hydrocarbons with light olefins (C_3–C_5) to produce isoparaffins (Fig. 3.3) was discovered by Ipatieff and Pines in 1932 [50].
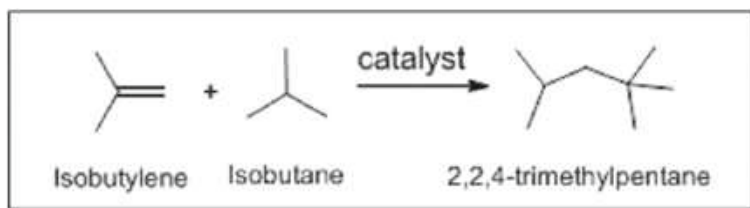
Fig. 3.3   Alkylation of alkenes with isobutane catalyzed by acid

This process is very important for the production of high octane motor fuel and occurs in the presence of an acid catalyst. Lewis catalysts with a small amount of hydrogen halides or Brønsted acids such as H_2SO_4 and HF were used in this alkylation reaction [7, 50, 51]. The reaction proceeded with saturated hydrocarbons containing tertiary carbon and olefins such as propylene, butylene, and amylenes. The alkylation product was the mixture of saturated stable isoparaffins that distilled in the gasoline range, which were the principal components of many high octane gasoline. The branched alkanes are the highest quality hydrocarbons for the gasoline due to the high octane number, very low sulfur content and are free of aromatic and olefins [52].

In the alkylation of isobutene with isobutene, for example, the reaction involves three main steps: the initial formation of a carbenium ion (initiation) by the protonation of the olefin; the attack of this cation by the isobutene (alkylation) resulting an octyl carbenium ion, C_8^+ and termination steps (hydride transfer) to produce the branched alkane, isooctane, as presented in Fig. 3.4 [53–55].

Until now, mineral acids such as HF (licensed by Conoco Phillips and UOP) and H_2SO_4 (licensed by DuPont/STRACTO, Kellog and Exxon Mobil) were used despite the problems of corrosion, toxicity, and generation of rejects [7, 16, 56, 57]. The substitution of these mineral acids by solid acids has been an important research goal. However, good heterogeneous catalysts should be acidic enough to form the
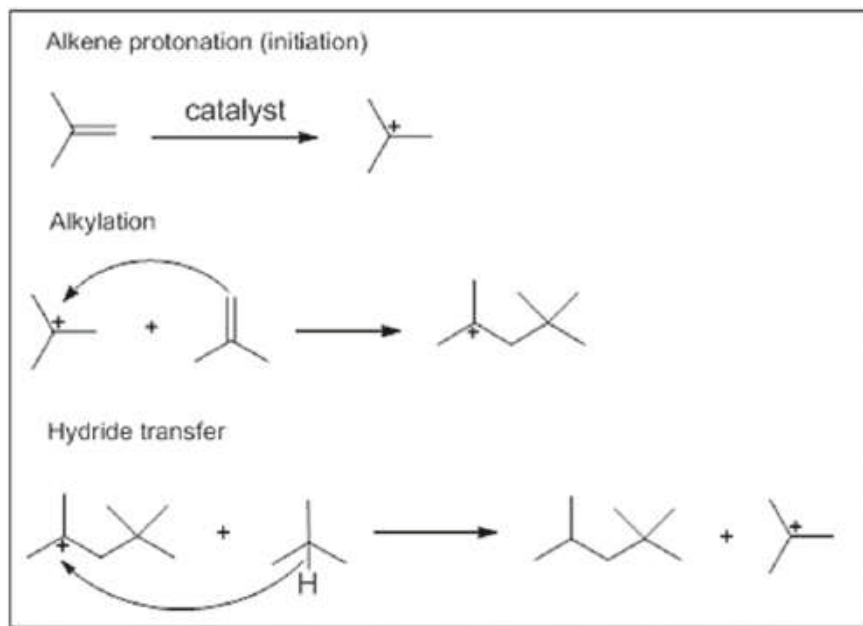
Fig. 3.4 Alkylation of isobutylene with isobutane [55]. Adapted and reproduced with permission. Copyright, 2005 American Chemical Society

intermediate carbocation and catalyze hydride transfers. Other characteristics are the pore sizes, which should be large enough to facilitate the diffusion of reactants and products, and the hydrophobic surface, which permits a higher paraffin concentration around the pore of the catalysts [58–61]. Among the solid acids evaluated for the reaction of alkenes with alkanes, Nafion resin [62, 63] has been the catalyst of choice for this reaction. Nafion resin is a copolymer of perfluorinated epoxide and vinyl sulfonic acid, and the presence of electron-withdrawing fluorine atoms in the structure increases the acidic strength of the sulfonic groups. Nafion has a strong solid acid and the strength is comparable to that of sulfuric acid [64]. The acidity of this Brønsted acid is around $H_0 \sim -10$ to -12 [51]. However, Nafion has low surface area and consequently a poor catalytic activity. A material with the high surface area, a higher density of available acid sites and consequently higher catalytic activity can be obtained by supporting Nafion on high surface area silica [65]. Nafion silica nanocomposite tested in the isobutene/isobutene alkylation showed good activity in the production of isooctane under batch conditions [66]. Nafion supported on mesostructured silica, SBA-16, presented better results in the alkylation of isobutene with isobutene than a commercial Nafion silica nanocomposite [59, 60]. These materials can be prepared by immobilization of perfluoro sulfonic acid groups on mesoporous materials by post-synthetic grafting [58, 67] or direct one-step synthesis [68] and present high surface area, large pore size, and high strength acid sites [69]. Shen and coworkers [59] demonstrated that Nafion resin supported on mesostructured SBA-15 modified by -OH capping has a high surface area (400 m^2 g^{-1}). The authors concluded that capping surface OH resulted in decrease of the silanol density on the surface and provides the hydrophobic environment for the isobutene/isobutene reaction [7, 43, 59].

3.5 The Reaction of Alkylation of Sulfur Compounds with Olefins

A new desulfurization technology for ultraclean gasoline, the olefinic alkylation of thiophenic sulfur (OATS), has been described in the literature and was first patented by Mobil Oil Corporation [70]. The aim of this process was to obtain sulfur compounds with higher molecular weight by alkylation with olefins over solid acid catalysts (Fig. 3.5). The heavier alkylated sulfur molecules were eliminated by further distillation to separate the high boiling compounds from the main gasoline stream. This process is interesting due to the mild operating conditions and low loss of octane number.

Solid acid catalysts such as ion-exchange resins have been evaluated for this reaction [71–75]. Amberlyst 35 (A35), a commercial macroporous sulfonic resin showed the higher activity among the investigated resins [75]. However, side reactions such as dimerization and polymerization of olefins can occur. Wang et al. evaluated the mechanism of the OATS process by calculation of density functional theory (DFT).
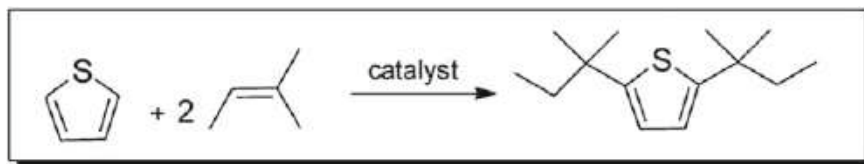
Fig. 3.5 Scheme of the alkylation of thiophene with an alkene

The authors showed that the alkylation rate of thiophenic compounds over A35 was faster than the dimerization of alkenes. The theoretical and experimental studies could help to optimize the reaction conditions for further application of A35 in the industrial process of alkylation desulfurization of gasoline [74].

3.6 Alkylation of Aromatic Compounds

The first example of alkylation reaction of aromatic compounds appeared in 1877 as a discovery by two researchers, Charles Friedel and James M. Crafts [1]. Friedel–Crafts reaction is an important reaction for forming carbon–carbon bond and is a very good tool for the synthesis of alkyl aromatic compounds both in the laboratory and on an industrial scale. The reaction is generally carried out with alkylating reagents such as alkenes, alkyl chloride, and alcohols using acid catalysts (Fig. 3.6).

Various reviews and books have been appeared discussing the developments in this subject [1, 11, 76–79]. The synthesis of valuable industrial pharmaceuticals, agrochemicals, and fine chemicals frequently involves electrophilic aromatic substitutions reactions. Two important classes of acidic forms of ion-exchange polymers used in alkylation of aromatic compounds are polystyrene-based materials (Amberlyst, DoweX, Lewatit) and perfluorinated sulfonic resin (Nafion). Our intention in the present topic is to give an update about the use of ion-exchange resins in alkylation of aromatic compounds.
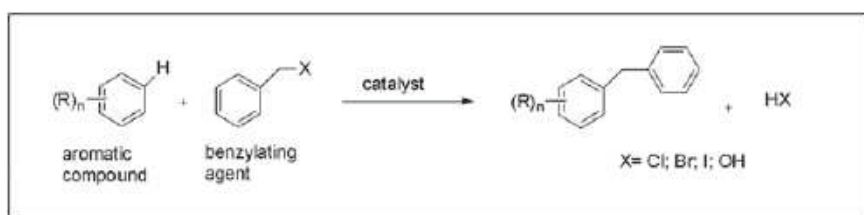
Fig. 3.6 Scheme of the aromatic alkylation reaction

3.6.1 The Reaction of Aromatic Compounds with Olefins

Alkylation of aromatic hydrocarbons with olefins has been applied on large scale in the chemical industry. The alkylation of aromatic compounds with olefins catalyzed by ion-exchange resins has been described in some reviews [17, 18, 20, 40, 43, 51].

The alkylation of benzene with C_{12} olefins to produce linear alkylbenzenes (LABs) is an important reaction because these compounds after sulfonation were used as detergent [6]. The products of the alkylation of benzene with C_{12} olefins contain a mixture of alkylbenzenes with the phenyl group attached to different C-atoms in the linear hydrocarbon chain. However, the 2-phenyl isomer is the most preferred product because of its high biodegradability compared to the branched isomers. In the petrochemical industry, benzene alkylation was carried out usually by HF despite their low selectivity and high corrosiveness. However, the use of solid acid catalysts grown up in the last years due to the environmental police [2, 5, 6].

The Nafion resin/silica nanocomposite presented good results for the reaction of benzene with 1-dodecene. The conversion was 99% at 80 °C. The authors found that the alkylation product distribution changed with benzene conversion. In general, at low conversion, more 2-phenyl dodecene was obtained [80, 81]. The nanocomposite was more active than the Amberlyst-15 and Nafion resin due to the greater accessibility to the strong acid sites and high surface area. The authors also studied the alkylation of toluene with heptane, cumene with propylene and naphthalene with propylene and compared the catalytic activities of Amberlyst-15, Nafion and Nafion resin/silica nanocomposite. The last catalyst presented better results [43].

The liquid-phase alkylation of toluene with 1-octene in the presence of different ion-exchange resins was evaluated [82, 83] and with Amberlyst 15, the major product obtained was the 2-octyl-toluene (Fig. 3.7).

The authors found that the resin Lewatit SP112 was practically inactive due to its low specific area and low exchanged capacity [82, 83].
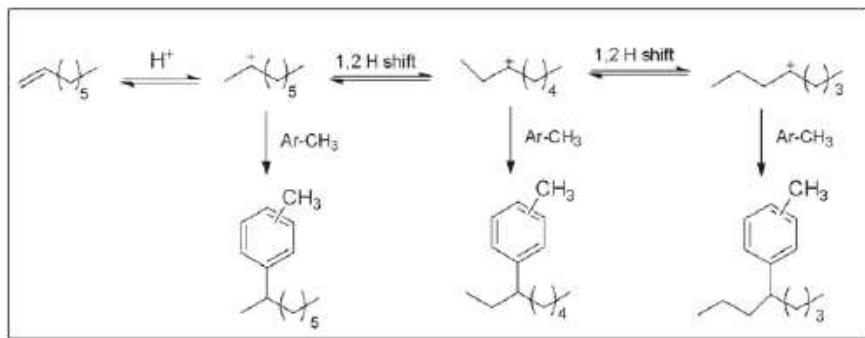
Fig. 3.7 Scheme of alkylation reaction [83]. Adapted and reproduced with permission. Copyright, 2005 Elsevier Ltd.

Nafion–silica catalysts used in the alkylation of benzene with olefins showed the selectivity to 2-phenylalkanes (25%) higher than the process using fluorinated silica alumina. The authors found that the selectivity decreased with the increase of Nafion content [43].

Ion-exchange resins Amberlyst 35 (A-35), Amberlyst 36 (A36), and Purolite CT275 were investigated as catalysts in the alkylation of toluene with 1-hexene [84]. The resins A-35 (Rohm & Haas) and CT275 (Purolite) have more sulfonic groups, 5.32 and 5.20 meq/g_{dry}, respectively. The resin A-46 (Rohm & Haas) sulfonated on the external surface showed 0.87 meq/g_{dry} of sulphonic groups. The authors evaluated the extension of isomerization and dimerization of 1-hexene besides the alkylation of toluene. Isomerization is the principal reaction with an excess of 1-hexene. The increase in the weight ratio of toluene to 1-hexene increased the alkylation and dimerization reactions. The best catalyst for isomerization was A-46 and the resins A-35, CT275 were the best catalysts for the dimerization and alkylation reactions due to the greater number of acidic sites in the gel phase. The mono-alkylation selectivity was higher for CT275 (42%) than for A35 (27%) due to the higher porosity which facilitated the accessibility to the acid sites on gel phase zones [84].

PS-SO$_3$H@phenylenesilica with yolk-double-shell nanostructures were evaluated in the alkylation of toluene and 1-hexene. These new materials were synthesized by sulfonation of polystyrene (PS) in the hollow interiors of silica-based hollow nanostructures and presented the highest stability than Amberlyst 15 in the alkylation reaction [21].

3.6.2 The Reaction of Aromatic Compounds with Alkyl Halides and Alcohols

In addition to the alkylation using olefins, the alkylation of aromatic compounds with alcohols and alkyl halides has also been well documented. The advantage of using an alcohol compared to olefin and alkyl halide is that with an alcohol, water is formed as a by-product and polymerization occurs with olefins and HCl with an alkyl halide.

Benzylated aromatic compounds, a class of alkylated aromatics, are very useful intermediates in petrochemical, cosmetic, and many other chemical industries [1, 4]. These compounds are formed by the replacement of a hydrogen atom of an aromatic compound by a benzyl group derived from a benzylating agent in the presence of an acid catalyst. Commercial ion-exchange resins (Lewatit SC-100, a gel resin) and Amberlyst-15, a macroreticular resin) were evaluated for the reaction of benzene with benzyl alcohol and benzyl chloride at 80 °C in liquid phase [85]. In the reaction with benzyl chloride, the monobenzylation product, diphenylmethane, was obtained in low yield with both resins (Fig. 3.6). In the reaction of benzene with benzyl alcohol (Fig. 3.8), the best results were obtained with the macroreticular resins Amberlyst 15. The authors evaluated the effect of molar ratio benzene: benzyl alcohol (1.5:1,
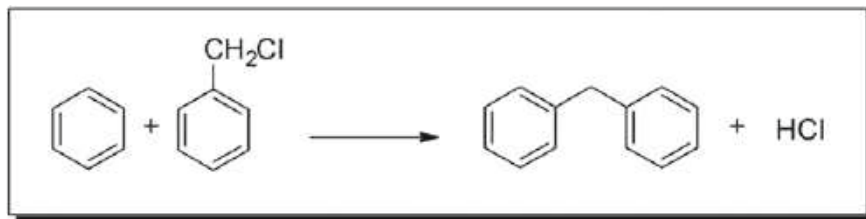
Fig. 3.8 Scheme of the reaction of benzene with benzyl chloride
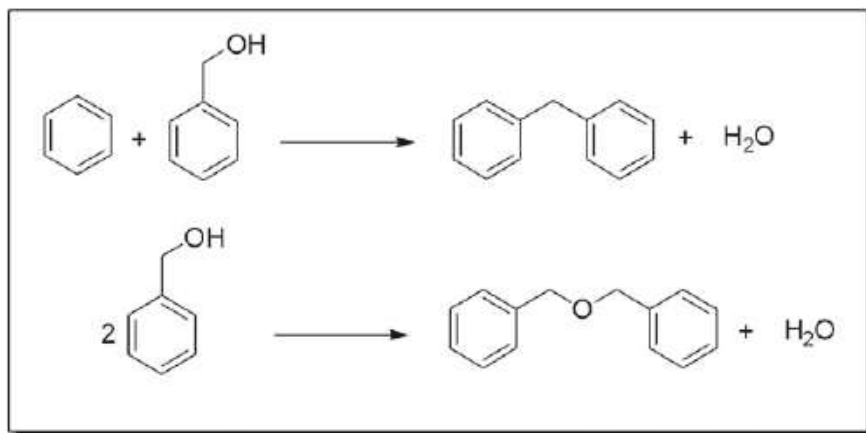
Fig. 3.9 Scheme of the reaction of benzene with benzyl alcohol

10:1) in selectivity to mono-alkylated products since the auto-etherification of benzyl alcohol, benzyl ether, may occur during the reaction (Fig. 3.9).

The results showed that an increase in molar ratio substrate: alcohol resulted in a decrease in the formation of benzyl ether. In the reaction with toluene and anisole the alcohol conversion, to monobenzylation product, was superior to 80% [85]. The same group evaluated the alkylation reaction of toluene with benzyl alcohol catalyzed by three different resins, two of which were commercial resins, (Amberlyst 15 and Lewatit, LWSP112) and a resin synthesized in the laboratory (MLS07). The properties of the resins are presented in Table 3.2 [86].

The results showed that Amberlyst 15 and the resin MLS07 presented better performance than Lewatit SP112. In all the reaction conditions, MLS07 showed the highest activity and selectivity in the formation of the desired product (*o-*,*m-*, and *p*-benzyltoluene, Table 3.3). This behavior may be mainly attributed to the fact that the MLS07 has the highest surface area and the highest number of acidic sites.

The alkylation of toluene with benzyl alcohol catalyzed by commercial ion-exchange resins was studied. The resins used were Amberlyst 15, Amberlyst 35, Amberlyst 36, and Amberlyst 70 which presented surface areas of 37.3, 40.7, 10.4, and 1 m^2 g^{-1}, respectively. The catalytic activity of resin Amberlyst 70 was com-

Table 3.2 Properties of the resins

Properties	Amberlyst-15	Lewatit SP112	MLS07
S (m^{2}g−1)	53.4	26.6	49.1
Vp (cm^3 g−1)	0.37	0.15	0.35
Dp (Å)	282	223	281
SO$_3$H meq g−1, dry resin	3.8	2.6	4.0

Table 3.3 Results in the alkylation of toluene with benzyl alcohol[a]

Resins	Alcohol conversion (%)	Products distributions		
		Alkylated (%)	Ether (%)	Others[b] (%)
Amberlyst-15	49.3	35.1	55	9.9
Lewatit SP112	20	22.6	71.6	5.5
MLS07	67.7	59.0	54.9	6.1

[a]Reaction conditions: temperature-80 °C, time-180 min, molar ratio of toluene: alcohol, 10:1
[b]Dialkylated products [86]

Table 3.4 Catalytic activity in the toluene alkylation[a] with benzyl alcohol

Catalysts	Conversion (%)	Selectivity (%)
H$_2$SO$_4$	4.9	50.1
Amberlyst-15	44	63.6
Nafion NR50	69.1	89.2
PS-SO$_3$H HNs	69.2	62.5
PS-SO$_3$H@mesosilicas HNs#	99.6	67.5
PS-SO3H@mesosilicas DSNs	99.1	72.7

[a]Reaction conditions: 80 °C, 7 h, 10 mL toluene; 23 mmol benzyl alcohol; 0.04 mmol acidic sites [21]

pared with the other resins presenting the highest thermal stability and resistant to de-sulfonation [87]. Nafion–silica has also evaluated in the reaction of *p*-xylene with benzyl alcohol and the catalytic activity was superior to Amberlyst 15 [43].

The influence of morphology on the acid strength of a resin is an important factor in benzylation reaction. A hybrid of silica and polystyrene resins (PS-SO3H) was synthesized and evaluated in the alkylation of toluene with benzyl alcohol [21] and the results are presented in Table 3.4. The PS-SO$_3$H@phenylenesilica was obtained by sulfonation of polystyrene (PS) in the interiors of the silica-based hollow nanostructure. The PS-SO$_3$H@mesosilicas DSNs are a PS@phenylenesilica-double-shell nanosphere.

The results presented in Table 3.4 show best activity of the resin PS-SO3H@mesosilicas DSNs, probably attributed to their strong acid strength and high local concentration of active sites.

3.7 Alkylation of Phenol

Ion-exchange resins play a key role as solid acid catalysts in a series of useful reactions such as etherification of olefins with alcohols, dehydration of alcohols to olefins or ethers, olefin hydration, ester hydrolysis, and alkylation of phenols to alkyl phenols. Alkylphenols and their derivatives have been widely used as antioxidants, herbicides, insecticides, polymerization inhibitors, and lubricants [88].

In 1957, Loev and Massengale [89] decided to investigate the catalysis of phenol alkylation promoted by cation-exchange resins for the first time. The reaction had previously been catalyzed by strong acids in homogeneous media [90]. They evaluated the following sulfonic acid resins: Amberlite IR-112 and IR-120, Dowex 5x12, and Permutite Q. It was observed that these resins were excellent catalysts for the alkylation of phenol with olefins such as isobutylene, diisobutylene, and 1-nonene. They also observed that the presence of water was deleterious to the reactions since the reaction required an oven-dried resin. The particular advantage of the cation-exchange resins over mineral acid catalysts was the simple filtration of the reaction mixture in an acid-free solution ready for distillation.

In the 90s, Sharma and coworkers published a series of papers in which ion-exchange resins were evaluated in phenol alkylation reactions. In 1990, they studied the alkylation of phenol with 1-dodecene (55–120 °C) and diisobutylene (50–100 °C) in the presence of Amberlyst 15, Amberlyst XN1010, monodisperse K2661, and Filtrol 24 clay [91]. They found satisfactory results when cation-exchange resins were used as catalysts. An equation to describe the overall kinetic of the process was also developed. Amberlyst 15 was the best catalyst for the alkylation of phenol with 1-dodecene. In order to obtain selective production of dodecylphenol, the reaction temperature has to be kept between 100 and 120 °C. On the other hand, the alkylation of phenol with diisobutylene gave better results with monodisperse K2661 since it suppressed the formation of tetraisobutylene. In order to obtain selective production of *p*-tert-octylphenol, the reaction temperature is kept between 90 and 100 °C and the mole ratio of phenol/diisobutylene should be greater than one. They also found that 85% yield in the production of *p*-tert-butyl phenol from phenol and diisobutylene can be obtained by conducting the reaction at 170 °C, in the presence of Nafion H as the catalyst.

In 1991, Sharma and coworkers [92] evaluated a series of heterogeneous catalysts (Amberlyst 15, Amberlyst XN1010, and Nafion NR50—cation-exchange resins; and Filtrol24 and Tonsil A/C—clay catalysts) and homogeneous catalysts (*p*-toluenesulfonic acid) in the mono-alkylation of phenol with a-methyl styrene (AMS) in the temperature range 60–120 °C. Propylene, 1-butene, isobutylene, isoamylene, and diisobutylene (DIB) were also evaluated as alkylating agents for phenol in order

to determine the ortho/para product distribution. They found that the ortho/para alkylated product ratio can vary considerably depending on the olefins used as alkylating agents, the reaction temperature, and the solid catalyst. Ag + -exchanged Amberlyst-15 resulted in ortho-alkylation of phenol with olefins such as DIB and 1-octene.

Sharma also studied the alkylation of phenol with cyclohexene in the presence of different cation exchangers and acid-treated clay (Filtrol-24) as catalysts [17, 93]. Different products, including *O*-alkylated and *C*-alkylated (*ortho*, *para,* and di-alkylated) products were formed. Amberlyst-15 was the best catalyst, considering activity. On the other hand, the acid-treated clay was the most selective catalyst (among those tried), considering etherification. They found that if the *O*-alkylation product is desired, the reaction should be carried out in the temperature range from 45–60 °C using Filtrol-24 as a catalyst, in the absence of solvent and phenol/cyclohexene mole ratio 1:1. On the other hand, if the objective is to obtain selective *C*-alkylation and high o/p ratio, the reaction should be carried out at 100 °C in the presence of Filtrol-24 as a catalyst. To reach selective *C*-alkylation, cyclohexanol can be used as the alkylating agent above 180 °C. However, at this temperature, *ortho* to *para* isomerization occurs.

The life of the ion-exchange resin catalysts is limited since these are deactivated after a few cycles. In addition, disposal of the used catalyst is also a problem for the industry. Malshe and Sujatha [94] tried to search for alternatives to regenerate the ion-exchange resin catalysts (Indion-130 and Amberlyst-15), previously used in the alkylation of phenol. In their approach, the physically adsorbed impurities were removed by solvent extraction and acid-alkali treatments, resulting in improved properties. However, ash analysis of the catalyst after solvent extraction evidenced that the impurities of phenol did not have a significant role in deactivating the catalyst. Another problem related to the use of this kind of resin was that the residual unsaturation content of the catalyst (around 6–7%) could react with the phenolic compounds. Thus, oxidation of the grafted phenolic compounds was performed by treatment with ozone and chlorine dioxide solutions. After the treatment, most of the characteristics of the catalyst were restored, and the catalyst was capable to be reused in alkylation application. However, the total exchange capacity was about 20% lower, because of the conversion of a part of the macroporous resin into gellular resin.

The same group, in 2000, developed an alternate catalyst based on styrene-substituted phenol and formaldehyde, instead of the conventional styrene/divinylbenzene matrix. In the case of styrene-DVB resins, the conversion of the second double bond of DVB at the end of the polymerization was limited due to diffusional resistance, resulting in residual double bonds on the matrix and the possibility of undesired side reactions with phenol, as mentioned before [95]. The strong advantage of the new catalyst was the absence of residual double bonds on its surface (Fig. 3.10).

The catalyst was evaluated using the synthesis of phenyl xylyl ethane (PXE), and an improvement was observed by comparing the performance of a new catalyst to the conventional ones. Phenolic resins acted as inhibitors for vinylic polymerization, and therefore no polymerization of monomers was seen on the pores of the catalyst.
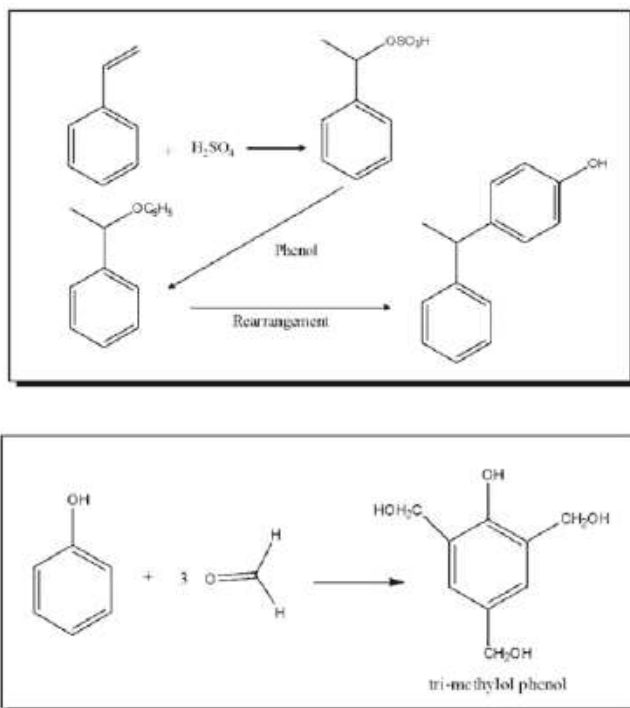
Fig. 3.10 Substitution of styrene with phenol and formation of tri-methylol phenol [95]. Adapted and reproduced with permission. Copyright, 2000 Elsevier Ltd

In addition, the new phenol-based catalysts were cheap when compared with the styrene-DVB equivalent products.

Harmer and Sun [18] proposed a different way to contour the problem of resin deactivation. They suggested a composite between Nafion® resin and silica as an alternative to the typical cation-exchange resins in alkylation of phenol, due to its higher thermal stability. Their experiments showed that the 13 wt% Nafion® resin/silica composite was efficient in catalyzing the alkylation of *p*-cresol with isobutene under mild conditions (50 °C). Additionally, they found that the composite was more active as well as selective (*C*-alkylation vs. *O*-alkylation) than the Nafion® resin pellets and Amberlyst®-15 catalyst.

It is known that Friedel–Crafts alkylation of phenols, using solid acids, resulted in the formation of both *O*- and *C*-alkylated products, and selectivity depends on parameters such as temperature, pore size, and nature of active sites present in the catalyst, an alkylating agent and solvent [96–98]. Yadav and Pathre [99] evaluated a series of solid catalysts such as sulfated zirconia, and the cation-exchange resins (Amberlyst-15 and Indion-130) in the case of the alkylation of guaiacol(2-methoxyphenol) with cyclohexene (Fig. 3.11).
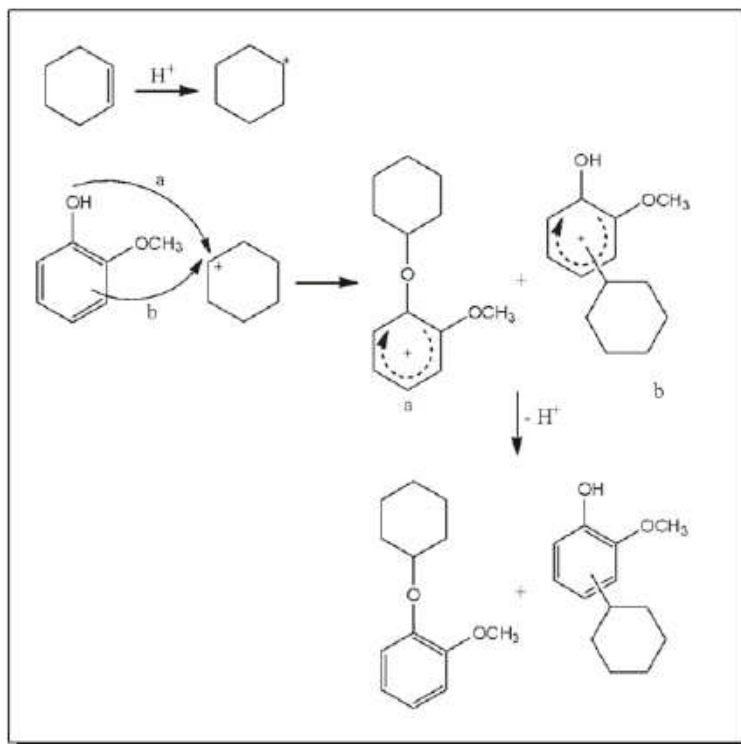
Fig. 3.11 Reaction path for the reaction between guaiacol and cyclohexene [99]. Adapted and reproduced with permission. Copyright, 2006 Elsevier Ltd

In their work, the aim was to achieve maximum selectivity for the *O*-alkylated product 1-cyclohexyloxy-2-methoxybenzene(cyclohexyl-2-methoxyphenyl ether), because of its use as a perfumery compound. However, both *O*- and *C*-alkylated products are useful in a variety of industries, and thus selectivity of one of the products is a challenging issue since costs related to the separation and purification would be reduced. Sulfated zirconia, with large mesopores, contains both Brønsted and Lewis acid sites, and hence the bulky *O*-product can be easily formed. Thus, this catalyst resulted in high conversion (74%) and selectivity for the *O*-alkylated product (72%). They suggested that a synergistic effect between Lewis and Brønsted acids occurred, resulting in *O*-alkylation selectivity. Amberlyst-15 and Indion-130, ion-exchange resins, have only Brønsted acidity, and hence resulted in good selectivity for *C*-alkylated products [93].

Aiming to understand the complex acid-catalyzed refining of bio-oil, Pittman and coworkers [100] studied liquid-phase reactions of 1-octene with phenol in different media such as water, acetic acid, methanol, and 2-hydroxymethylfuran using acid catalysts including 30 wt% acidic salt $Cs_{2.5}H_{0.5}PW_{12}O_{40}$ supported on K-10 clay (30%Cs2.5/K-10), Nafion (NR50), and Amberlyst-15. In their study, the temperature
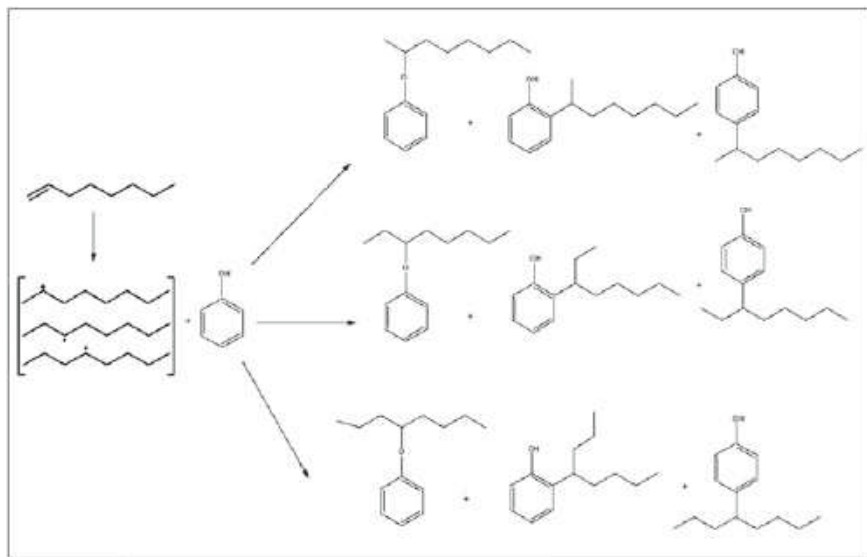
Fig. 3.12 Main reactions in alkylation of phenol with 1-octene [100]. Adapted and reproduced with permission. 2010 American Chemical Society

was kept in the range 40–120 °C. In the alkylation of phenol with 1-octene, both *O*- and *C*-alkylated products were formed, including isomeric octyl phenyl ethers (*O*-alkylates) and octyl phenols (*ortho/para*-*C*-alkylates), as illustrated in Fig. 3.12.

Both catalysts evaluated had a high activity and selectivity for *O*-alkylation of phenol with 1-octene, and it was observed that phenol conversion increased significantly with increasing temperature in cases of both Amberlyst-15 and 30%Cs2.5/K-10, suggesting a kinetic control. *O*-alkylation selectivity decreased with increasing temperature, from 60 to 100 °C as equilibrium control increasingly dominates. At high temperature, the formation of *O*-alkylated product was reversible [93] and the more thermodynamically stable *C*-alkylated products were formed. Differences between the reactivities of 1-octene, 2,4,4-trimethylpentene, and cyclohexene with phenol were also examined during their studies. Amberlyst-15 and 30%Cs2.5/K-10 exhibited similar activities and selectivities. However, the olefins that form more reactive carbocations (secondary) reacted faster than 2,4,4-trimethylpentene, which forms a tertiary carbocation upon protonation. They found that tertiary and secondary carbocations reacted most rapidly to form *O*-alkylated products. On the other hand, phenyl *t*-alkyl ethers isomerized more rapidly to *C*-alkylated products than phenyl *sec*-alkyl ethers. Isomerization of *O*-alkylated product phenyl-1,1,3,3-tetramethylbutyl ether to the C-alkylated products (*o*- and *p*- isomers) was faster because ether cleavage to the tertiary dimethyl neopentyl carbenium ion required lower activation energy than the corresponding cleavage of 2-phenyoxyoctane. The presence of water, acetic acid, and methanol lowered the yield of alkylated phenols by the competitive formation of octanols and dioctyl ethers, octyl acetates, and methyl ethers, respectively. They

found that 30%Cs2.5/K-10 was tolerant to water, while Amberlyst-15 decomposed at high temperatures and high water content. In addition, 2-hydroxymethylfuran deactivated catalysts, indicating future problems related to furan derivatives in bio-oil. Considering the desired application, these reactions constitute bio-oil upgrading possibilities and need to be taken into account to design adequate catalysts and choose the best conditions to use in exploring a process design for refining bio-oil.

Recently, Ramos and coworkers [101] studied the liquid-phase alkylation of phenol with linear and branched olefins (1-octene and diisobutylene) in a batch reactor, comparing conversion and selectivity trends while using homogeneous (sulfuric acid) and heterogeneous (Amberlyst-15) acid catalysts. They found that heterogeneous Amberlyst-15 showed satisfactory conversions with both olefins, despite being less active than sulfuric acid. Higher conversions were obtained with diisobutylene than with 1-octene. *C*-alkylation was dominant in the reaction with diisobutylene, but *O*-alkylation was predominantly observed under mild reaction conditions in the reactions with 1-octene. The temperature was the key parameter to define conversion and selectivity trends, as evidenced by factorial experimental design. In addition, the highest yields of di- and tri-alkylated products were obtained at high temperatures.

Vavasori and coworkers [102] studied the kinetics of phenol cyclohexylation catalyzed by sulfonic resins, taking into account equilibria and side reactions. The influence of different sulfonic resins (Amberlyst-15-SO_3 H and Amberlyst-36-SO_3H) was evaluated and only a small variation of the catalyst activity, referring to the acid amount, was observed. They found that selectivity is not affected by the type of the catalyst. In order to study the kinetics of the reaction, the effect of reagent concentration on the reaction rate has also been studied, together with the reactivity of the cyclohexyl phenyl ether as intermediate. From the obtained results, a reaction mechanism with the occurrence of both strong phenol–cyclohexene adsorption and strictly dependence of the rate of reaction from the phenol concentration simultaneously was proposed. Thus, a surface complex is formed by phenol and cyclohexene adsorbed on the sulfonic groups of the resin, and this complex reacted with a molecule of phenol in solution. From this and other evidence, an Eley–Rideal-type kinetic model was proposed, and it was possible to obtain the kinetic constant of each stage. In addition, it was concluded that the rearrangement of the ether and its decomposition were catalyzed by the free acid sites. The model satisfactorily fits the obtained results, and thus it is providing a comprehensive explanation of the different aspects of the reaction.

Krymkin et al. [103] investigated the liquid-phase alkylation of phenol with diisobutylenes (DIB) in the presence of the ion-exchange resin, Amberlyst-36 Dry. They observed that the alkylation of phenol with DIB occurred only in the aromatic ring to form 2-TOPh and 4-TOPh (2- and 4-tert-octylphenol) under selected reaction conditions. Alkyl phenyl ethers were not formed. It was also observed that 4-TOPh can be obtained with high selectivity over acid catalysis, even considering that phenol and DIB are high-reactive substances. At low temperature (329 K), the amount of 4-TOPh was almost 120 times higher than 2-TOPh at equilibrium. However, the ratio 4-TOPh/2-TOPh decreased when temperature increased. They observed that low temperatures improved the overall selectivity of the phenol alkylation process with
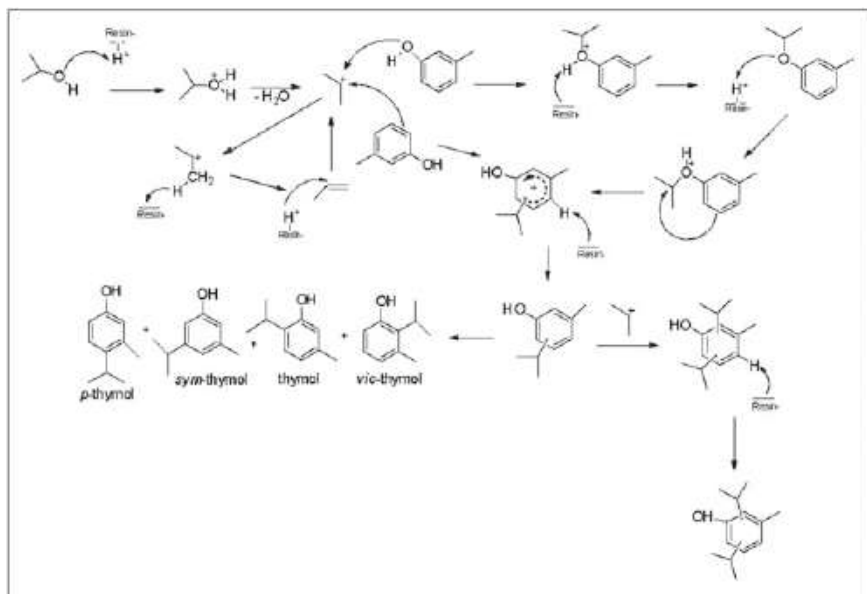
Fig. 3.13 Reaction route of alkylation of *m*-cresol with isopropyl alcohol [104]

DIB. In addition, the results obtained in the kinetic study showed that the activation energy of destructive transalkylation was higher than the other reactions considered. Thus, low-temperature reaction led to a decrease in the amount of tert-butyl phenol (TBPhs).

Sandulescu and coworkers [104] investigated the alkylation of *m*-cresol with iso-propyl alcohol (IPA) using strong acid resin catalysts (CT-151 DR Resin and Nafion NR-50) under microwave irradiation and conventional heating, in the absence of solvent, in order to prepare alkylphenols, especially mono-alkylphenols. Figure 3.13 shows the proposed mechanism that may lead to mono-alkylated products, but di-alkylated products may also be formed since the isopropyl cation can attack the aromatic ring of the mono-alkylated products, formed in the first step.

They found that under conventional heating, the time of the reaction and the catalyst loading can influence the selectivity of the reaction, resulting in thymol, *p*-thymol, and *sym*-thymol as main products. On the other hand, use of microwave-assisted synthesis, resulting in a shorter reaction time and different product distributions, producing thymol, *p*-thymol, and *vic*-thymol as main products. If the time is too short, the *O*-alkylated compound is obtained in significant amounts. However, within 30 min, the product is completely converted to *C*-alkylated. Thus, the reaction is significantly influenced by reaction parameters, and selectivity can be adjusted by choosing the appropriate reaction conditions. In another approach, Tang and coworkers [105] used ab initio density functional theory (DFT) to study the mechanism of phenol alkylation in the presence of a cation-exchange resin catalyst, Amberlyst-15,
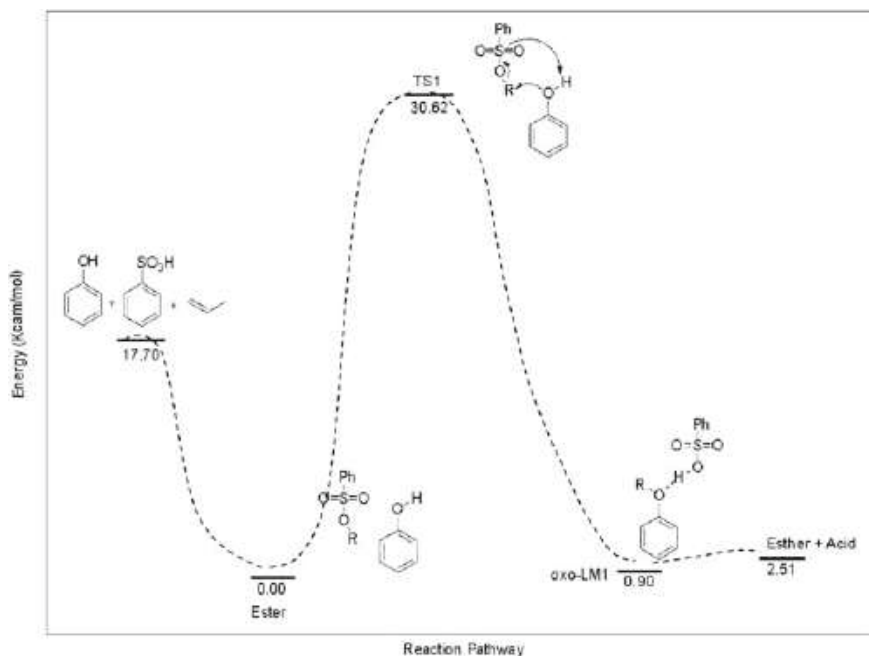
Fig. 3.14 Reaction pathway proposed for the direct *O*-alkylation [105]. Adapted and reproduced with permission. 2006 American Chemical Society

which was modeled with the benzene sulfonic acid. In their study, the effect of the modeled acid catalyst on olefins such as isopropene (*i*-Pr) and tributene (*t*-Bu) in a phenol solution was evaluated, in an attempt to mimic the experimental conditions. They proposed a combination of neutral and ionic multistep reaction mechanism, in which an exothermic reaction between olefin and the benzene sulfonic acid forms an ester, and then three reaction pathways would lead to direct *O*-alkylation, *o*-*C*-alkylation, and *p*-*C*-alkylation. From calculations, they found that in neutral conditions, *O*-alkylation was the most energetically favorable way. Figure 3.14 shows the reaction pathway to direct *O*-alkylation of phenol.

Formation of *C*-alkylphenols, on the other hand, can be explained by intramolecular migrations of the alkyl group from *O*-alkylated products, in an ionic rearrangement, resulting in *o*-*C*-alkylphenol and *p*-*C*-alkylphenol (Fig. 3.15). Protonation reduced transition barriers for these migrations to occur, and the competition between R and H at the substitutive size determined the ortho/para ratio of the *C*-alkylated products.

Bilenchenko et al. [106] performed an experimental study on the kinetics of reactions occurring in the alkylation of phenol with straight-chain alkenes (C9, C16) over a series of sulfonic acid cation-exchange resins such as Amberlyst-15 Dry, Amberlyst-35 Dry, Amberlyst-36 Dry, Amberlyst-70, Amberlyst DT, Tulsion 66 MP, Lewatit K2640, Lewatit K2431, and Relite EXC8D. The effects of process
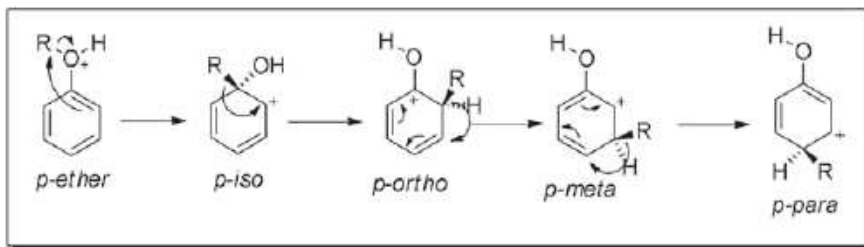
Fig. 3.15 Five possible protonated configurations, *p*-ether, *p*-ipso, *p*-ortho, *p*-meta, and *p*-para, for migrations of the alkyl group in the proposed ionic pathway [105]. Adapted and reproduced with permission. 2006 American Chemical Society

parameters such as reaction temperature, water content, and alkene chain length on the kinetics of various types of reactions were analyzed. They found that rate constants of all evaluated reactions decreased on passing from 1-nonene to straight-chain hexadecene. In the alkylation reactions of phenol with straight-chain alkenes, the *ortho/para*-alkylphenol ratio was basically equal to the statistical ratio for all of the resins examined in their work. Lewatit K2640, Lewatit K2431, Tulsion 66 MP, and Amberlyst-15 presented comparable activities in alkylation reactions of phenol with nonene, showing the best performances among the evaluated resins, in the absence of water. However, it was found that increasing amounts of water decreases the rate constants of all reactions, and increases activation energies and the relative yield of alkyl phenyl ethers. In addition, it also diminished the alkylphenol selectivity of the reactions.

3.8   Alkylation of Furan and Indol Derivatives

The alkylation of heterocyclic systems such as furan and indole is a fascinating procedure that has found application in differentiated fields [19, 106]. The indole is a biologically privileged structure, whose derivatives have shown utility mainly as drugs or precursors of these. On the other hand, furan is a less required scaffold to access drugs, but their alkylated derivatives have received attention for applications related to obtaining synthetic fuels. The importance and application of ion-exchange resins as catalysts in alkylation reactions of these two heterocyclic systems of great interest are presented in the following section.

Indole **1** and furan **2** are aromatic heterocyclic electron-rich compounds, whose functionalization takes place preferentially on C-3, C-2, and C-5, respectively, through electrophilic aromatic substitution (Fig. 3.16). Due to this, the procedures developed to date for the alkylation of indole and furan catalyzed by ion-exchange resins are a matter that involves reactivity only in the indicated position. The widely
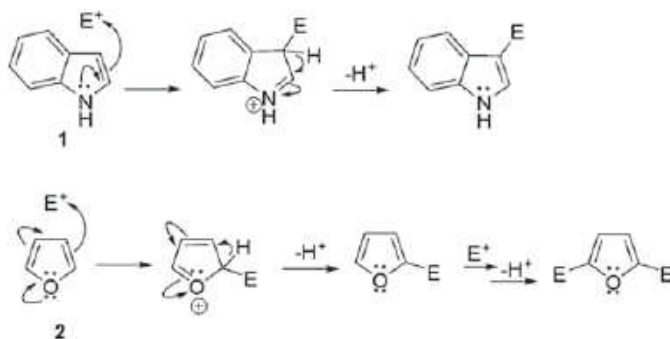
Fig. 3.16 Electrophilic aromatic substitution on C-3 to the indole and C-2 and C-5 to the furan

recognized Friedel–Crafts alkylation reaction is the route through which the formation of CAr-Csp^3 bonds occurs in this type of systems.

3.8.1 Indole Alkylation

During the last 20 years, several alkylation protocols have been developed to introduce structural diversity in the indole ring using cation-exchange resins as catalysts. In these procedures, unsaturated substrates such as carbonyl compounds, activated alkenes, and imines have found large application as electrophiles [107–110].

Work performed by the Zhao group showed that commercial Amberlyst type [108, 109] and synthetized p-(ω-sulfonic-perfluoroalkylated)polystyrene (FPS) [110] ion-exchange resins can be used for alkylation of indole with hexanal **2** and benzylideneaniline **4** (Fig. 3.17). FPS resin was the most efficient since high yields of bis-indolylmethanes **3** and **6** were obtained with only half the reaction time (12 h) required in the presence of the other resins tested. The synthesis of bis-indolylmethanes was also explored with other carbonyl compounds and Amberlyst-15 as a catalyst, reaching to the yield of up to 100% [109]. Similar research found that Zeokarb-225 resins [111] and Indion Ina 225H [112] have higher efficiencies than Amberlyst-15 and FPS, in the preparation of **6** using benzaldehyde **5** as an alternative alkylating reagent. Zeokarb-225 also provided high yields in obtaining a varied set of bis- and tris-indolylmethanes from the alkylation of indole, 2-phenylindole, and 2-methylindole with aryl aldehydes. The same happened with the alkylation of indole, 5-bromoindole, and 5-hydroxylindole with aryl aldehydes and alkyl aldehydes using Indion Ina 225H as a catalyst.

Bandini et al. [113] described the alkylation of 2-methylindole **6** with α,β-unsaturated carbonyls and nitro compounds, as a novel heterogeneously catalyzed Friedel–Crafts Michael-type addition (Fig. 3.18). Sulfonic resins such as Amberlyst-15, 35, 36, and 40, employed at 20% wt allowed **8** to be isolated with a yield
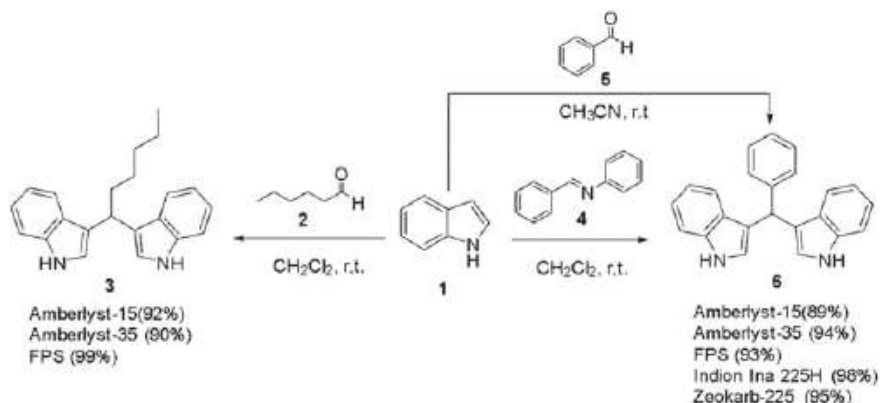
Fig. 3.17 Alkylation of indole with hexanal **2**, benzylideneaniline **4** and benzaldehyde **5**
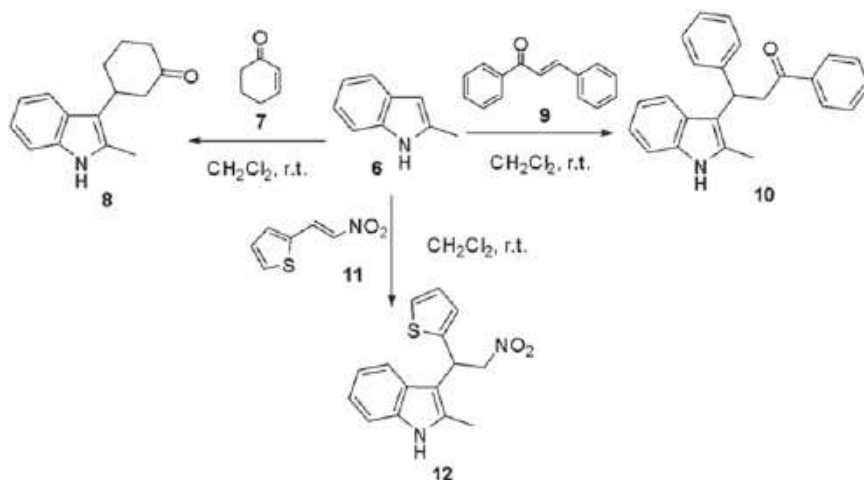
Fig. 3.18 Alkylation of 2-methylindole with α,β-unsaturated carbonyls and nitro compounds

of 61 to 76% after 24 h of reaction. By contrast, when the perfluorinated resin-sulfonic acid Nafion-H was examined, the adduct **8** was obtained with moderated yield (46%). Additional experiments with Amberlyst-15 showed that chemical outcomes are improved by increasing the electro-deficiency of the double bond of the alkylating reagent by linking aryl and nitro groups. For instance, **9** and **11** allowed access to **10** and **12** products with yields of 95 and 96%, respectively. The authors also reported the use of Amberlyst-15 as a convenient catalyst to carry out a practical, continuous, and highly atom economic semicontinuous process using common laboratory equipment and mild experimental conditions.

Amberlyst-15 was introduced as a catalyst for the transformation of indole and substituted derivatives with novels electrophiles: propargylic acetates **19** [114] and
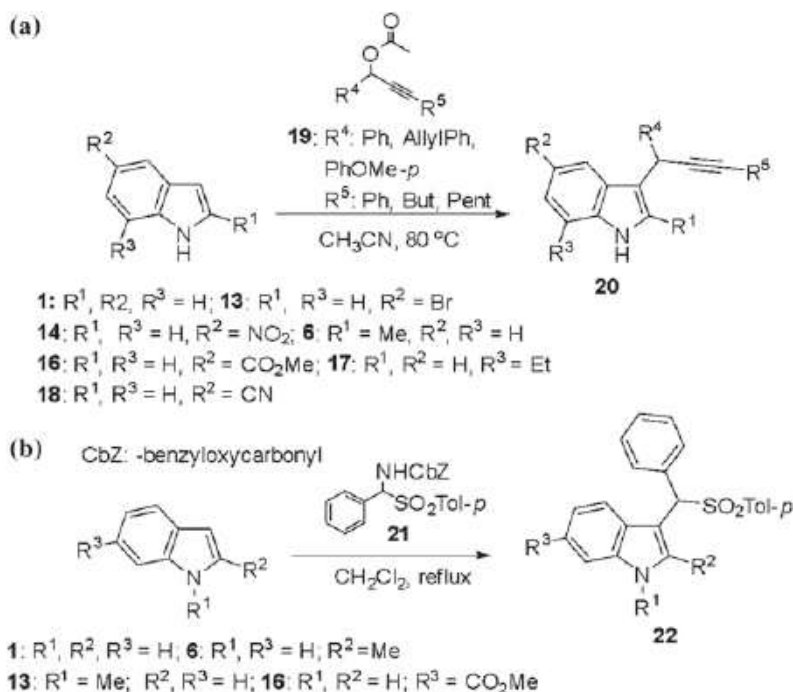
Fig. 3.19 Amberlyst-15-catalyzed alkylation of indole and substituted derivatives with **a** propargylic acetates and **b** *N*-benzyloxycarbonylamino phenyl *p*-tolylsulfone [115]. Adapted and reproduced with permission. 2004 American Chemical Society

α-amido sulfone **21** [115] (Fig. 3.19). With **19,** the resin promoted high yields for the alkylated products **20** (84–93%), while the yields obtained with **21** for the synthesis of **22** were moderate (45–51%).

Asymmetric catalysis, despite being one of the most prominent lines of research in modern organic chemistry, exhibits some important limitations. The high cost and resulting metallic impurities, both associated with the catalysts themselves, limit their use on a large scale and make it difficult to purify the synthesized products, respectively [116]. In order to reduce the impact of the aforementioned problems, ion-exchange resins have been introduced in this field. However, in this type of process, the resin does not properly constitute the catalyst. This is used as an organic support to immobilize the catalytic species, which facilitates their reuse and separation from target products. Evidently, the developed catalysts could be considered as cation-exchange systems since the reaction, as well as all the others treated in this section, occurs through the Friedel–Crafts alkylation reaction. Indoles with stereocenter in the α-, β-positions of the side chain in the ring have been obtained through this versatile catalytic system.

Desyatkin et al. [117] have recently immobilized the complex of copper(II) trifluoromethanesulfonate with chiral isopropyl bis(oxazoline) ligand (i-Pr-Box) on
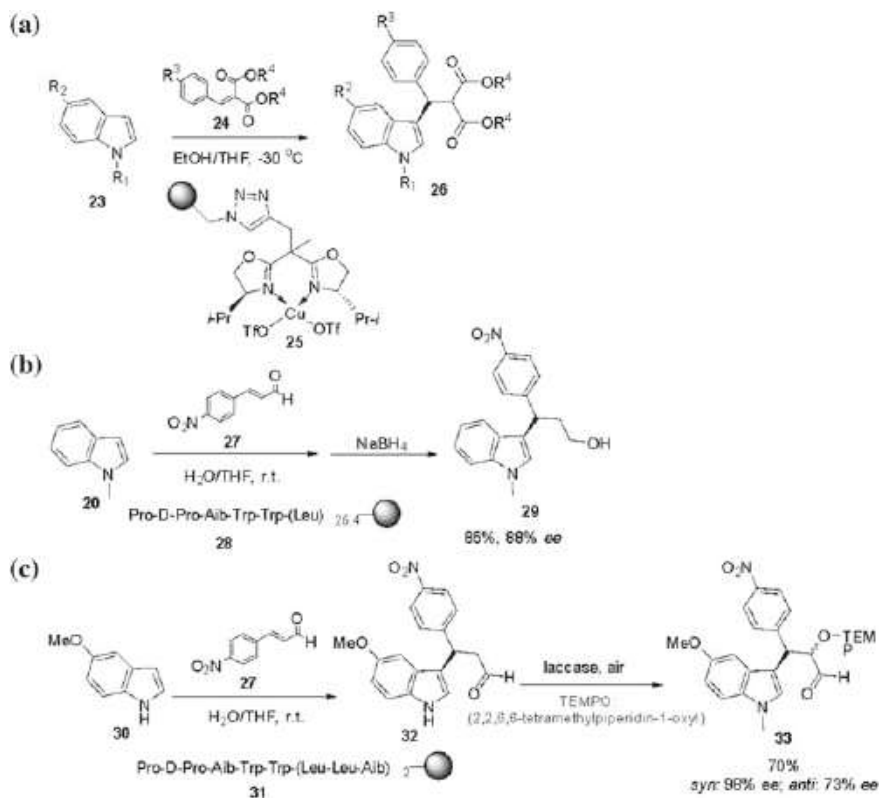
Fig. 3.20 Alkylation asymmetric of indoles assisted by the resin-supported catalyst

Merrifield resin following "click" procedure. The resulting catalytic system **25** was used to perform the asymmetric Friedel–Crafts alkylation of a set of indol and 1,5-indole substituted **23** with benzylidenemalonates **24** (Fig. 3.20a). The desired product **26** was obtained with a high yield (up to 99%) and enantiomerically enriched (up to 97% ee), after being recycled several times. The results showed that the catalyst can be recycled five times without appreciable loss of activity and enantioselectivity. In other work, organic catalysts were developed by Kudos's group to affect the asymmetric Friedel–Crafts alkylation of indolic substrates in an aqueous medium. The catalysts were *N*-terminal prolyl peptides supported on an amphiphilic polyethyleneglycol-grafted cross-linked polystyrene (PEG-PS) resins (**28** and **31**) [118, 119]. Two representative examples from these works showed the good yields and the high enantioselectivity achieved with these catalytic systems (Fig. 3.20b,c).

Conventional metal catalysts supported on cation-exchange resins have opened pathways for obtaining achiral indole derivatives. Yu et al. [120] checked the performance of several different Ytterbium(III)-Resins in the alkylation of indole with hexanal, to synthesize the product **3** (Fig. 3.17). The most efficient catalytic systems

were obtained with Amberlyst XN-1010 and Amberlyst-15, achieving yields of 93 and 90%, respectively. The use of resins such as Amberlite CG-50 and Amberlite IRP-6 constituted weak acids (carboxylic acids) and provided the product with low yields. Similarly, Havránková et al. [121] recently reported an alternative catalyst for obtaining bis-indolylmethane **6** with benzaldehyde **5** (Fig. 3.17). The synthesis of this and other indole derivatives was catalyzed by Cerium (III) supported on Purolite C104 Plus resin, a weakly acidic macroporous material which showed at least the same or better catalytic activity as that of $CeCl_3.7H_2O$ and other catalytic systems [121].

3.8.2   Furan Alkylation

In principle, the furan ring could undergo alkylation with the same kinds of electrophiles that were described for indole. However, as the focus of application has been on acquiring appropriated intermediaries to obtain diesel, gasoline, or jet fuel synthetics, the reported works limited to the range of alkylating agents, mainly in carbonyl compounds. Cationic-exchange resin catalysts have played a very important role in the development of this important research niche.

Although the development of works related to obtaining synthetic fuel intermediaries began at the beginning of this century [122], the previous works already reported protocols for the hydroxyalkylation and alkylation of furan **2** and 2-methylfuran (2-MF) (or Sylvan) **41** using cation-exchange resins as catalysts [123, 124] (Fig. 3.21). Iovel et al. [123] found that the reaction between furan **2** and formalin in the presence of Amberlyst-15 and Dowex 50WX4 yielded furfuryl alcohol **35** and 2,2′-bisfurylmethane **36**. While, in the same reaction, in presence of Amberlyst-15, 2,5-bis (2-furanylmethyl) furan **37** was also found (Fig. 3.21a). Amberlite IRC-50 did not promote this reaction. Appropriate conditions such as low amounts of Amberlyst-15 (5–10 mol% relative to the substrate) and a ratio 2:34 of 1:2.5-3 were found to limit the reaction to the hydroxymethylation allowing the product **35** with yields greater than 90% to be obtained. A greater amount of the catalyst promoted higher yields of **36**, **37**. On the other hand, in the hydroxymethylation of **41**, the checked resins showed an increasing efficiency in accordance with the increase in their acid strength: Amberlite IRC-50 ≪ Dowex 50WX4 ≤ Amberlyst-15. The main product of the reaction was **43** with achieved yield up to 95% with Amberlyst-15 (Fig. 3.21b). Amberlyst-15 also showed good efficiency in the alkylation of **2** with t-butanol **38** (Fig. 3.21a). When the reaction was carried out in a ratio **2:38**: resin of 7.5:1:1.15, the product of the first alkylation **39** was obtained with 80% yield. Under similar reaction conditions, but with a ratio of 4:1:2.15, the majority product was **40** (75%) [124].

The 2-MF, an abundant product derived from biomass, is presently the main substrate used in research dealing with the obtaining of synthetic fuel precursors by catalysis with cation-exchange resins, under solvent-free conditions. The advantages offered by this building block, in comparison to the furan, include its greater reac-
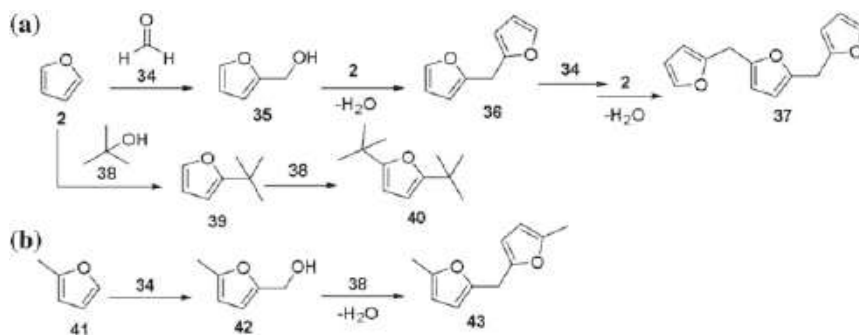
Fig. 3.21 Hydroxymethylation and alkylation of **a** furan with aqueous formaldehyde and t-butanol and **b** 2-MF with aqueous formaldehyde

tivity and limited extension of the alkylation reactions, the latter necessary to obtain biocarburants with a suitable number of carbons. Pioneering work in this research line was carried out by the Corma group [125, 126], which checked sulfonic resins as well as other types of acid catalysts. As part of this work, the authors used butananal **44** and 5-hydroxymethylfurfural **45** as alkylating electrophiles and Amberlyst-15 and Dowex 50WX2-100 resins as acid catalysts (Fig. 3.22). The catalysts had, in general, a good and comparable efficiency, obtaining yields for **42** of up to 90% with Amberlyst-15, and up to 80% with Dowex 50WX2-100, when the butanal was used as an alkylating reagent. Catalyst regeneration was identified as the critical step with sulfonic resins [124].

Subsequent works performed by the Zhang group explored more extensively the alkylation of 2-MF with a diverse set of resins and electrophiles. These studies evaluated the use of Nafion-115, -212, -1135 and Amberlyst-15, -36 with acetone **47** and furfural **49** [127]; Nafion-212 with acetone **47** and butanal **44** [128]; Nafion-212, -115 and Amberlyst-15, -36 with hydroxyacetone **52** [129]; and Nafion-2012
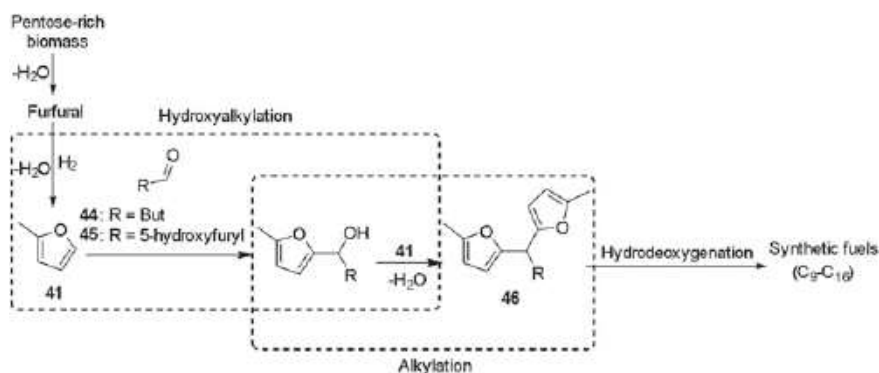
Fig. 3.22 Hydroxyalqylation/alkylation of 2-MF with butananal and 5-hydroxymethylfurfural
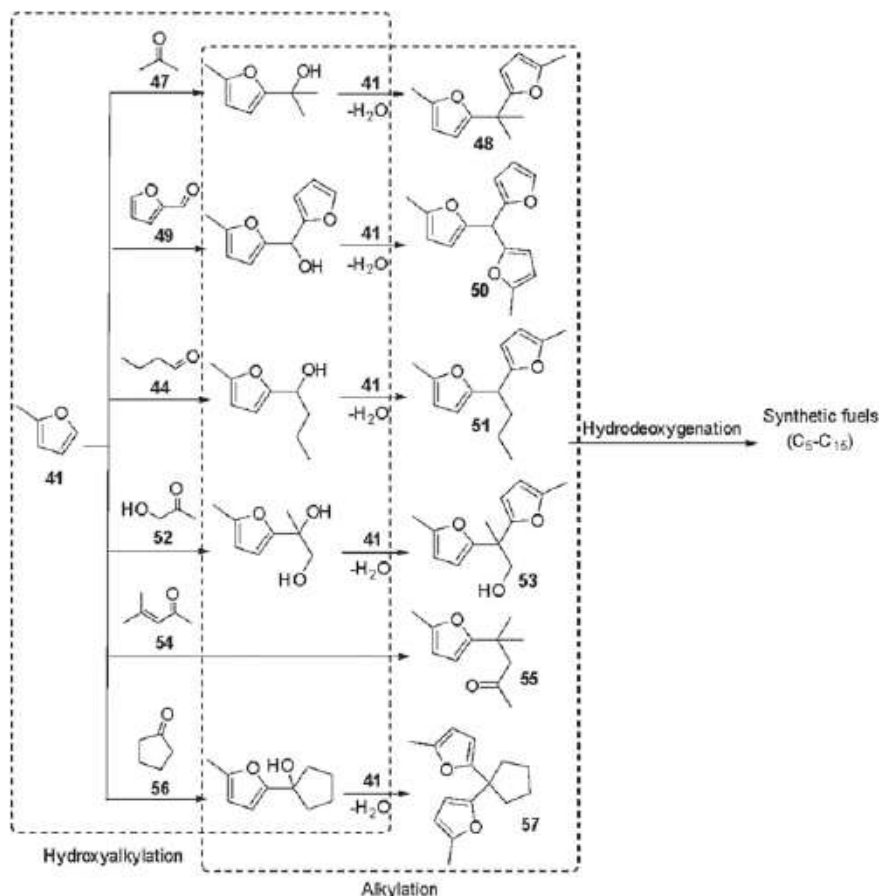
Fig. 3.23 Hydroxyalqylation/alkylation of 2-MF performed by the Zhang's group

and Amberlyst-15, -36 with mesityl oxide **54** [130, 131] and cyclopentanone **56** [130, 131]. Among the investigated catalysts, Nafion-212 resin exhibited the highest activity and stability (Fig. 3.23).

Deng et al. [132] used cyclohexane as alkylating reagent. Nafion-2012 allowed access to the hydroxyalkylation/alkylation product with a high yield (89%); and Amberlyst-15 showed to be effective in controlling the reaction, reaching a yield of 76% for the hydroxyalkylation product. In other research, Zhu et al. [122] proposed 3-hydroxy-2-butanone as electrophile to react with 2-MF and other analogous systems. It should be noted that within the different proposed reactions, the route with 2-MF was the only one that involved furan ring alkylation. Among the 12 catalysts evaluated, the Nafion-2012 and Amberlyst-15 resins allowed the product with comparable yields (80 and 78%, respectively) to be obtained, these being the catalysts
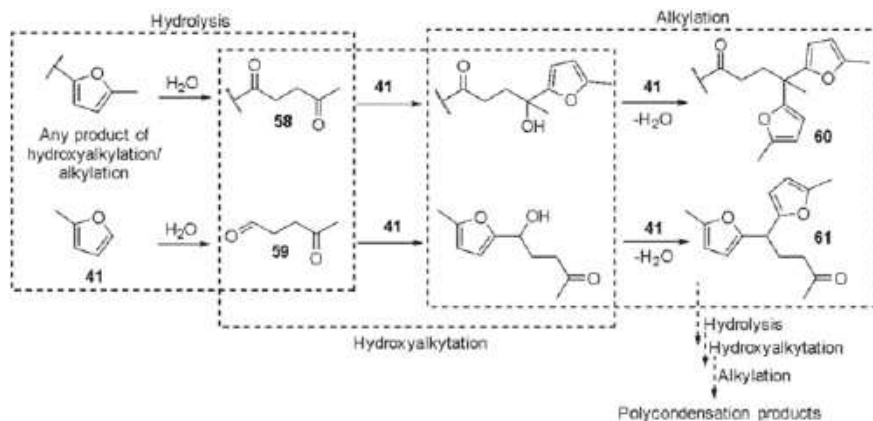
Fig. 3.24 Side reactions promoted by the acid catalyst in the presence of water

that showed the highest efficiency after zirconia supported trifluoromethanesulfonic acid (TFA-ZrO$_2$).

Whenever an aldehyde (**44** or **47**) was compared with acetone, the highest yields were obtained with the former [127, 129]. The authors attributed this observation to the higher reactivity of the aldehyde and the deactivating effect on the catalyst that could have products of side reactions, favored by the presence of acetone. In acid catalytic sites, water generated during hydroxyalkylation/alkylation can hydrolyze the furan ring present in the products of this reaction and 2-MF **41**, to produce diketones **58** and 4-oxopentanal **59**, respectively (Fig. 3.24). These are then attacked by two molecules of 2-MF, as side reaction of hydroxyalkylation/alkylation (Fig. 3.17). Hydrolysis/Hydroxyalkylation/alkylation sequences can continue to occur due to the reactivity of the furan ring and the ketone group present in **60** and **61**. Products resulting from this polycondensation plug the pores of the catalyst affecting their activity. In the presence of an aldehyde as an electrophile, 2-MF is consumed more quickly than in the presence of acetone, decreasing the polycondensation. Water produced also reduces catalyst activity by means of acid leveling effect, as pointed out by other authors [19, 132]. As expected, hydroxyacetone **52** (acetone containing the electron-withdrawing hydroxyl group) was more reactive than acetone allowing to improve the product yield in relation to previous results [129].

In order to minimize the loss of activity induced by water, recently Zhang et al. [19] synthesized hydrophobic mesoporous resins with a sulfonic acid group (PS) and fluoride sulfonic acid group (PCS) by a simple solvothermal reaction and ion-exchange treatment. The new water-resistant materials were tested in the hydroxyalkylation/alkylation of 2-MF with cyclic ketones (cyclopentanone and cyclohexanone). The results showed that PS has higher activity and selectivity than Amberlyst-15 while PCS surpassed Nafion-212. Furthermore, both PS and PCS have good recycling stabilities for consecutive five runs.

3.9 Conclusions

Ion-exchange resins have interesting applications as catalysts in alkylation reaction, which is widely employed in different areas such as fuels, cleaning products, and pharmacological products. Recently, the use of biomass as a raw material to produce chemicals and renewable fuels has been showed to be an alternative source of fossil feedstock and some examples using ion-exchange resins have emerged. The interest in ion-exchange resins such as polystyrene sulfonic acid resins is due to their mild and highly selective properties, environmentally benign character, and commercial availability. However, solid acid catalysts showed lower strength than the homogeneous catalysts and some aspects such as diffusional and stability problems may be considered. A recent promising new approach is the synthesis of materials such as Nafion–silica nanocomposites and sulfonated polystyrene encapsulated within the confined nanospace of hollow silica nanospheres. These nanocomposite materials have shown good catalytic activity and stability in alkylation reactions and hoped to contribute to the development of future industrial processes.

References

1. Olah GA (1963) Friedel-Crafts and related reactions. Wiley-Interscience, New York
2. Tanabe K, Holderich WF (1999) Industrial application of solid acid-base catalysts. Appl Catal A 181:399–434
3. Perego C, Ingallina P (2002) Recent advances in the industrial alkylation of aromatics: new catalysts and new processes. Catal Today 73:3–22
4. Busca G (2007) Acid catalysts in industrial hydrocarbon chemistry. Chem Rev 107:5366–5410
5. Wang H, Meng X, Zhao G, Zhang S (2017) Isobutane/butene alkylation catalyzed by ionic liquids: a more sustainable process for clean oil production. Green Chem 19:1462–1489
6. Wang JJ, Chuang YY, Hsu HY, Tsai TC (2017) Toward industrial catalysis of zeolite for linear alkylbenzene synthesis: a mini review. Catal Today 298:109–116
7. Singhal S, Agarwal S, Arora S, Singhal N, Kumar A (2017) Solid acids: potential catalysts for alkene-isoalkane alkylation. Catal Sci Technol 7:5810–5819
8. Dolganova I, Ivanchina E, Ivashkina E (2018) Alkylaromatics in detergents manufacture: modeling and optimizing linear alkylbenzene sulfonation. Surfct Deterg 21:175–184
9. Weissemel K, Arpe HJ (1997) Industrial organic chemistry, 3rd edn. VCH, Weinheim, p 358
10. Pal R, Sarkar T, Khasnobis S (2012) Amberlyst-15 in organic synthesis. Arkivoc 1:570–609
11. Dasgupta S, Török B (2008) Environmentally benign contemporary Friedel-Crafts chemistry by solid acids. Curr Org Synth 5:21–342
12. Zhang X, Zhao Y, Xu S, Yang Y, Liu J, Wei Y, Yang Q (2014) Polystyrene sulphonic acid resins with enhanced acid strength via macromolecular self-assembly within confined nanospace. Nat Commun 5:3170
13. Li H, Riisager A, Sravanamurugan S, Pandey A, Sangwan RS, Yang S, Luque R (2018) Carbon-increasing catalytic strategies for upgrading biomass into energy-intensive fuels and chemicals. ACS Catal 8:148–187
14. Alfs H, Steiner H, Grunheit KH (1979) Bohm, G. Process for continuous alkylation of phenol using ion exchange resins. USA 4,168,390
15. Li L, Zhang J, Du C, Luo G (2018) Process intensification of sulfuric acid alkylation using a microstructured chemical system. Ind Eng Chem Res 57:3523–3529

16. Li Y, Liu R, Zhao G, Zhou Z, Zhang J, Shi C, Liu X, Zhang X, Zhang S (2018) Simulation and optimization of fixed bed solid acid catalyzed isobutane/2-butene alkylation process. Fuel 216:686–696

17. Sharma MM (1995) Some novel aspects of cationic ion-exchange resins as catalysts. React Funct Polym 26:3–23

18. Harmer MA, Sun Q (2001) Solid acids catalysis using ion exchange resins. Appl Catal A Gen 221:45–62

19. Zhang X, Deng Q, Han P, Xu J, Pan L, Wang L, Zou JJ (2017) Hydrophobic mesoporous acidic resin for hydroxyalkylation/alkylation of 2-methylfuran and ketone to high-density biofuel. AIChE J 63:680–688

20. Gelbard G (2005) Organic synthesis by catalysis with ion-exchange resins. Ind Eng Chem Res 44:8468–8498

21. Zhang X, Yaopeng ZY, Yang Q (2014) PS-SO$_3$H@phenylenesilica with yolk–double-shell nanostructures as efficient and stable solid acid catalysts. J Catal 320:180–188

22. Teixeira VT, Coutinho FMB (2010) Morphological study on the reactivity of styrene-divinylbenzene copolymers in a chloromethylation reaction. J Appl Polym Sci 118:2389–2396

23. Kunin R, Meitzner E, Bortnick N (1962) Macroreticular ion exchange resins. J Chem Soc 84:305–306

24. Millar JR, Smith DG, Marr WE, Kressman TRE (1963) Solvent modified polymer networks. Part I. The preparation and characterisation of expanded-network and macroporous styrene-divinylbenzene copolymers and their sulphonates. J Chem Soc: 218–225

25. Kun KA, Kunin R (1964) Pore structure of some macroreticular ion exchange resin. Polym Lett 12:587–591

26. Sederel WL, de Jong GJ (1973) Styrene-divinylbenzene copolymers. Construction of porosity in styrene divinylbenzene matrices. J Appl Polym Sci 17:2835–2846

27. Poinescu IC, Beldie C, Vlad C (1984) Styrene divinylbenzene copolymers: influence of the diluent on network porosity. J Appl Polym Sci 29:23–34

28. Okay O, Balkas TI (1986) Heterogeneous styrene-divinylbenzene copolymers in collapsed and reexpanded states. J Appl Polym Sci 31:1785–1795

29. Rabelo D, Coutinho FMB (1994) Structure and properties of styrene-divinylbenzene copolymers I. Pure solvents as pore forming agents. Polym Bull 33:479–486

30. Okay O (1999) Phase separation in free-radical crosslinking copolymerization: formation of heterogeneous polymer networks. Polymer 40:4117–4129

31. Barton AF (1991) Handbook of solubility parameters and other cohesion parameters. CRC Press, Boca Raton

32. Hansen CM (2007) Hansen solubility parameters: a user's handbook. CRC Press, Boca Raton

33. Millar JR, Smith DG, Kressman TRE (1965) Solvent modified polymer networks. Part IV. Styrene-divinylbenzene copolymers made in the presence of non-sovating diluents. J Chem Soc: 304–310

34. Howard GJ, Midgley CA (1981) The formation and structure of suspension polymerized styrene-divinylbenzene copolymers. J Appl Polym Sci 26:3845–3870

35. Wieczorek PP, Kolarz BN, Galena H (1984) Porous structure of highly crosslinked styrene-divinylbenzene copolymers. Angew Makromol Chem 126:39–50

36. Costa LC, Gomes AS, Coutinho FMB, Teixeira VG (2010) Chelating resins for mercury extraction based on grafting of polyacrylamide chains onto styrene-divinylbenzene copolymers by gamma irradiation. React Funct Polym 70:738–746

37. Aguiar LG, Moura JOV, Neto TGS, Lopes VMP, Dias JR (2017) Prediction of resin textural properties by vinyl/divinyl copolymerization modeling. Polymer 129:21–31

38. Ahmad A, Siddique JA, Laskar MA, Kumar R, Mohd-Setapar SH, Khatoon A, Shiekh RA (2015) New generation Amberlite XAD resin for the removal of metal ions: a review. J Environ Sci 31:104–123

39. Antunes BM, Rodrigues AE, Lin Z, Portugal I, Silva CM (2015) Alkenes oligomerization with resin catalysts. Fuel Process Technol 138:86–99

40. Chakrabarti A, Sharma MM (1993) Cationic ion exchange resins as catalyst. Reac Polym 20:1–45
41. Jerabek K, Hanková L, Holub L (2010) Working-state morphologies of ion exchange catalysts and their influence on reaction kinetics. J Mol Catal A Chem 333:109–113
42. Buttersack C, Widdecke H, Klein J (1986) The concept of variable active centers in acid catalysis. PART I alkylation of benzene with olefins catalyzed by ion exchange resins. J Mol Catal 38:365–381
43. Molnár A (2011) Nafion-silica nanocomposites: a new generation of water-tolerant solid acids of high efficiency-an update. Curr Org Chem 15:3928–3960
44. Thomas JM, Thomas WJ (2015) Principles and practice of heterogeneous catalysis, 2nd edn. Wiley, KGaA
45. Luyben WL (2007) Chemical reactor design and control. Wiley, London
46. Unnikrishnan P, Srinivas D (2016) Heterogeneous catalysis. In: Industrial catalytic processes for fine and specialty chemicals. Elsevier, Joshi SS, Ranade VV (eds) CSIR-national chemical laboratory, Pune, India
47. Radcliffe WH, Kiel WL, Gosling SD, Sechrist PA, Anderson P (2004) Apparatus for alkylation using solid catalyst particles in a transport reactor USA 6,814,943 B2
48. Kaufman S, Brunswick E, Nicol RE (1969) Process for continuous alkylation of aryl hydroxides using ion- exchange resins. USA 3,422,157
49. Skripek M (1966) Process for alkylating aromatic hydrocarbons using a sulfonated resin catalyst. USA 3,238,266
50. Pines H (1981) The Chemistry of catalytic hydrocarbon conversions. Academic Press, New York
51. Olah GA, Prakash GKS, Sommer J (1985) Superacids. Wiley, New York
52. Corma A, Martinez A (1993) Chemistry, catalysts, and processes for isoparaffin-olefin alkylation: actual situation and future trends. Catal Rev-Sci Eng 35:483–570
53. Olah GA, Btamack P, Deffieux D, Török B, Wang Q, Molnár A, Prakash GKS (1996) Acidity dependence of the trifluoromethanesulfonic acid catalyzed isobutane-isobutylene alkylation modified with trifluoroacetic acid or water. Appl Catal A 146:107–117
54. Feller A, Zuazo I, Guzman A, Barth JO, Lercher AJ (2003) Common mechanistic aspects of liquid and solid acid catalyzed alkylation of isobutane with n-butene. J Catal 216:313–323
55. Esteves PM, Araujo CL, Horta BAC, Alvarez LJ, Wilson-Zicovich CM, Solis-Ramirez A (2005) The isobutylene-isobutane alkylation process in liquid HF revisited. J Phys Chem B 109:12946–12955
56. Albright LF (2009) Present and future alkylation processes in refineries. Ind Eng Chem Res 48:1409–1413
57. Hidalgo JM, Zbuzek M, Cerný R, Jísa P (2014) Current uses and trends in catalytic isomerization, alkylation and etherification processes to improve gasoline quality. Cent Eur J Chem 12:1–13
58. Shen W, Dube D, Kaliaguine S (2008) Alkylation of isobutane/1-butene over periodic mesoporous organosilica functionalized with perfluoroalkylsulfonic acid group. Catal Commun 10:291–294
59. Shen W, Gu Y, Xu H, Dubé D, Kaliaguine S (2010) Alkylation of isobutane/1-butene on methyl-modified nafion/SBA-15 materials. Appl Catal A 377:1–8
60. Shen W, Gu Y, Xu H, Che R, Dubé D, Kaliaguine S (2010) Alkylation of isobutane/1-butene on methyl-modified nafion/SBA-16 materials. Ind Eng Chem Res 49:7201–7209
61. Gobin OC, Huang Q, Vinh-Thang H, Kleitz F, Eic M, Kaliaguine S (2007) Mesostructured silica SBA-16 with tailored intrawall porosity part 2: diffusion. J Phys Chem C 111:3059–3065
62. Botella P, Corma A, Lopez-Nieto JM (1999) The influence of textural and compositional characteristics of nafion/silica composites on isobutane/2-butene alkylation. J Catal 185:371–377
63. Lyon CJ, Sarsani VSR, Subramaniam B (2004) 1-butene + isobutane reactions on solid acid catalysts in dense CO_2-based reaction media: experiments and modeling. Ind Eng Chem Res 43:4809–4814

64. Harmer MA, Farneth WE, Sun Q (1998) Towards the sulfuric acid of solids. Adv Mater 10:1255–1257

65. Heidekum A, Harmer MA, Holderich WF (1998) Highly selective fries rearrangement over zeolites and Nafion in silica composite catalysts: a comparison. J Catal 176:260–263

66. Kumar P, Vermeiren W, Dath JP, Hoelderich WF (2006) Alkylation of raffinate II and isobutane on Nafion silica nanocomposite for the production of isooctane. Energy Fuels 20:481–487

67. Alvaro M, Corma A, Das D, Fornés V, Gracia H (2004) Single step, preparation and catalytic activity of mesoporous MCM-41 and SBA-15 silicas functionalized with perfluoroalkylsulfonic acid groups analogous to Nafion. Chem Commun: 956–957

68. Macquarrie DJ, Tavener SJ Harmer MA (2005) Novel mesoporous silica-perfluorosulfonic acid hybrids as strong heterogeneous bronsted catalysts. Chem Commun: 2363–2365

69. Martinez F, Morales G, Martin A, van Grieken R (2008) Perfluorinated Nafion-modified SBA-15 materials for catalytic acylation of anisole. Appl Catal A Gen 347:169–178

70. Collins NA, Trewella JC (1997) Alkylation process for desulfurization of gasoline. US. Patent No.5, 599,441

71. Guo B, Wang R, Li Y (2010) The performance of solid phosphoric acid catalysts and macroporous sulfonic resins on gasoline alkylation desulfurization. Fuel Process Technol 91:1731–1735

72. Guo B, Wang R, Li Y (2011) Gasoline alkylation desulfurization over amberlyst 35 resin: influence of methanol and apparent reaction kinetics. Fuel 90:713–718

73. Wang R, Wan J, Li Y, Sun H (2014) An insight into effect of methanol on catalytic behavior of amberlyst 35 resins for alkylation desulfurization of fluid catalytic cracking gasoline. Fuel 115:609–617

74. Wang R, Wan J, Li Y, Sun H (2015) A further catalysis mechanism study on amberlyst 35 resins application in alkylation desulfurization of gasoline. Chem Eng Sci 137:59–68

75. Xu W, Li Y (2015) Alkylation desulfurization of the C9 fraction over amberlyst 36 resin. RSC Adv 5:2908–2913

76. Olah GA (1973) Friedel-Crafts chemistry. Wiley, New York

77. Olah GA, Iyer PS, Prakash GKS (1986) Perfluorinated resin sulfonic acid (Nation–H) catalysis in synthesis. Synthesis 7:513–531

78. Olah GA, Molnar A, Prakash GKS (2018) Hydrocarbon chemistry, 3rd edn. Wiley, New York

79. Roberts RM, Khalaf AA (1984) Friedel-Crafts alkylation chemistry: a century of discovery. Marcel Dekker, New York

80. Harmer MA, Sun Q, Farneth WE (1996) High surface area Nafion† Resin/Silica Nanocomposites: a new class of solid acid catalyst. J Am Chem Soc 118:7708–7715

81. Harmer MA, Sun Q, Vega AJ, Farneth WE, Heidekum A, Hoelderich WF (2000) Nafion resin-silica nanocomposite solid acid catalysts. Microstructure—processing—property correlations. Green Chem 6:7–14

82. Lachter ER, San Gil RAS, Tabak D, Costa VG, Chaves CPS, Santos JA (2000) Alkylation of toluene with aliphatic alcohols and 1-octene catalyzed by cation-exchange resins. React Funct Polym 44:1–7

83. Fernandes RM, Lachter ER (2005) Evaluation of sulfonic resins for liquid phase alkylation of toluene. Catal Commun 6:550–554

84. Cadenas M, Bringué R, Fité C, Iborra M, Ramírez E, Cunill F (2014) Alkylation of toluene with 1-hexene over macroreticularion-exchange resins. Appl Catal A Gen 485:143–148

85. Silva MSM, Costa CL, Pinto MM, Lachter E (1995) Benzylation of benzene, toluene and anisole with benzyl alcohol catalyzed by cation-exchange resins. React Polym 25:55–61

86. Coutinho FMB, Aponte ML, Barbosa CCR, Costa VG, Lachter ER, Tabak D (2003) Resinas Sulfônicas: Síntese, Caracterização e Avaliação em Reações de Alquilação. Polímeros: Ciência e Tecnologia 13: 141–146

87. Siril PF, Cross HE, Brown DR (2008) New polystyrene sulfonic acid resin catalysts with enhanced acidic and catalytic properties. J Mol Catal A Chem 279:63–68

88. Rosenwald RH (1978) In: Alkylphenols, M. Grayson (eds) Kirk-othmer encyclopedia of chemical technology, Wiley, New York

89. Loev B, Massengale JT (1957) Cation exchange resins as catalysts in the alkylation of phenol. J Org Chem 22:988–989
90. Niederl JB (1938) Disobutylphenol synthesis-structure-properties-derivatives. Ind Eng Chem 30:1269–1274
91. Sharma MM, Patwardhan AA (1990) Alkylation of phenol with 1-dodecene and diisobutylene in the presence of a cation exchanger as the catalyst. Ind Eng Chem Res 29:29
92. Chaudhuri B, Sharma MM (1991) Alkylation of phenol with α-methylstyrene, propylene, butenes, isoamylene, 1-octene, and diisobutylene: heterogeneous vs homogeneous catalysts. Ind Eng Chem Res 30:227–231
93. Chakrabarti A, Sharma MM (1992) Alkylation of phenol with cyclohexene catalysed by cationic ion-exchange resins and acid-treated clay: O-versus C-alkylation. React Polym 17:331–340
94. Malshe VC, Sujatha ES (1997) Regeneration and reuse of cation-exchange resin catalyst used in alkylation of phenol. React Funct Polym 35:159–168
95. Malshe VC, Sujatha ES (2000) Phenol based resin as alkylation catalyst. React Funct Polym 43:183–194
96. Yadav GD, Rahuman MSM (2003) Efficacy of solid acids in the synthesis of butylated hydroxy anisoles by alkylation of 4-methoxyphenol with MTBE. Appl Catal A 253:113–123
97. Yadav GD, Murkute AD (2004) Novel efficient mesoporous solid acid catalyst UDCaT-4: dehydration of 2-propanol and alkylation of mesitylene. Langmuir 20:11607–11619
98. Yadav GD, Salgaonkar SS (2005) Selectivity engineering of 2,6-diisopropylphenol in iso-propylation of phenol over $Cs_{2.5}H_{0.5}PW_{12}O_{40}$/K-10 clay. Ind Eng Chem Res 44:1706–1715
99. Yadav GD, Pathre GS (2006) Chemoselective catalysis by sulphated zirconia in O-alkylation of guaiacol with cyclohexene. J Mol Catal Chem 243:77–84
100. Pittman CU, Yang X, Chatterjee S, Zhang Z, Zhu X (2010) Reaction of phenol, water, acetic acid, methanol, and 2-hydroxymethylfuran with olefins as models for bio-oil upgrading. Ind Eng Chem Res 49:2003–2013
101. Freire MA, Mendes DTSL, Freitas LS, Beerthuis R, Amarante SF, Ramos ALD (2017) Acid-catalyzed liquid-phase alkylation of phenol with branched and linear olefin isomers. Catal Today 289:192–203
102. Ronchin L, Quartarone G, Vavasori A (2012) Kinetics and mechanism of acid catalyzed alkylation of phenol with cyclohexene in the presence of styrene divinylbenzene sulfonic resins. J Mol Catal Chem 353:192–203
103. Krymkin NY, Shakun VA, Nesterova TN, Naumkin PV, Shuraev MV (2016) Theory and practice of alkyl phenol synthesis. tert-octylphenols. Ind Eng Chem Res 55:9829–9839
104. Teodorescu F, Enache A, Sandulescu M (2017) Selective alkylation of m-cresol with isopropyl alcohol under solvent-free conditions. Arkivoc 5:58–66
105. Ma Q, Chakraborty D, Fglioni F, Muller P, Goddard WA, Harris T, Campbell C, Tang YC (2006) Alkylation of phenol: a mechanistic view. J Phys Chem A 110:2246–2252
106. Bilenchenko NV, Nesterova TN, Chernyshov DA, Shakun VA, Krymkin NY, Tarasov AV, Voronin IO (2016) Sulfonic acid cation-exchange resins in the synthesis of straight-chain alkylphenols. Catal Ind 8:16–22
107. Iovel I, Goldberg YS, Shymanska M (1991) Hydroxymethylation of methylsubstituted pyrrole, thiophene, and furan in the presence of H⁺ cation exchangers. Chem Heterocycl Comp 27:1316–1318
108. Feng XL, Guan CJ, Zhao CX (2003) Ion exchange resin catalysed reactions of indole with imines: formation of diindolylmethanes. J Chem Res (S) 11:744–745
109. Feng XL, Guan CJ, Zhao CX (2004) Ion exchange resin catalyzed condensation of indole and carbonyl compounds-synthesis of bis-indolylmethanes. Synth Commun 34:487–492
110. Lin ZH, Guan CJ, Feng XL, Zhao CX (2006) Synthesis of macroreticular p-(ω-sulfonic perfluoroalkylated)polystyrene ion-exchange resin and its application as solid acid catalyst. Mol Catal A Chem 247:19–26
111. Magesh CJ, Nagarajan R, Karthik M, Perumal PT (2004) Synthesis and characterization of bis(indolyl)methanes, tris(indolyl)methanes and new diindolylcarbazolylmethanes mediated

by Zeokarb-225, a novel, recyclable, eco-benign heterogenous catalyst. Appl Catal A Gen 266:1–10

112. Surasani R, Kalita D, Chandrasekha KB (2013) Indion Ina 225H resin as a novel, selective, recyclable, eco-benign heterogeneous catalyst for the synthesis of bis(indolyl)methanes. Green Chem Lett Rev 6:113–122

113. Bandini M, Fagioli M, Umani-Ronchi A (2004) Solid acid-catalysed michael-type conjugate addition of indoles to electron-poor C=C bonds: towards high atom economical semicontinuous processes. Adv Synth Catal 346:545–548

114. Yadav JS, Reddy BUS, Kumar GGKSN, Rao KUR (2007) Cation-exchange resin as efficient, cost-effective and recyclable catalyst for the synthesis of 3-propargylindoles. Chem Lett 36:942–943

115. Kadam S, Thirupathi P, Kim SS (2009) Amberlyst-15: an efficient and reusable catalyst for the Friedel-Crafts reactions of activated arenes and heteroarenes with α-amido sulfones. Tetrahedron 65:10383–10389

116. Wang Z, Ding K, Uozumi Y (2008) An overview of heterogeneous asymmetric catalysis. In: Din K, Uozumi Y (eds) Handbook of asymmetric heterogeneous catalysis, Wiley, New York

117. Desyatkin VG, Anokhin MV, Rodionov VO, Beletskaya IP (2016) Polystyrene-supported Cu(II)-R-box as recyclable catalyst in asymmetric Friedel-Crafts reaction. Russ J Org Chem 52:1727–1737

118. Akagawa K, Yamashita T, Sakamoto S, Kudo K (2009) Friedel-Crafts-type alkylation in aqueous media using resin-supported peptide catalyst having polyleucine. Tetrahedron Lett 50:5602–5604

119. Akagawa K, Umezawa R, Kudo K (2012) Asymmetric one-pot sequential Friedel–Crafts-type alkylation and α-oxyamination catalyzed by a peptide and an enzyme. Beilstein J Org Chem 8:1333–1337

120. Yu L, Chen D, Li J, Wang PG (1997) Preparation, characterization, and synthetic uses of lanthanide (III) catalysts supported on ion exchange resins. J Org Chem 62:3575–3581

121. Havránková E, Csöllei J, Pazdera P (2017) Comparative study for 3, 3′-[(4-X-phenyl)-methanediyl] bis(1H-indoles) synthesis catalyzed by Ce(III) cations. Int J Engin Res Sci 3:9–14

122. Zhu C, Shen T, Liu D, Wu J, Chen Y, Wang L, Guo K, Ying H, Ouyang P (2016) Production of liquid hydrocarbon fuels with acetoin and platform molecules derived from lignocellulose. Green Chem 18:2165–2174

123. Iovel I, Goldberg Y, Shymanska M (1989) Hydroxymethylation of furan and its derivatives in the presence of cation-exchange resins. J Mol Cat 57:91–103

124. Iovel IG, Lukevics E (1998) Hydroxymethylation and alkylation of compounds of the furan, thiophene, and pyrrole series in the presence of H$^+$ cations (review). Chem Heterocycl Comp 34:1–12

125. Corma A, de la Torre O, Renz M, Villandier N (2011) Production of high-quality diesel from biomass waste products. Angew Chem Int 50:2375–2378

126. Corma A, de la Torre O, Renz M (2012) Production of high quality diesel from cellulose and hemicellulose by the Sylvan process: catalysts and process variables. Energy Environ Sci 5:6328–6344

127. Li G, Li N, Wang Z, Li C, Wang A, Wang X, Cong Y, Zhang T (2012) Synthesis of high-quality diesel with furfural and 2-methylfuran from hemicellulose. Chem Sus Chem 5:1958–1966

128. Li G, Li N, Yang J, Wang A, Wang X, Cong Y, Zhang T (2013) Synthesis of renewable diesel with the 2-methylfuran, butanal and acetone derived from lignocellulose. Bioresour Technol 134:66–72

129. Li G, Li N, Li S, Wang A, Cong Y, Wang X, Zhang T (2013) Synthesis of renewable diesel with hydroxyacetone and 2-methyl-furan. Chem Commun 49:5727–5729

130. Li S, Li N, Li G, Wang A, Conga Y, Wang X, Zhang T (2014) Synthesis of diesel range alkanes with 2-methylfuran and mesityloxide from lignocellulose. Catal Today 234:91–99

131. Li G, Li N, Yang J, Wang A, Wang X, Cong Y, Zhang T (2014) Synthesis of diesel or jet fuel range cycloalkanes with 2-methylfuran and cyclopentanone from lignocellulose. Energy Fuels 28:5112–5118
132. Deng Q, Han P, Xu J, Zou JJ, Wang L, Zhang X (2015) Highly controllable and selective hydroxyalkylation/alkylation of 2-methylfuran with cyclohexanone for synthesis of high-density biofuel. Chem Eng Sci 138:239–243

Chapter 4
Ion Exchange Resins Catalysed Esterification for the Production of Value Added Petrochemicals and Oleochemicals

Sim Yee Chin, Nurwadiah Azizan, Mohd Amirul Asyraf Ahmad and Muhammad Ridzuan Kamaruzaman

Abstract This book chapter is formulated with the aim to review the literature relevant to the esterification reactions catalysed by strong acidic ion exchange resins. Priority has been given to the works that have been published during the last 15 years. Industrially important esterification reactions in the petrochemical and oleochemical industries have been delineated. Various types of strongly acidic ion exchange resins produced by different manufacturers have been used to accelerate the rate of esterification reactions. In the esterification reactions in both petrochemical and oleochemical industries, gel-type resins showed comparable activity with the macro-reticular type resins after swollen by the polar solvents during the reactions, otherwise the macroporous-type resins always performed better. Gel-type resins were also preferred, in particular, for the esterification reactions involved bulky reactant molecules due to the mass transfer restriction of the macro-reticular type resins. In contrast to the comprehensive studies on the activity of ion exchange resin in the esterification reactions, the works that are related to the reusability, recovery and regeneration of these resin catalysts are rather scarce. In order to scale up the esterification processes catalysed by strongly acidic ion exchange resins to the industrial level, future works should be focusing on the solutions to overcome of the aforementioned constraints and limitations.

S. Y. Chin (✉) · N. Azizan · M. A. A. Ahmad · M. R. Kamaruzaman
Faculty of Chemical and Natural Resources Engineering, Universiti Malaysia Pahang,
Lebuhraya Tun Razak, 26300 Gambang, Kuantan, Pahang, Malaysia
e-mail: chin@ump.edu.my

S. Y. Chin
Centre of Excellence for Advance Research in Fluid Flow, Universiti Malaysia Pahang,
Lebuhraya Tun Razak, 26300 Gambang, Kuantan, Pahang, Malaysia

4.1 Introduction

Esterification is an important organic synthesis process in the petrochemical and oleochemical industries. The main esters in the petrochemical industries with considerable economic importance in various applications include acrylate, acetate, lactate and maleate esters derived from acrylic, acetic, lactic and maleic acids respectively. These esters are typically used in the production of fibres, films, adhesives and plastics. Some of the volatile petrochemical esters are used as aromatic materials in perfumes, cosmetics and foods [45]. In recent years, the esters derived from oleochemical (renewable resources like natural fats and oils) have been intensively studied to substitute the petrochemical esters due to their biodegradability. Oleochemical esters can be categorised into four groups, namely fatty acid esters, glycerol esters, polyol esters and complex esters. Oleochemical esters can be produced through the esterification of fatty acids with various alcohols. These oleochemical esters exhibit different superior technical properties combined with very favourable ecological properties, making them suitable as raw materials for the development the various derivative products. The simple fatty acid esters produced with lower chain alcohols are used as biodiesel, solvents, adhesives, emollients and lubricants; whereas the polyol esters and glycerol esters are consumed in the polymer industries [48].

Most of the industrial liquid phase esterification processes employ homogeneous mineral acid catalysts such as hydrochloric acid, hydrofluoric acid, sulphuric acid and *p*-toluene sulphonic acid or Lewis acid catalysts like tin octoate [43]. These homogeneous catalysts possess lower cost, good thermal and chemical stability but it is corrosive and difficult to be separated from the ester products. There is an impending need to substitute the homogeneous catalyst with a more eco-friendly heterogeneous catalyst for a greener and sustainable esterification reaction. Ion exchange resin (IER) in particular the strong acid resin is one of the potential heterogeneous catalysts that could facilitate the esterification reaction.

Strong acidic IER is functionalised with sulphonic acid group that performs in the same way as that of homogeneous sulphuric acid catalyst through the dissociation of acid, H^+ species. Commercially, the ion exchange resins are available in spherical resin beads. The capacity of these IER as catalyst counts on its highly porous nature that directly influences the rate of overall catalytic process. In general, the overall rates are determined by the rate of pore diffusion and rate of chemical reaction. The IER catalysts can be categorised into gel-type resins and macroporous-type resins on the basis of its pore structure to minimise the pore diffusion resistances. The microporosity (<2 nm) and high surface area of the gel-type resins can only be exhibited when it swells. It usually possesses very low crosslinking agent, di-vinyl benzene (DVB) content since swelling is a very important effect to the gel-type resins. It can only be used in the esterification reactions that involved the swelling solvents (Van de Steene et al. [46]. On the other hand, the micropore areas of the macroporous (2–50 nm) type resins are embedded in macroporous bead. It has relatively lower surface area but swelling is not an important effect to demonstrate its catalyst capac-

ity. Therefore, the macroporous type resins are widely applied in the esterification reactions involve aqueous, non-aqueous and non-polar solvents [4].

Over the past 15 years, commercial IER such as Amberlyst ion exchange catalysts, Amberlite resins, Dowex resins, Indion catalyst-grade resins, Tulsion catalyst resins and Purolite catalyst resins were tested in the esterification process for the production of value added petrochemicals and oleochemicals. Nevertheless, most of these processes was remained at the laboratory scale. Industrial esterification processes that employ IER as catalyst are very limited. In this regard, the present review discusses the activity, selectivity and stability of the IER used to catalyse various important esterification processes in the petrochemical and oleochemical industries. The limitations and constraints to commercialise these processes are delineated. The future prospect of IER catalyst in catalysing these esterification reactions is also summarised.

4.2   Ion Exchange Resin Catalysed Esterification for the Production of Petrochemicals

4.2.1   Esterification of Acetic Acid

Most of the acetic acid (AcH) produced in the industry are used for the manufacture of acetates. These acetates usually in the form of polymers are produced by esterifying AcH with alcohols. Butanol is among the most frequent used alcohols [5, 16, 19] followed by ethanol [32] and hexanol [35].

Ion exchange resin (IER) is commonly used in the esterification of AcH. Gangadwala et al. [16] compared the activity of a macroporous-type IER Amberlyst 15 (A15) with gel-type IER Amberlite IR-120 (AIR120) and with its counterparts Indion 130 (I130) and Tulsion TX-66 (TX66) in the esterification of AcH with butanol. The activities of these IERs are dictated by their properties as shown in Table 4.1. The batch-wise reaction catalysed by A15 achieved an AcH conversion of 60% after 1.5 h at a temperature of 356 K, mole ratio of AcH:butanol of 1:1 and catalyst loading of 6.67 g of catalyst/gmol of AcH. The gel-type AIR120 showed comparable activity with A15 because of the improved accessibility to its active sites as it was swollen by the substantial amount of water in the reaction mixture.

Blagov et al. [5] compared the performance of IER catalysts with a similar macroreticular matrix but different sulphonation for the same esterification reaction in a fixed bed reactor. Purolite CT 269 (PCT269) and Amberlyst 48 (A48) are fully monosulphonated and bi-sulphonated respectively in the gel phase, whereas Amberlyst 46 (A46) is only surface-sulphonated. A46 is only surface-sulphonated. Despite the lower ion exchange capacity of A46 as shown in Table 4.1, its activity showed only very minor differences from the activity of PCT269 and A48 due to the negligible side reactions during the esterification of AcH with butanol catalysed by A46. It validated that the active sites on the external surfaces were mainly responsible to

Table 4.1 The properties of the IER used in the esterification of acetic acid with various alcohols

Properties	A15[a]	I130[a]	TX66[a]	AIR120[a]	PCT269[c]	A48[c]	A46[c]	D502[d]	A70[e]	PCT124[f]	DM650C[g]
Matric type	Styrene (Styr) DVB	Styr DVB	Styr DVB	Styr DVB	Styr DVB	Styr DVB	Styrene DVB	Styr DVB	Styr DVB	Styr DVB	Styr DVB
Form	Macro-reticular	Macro-reticular	Macro-reticular	Gel	Macro-reticular	Macro-reticular	Macro-reticular	Gel	Macro-reticular	Gel	Gel
Total exchange capacity											
(a) Dry basis (mmol H^+/g)	4.7	4.8	4.2	4.44	5.12	5.62	1.10	4.8	2.55	5.0	b
(b) Wet basis (mmol H^+/mL)	1.8	b	b	1.9	b	b	0.43	0.6	b	1.2	2
Maximum operating temperature (°C)	120	130	120	120	b	b	120	150	190	145	130
Surface area (m^2/g)	55	b	b	1.532[d]	35–50	44	75	6.94	31–36	b	b

(continued)

Table 4.1 (continued)

Properties	A15[a]	I130[a]	TX66[a]	AIR120[a]	PCT269[c]	A48[c]	A46[c]	D502[d]	A70[e]	PCT124[f]	DM650C[g]
Average pore diameter (nm)	38	b	b	28.85[d]	33.8	30	23.5	8.534	19.5–22	b	b
Total pore volume (cm^3/g)	b	b	b	[d]1.10×10^{-2}	0.4	0.35	0.44	1.48×10^{-2}	0.15–0.33	b	b
Crosslinking density (% DVB)	20–25	b	b	8	b	b	b	2	b	b	7
Average particle size (mm)	0.5	0.55	0.57	0.5	0.55	0.95	0.8	0.05–1.5	0.5	0.35–1.00	0.65

[a]Data adopted from [16] unless stated otherwise
[b]Data not available
[c]Data adopted from Blagov et al. [5] unless stated otherwise
[d]Data adopted from Izci and Bodur [19] unless stated otherwise
[e]Data adopted from Orjuela et al. [32] unless stated otherwise
[f]Data adopted from Patel and Saha [35] unless stated otherwise
[g]Data provided by DOW Chemical unless stated otherwise

enable the occurrence of main reactions while the active sites in the pore contributed to the side reactions.

On the other hand, Izci and Bodur [19] esterified AcH with butanol using Dowex 50WX2 (D50WX2) and AIR120 as the catalysts and 1,4-dioxan as a solvent. Both catalysts were gel-type IERs with the properties as displayed in Table 4.1. They found that D50WX2 with higher total exchange capacity, surface area and pore volume, had resulted higher activity than AIR120. D50WX2 was then tested in the reactions at various temperatures ranged between 318–348 K, while maintaining the AcH:butanol molar ratio at 1:1, catalyst weight at 5 g dry resin L^{-1} and stirring speed at 500 rpm. An equilibrium conversion of approximately 67% was achieved in the reactions carried out at all these temperatures, concluding that the equilibrium conversion was independent between temperatures 318–348 K. Nevertheless, the time taken to achieve equilibrium in the reaction at a temperature of 348 K was seven times shorter than the reaction at a temperature of 318 K.

A more thermally stable macroporous IER, Amberlyst 70 (A70) was employed in the esterification of AcH with ethanol [32]. In comparison to the traditional A15, this sulphonic resin displayed higher activity ascribed to its higher thermal stability. The reaction carried out at a temperature of 383 K with catalyst loading, $w_{CAT} = 0.011$ wt% and mole ratio ethanol:AcH = 4.29 achieved equilibrium conversion of 89% within 150 min.

A gel-type IER, Purolite CT124 (PCT124) was used as the catalyst to esterify AcH with a bulkier alcohol, *n*-hexanol [35] in a batch chromatographic reactor column (BCRC). A complete conversion (100%) of AcH was achieved in the reaction performed at a temperature of 353 K, feed molar ratio (*n*-hexanol:AcH) of 3:1, feed flow rate of 0.2 mL/min, and reaction and regeneration step times of 75 min each. PCT124 was regenerated using *n*-hexanol. Similarly, Mariana Reinoso and Marta Tonetto [30] also used gel-type IER, Dowex Monosphere 650 °C (DM650C) in the esterification of glycerol with AcH for the production of bio-additives. The optimum condition was obtained at a temperature of 393 K and molar ratio AcH:glycerol of 9:1 with the catalyst concentration of 4 wt% and reaction time of 240 min. The corresponding glycerol conversion was 99.6% while the elevated selectivity towards the interest products triacetylglycerol (TAG) was 34% and diacetylglycerol + triacetylglycerol mixture (DAG + TAG) was 88%. DM650C was also proven to maintain its activity and selectivity for five catalytic cycles without regeneration as no leaching of the active species was detected. In spite of its comparable or lower ion exchange capacity as given in Table 4.1, it was found to be more stable than the other macroreticular types IERs used in the same reaction, e.g. A15 [51] and A70 [22] that could only retain its activity but not selectivity during the reuse. Table 4.2 summarises all the comparison studies carried out for the esterification of AcH using different alcohols and different IER catalysts.

Table 4.2 Comparison studies of the esterification of AcH using different types of IER

Catalysts involved	Alcohol	Best catalyst and operating condition	References
PCT269, A46, A48	1-butanol	A48	[5]
A15, AIR120, TX66 and I130	*n*-butanol	A15. The batch-wise reaction achieved an AcH conversion of 60% after 1.5 h at a temperature of 356 K, mole ratio of AcH:butanol of 1:1 and catalyst loading of 6.67 g of catalyst/gmol of AcH	[16]
D50WX2, AIR120	isobutanol	D50WX2. An equilibrium conversion of 67% was achieved at temperatures ranged between 318–348 K, while maintaining the AcH:butanol molar ratio at 1:1, catalyst weight at 5 g dry resin/L and stirring speed at 500 rpm	[19]

4.2.2 Esterification of Acrylic Acid

Acrylate esters are one of the key petrochemicals that are extensively used to produce homopolymers and copolymers for the manufacturing of adhesives, printing inks and binders for paints. They are also applied in the production of elastomers, super absorbent polymers, flocculants and fibres [25]. Considering industrial importance, the synthesis of acrylate esters through a more environmental process employing heterogeneous catalyst like IER has long been the research subject.

To produce various types of acrylate esters through the IER catalysed esterification reaction, acrylic acid (AA) was esterified mainly with butanol [12, 23, 39], followed by 2-ethyl hexanol [2, 8, 25] and other alcohols such as ethanol, propylene glycol and hexanol [3, 7]. Table 4.3 lists the properties of the IER catalysts involved in the aforementioned studies.

The IER catalysts, macro-reticular type Amberlyst 15 (A15) as well as gel-type Amberlyst 131 (A131) and Dowex 50WX400 (D50WX400) were screened for activity in the batch-mode esterification of AA with *n*-butanol and isobutanol by Sert et al. [39] and Karakus et al. [23] respectively. The gel-type resins exhibited higher activity because of their swelling effect due to the water produced during the esterification. The accessibility to the active sites highly depends on the degree of swelling of the gel-type resins. Between the two gel-type resins, A131 performed better because of its higher ion exchange capacity. At the best operating conditions, the same maximum AA conversion of 50% was achieved in the esterification with *n*-butanol and isobutanol respectively at 358 K with the catalyst loading of 10 g/L. Nevertheless, a higher butanol-to-AA mole ratio was required for the process using iso-butanol for

Table 4.3 The characteristics of the IER used in the esterification of acrylic acid

Properties	A15[e]	A131[e]	D50WX400[e]	A36[f]	A39 [g]	A46 [g]	A70 [g]
Matric type	Styrene (Styr) DVB	Styr DVB	Styr DVB	Styr DVB	Styr DVB	Styr DVB	Styr DVB
Form	Macro-reticular	Gel	Gel	Macro-reticular	Macro-reticular	Macro-reticular	Macro-reticular
Total exchange capacity							
(a) Dry basis (meq H$^+$/g)	4.7	4.8	c	5.4	4.5	0.98	2.55
(b) Wet basis (meq H$^+$/mL)	1.8	1.35	1.1	c	c	0.43	0.9
Maximum operating temperature (°C)	120	120	150	150	130	120	190
Surface area (m^2/g)	50	d	d	33	32	75	36
Average pore diameter (nm)	38	d	d	c	23	23.5	22
Particle size (mm)	0.23–0.6	0.4–0.5	c	c	0.6–0.7	0.8–0.9	0.5
$^a V_{sp}$ (cm^3/g)	c	c	c	c	1.45	0.16	1.4
^{b}PFD (nm/nm^3)	c	c	c	c	0.8–1.5	1.5–2.0	0.4–0.8

^{a}Volume of the swollen polymer phase
^{b}Polymer fraction density
^{c}Data not available
^{d}Data not applicable
^{e}Data adopted from Sert et al. [39] unless stated otherwise
^{f}Data adopted from Altıokka and Ödeş [3] unless stated otherwise
^{g}Data adopted from Komon et al. [25] unless stated otherwise

achieving the same conversion within 4 h. The steric hindrance effect of iso-butanol structure has resulted in lower rate of reaction. It is worth noting that the A131 gave conversions that were comparable to the fresh catalyst after it was reused for four times. A131 was also revealed by Buluklu et al. [7] as the best catalyst among A15, A131 and D50WX400, in their study to elucidate the kinetic mechanism for the esterification of AA with hexanol. Compared to the esterification of AA with butanol, the AA conversion can only reach ≥50% when it was esterifying with hexanol at a reaction temperature of 358 K with higher hexanol to AA mole ratio and catalyst loading (either hexanol to AA mole ratio of 3 or catalyst loading of 20 g/L).

Despite the inferior activity of A15 for the esterification of AA with butanol, Constantino et al. [9] packed and evaluated this porous IER in a fixed bed adsorptive reactor for the esterification reaction of AA with 1-butanol. Attributing to the simultaneous reaction and separation steps, the maximum butyl acrylate concentration obtained was 38% higher than the equilibrium concentration at a reaction temperature of 363 K with an equimolar reactants ratio solution and a feed flow rate of 0.9 mL/min. A15 was also used to accelerate the esterification of AA with methanol in another continuous system, a simulated-moving-bed reactor (SMBR). The operation at its optimal point yielded about 12 mol of methanol per mol of methyl acrylate with the corresponding AA conversion of 98% at a relatively low operating tempera-

ture (60 °C). In addition, A15 was also compared with Amberlyst 36 (A36) in terms of its activity in the esterification AA with propylene glycol [3]. Although the higher ion exchange capacity of A36 has resulted in higher rate of reaction, at the same time it promoted side reactions. In spite of the longer duration required to achieve the comparable conversion, A15 was found as the best catalyst as its selectivity (73.6%) was almost 1.5-folds of the selectivity obtained in the reaction catalysed by A36. The comparison studies were carried out at 353 K using propylene glycol to AA mole ratio of 1:1 in the presence of 5.5 wt% of resin catalyst and 0.3 wt% inhibitor.

The synthesis of another acrylate ester of industrial significance, 2-ethyl hexyl acrylate was also investigated extensively through the esterification of AA with 2-ethyl hexanol accelerated by the IER catalysts. Komon et al. [25] compared the activities of macroporous-type resins Amberlyst 39 (A39), Amberlyst 46 (A46) and Amberlyst 70 (A70) with gel-type resin A131 in the esterification of AA with 2-ethyl hexanol. A131 showed the poorest activity as its active sites could not be fully accessed in a non-polar reaction system that did not cause swelling effect to the gel-type resin. Among the macroporous resins, A70 overtook the others and gave the highest conversion and yield of 76 and 71.6% respectively after 360 min of reaction performed at a temperature of 373 K with initial 2-ethyl hexanol to AA mole ratio of 1, inhibitor concentration of 0.2 wt% and catalyst loading of 5 wt%. A70 performed better than Amberlyst 39 even though A70 has lower number of the acid centers. Its highest activity could be attributed to the enhanced acidic strength of the active sites by the chlorine atom in the matrix of the resin [42]. In addition, A70 has lower polymer density and therefore larger space between polymer chains than A39 to allow higher accessibility of reactants to the acid sites (resin properties as shown in Table 4.3).

On the related note, A15 was employed for 2-ethyl hexyl acrylate synthesis by esterifying AA with 2-ethyl hexanol [8]. The highest yield, 70% was obtained within 500 min in the reaction carried out at 388 K with initial mole ratio AA to 2-ethyl hexanol of 1:3 and catalyst loading of 10 wt%. The reusability studies showed that approximately 20% reduction was observed in the yield after the 1st use of the A15, inferring the blockage of catalyst active sites by the co-produced water. Table 4.4 includes the significant findings of the comparison studies for the esterification of AA using different types of resins and alcohols.

4.2.3   Esterification of Lactic Acid

Lactic acid (LA) with a hydroxyl group adjacent to the carboxyl group in its molecular structure is classified as an alpha-hydroxy acid. It can be esterified with various alcohols to produce lactate esters that act us flavour, preservative and solvent in the pharmaceutical, cosmetic and food industries. Lactic acid was esterified with ethanol [14] and isopropanol respectively [47] using Amberlyst 15 as a catalyst. The equilibrium LA conversions of about 30 and 15% were attained within 300 min when LA was esterified using ethanol (EtOH) and isopropanol (IPA) respectively

Table 4.4 Significant findings of the comparison studies for the esterification of AA using different types of resins and alcohols

Catalyst involved	Alcohol	Best catalyst and best operating condition	References
A15, A36	Propylene glycol	Amberlyst 15. AA conversion of 45% with selectivity of 74% was achieved in the reactionat a temperature of 353 K and propylene glycol to AA mole ratio of 1:1 in the presence of 5.5 wt% of resin catalyst and 0.3 wt% inhibitor	[3]
A39, A46, A70 and A131	2-Ethyl hexanol	Amberlyst 70. Highest conversion and yield of 76 and 71.6% respectively were achieved after 360 min of reaction performed at a temperature of 373 K with initial 2-ethyl hexanol to AA mole ratio of 1, inhibitor concentration of 0.2 wt% and catalyst loading of 5 wt%	[25]
A15, A131, and D50WX400	Hexanol	Amberlyst 131. Max. conversion of 54% was obtained in the reaction at 358 K with molar ratio acid to alcohol 1:1 and 20 g/L catalyst loading	[7]
A15, A131, and D50WX400	Isobutanol	Amberlyst 131. Max. conversion of 50% was obtained in the reaction at 358 K with molar ratio acid to alcohol 3:1 and 10 g/L catalyst loading	[23]
A15, A131, and D50WX400	*n*-Butanol	Amberlyst 131. Max. conversion of 50% was obtained in the reaction at 358 K with molar ratio acid to alcohol 1:1 and 10 g/L catalyst loading	[39]

Table 4.5 The physicochemical characteristics of the IER used in the esterification of lactic acid and maleic acid

Properties	WD80[a]	WD009[a]	I225H[b]	A15[b]
Matrix type	Macro-reticular	Macro-reticular	Gel	Macro-reticular
Operating pH	Styrene (Styr) DVB	Styr DVB	Styr DVB	Styr DVB
Ionic form	H^+	H^+	H^+	H^+
Total exchange capacity	0–14	0–14	c	c
(a) Dry basis (meq H^+/g)	4.9	5	1.8	4.7
(b) Wet basis (meq H^+/mL)	1.6	1.15	c	c
Moisture (%)	50–60	60–68	c	c
Maximum operating temperature (K)	393	403	393	393
Particle size (mm)	0.3–1.25	0.3–1.25	0.3–1.2	0.5
Surface area (m²/g)	25–40	25–40	c	34.85
Total pore volume (cm³/g)	0.3–0.5	0.3–0.5	c	c
Average pore diameter (nm)	200–400	200–400	c	c
Crosslinking (% DVB)	c	c	c	20

[a]Data adopted from Qu et al. [36] unless stated otherwise
[b]Data adopted from Mulay and Rathod [31] unless stated otherwise
[c]Data not available

at a temperature of 353 K, a molar ratio alcohol:LA of 3 and a catalyst loading of approximately 6 wt%. Weblyst D009 and Weblyst D80 macro-reticular resins with the properties as shown in Table 4.5 were compared in the esterification of LA with *n*-butanol and iso-butanol [36]. As a result of slightly higher ion exchange capacity and maximum operating temperature of Weblyst D009 (WD009), it showed a remarkable higher activity than Weblyst D80 (WD80). In addition, WD80 was also mechanically less stable as a larger part of WD80 cracked into small particles in the reaction medium. At a reaction temperature of 353 K, molar ratio alcohol:LA of 3 and catalyst loading of 3 wt%, the equilibrium LA conversions of about 30 and 35% were attained within 1200 min for the esterification of LA with iso-butanol and *n*-butanol respectively. The time required to reach equilibrium in the process of esterifying LA with butanol was longer than the esterification of LA with shorter carbon chain alcohol such as ethanol and isopropanol. A lower rate of reaction of the esterification of LA with butanol could be ascribed to the effect of polarity and steric hindrance.

4.2.4   Esterification of Maleic Acid

Maleic acid (MA) is an organic dicarboxylic acid, a molecule with two carboxyl groups. Dibutyl maleate could be produced by esterifying the MA with butanol and it can be used as plasticizer and copolymer on top of its applications in the manufacturing of plastisols, dispersions, coatings and adhesives. Esterification of MA with butanol catalysed by IER was studied by Mulay and Rathod [31] at a temperature of 80 °C and mole ratio of 1:4 for the MA:butanol with the catalyst loading of 2% and agitation speed of 300 rpm. The corresponding MA conversions achieved after 4 h in the reaction catalysed by A15 and Indion-225 H (I225H) were comparable (48 and 44% respectively) although the ion exchange capacity of A15 (4.7 meq/g) was threefolds as compared to I225H (1.8 meq/g). A swollen gelular type-I225H with larger pore eliminated the internal mass transfer resistance. As a consequence, its low ion exchange capacity was offset. The properties of these cation exchange resins are provided in Table 4.5. The further studies that used A15 as catalyst resulted a maximum MA conversion of 76% at 90 °C, MA to butanol mole ratio of 1:4, catalyst and molecular sieves loading of 4% each and the agitation speed of 300 rpm. The additional molecular sieves in the reaction mixture increased the conversion (40–68%) because of the water adsorption in the molecular sieves pores which reduced the water poisoning on the IER active sites.

4.3   Ion Exchange Resin Catalysed Esterification for the Production of Oleochemicals

4.3.1   Esterification of Oleic Acid

Macro-reticular ion exchange resins (IERs) such as aminophosphonic acid resin (D418) and sulphonated resins (Amberlyst 15 and CH-A) were used as the catalyst in the esterification of oleic acid and ethanol with the intent to produce biodiesel [17, 20, 24, 49]. These resins have been used in the reaction systems with various operating mode and conditions and the performances achieved are summarised in Table 4.6.

Amberlyst 15(A15) was tested in the both batch reactor [17] and packed bed reactor [24] for the synthesis of ethyl oleate. The conversion (43.8%) achieved in the packed bed reactor was lower than the conversion (53%) achieved in the batch reactor at a temperature of 75 °C. It happened due to the shorter contact time, nonideal mixing or mass transfer resistances in the packed bed reactor.

In comparison to the IER CH-A tested in a batch system, A15 has resulted lower conversion owing to its inferior properties in the pore diameter and moisture content of the A15. A smaller pore diameter restricts the access of reactant to the active sites while the higher moisture content causes reduction in the available active sites due

Table 4.6 The reaction conditions and performance of IER catalyst in the esterification oleic acid with ethanol

Catalyst	Conditions	OA conversion (%)	References
Amberlyst 15	Batch reactor with $M_{EtOh:OA}$ of 6, temperature at 75 °C, catalyst loading of 20 wt% and reaction time of 6 h	53	[17]
Amberlyst 15	Packed bed reactor with $M_{Etoh:OA}$ of 1, temperature at 75 °C, 3 g of catalyst loading, flow rate of 0.25 ml/min and corresponding residence time of 15 min	43.8	[24]
D418, aminophosphonic acid resin	Batch reactor with $M_{Etoh:OA}$ of 14, temperature at 115 °C, catalyst loading of 10.2 wt% and reaction time of 10 h	92	[49]
CH-A, Sulfonated cation exchange resin	Batch reactor with $M_{Etoh:OA}$ of 9, temperature at 82 °C, 20 g of catalyst loading and reaction time of 8 h	93	[20]

to the preoccupation of the water on it. The hydrogen bond of water interacts with the ion sulphonic, SO_3H easily to active site which reduces the activity.

Despite the poorer properties of aminophosphonic acid resin (D418), the higher reaction temperature and molar ratio of ethanol to oleic acid ($M_{Etoh:OA}$) in the reaction catalysed by D418 caused an identical conversion with the one achieved by the reaction catalysed by CH-A. The properties of the IERs are compared in Table 4.7.

In addition, the biodiesel has also been produced by esterifying the oleic acid with methanol using different types of IERs as catalyst. Kouzu et al. [26] compared the reaction rates and oleic acid conversion during esterification of oleic acid with methanol catalysed by the gelular type (Amberlyst 31) and macrorecticular type (A15) IERs. The reaction carried out at 333 K with catalyst loading of 0.5 g and molar ratio of methanol to oleic acid (OA) of 210 for 1.5 h achieved higher reaction rate as well as the OA conversion when it was catalysed by powdered form Amberlyst 31 (A31). The powdered form IER possesses higher surface area and hence larger amount of OA came into contact with the active sites. The gelular-type IER A31 has shown better performance as compared to macro-reticular type due to its higher ion exchange capacity. The increased reaction rate and OA conversion with A31 can also be explained by its lower percentage of crosslinking degree that allowed the

Table 4.7 The properties of macro-reticular IER used in the esterification of oleic acid with ethanol

Properties	Amberlyst 15[a]	CH-A[b]	D418[c]
Matrix	Styrene divinylbenzene		
Form	H$^+$	H$^+$	Na$^+$
Total ion exchange capacity (mmol/g)	4.7	$\geq$5.2 (wet) $\geq$1.5 (dry)	$\geq$0.35 mmol/ml
Surface area (m^2/g)	53	46	NA
Average pore diameter (nm)	30	38	NA
Bead size (mm)	0.60–0.85	$\geq$95% 0.32–1.25	$\geq$95% 0.315–1.25
Moisture content (%)	$\leq$1.6	$\leq$10	55–60
Density (wet): True (g/ml) Apparent (g/ml)	d d	1.25–1.28 0.75–0.85	1.1–1.18 0.7–0.8

[a]Provided by DOW Chemical
[b]Adopted from Jiang et al. [20] unless stated otherwise
[c]Provided by supplier of Tianjin Yunkai Resin Technology
[d]Data not available

Table 4.8 Characteristic of IER used in esterification of oleic acid with methanol

Properties	Gelular (A31)		Macro-reticular (A15)	
	Bead	Powder	Bead	Powder
Reaction rate[a]	0.55	1.19	0.38	0.49
Conversion[a]	82.1	98.9	69.1	74.0
Particle sized, swelled (mm)	0.55–0.70	0.04–0.22	0.60–0.85	0.03–0.20
Ion exchange capacity (mmol/g)	7.1		5.4	
Cross linking degree (%)	4		20	

[a]catalyst loading of 0.5 g $M_{Metoh:OA}$ of 209 at 333 K for 1.5 h

catalyst to swell easily with the increase in porosity. The increased porosity of the resin enabled the access of reactant molecules to the active nuclear sulphonic acid groups residing in the pores of the resin. Table 4.8 summarises the properties and performances of A31 and A15 in the esterification of OA with methanol.

In recent years, the oleic acid has been esterified with polyol such as trimethyl-propane (TMP) and glycerol (Gly) using IER as solid acid catalyst. It is important to highlight that these reactions require elevated reaction temperature (>130 °C) which exceeds the maximum allowable temperature of the typical IERs. IER catal-ysed esterification of oleic acid with trimethylpropane (TMP) was investigated by Kuzminska et al. [27, 28]. A pre-swelling in TMP significantly increased the activ-ity of the gelular-type resin, D50WX2 but not the other macro-reticular resins (A36, Purolite CT482 and Purolite CT275DR). The activities of the macroporous IERs with high divinylbenzene (DVB) crosslinking degree such as Purolite CT482 (PCT482) and Purolite CT275DR (PCT275DR) were not affected by pre-swelling because the

Table 4.9 Characteristics of the IER used in esterification of oleic acid with polyol [27, 28]

Properties	Gelular	Macroporous		
		Low crosslinking	High crosslinking	
Catalyst	Dowex	A36	PCT275DR	PCT482
DVB (%)	2	12	>12	
Maximum operating temperature (°C)	150	150	180	190
Ion exchange capacity (meq H$^+$/g)	3.9	4.4	4.7	3.2
Median pore diameter (nm)	–	27	40–70	26.8

high degree of crosslinking forbade the IER to expand. The pre-swollen D50WX2 provides a good accessibility due to its enhanced resin cavities in a wet state. Among these IERs, D50WX2 in pre-swollen state and PCT275DR showed the highest activity in producing triester for 24 h. A higher activity of PCT275DR was due to the bigger pore size and higher ion exchange capacity that gave larger number of active sites. The properties of all the resins used are shown in Table 4.9. Despite the highest degree of leaching in the dimethylformamide, the pre-swollen D50WX2 and PCT275DR retained its superiority in activity in the subsequent recyclability tests after its first use. The activity decay after the first use may be ascribed to the partial blocked active sites by the water by-product.

The effect of water on the activity of IER A15 for the esterification of oleic acid with methanol was also verified by Son et al. [44] in the different reactor systems. The three phase fixed bed reactor was declared as the better system to process the low quality oil that contained considerable amount of water. The reaction carried out in a three-phase fixed bed reactor showed higher fatty acid methyl ester (FAME) yield than those obtained using a batch reactor. The continuous removal of co-produced water by evaporation attributed to the stable catalyst activity that led to the increasing yield in a fixed bed reactor. Moreover, a shift of reaction equilibrium towards the products also contributed to the increased yield. In a batch system, the active sites of IER A15 were blocked by the water, hindering the access of polar OA to the catalyst active sites. The optimal conditions occurred at increased methanol flow rate and bed height yielded 97.5% OA conversion [44]. Nevertheless, it was reported that the large amount of methanol not only blocked the active sites of the IER, but also caused bi-phasic reaction system that prevented the interaction between the methanol and OA [18].

Table 4.10 Characteristics of the IER used in the esterification of butyric acid with various alcohol (adopted from [34] unless stated otherwise)

Catalyst	Type	Acid site density (mol H⁺/kg)	Surface area (m²/g)	Average pore diameter (nm)	Maximum operating temperature (°C)
A35	macro-reticular	5.32[a]	34[a]	32.9[a]	150[b]
A36	macro-reticular	5.40	33	24	150
A70	macro-reticular	2.70	36	22	190
ABD20	Gelular	5.10	<0.1	[c]	[d]

[a][41]
[b]Provided by supplier Rohm and Haas
[c]Not applicable
[d]Not available

4.4 Esterification of Butyric Acid

The growing interest in producing butyric acid (BA), a short chain fatty acid by fermentation from bio-renewable resources has made BA as a platform molecule to be esterified with various alcohols for the synthesis of BA esters, the biofuel constituents. Pappu et al. [34] evaluated the effect of different types of alcohols (linear and branched) in esterifying the BA employing IER catalysts that included macro-reticular types IER (A15, A36, and A70) and gel-type IER (Amberlyst BD 20). The reaction study was carried out at the temperature ranged from 100 to 150 °C. Identical to the reaction trend of the paratoluene sulphonic acid homogeneously catalysed reaction, the rate of IER catalysed BA esterification decreased with the increase of the carbon chain length of the linear alcohol. The decrease in esterification reactivity from methanol to octanol was due to the decrease in polarity and increase in steric hindrance. At the same time, the increase of steric hindrance was also the reason for the decline of rate of BA esterification with the increasing of the branches in butanol and octanol. Among the IERs tested in the BA esterification, Amberlyst BD 20 (ABD20) exhibited highest activity per unit mass because of its higher active site density while A70 showed high activity per acid site because of its higher thermal stability that resulted from its halogenated polymer backbone. Nevertheless, the turnover frequency (TOF) for the BA esterification catalysed by paratoluene sulphonic acid was 10–12 times higher than that due to A70. Pappu et al. [34] supposed that the lower TOF of the BA esterification using A70 as catalyst was due to the reduced active sites activity and accessibility as a result of the IER swelling/hydrophilicity or restricted conformation of the intermediate complexes adsorbed on acid sites in the porous structure of the IER. Table 4.10 compares the characteristics of IER used in the esterification of butyric acid with various alcohols.

The activity of A15 was compared with the activity of another type of macro-reticular resin, A35 for the esterification of BA with ethanol by Singh et al. [41]. The reaction study was carried out in a batch system at a catalyst loading of 48.8 kg/m3, temperature of 75 °C and molar ratio of ethanol to BA of 1 : 10 (butyric acid : ethanol). The BA conversion of the reaction catalysed by A15 (70%) was almost double of the conversion attained in the A35 catalysed reaction. The superior structural properties like higher surface area, pore size and pore volume of A15 resulted an easy access of reactants to the active sites. The properties of the A35 are compared with the other catalysts in Table 4.10.

Owing to the good structural properties of A15, it was employed by Dange and Rathod [11] in the esterification of butyric acid with methanol, irradiated by microwave (MW). At the optimum reaction condition that maximising the MW energy absorption, the molar ratio of methanol to BA and catalyst loading were set to 1:1 and 8.1 wt% respectively. The co-produced water was absorbed using 10.8% of molecular sieves to prohibit the reverse reaction. The resulted BA equilibrium conversion of 92.6% at a reaction temperature of 70 °C was achieved in less than 60 min. The time taken was four times shorter than the conventional batch system. The direct interaction of the MW energy with the reactants and catalysts produced efficient internal heating that enhanced the reaction rate. Furthermore, the rate improvement could also be due to the polarity enhancement originated by ionic dissociation of methanol under MW irradiation.

The esterification of BA by *n*-butanol catalysed by gel-type D50WX8 has been intensified using reactive distillation [21]. The reactive distillation system removed the water byproduct simultaneously during the reaction and hence minimising the reverse reaction. In a reaction with equimolar of *n*-butanol and BA and temperature of 110 °C, the BA conversion was achieved (90%) within 120 min. BA conversion increased almost to 100% when the molar ratio of *n*-butanol to BA was raised to 4.

4.5 Esterification of Palmitic Acid

Esterification of palmitic acid (PA) with methanol catalysed by gel-type AIR120 resin was investigated by Dang and Chen [10] in a batch reactor with the intention to produce biodiesel. The optimal conditions predicted for devising a statistical strategy in experimental design occurred at a reaction temperature 61 °C, methanol to palmitic acid molar ratio of 8:1, reaction time of 10.5 h, catalyst loading at 10 wt% of palmitic acid and stirring speed of 600 rpm. The swelling AIR120 resin in the excess methanol exhibited high activity and resulted into high PA conversion efficiency of $98.3 \pm 0.42\%$.

de Aguiar et al. [13] synthesised sulphonated poly-divinylbenzene (SPDVB) resin and evaluated its activity in the esterification of palmitic acids with methanol. The best reaction under conditions with molar ratio methanol/PA of 20/1 using 5 wt% of as-synthesised SPDVB resin at 120 °C for 8 h, the corresponding PA conversion was 94%. Although the ion exchange capacities of the as-synthesised SPDVB resin

(2.26 mmol H$^+$/g) was only half of the ion exchange capacities of the commercial resins A35 and A36, it exhibited similar catalytic activity with these commercial macroporous resins. This was owing to its superior properties like specific surface area (419 m^2/g) and pore volume (0.56 cm^3/g). Its catalytic activity also remained good when used to convert the PA present in the fatty acid residue from the palm and soybean oil refining industries.

4.6   Esterification of Nanonoic Acid

Propyl nonanoate is used in chemical industries for the production of synthetic flavours, cosmetics, pharmaceuticals and corrosion inhibitors. It can be produced by esterifying nonanoic acid with 1-propanol in the presence of IER catalyst such as A15 [40]. The activity studies using a batch system indicated that the nonanoic acid conversion of approximately 85% can be achieved when the reaction was carried out for 7 h at a temperature of 363.15 K, mole ratio nonanoic acid to 1-propanol of 1:10 with catalyst loading of 8% (w/v) and stirring speed 500 rpm. Identical to the other fatty acids esterification reactions, the conversion of nonanoic acid decreased when the longer carbon chain and branched alcohols were used due to the effect of polarity and steric hindrances.

4.7   Esterification of Free Fatty Acid in Plant Oil

Esterification of the free fatty acids (FFA) present in the waste cooking oil (WCO) with methanol is commonly used to pretreat the WCO before it is used to produce biodiesel. Table 4.11 summarises the performance of different types of IERs in esterifying the FFA in the WCO. The catalytic activities of these IERs were highly influenced by characteristic of the resins such as surface area, sulphur content and acid capacity [15, 33, 37, 1, 50]. Among these IER catalysts, the gel-type resin (EBD100) and hyper-crosslinked resin (Purolite D5081) displayed higher catalytic activities than the macroporous resins. The reaction only took place on the superficial sulphonic acid groups of the macroporous resins as the access to the active sites in the pore was limited by the internal diffusion resistances. The internal diffusion resistances were minimised in the swelling gelular resin and hyper-crosslinked resin due to the large surface area and pore size. The properties of these resins are tabulated in Table 4.12 for comparison purposes.

In contrary, macroporous resin A15 and PCT275DR showed better catalytic performance when they were compared with the gel-type resin Dowex 50WX8 in esterification of castor oil (content approximately 90% of ricinoleic acid) and 2-ethylhexanol [38]. This catalytic study was carried out at 100 °C with mole ratio alcohol to castor oil of 2:1 for 4 h. The resulted fatty acid conversion of almost 100% was reached in a reaction catalysed by Amberlyst 15 while the fatty acid conversion was only 27%

Table 4.11 Catalytic performance of the IER used in the esterification of FFA in the WCO

Resin	Alcohol	Operating condition	FFA conversion (%)	Reusability	References
A15 (Macrop-orous)	Methanol	65 °C, 12:1 ($M_{MeOH:oil}$), 3 wt% and 9 h in a batch reactor	41	No significant loss of catalytic activity after 3 cycles of reuse	[6]
		60 °C, 20% v/v methanol, 2 wt% and 3 h	45.7	–	[33]
NKC9 (Macrop-orous)	Methanol	64 °C, 3:1 ($M_{MeOH:oil}$), 20 wt% and 4 h in a fixed bed reactor	94.5	The conversion of FFA kept unchanged at the first 10 runs	[15]
	Ethanol	80 °C, 3:1 ($M_{MeOH:oil}$), 15 wt% and 6 h in a fixed bed reactor	67	The catalyst was recycled for 5 times. The conversion of FFA dropped approximately 8.6% between each run	[29]
EBD100 (Gel)	Methanol	120 °C, 12:1 ($M_{MeOH:oil}$), 1 wt% and 24 h in a batch reactor	97.7	The rate of reaction drop significantly when the IER was reused for the first time. Much lower activity loss took place in the subsequent reuse	[37]
SK104H (Gel)	Methanol	60 °C, 6:1 ($M_{MeOH:oil}$), 3 wt% and 8 h	78	–	[50]
Purolite D5081 (Hyper-crosslinked)	Methanol	60 °C, 6:1 ($M_{MeOH:oil}$), 1.25 wt% and 8 h	92	The catalyst was recycled for 4 times. The conversion decreased by 8–10% per cycle	[1]

Table 4.12 Physiochemical properties of the IER used in the esterification of FFA in the plant oil

Properties	A15[a]	NKC9[b]	EBD100[c]	SK104H[d]	Purolite D5081[e]	PCT275DR[f]	D50WX8[f]
Type	Macro-reticular	Macro-reticular	Gel	Gel	Hyper-crosslinked	Macro-reticular	Gel
Matrix	Styrene (Styr) DVB	Styr DVB	Styr DVB	Styr DVB	g	Styr DVB	Styr DVB
Divinylbenzene (%)	20	g	g	4	g	>12	8
Operating pH	0–14	g	g	g	g	0–14	0–14
Cation type	H^+	H^+	H^+	H^+	H^+	H^+	H^+
Particle size range (μm)	600–850	40–125	g	300–1180	396–638	650–900	425–525
Total exchange capacity							
(a) Dry basis (meq H^+/g)	5.2	4.7	5.37	g	1.59	5.69	4.1
(b) Wet basis (meq H^+/mL)	g	1.5	g	1.1	g	g	g
Average pore diameter (nm)	30	56	g	369	g	g	g
S_{BET} (m^2 g^{-1})	53	77	g	g	514.18	26	~0
Maximum operating temperature (°C)	120	g	130	120	g	180	150

[a] Data adopted from Özbay et al. [33] unless stated otherwise
[b] Data adopted from Feng et al. [15] unless stated otherwise
[c] Data adopted from Russbueldt et al. [37] unless stated otherwise
[d] Data adopted from Yunus et al. [50] unless stated otherwise
[e] Data adopted from Abidin et al. [1] unless stated otherwise
[f] Data adopted from Saboya et al. [38] unless stated otherwise
[g] Data not available

in the reaction that used D50WX8 as catalyst. The reactant, 2-ethylhexanol with low polarity could not swell the gel-type D50WX8 hence the access to the active sites was limited. The physiochemical properties of these IER are demonstrated in Table 4.12.

4.8 Summary and Future Prospects

Strongly acidic ion exchange resins have been employed for more than 50 years as industrial catalysts. Both gelular and macroporous types strongly acidic IERs were found to be the potent catalyst for the esterification processes in the petrochemicals and oleochemicals industries from the environmental benefits point of view. The gelular-type acidic IERs performed as good as or even better than the macroporous-type acidic IERs in the esterification reactions that involved polar solvents. It also showed higher catalytic activity when bulkier reactant molecules such as glycerol, polyol, long-chain alcohol and organic acids, were used in the esterification reactions. Otherwise, the macroporous-type acidic IER was always favoured as it allowed ion exchange catalysis in aqueous, non-aqueous and non-polar solvents. The macroporous-type acidic IER is also suitable to be used in a stirred system as it possesses excellent resistance to various types of attrition.

Nonetheless, the catalytic activities of strongly acidic IERs were far lower than the homogeneous mineral acid catalysts used in the commercial esterification processes. The poor thermal stability of acidic IERs has also limited their applications in the processes requiring higher temperature such as esterification of fatty acid with polyol. The low surface area and pore size of the macroporous-type acidic IERs also restricted the access of bulkier molecules to the acid sites in the pore. In contrast to the comprehensive activity studies of the strongly acidic IERs catalysts in the esterification processes, the studies on their deactivation, stability, reusability, recovery and regeneration are very limited.

Consequently, additional efforts are required to improve this broad class of acidic IER catalysts with innovations. For instance, more thermally stable strongly acidic IERs with increased surface area and enhanced anti-swelling properties could be prepared using the polymer/silica hybrid composites as the support. The precisely structured polymeric supports to place sulphonic acid groups could also be investigated to develop the acidic IER with least leaching. Furthermore, the stability of this strongly acidic IER could be investigated in detailed to identify the cause of deactivation during the reaction. The used acidic IER catalysts from the esterification processes need to be recovered and regenerated using the standard methods recommended by the IER manufacturers to evaluate the methods effectiveness. In addition, effective methods of disposing waste catalysts also needed to be developed.

References

1. Abidin SZ, Haigh KF, Saha B (2012) Esterification of free fatty acids in used cooking oil using ion-exchange resins as catalysts: an efficient pretreatment method for biodiesel feedstock. Ind Eng Chem Res 51:14653–14664

2. Ahmad MAA, Kamaruzzaman MR, Chin SY (2014) New method for acrylic acid recovery from industrial waste water via esterification with 2-ethyl hexanol. Process Saf Environ Prot 92(6):522–531

3. Altıokka MR, Ödeş E (2009) Reaction kinetics of the catalytic esterification of acrylic acid with propylene glycol. Appl Catal A 362(1–2):115–120

4. Bhandari VM, Sorokhaibam LG, Ranade VV (2016) Ion exchange resin catalysed reactions-an overview. In: Joshi S, Ranade V (eds) Industrial catalytic processes for fine and specialty chemicals. Elsevier, Amsterdam, pp 393–426

5. Blagov S, Parada S, Bailer O, Moritz P, Lam D, Weinand R, Hasse H (2006) Influence of ion-exchange resin catalysts on side reactions of the esterification of—Butanol with acetic acid. Chem Eng Sci 61(2):753–765

6. Boz N, Degimenbasi N, Kalyon DM (2015) Esterification and transesterification of waste cooking oil over amberlyst 15 and modified amberlyst 15 catalysts. Appl Catal B 165:723–730

7. Buluklu AD, Sert E, Karakuş S, Atalay FS (2014) Development of kinetic mechanism for the esterification of acrylic acid with hexanol catalyzed by ion-exchange resin. Int J Chem Kinet 46(4):197–205

8. Chin SY, Ahmad MAA, Kamaruzaman MR, Cheng CK (2015) Kinetic studies of the esterification of pure and dilute acrylic acid with 2-ethyl hexanol catalysed by Amberlyst 15. Chem Eng Sci 129:116–125

9. Constantino DS, Pereira CS, Faria RP, Ferreira AF, Loureiro JM, Rodrigues AE (2015) Synthesis of butyl acrylate in a fixed-bed adsorptive reactor over Amberlyst 15. AIChE J 61:1263–1274

10. Đặng T, Chen B (2013) Optimization in esterification of palmitic acid with excess methanol by solid acid catalyst. Fuel Process Technol 109:7–12

11. Dange PN, Rathod VK (2017) Equilibrium and thermodynamic parameters for heterogeneous esterification of butyric acid with methanol under microwave irradiation. Resour Efficient Technol 3:64–70

12. Darge O, Thyrion FC (1993) Kinetics of the liquid phase esterification of acrylic acid with butanol catalysed by cation exchange resin. J Chem Technol Biotechnol 58(4):351–355

13. de Aguiar VM, de Souza ALF, Galdino FS, da Silva MMC, Teixeira VG, Lachter ER (2017) Sulfonated poly(divinylbenzene) and poly(styrene-divinylbenzene) as catalysts for esterification of fatty acids. Renew Energy 114Part B 725–732

14. Delgado P, Sanz MT, Beltran S (2007) Kinetic study for esterification of lactic acid with ethanol and hydrolysis of ethyl lactate using an ion-exchange resin catalyst. Chem Eng J 126:111–118

15. Feng Y, He B, Cao Y, Li J, Liu M, Yan F, Liang X (2010) Biodiesel production using cation-exchange resin as heterogeneous catalyst. Bioresour Technol 101(5):1518–1521

16. Gangadwala J, Mankar S, Mahajani S, Kienle A, Stein E (2003) Esterification of acetic acid with butanol in the presence of ion-exchange resins as catalysts. Ind Eng Chem Res 42:2146–2155

17. Hykkerud A, Marchetti JM (2016) Esterification of oleic acid with ethanol in the presence of Amberlyst 15. Biomass Bioenerg 95:340–343

18. Ilgen O (2014) Investigation of reaction parameters kinetics and mechanism of oleic acd esterification with methanol by using Amberlyst 46 as a catalyst. Fuel Process Technol 123:134–139

19. Izci A, Bodur F (2007) Liquid-phase esterification of acetic acid with isobutanol catalyzed by ion-exchange resins. React Funct Polym 67(12):1458–1464

20. Jiang Y, Lu J, Sun K, Ma L, Ding J (2013) Esterification of oleic acid with ethanol catalyzed by sulfonated cation exchange resin: experimental and kinetic studies. Energy Convers Manag 76:980–985

21. Ju IB, Lim H-W, Jeon W, Suh DJ, Park M-J, Suh Y-W (2011) Kinetic study of catalytic esterification of butyric acid and n-butanol over Dowex 50WX8-400. Chem Eng J 168:293–302

22. Kale S, Umbarkar S, Dongare M, Eckelt R, Armbruster U, Martin A (2015) Selective formation of triacetin by glycerol acetylation using acidic ion-exchange resins as catalyst and toluene as entrainer. Appl Catal 490:10–16
23. Karakus S, Sert E, Buluklu D, Atalay FS (2014) Liquid phase esterification of acrylic acid with isobutyl alcohol catalyzed by different cation exchange resins. Ind Eng Chem Res 53:4192–4198
24. Khan JA, Jamal Y, Shahid A, Boulanger BO (2016) Esterification of acetic acid and oleic acids within the Amberlyst 15 packed catalytic column. Koren J Chem Eng 33:582–586
25. Komoń T, Niewiadomski P, Oracz P, Jamróz ME (2013) Esterification of acrylic acid with 2-ethylhexan-1-ol: Thermodynamic and kinetic study. Appl Catal A 451:127–136
26. Kouzu M, Nakagaito A, Hidaka J-S (2011) Pre-esterification of FFA in plant oil tranesterified into biodiesel with the help of solid acid catalysis of sulfonated cation-exchange resin. Appl Catal A 405:36–44
27. Kuzminska M, Backov R, Gaigneaux (2015a) Behaviour of cation-exchange resin employed as heterogeneous catalysts for esterification of oleic acid with trimethylolpropane. Appl Catal A Gen 504:11–16
28. Kuzminska M, Backov R, Gaigneaux (2015b) Complementarity of heterogeneous and homogeneous catalysis for oleic acid esterification with trimethylolpropane over ion-exchange resins. Catal Commun 59: 222–225
29. Liu L, Liu Z, Tang G, Tan W (2014) Esterification of free fatty acids in waste cooking oil by heterogeneous catalyst. Trans Tianjin Univ 20:266–272
30. Mariana Reinoso D, Marta Tonetto G (2018) Bioadditives synthesis from selective glycerol esterification over acidic ion exchange resin as catalyst. J. Environ Chem Eng 6:3399–3407
31. Mulay A, Rathod VK. (2017) Esterification of maleic acid and butanol using cationic exchange resin as catalyst. J Chem Sci 129: 1713–1720
32. Orjuela A, Yanez AJ, Santhanakrishnan A, Lira CT, Miller DJ (2012) Kinetics of mixed succinic acid/acetic acid esterification with Amberlyst 70 ion exchange resin as catalyst. Chem Eng J 188:98–107
33. Özbay N, Oktar N, Tapan NA (2008) Esterification of free fatty acids in waste cooking oils (WCO): role of ion-exchange resins. Fuel 87(10–11):1789–1798
34. Pappu VKS, Kanyi V, Santhanakrishnan A, Lira CT, Miller DJ (2013) Butyric acid esterification kinetics over Amberlyst solid acid catalysts: the effect of alcohol carbon chain length. Bioresour Tehnol 130:793–797
35. Patel D, Saha B (2012) Esterification of acetic acid with n-hexanol in batch and continuous chromatographic reactors using a gelular ion-exchange resin as a catalyst. Ind Eng Chem Res 51(37):11965–11974
36. Qu Y, Peng S, Wang S, Zhang Z, Wang J (2009) Kinetic study of esterification of lactic acid with isobutanol and n-butanol catalysed by ion-exchange resins. Chin J Chem Eng 17:773–780
37. Russbueldt BME, Hoelderich WF (2009) New sulfonic acid ion-exchange resins for the preesterification of different oils and fats with high content of free fatty acids. Appl Catal A 362(1–2):47–57
38. Saboya RMA, Cecilia JA, García-Sancho C, Sales AV, de Luna FMT, Rodríguez-Castellón E, Cavalcante CL (2017) Synthesis of biolubricants by the esterification of free fatty acids from castor oil with branched alcohols using cationic exchange resins as catalysts. Ind Crops Prod 104:52–61.
39. Sert E, Buluklu AD, Karakuş S, Atalay FS (2013) Kinetic study of catalytic esterification of acrylic acid with butanol catalyzed by different ion exchange resins. Chem Eng Process 73:23–28
40. Sharma M, Wanchoo RK, Toor AP (2014) Amberlyst 15 catalyzed esterification of nonanoic acid with 1-propanol: kinetics, modeling, and comparison of its reaction kinetics with lower alcohols. Ind Eng Chem Res 53:2167–2174
41. Singh N, Kumar R, Sachan PK (2013) Kinetic study of catalytic esterification of butyric acid and ethanol over Amberlyst 15. ISRN Chem Eng 2013:6

42. Siril PF, Cross HE, Brown DR (2008) New polystyrene sulfonic acid resin catalysts with enhanced acidic and catalytic properties. J Mol Catal A Chem 279(1):63–68
43. Sirsam R, Hansora D, Usmani GA (2016) A Mini-Review on solid acid catalysts for esterification reactions. J Inst Eng India Ser E
44. Son SM, Kimura H, Kasukabe K (2011) Esterification of oleic acid in a three-phase, fixed-bed reactor packed with a cation exchange resin catalyst. Biores Technol 102:2130–2132
45. Speight JG (2016) Environmental organic chemistry for engineers. Butterworth-Heinemann
46. Van de Steena E, De Clereq J, Thybaut JW (2014) Ion exchange resin catalysed transesterification of ethyl acetate with methanol: gel versus macroporous resins. Chem Eng J 242:170–179
47. Toor AP, Sharma M, Thakur S, Wanchoo RK (2011) Ion-exchange resin catalyzed esterification of lactic acid with isopropanol: a kinetic study. Bull. Chem. React Eng Catal 39–45
48. Willing A (1999) Oleochemical esters—environmentally compatible raw materials for oils and lubricants from renewable resources. Fett/Lipid 101:192–198
49. Yin P, Chen L, Wang Z, Qu R, Liu X, Xu Q, Ren S (2012) Biodiesel production from esterification of oleic acid over aminophosphonic acid resin D418. Fuel 102:499–505
50. Yunus NBM, Roslan NAB, Chin SY, Abidin SZ (2016) Esterification of free fatty acid in used cooking oil using gelular exchange resin as catalysts. Procedia Engineering 148:1274–1281
51. Zhou L, Al-Zaini E, Adesina A (2013) Catalytic characteristics and parameters optimization of the glycerol acetylation over solid acid catalysts. Fuel 103:617–625

Chapter 5
Synthesis and Control of Silver Aggregates in Ion-Exchanged Silicate Glass by Thermal Annealing and Gamma Irradiation

Khaled Farah, Faouzi Hosni and Ahmed Hichem Hamzaoui

Abstract Samples of commercial silicate glass have been subjected to ion exchange by silver ions. The ion exchange was performed at 320 °C for periods from two minutes to one hour, in a molten mixture of $AgNO_3$ and $NaNO_3$ with a molar ratio of 1:99, 5:95 and 10:90. The ion exchange process was followed by different treatments: thermal annealing, gamma irradiation and their combined role in order to initiate the synthesis and control of silver aggregates in the surface of the glass matrix. UV-Visible absorption spectrometry results indicated that various states of silver existing in these glasses depend on heat treatment conditions. The silver ions (Ag^+) exist in almost all conditions, neutral silver atoms (Ag^0) exist only in samples subjected to heat treatment in the range of 250–450 °C, neutral silver aggregates (Ag^0) produced by thermal annealing at 550 °C were responsible for the absorption bands observed from 305, 350 and 450 nm, respectively. The effect of gamma irradiation in doses from 10 to 100 kGy and thermal annealing on glass samples was also investigated. The main modification induced by gamma rays on the structure of silicate glass was the creation of colour centres, Non-Bridging Oxygen Hole Centres (NBOHCs) and trapped electrons. The (NBOHCs) defects caused the absorption of light. The Ag^+ ions trapped electrons to form neutral silver Ag^0. The first step of silver aggregation was observed, following the irradiation by gamma rays, as well as after thermal annealing. After annealing at 550 °C, silver atoms spread out over glass surface to form silver aggregates. An absorption band at 430 nm was observed

K. Farah · F. Hosni
Energy and Matter Research Laboratory (LR16CNSTN02), National Centre for Nuclear Sciences and Technology, 2020 Sidi-Thabet, Tunisia

K. Farah (✉)
Higher Institute of Transportation and Logistics, University of Sousse, P.B. 247, 4023 Sousse, Tunisia
e-mail: kafarah@gmail.com

F. Hosni
Faculty of Sciences, University of Bisha, P.B. 551, Bisha 61922, Saudi Arabia

A. H. Hamzaoui
Laboratoire de Valorisation des RessourcesNaturelles et Matériaux de Récupération, Centre National de Recherecheen Sciences des Matériaux, B.P. 95, 2050 Borj-Cedria, Hammam-Lif, Tunisia

characterizing the Surface Plasmon Resonance (SPR) of silver aggregates. The calculated average radius increases from 0.9 to 1.35 nm as the annealing time increased from 10 to 490 min. The average radius of nanoparticles varied as a function of absorbed dose. Unexpectedly, 10 kGy was found to be the optimally absorbed dose corresponding to the maximum of the nanoparticle's average radius. The average radius of nanoparticles was decreased at a higher dose.

5.1   Introduction

The introduction of metals into vitreous matrices is the origin of many interesting phenomena. Particularly, the silver-doped glasses have been the subject of much research because of their various applications.

These include the colouring of glasses [1–4], the dosimetry of ionizing radiation [5] and recently the manufacture of optical devices [6]. The useful properties in all the mentioned applications depend mainly on the state of oxidation and silver aggregation degree in glass.

The ion exchange technique has been considered as one of the substantial methods for introducing noble metals into the glass surface. This doping method is easy to carry out and does not need elaborated equipment. Silver, gold and copper nanoparticles can be synthesized on the ion exchange glass surface by thermal annealing [7–9]. On the other hand, the role played by silver species is not still clear because of the complexity of the silver–glass interaction and the difficulties inherent in the identification of valence states and the possible aggregation of silver atoms. Little information is available in the literature concerning the UV-Visible spectral characteristics of such glasses during the different steps of the colouring process and their relation to different states of silver [10].

Recently, some papers have been published on the uses of ionizing radiation such as gamma rays, X-ray, laser beam, electron beam, or heavy ions with or as an alternative to thermal annealing to synthesize silver nanoparticles in ion-exchanged glasses [11–14]. It is well known that the main changes induced by ionizing radiation in glasses are the stable defects valence state change of the doping ions and the preexisting impurities in the glass. The defects created by irradiation become the origins of the light absorption and, as a result, they are called "colour centres". These centres are of different types depending on the composition of the glass. They are characterized by UV-Vis spectroscopy. The effects of gamma rays induced colour centres in non-exchanged silicate glasses have been presented in our previously published works [15, 16]. Only a few articles have appeared dealing with the combination of gamma rays and thermal treatment on the formation of silver nanoparticles in ion-exchanged glasses. More investigations are required to throw light on the relationship between the gamma rays dose and the formed silver nanoparticles size.

In this work, we investigated by optical absorption spectroscopy, the oxidation states of silver species in exchanged silicate glasses for different silver concentrations and ion exchange times. The exchanged samples are then subjected to heat treatments,

at different temperatures at different times, also to gamma irradiations, with different doses, followed by isochronal and isothermal annealing. The mechanism of the silver aggregates formation was also investigated.

5.2   Materials and Methods

5.2.1   Glass Composition

For optical measurements purpose UV-V, commercial silicate glasses were cut into pieces of $11 \times 30 \times 1.5$ mm^3 dimensions. Prompt gamma activation analysis technique was used to determine the glass composition (constituents in wt%: 68.5 SiO_2, 13.8 Na_2O, 8.2 CaO, 4.3 MgO, 1 Al_2O_3, 0.6 K_2O, 0.1 Fe_2O_3 and 3.5% of other components).

5.2.2   Ion Exchange

Ion exchange was carried out by submerging glass samples in a bath of molten salts formed by a combination of 10 g of $AgNO_3$ and $NaNO_3$ in an alumina crucible. The composition of the mixture was (1% $AgNO_3$: 99% $NaNO_3$), (5% $AgNO_3$: 95% $NaNO_3$) and (10% $AgNO_3$: 90% $NaNO_3$). The ion exchange occurred at a temperature of 320 °C for 2, 5, 10, 15, 20, 30, 40 and 60 min for each of the given concentrations. In the course of this stage, Ag^+ ions were diffused from the salt bath to penetrate into the glass surface. In order to remove any silver nitrate remaining on their surface, glass samples were washed with distilled water and acetone.

5.2.3   Gamma Irradiation and Thermal Treatment

Gamma irradiations of exchanged glasses were carried out at the Tunisian cobalt-60 gamma irradiation pilot plant [17] at the doses between 1 and 250 kGy. The dose rate was 8.5 kGy/h.

Thermal treatment was performed in an electrical furnace in the air with a temperature varying from 100 to 600 °C for time intervals from 10 to 492 min.

5.2.4 UV-Vis Optical Absorption Spectrometry

Absorption spectra of the glass samples were recorded with a Shimadzu UV-VIS spectrophotometer (Model Pharma Spec UV-1700) between 200 and 700 nm.

The measurements were made against a glass sample not exchanged and not irradiated.

5.3 Results and Discussion

5.3.1 Effect of Ion Exchange Conditions

The glass samples used in this study were colourless. After ion exchange, the glass developed a weak yellow colour which deepened slightly with increasing of ion exchange time or percentage of silver nitrate in the mixture ($AgNO_3$: $NaNO_3$).

The obtained results, summarized in Fig. 5.1, show the effect of these two parameters on the absorption spectrum. In general, the spectra are characterized by a narrow and asymmetric absorption band, similar to those obtained by Ahmed et al. [10] for silicate glass of similar composition. It is important to note that the asymmetrical shape of this band may be due to the spectrometer loss sensitivity in the UV range and does not correspond to the maximum of the band. This band is more pronounced for ion exchange times greater than 10 min. Its intensity increases with the increasing time of ion exchange. The maxima of this band appear between 305 and 309 nm.

5.3.2 Effect of Thermal Annealing Conditions

The effect of the thermal annealing was carried out only on the glass samples exchanged at 60 min with 1 and 10% of $AgNO_3$. These samples were annealed at the desired temperature between 250 and 550 °C. The heat treatment time was set at 30, 60 and 120 min for each temperature. The increase in temperature or time of heat treatment was manifested by a change in the colour of the glass: from faint yellow (before heat treatment) to bright yellow or brown. The UV-visible spectra of the glass samples subjected to thermal annealing are shown in Figs. 5.2 and 5.3.

It seems that these absorption bands are constituted by the superposition of different absorption bands corresponding to different absorbent centres. Assuming that the dispersion of these centres does not allow them to interact, the absorption envelope is a superposition of independent bands that can be modelled by Lorentzians. Absorption (A) at a wavelength λ can be described by (5.1).

$$A(\lambda) = \frac{A_{\mathrm{m}}}{1 + 4\left(\frac{\lambda - \lambda_0}{W}\right)^2} \tag{5.1}$$
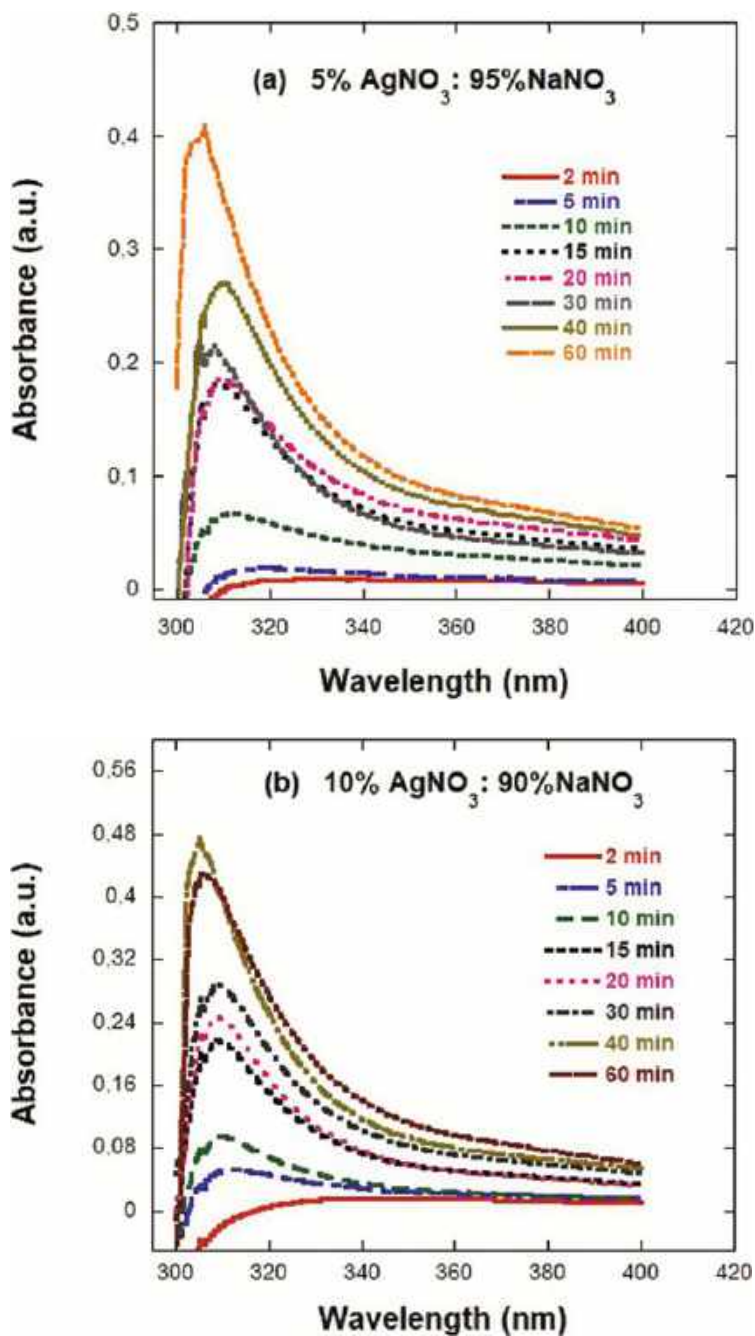
Fig. 5.1 Absorption spectra of glasses after ion exchange at 5% (**a**) and 10% (**b**) of $AgNO_3$ as a function of time in the $AgNO_3$: $NaNO_3$ mixture
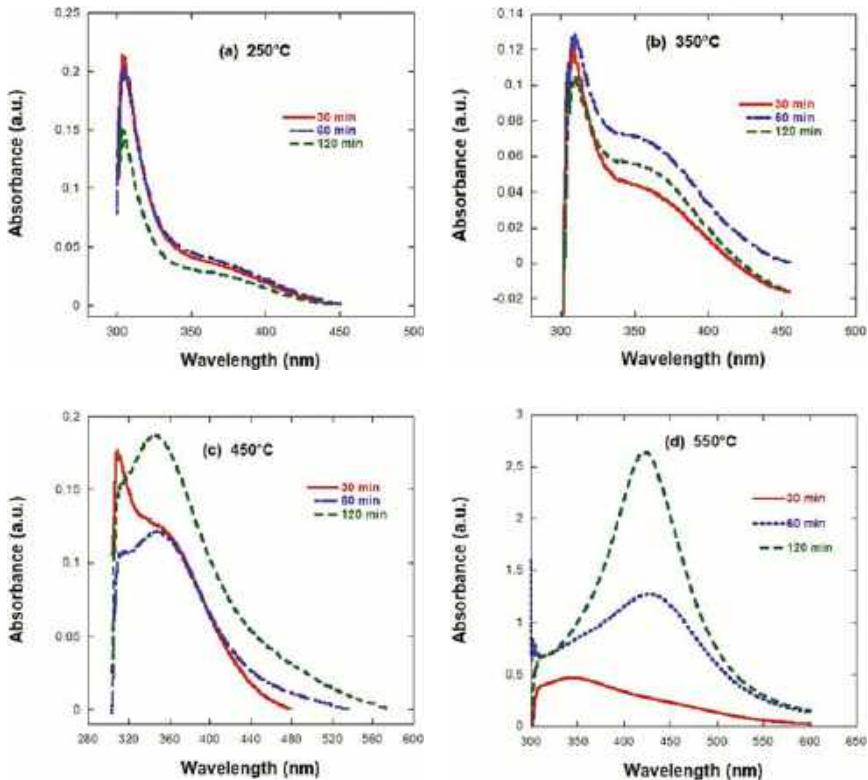
Fig. 5.2 Absorption spectra of the glasses after ion exchange at 1% AgNO$_3$ for temperatures of 250 °C (**a**), 350 °C (**b**), 450 °C (**c**) and 550 °C (**d**) as a function of the annealing time

where: λ_0 is the wavelength position of the absorption peak, W is the half-height width, and (A_m) is the relative intensity of the peak.

Based on the hypothesis of the absence of interaction between the different centres, the behaviour of each absorption band was treated independently.

The absorption band around 305 nm was observed in the two families of spectra corresponding to ion exchange and heat-treated glasses. For a mixture containing 10% AgNO$_3$, this band was observed at temperatures between 250 and 450 °C for all time periods of heat treatment.

On the other hand, for the mixture containing 1% AgNO$_3$, it appeared only at the temperatures of 250 and 350 °C and was independent of the annealing time. Furthermore, the intensity of this band (~305 nm) was increased with increasing of silver concentration and decreased gradually with increasing temperature and annealing time with an exception observed for samples treated for 30 min in 10% AgNO$_3$ where the intensity apparently increases with temperature (Fig. 5.3).

Ion exchange process occurred by diffusion of the silver ions of the molten salts towards the surface of the glass and by substitution of sodium ions Na$^+$. Considering
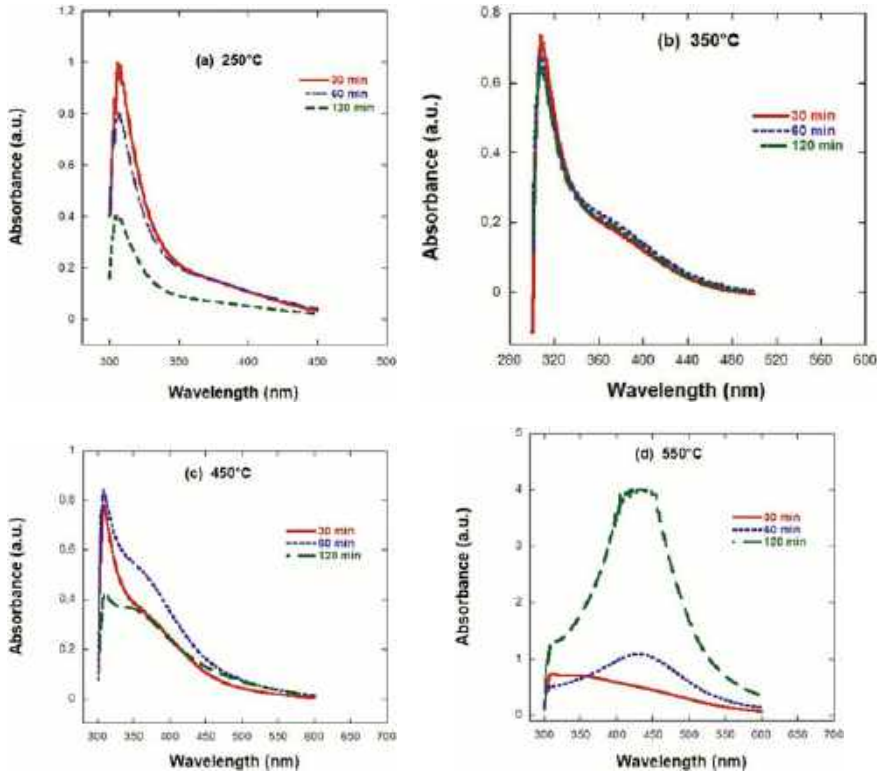
Fig. 5.3 Absorption spectra of the glasses after ion exchange at 10% AgNO$_3$ for temperatures of 250 °C (**a**), 350 °C (**b**), 450 °C (**c**) and 550 °C (**d**) as a function of the annealing time

that the Na$^+$ and Ag$^+$ ions being the only species participating in the doping process, it can be concluded that the observed changes in the UV region of absorption spectra of ion exchanged glass sample resulted due the change in composition of glass surface by replacing Na$^+$ ions by Ag$^+$ [18] as illustrated by (5.2) [10].

$$Ag^+NO_3^- + \equiv Si-O-Na^+ \rightarrow \equiv Si-O-Ag^+ + Na^+NO_3^- \qquad (5.2)$$
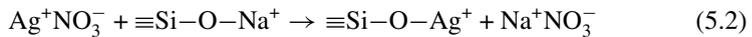
The number of silver ions diffused into the glass surface was proportional to the temperature and the time of ion exchange [10]. The layer containing the Ag$^+$ ions on the surface of the glass was colourless. The existence of this band was probably reported for the first time by Ito in 1962 [19] in a soda-lime silicate glass. He observed an absorption band at 314 nm, which increased in intensity with increasing either the temperature or time of ion exchange. The glass was yellow and not fluorescent, which led to attribute this band to the Ag$^+$ ions. Similar results have also been published by Ahmed et al. [10].

Some workers [20, 21] have studied the optical absorption of silver in borate glasses as a function of Ag_2O concentration. Three bands at 250, 310 and 407 nm have been identified. The intensities of these bands were observed to increase with increasing Ag_2O concentration in the glasses.

The absorption band at 407 nm could be linked with the colloidal silver responsible for the colouration of glass since this band appeared nearly at the same wavelength as that observed in silicate glasses and its intensity also varied in the same way as a function of silver oxide concentration [20, 22]. The origin of the bands at 250 and 310 nm was not obvious. The dependence of their intensities on the silver oxide concentration confirmed the existence of silver in the glass matrix.

Spierings et al. have also observed these two bands at 230 and 250 nm in the spectra of a silver-doped sodium borosilicate glass because of ion exchange [23]. These values were very close to those observed in the case of free Ag^+ ions [24].

Both bands were assigned to the 4d-5s electronic transition [21–23]. Spierings et al. explained the shift observed by the influence of the glass preparation method on the ionic character of the Ag–O bond. In the case where the doping has been carried out by ion exchange, the Ag–O bond is more ionic. In fact, the Ag^+ ions occupy the positions which were earlier occupied by the Na^+ ions. If the temperature is well below Tg, the ion exchange occurs without or with the only partial relaxation of glass network. Studies on the photoluminescence of several types of silver-doped glasses, with a low concentration [24], confirmed the luminescent behaviour of Ag^+ ions. In fact, the excitation of Ag^+-doped glasses with a wavelength of 228 nm showed a peak at around 330 nm. [25, 26]. This observation confirmed that the glass remained colourless after doping with silver.

The relaxation of Ag^+ ion from the excited state to the fundamental state may be used to explain the origin of the 330 nm emission peaks. A donor–acceptor pair recombination mechanism might be also proposed, in which the Ag^+ ion would be involved [25].

The absorption band around 350 nm also appeared for the samples annealed at 250 °C.

Initially, it was observed as a shoulder which became more pronounced depending on the temperature and/or the annealing time. The formation and stability of this band were critically dependent on the $AgNO_3$ concentration in the mixture as well as the annealing time and temperature as evident from Fig. 5.4a, b. In the case of a mixture containing 1% $AgNO_3$, the band at 350 nm was observed for heat-treated glasses at 450 °C for heat treatment time of 60 min. Its intensity increases with increasing heat treatment time and reached its maximum at 120 min. However, at 550 °C, the intensity of this band also increased but became less resolved for 30 and 60 min of annealing times and disappear completely after annealing for 120 min.

On the other hand, this band is retained when the mixture containing 10% $AgNO_3$ was used, but less pronounced and resolved than in the previous case with 1% $AgNO_3$. Its existence could be verified by a multi-Lorentzian resolution of the optical spectrum of glass sample annealed at 450 and 550 °C for 60 and 30 min, respectively (Figs. 5.5 and 5.6). This band can be observed only if the ion-exchanged glass is subjected to heat treatment.
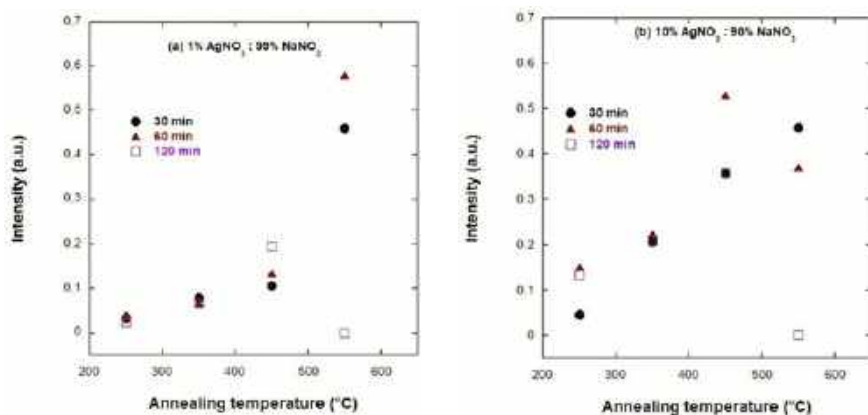
Fig. 5.4 Evolution of the maximum intensity of the band at 350 nm as a function of the temperature and time of the heat treatment for the silver ion-exchanged samples **a** 1% AgNO$_3$: 99% NaNO$_3$ and **b** 10% AgNO$_3$: 90% NaNO$_3$

The concentrations of both Ag$^+$ and Ag^0 species were determined from the relative intensities of their respective absorption bands. It was, therefore, expected that the conversion of Ag$^+$ ions into neutral Ag^0 atoms by heat treatment was correlated with the gradual decrease in the Ag$^+$ concentration, i.e., the gradual decrease of the absorption band intensity at 305 nm. This conversion was verified by this work with the exception of the sample containing 10% of AgNO$_3$ and annealed for 30 min, where the intensity at 305 nm apparently increased with the increase of the annealing temperature (Fig. 5.4). The persistence of the Ag$^+$ ions was expected, but with the gradual decrease of its intensity with increasing of temperature and time of the heat treatment because the Ag$^+$ ions were not all reduced to Ag^0 even after heat treatments at high temperatures and for longer times. Indeed, the reduction of Ag$^+$ ions can be influenced by Fe^{2+} ions, which are capable to release an electron by oxidation to Fe^{3+} ions. The glass used in this study contained a small amount of iron as an impurity of ~0.13%. EPR spectrum of the glass before the ion exchange showed the presence of ferric ions (Fe^{3+}) at $g = 4.3$ (Fig. 5.7). Since glass is usually made under reducing conditions, a significant part of the iron is in the ferrous state. The presence of a too small quantity of Fe^{3+} ions in glass could be the reason for the appearance of the band at 305 nm, regardless of the heat treatment conditions. However, such interpretation does not explain why Ag$^+$ acquired a higher concentration than that previously introduced by ion exchange. Nevertheless, this apparent contradiction, also observed by Ahmed et al. [10], can be explained by taking into account that the Ag$^+$ concentration in glass samples can be determined from the calculation of air under the peak which is proportional to the total of silver ions in the glass. In this case, it is obvious that Ag$^+$ ion concentration decreases with the increase of annealing temperature (Table 5.1), and the apparent contradiction between the results and the proposed assignment of the band can be eliminated.
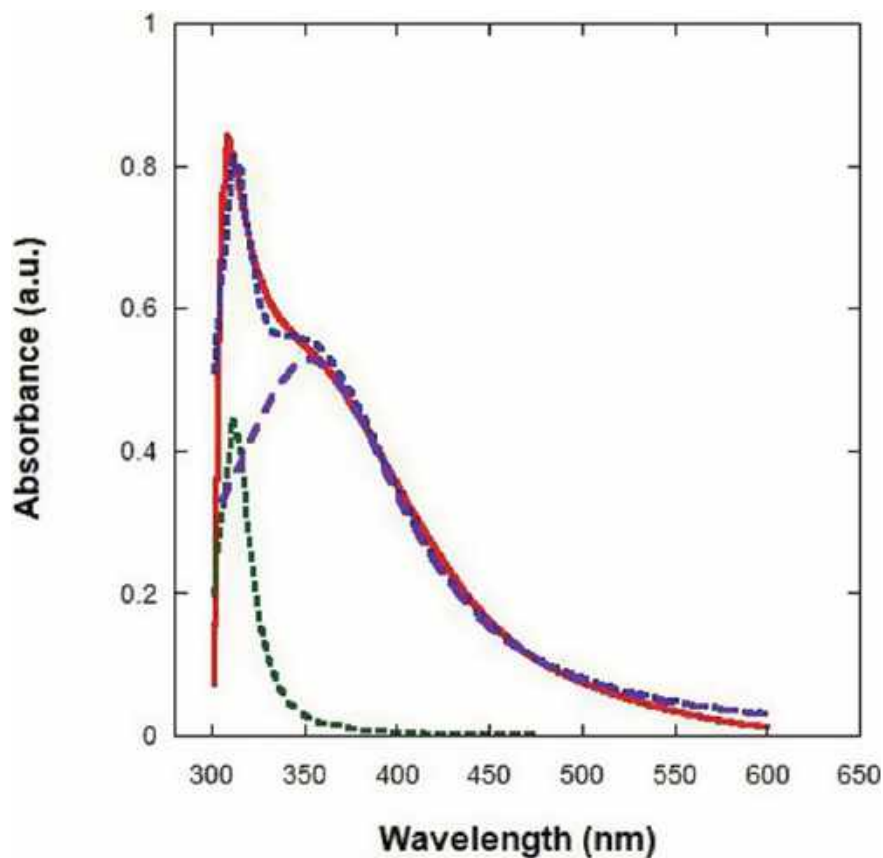
Fig. 5.5 Multi-Lorentzian fit of the absorption spectrum of a glass sample exchanged at 10% $AgNO_3$ and annealed at 450 °C for 1 h

Table 5.1 Area under absorption band at 305 nm as a function of heat treatment temperature and time, and the concentration of silver

Percentage of AgNO₃	Heat treatment time (min)	Area under peak (a.u.)			
		Annealing temperature			
		250 °C	350 °C	450 °C	550 °C
1%	30	5.02	4.11	2.47	0
	60	4.96	3.36	0	0
	120	3.44	1.68	0	0
10%	30	25.96	21.02	19.96	0
	60	25.9	19.99	10.6	0
	120	22.14	19.53	6.46	0
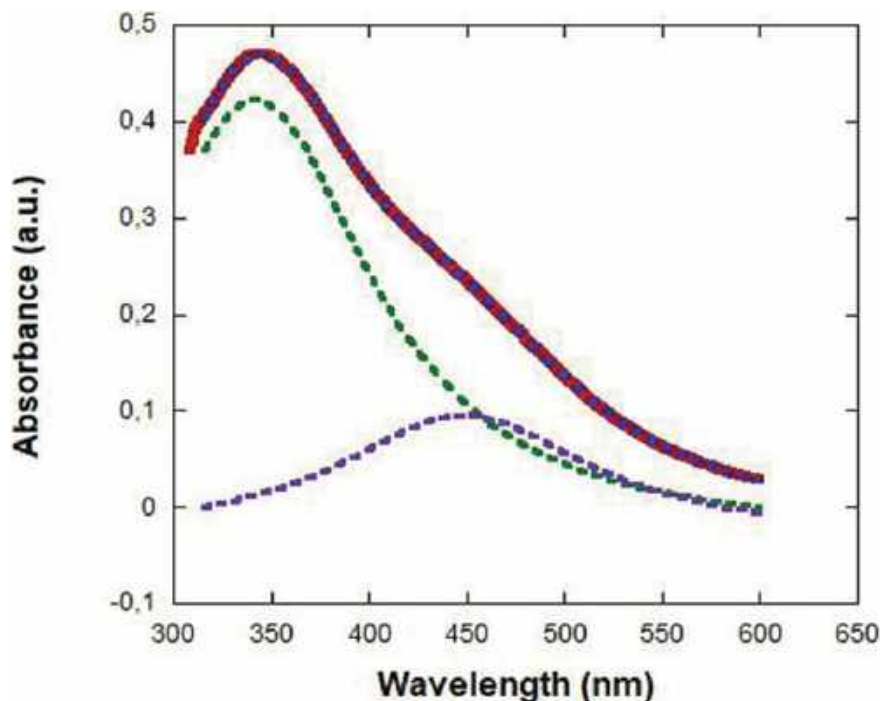
Fig. 5.6 Multi-Lorentzian fit of the absorption spectrum of a glass sample exchanged at 10% $AgNO_3$ and annealed at 550 °C for 0.5 h

In general, to develop the yellow colour, that is, to reduce the neutral silver atom, the silver ions must pass through an intermediate stage [27]. Indeed, the glass should contain a reducing agent or a polyvalent element, such as As_2O_3 or Fe_2O_3 [24, 28] or it must be subjected to a hydrogen atmosphere at moderate temperatures [27, 29] for reducing silver ions during the heat treatment. However, it has been mentioned in the literature that heat treatment alone was not sufficient to reduce silver ions. The resulting glass was colourless. This could be explained by the variation in the silver oxidation degree that strongly depends on the states of the valence of some polyvalent dopants such as iron usually existing in glasses in oxide form.

These show the reducing role of the arsenic ion, which is usually added as an impurity in the form of As_2O_3 the role of which is twofold, i.e. to remove bubbles; and causing the discolouration by oxidizing a portion of Fe^{2+} to Fe^{3+}. In addition, previous work has indicated that arsenic can modify the diffusion of silver in silicate glasses [24] and sol-gel silica [30].

On the other hand, results reported in the literature [31, 32] on the photoluminescence of silver-doped glasses have shown that the thermal treatment of these glasses develops a strong luminescence band around 500 nm, assigned to neutral silver Ag^0 approximately in the same temperature range where the appearance and disappear-
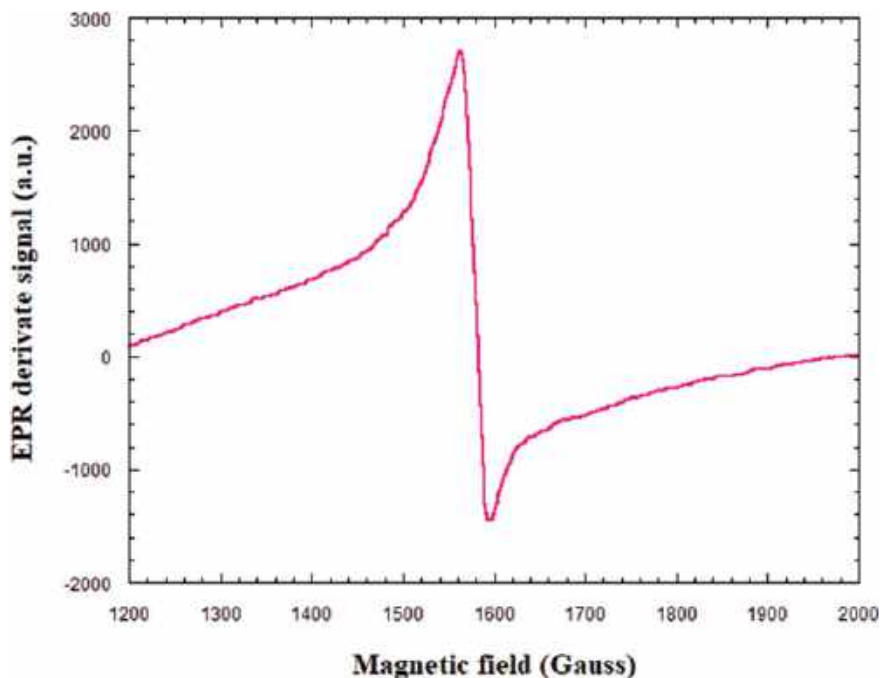
Fig. 5.7 Fe^{3+} signal in EPR spectrum of nonirradiated glass

ance of the absorption band at 350 nm was observed. The luminescence data and the formation sequence of the absorption band at 350 nm support its assignment to Ag^0.

The absorption band around 450 nm is characterized by a strong absorption and the glass turns brown. It is observed in the spectra of glasses annealed at 550 °C (Figs. 5.2d and 5.3d). For annealing times of 30 and 60 min, the absorption spectra composed of two separate bands at 350 and 430 nm. Beyond 60 min of thermal annealing, the resolution of the band at 430 nm increases sharply and is accompanied by a strong decrease until the disappearance of the band at 350 nm. On the other hand, a small shift of the absorption peak of this band to shorter wavelengths as well as its amplification has been observed if the annealing time increases from 30 to 120 min. Finally, its width decreases with increasing of thermal treatment time. The various parameters of this band obtained by multi-Lorentzian fit are shown in Table 5.2.

These results show that the peak position is independent of the silver concentration. On the other hand, the Full Width at Half Maximum (FWHM), the area under the peak and the maximum of absorbance are a function of the silver concentration in the mixture ($AgNO_3$: $NaNO_3$). The FWHM is slightly larger for the smaller amount of $AgNO_3$. In contrary, the area and the maximum of absorbance are proportional to the silver concentration introduced into the glass.

Table 5.2 Multi-Lorentzian fitting parameters of the absorption band around 450 nm as a function of annealing time, at 550 °C, and the concentration of silver

Percentage of AgNO$_3$	Annealing time (min)	λ (nm)	FWHM (nm)	Area under peak	Maximum of absorbance	Average aggre-gates radius
1%	30	449.3	145.8	1.4	0.01	1.02
	60	434.9	106	59.5	0.59	1.32
	120	420.6	98	243.7	2.49	1.34
10%	30	448.2	120.5	42.7	0.29	1.23
	60	436.1	101.5	89.3	0.84	1.39
	120	426.1	96	358.9	3.74	1.40

As reported in the literature [33, 34], the average radii R of the nanoparticle aggregates introduced into the vitreous matrix can be calculated using (5.3) [35]:

$$R = \frac{V_f \times \lambda_m^2}{2\pi \times C \times \Delta\lambda} \tag{5.3}$$

where:

V_f Electron Fermi velocity in silver $= 1.39.10^8$ cm/s

$\Delta\lambda$ FWHM of the absorption band

λ_m Characteristic wavelength at which the Plasmon surface resonance occurs

C Light velocity in a vacuum (3.10^8 m.s^{-1})

The calculated values of λ_m and $\Delta\lambda$ depend on the substrate and the silver aggregate size of the composite.

The average radii of the aggregates were calculated and are listed in Table 5.2. The results show that the aggregates radius, depend on the annealing time and the quantity of silver introduced into the glass surface. The values ranged between 1 and 1.4 nm.

The shape, intensity and absorption peak position around 450 nm are substantially affected by changes in temperature or thermal annealing time. The maximum intensity of the band increases with the increasing of silver concentration and time of the heat treatment. The absorption spectra became sharper and shifted to the shortest wavelengths.

Heat treatment has been shown to induce the reduction of silver ions to neutral silver atoms that get precipitated to form silver aggregates. As the heat treatment time increases, the number of Ag^0 atoms increases. Accordingly, the number and size of aggregates increase.

As the annealing time increases, silver aggregates that are not spherical tend to be, leading to a shift of λ_m to shorter wavelengths [7]. As a result, the increase in

the intensity of the absorption band at 450 nm with increasing of heat treatment time is ascribed to the increase in the number of Ag^+ atoms forming the nanosized particles. At the same time, the band becomes sharper, indicating the rapid growth of the aggregates.

The literature review revealed the agreement between different authors about the assignment of the band near 450 nm which has been ascribed to the silver aggregates [8, 33]. This band was found by Doremus at 405 nm in an aluminosilicate sodium glass [8] and in the 400–420 nm range by Piquet and Shelby in a float glass [20]. Sarker et al. [33] investigated the absorption spectra of ion-exchanged silver oxide glasses, they were able to observe only an absorption band at around 400 nm, which they attributed to the metallic silver particles in the glass matrix. The observed small variation of this band position could be explained by the difference of the glasses compositions or by the difference in the silver nanoparticles size. This band was due to the surface plasmon resonance of silver nanoparticles. In metal aggregates, the state density was too high to observe individual transitions between levels. These were the collective oscillations of the conduction electrons that were observed in the form of a plasmon resonance.

The previous behaviour, order of their appearance and the ranges of stability of the different bands observed in the absorption spectra of ion-exchanged glasses before and after the heat treatment suggest that each absorption band corresponds to a specific state of silver in the material. Therefore, it is expected that three different states of silver existed in these glasses, each of which is stable under given conditions. It can also be noted that each set of conditions (the amount of $AgNO_3$ introduced into the glass and the heat treatment time) can favour the formation of one, two or three silver states.

The mechanism of colouring the glass surface can be divided into three steps: (1) ion exchange reaction, (2) reduction of silver ions and (3) formation of colour centres. The yellow colour of the doped glass develops only after the aggregation of silver atoms Ag^0 following heat treatment to form silver crystallites $(Ag)_n$. The absorption bands observed in this study can therefore be ascribed to the following silver states: the band at 305 nm is assigned to the Ag^+ ions, the band at 350 nm is assigned to the neutral atoms Ag^0 and the band at 450 nm is assigned to the aggregates $(Ag^0)_n$, where n is the number of silver atoms forming the aggregate.

From the foregoing, it can be deduced that after the ion exchange only the band at 305 nm was observed, the glass samples were colourless. The 350 nm band, which was observed in the early stages of heat treatment, remained stable in a limited range of temperatures and times of heat treatment. Thus, these reduction processes occurred at the initial stage of heat treatment, did not absorb light in the visible range, and thus do not affect the colour of the glass. Increasing the annealing temperature up to 550 °C leads to the aggregation of the silver atoms to develop silver particles of colloidal dimensions $(Ag^0)_n$, inducing the characteristic band at 450 nm, and the glass becomes brown. These conclusions are in agreements with data published in the literature on similar glasses, particularly that of Ahmed et al. [10].

5.3.3   *Effect of Gamma Irradiation*

Samples of ion-exchanged glasses were irradiated by gamma doses ranging between 1 and 100 kGy. Figure 5.8a, b show the effect of increasing dose up to 100 kGy on the absorption spectra from 300 to 700 nm for samples ion-exchanged respectively at 1 and 10% $AgNO_3$.

In accordance with what reported by many authors, bands near 400 and 610 nm have been ascribed to "non-bridging oxygen hole centres" (NBOHCs: $\equiv Si-O^{\cdot}$) [34, 36]. The broad absorption spectrum around 400 nm is expected to be the superposition of two absorption bands at 350 and 410 nm. The additional band near 350 nm may be due to silver ion-exchange process. This could be verified by making a comparison between the spectrum of silver exchanged glass sample to that non-exchanged. The two samples were subjected together to gamma irradiation at 250 kGy [37] (Fig. 5.9).

The observation of this band, which was attributed to Ag^0 atoms, indicating that the induced photoelectrons have reduced silver ions according to the following reactions [13, 14]:

$$glass \overset{\gamma-irradiation}{\rightarrow} h^+ + e^- \tag{5.4}$$

$$Ag^+ + e^- \rightarrow Ag^0 \tag{5.5}$$

where h^+ is a hole centre.

Figure 5.8a, b, indicate the existence of Ag_2^+ ions. The shifting of the peak from 305 to 312 nm was also observed in the spectra of samples irradiated with absorbed dose above 1 kGy.
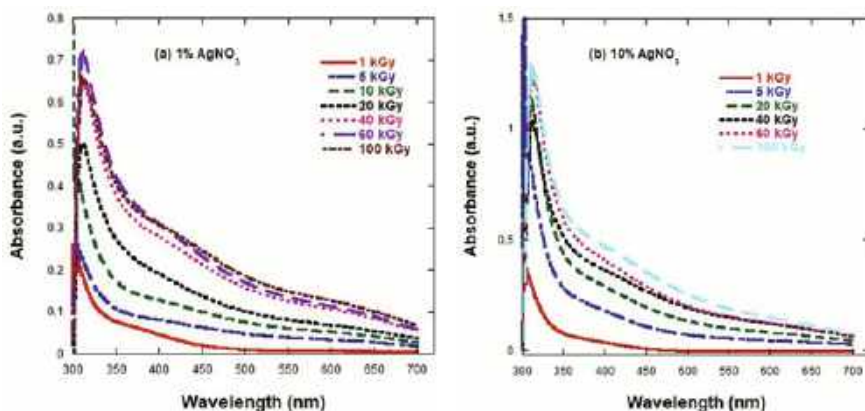
Fig. 5.8   Absorption spectra of glass sample ion-exchanged at 1% $AgNO_3$ (**a**) and at 10% $AgNO_3$ (**b**) and irradiated with gamma rays in the dose range of 1–100 kGy
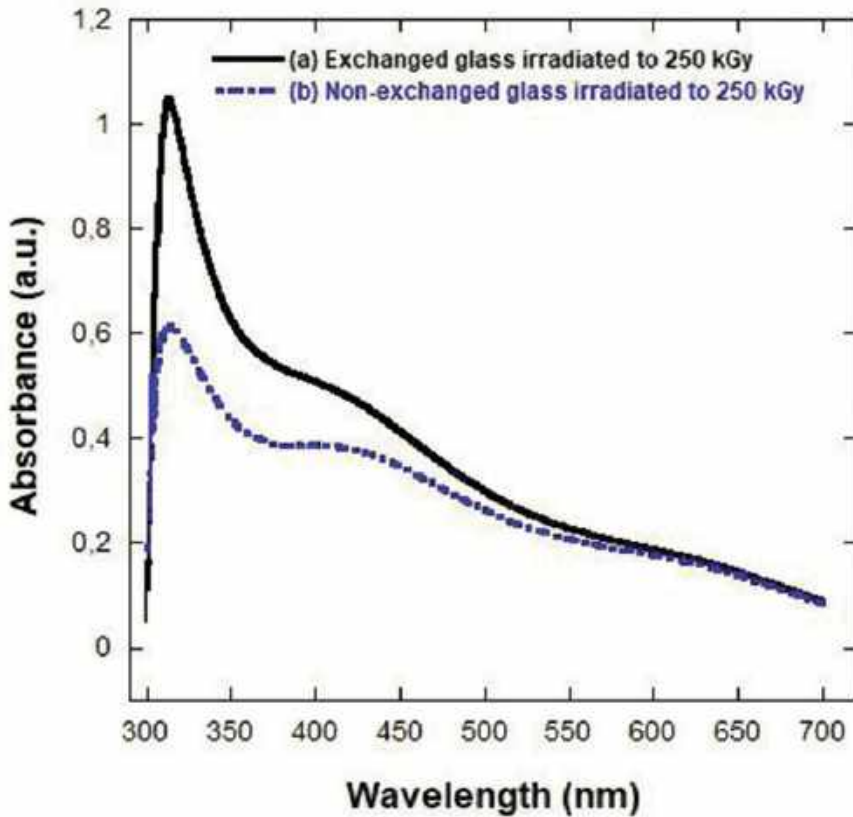
Fig. 5.9 Absorption spectra of the glass irradiated with gamma rays at 250 kGy: **a** spectrum of 10% AgNO$_3$ exchanged glass and **b** spectrum of non-exchanged glass

We assigned this peak (312 nm) to Ag$_2^+$. This peak was also identified by Bellouni and Mostafavi in radiolyzed aqueous solutions containing Ag$_2^+$ ions [38]. De Lamaëstre identified the peak at 312 nm in a silver-doped silicate glass subjected to combined effects of gamma rays and heat treatment [13].

Figure 5.10 shows the specific absorbance of non-bridging oxygen hole centres (NBOHC) ($\lambda \sim 400$ nm) in gamma-irradiated glasses with doses between 1 and 100 kGy as a function of the concentration of AgNO$_3$ introduced into the glasses by ion exchange. In the absence of silver, the concentration growth of NBOHC was rapid up to 40 kGy. For doses between 40 and 100 kGy, the specific absorbance continued to increase, but slowly without reaching saturation. The nonlinear dependence of the absorbance as a function of the dose can be explained by the simultaneousexistence of two different mechanisms involved in the colour centres formation [39, 40]:
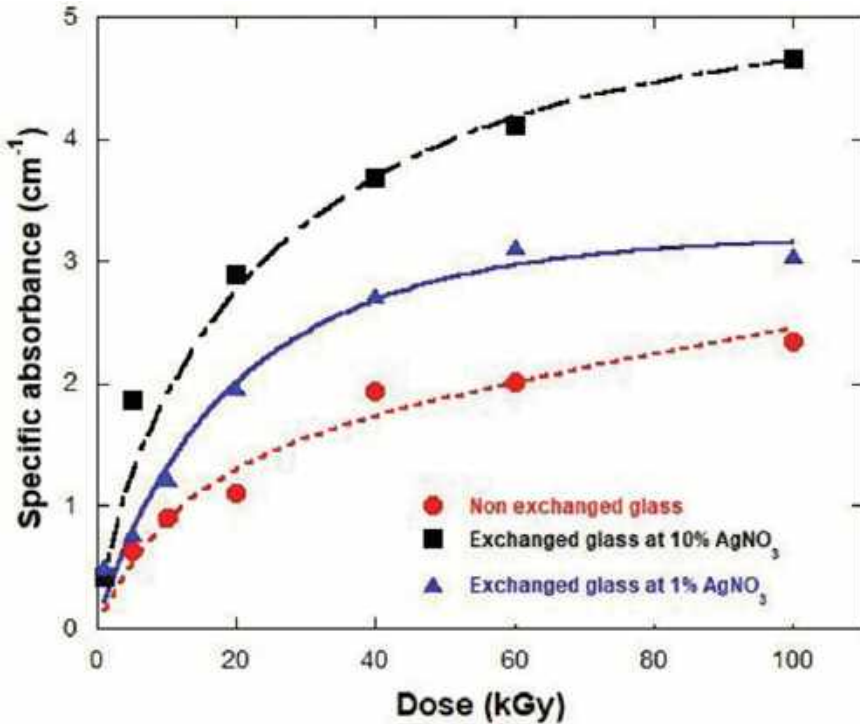
Fig. 5.10 Dose response curves of NBOHC trapped holes ($\lambda \sim 400$ nm) in glasses irradiated with gamma radiation in the dose range between 1 and 100 kGy as a function of the concentration of $AgNO_3$ introduced into glass by ion-exchange

(1) Extrinsic process: Activation of a fixed number of preexisting precursors (Reaction 5.6) which saturate with irradiation dose because of their limited concentration.

$$\equiv Si - O - X + h\nu(\gamma \text{ rays}) \rightleftharpoons Si-O^{\cdot} + {}^{\cdot}X \qquad (5.6)$$
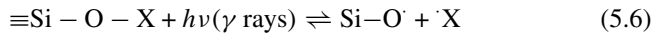
(2) Intrinsic process: Creation of unlimited new defects during $\equiv Si-O-Si\equiv$ bond breaking (Reaction 5.7).

$$\equiv Si-O-Si\equiv + h\nu(\gamma \text{ rays}) \rightarrow \equiv Si-O^{\cdot} + {}^{\cdot} Si\equiv \qquad (5.7)$$
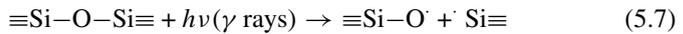
In the presence of silver, the specific absorbance of the NBOHC was proportional to the dose up to 60 and 80 kGy for the samples exchanged respectively at 1 and 10% of $AgNO_3$, then reached to saturation at high doses contrary to samples that to the samples that have not been subjected to silver ion exchange. This showed that

Table 5.3 Characteristics of the plasmon resonance band, obtained by Lorentzian fitting, of two glass samples exchanged at 1% AgNO$_3$ and subjected to different treatments

Treatment underwent by the glass sample	Peak position (nm)	FWHM (nm)	Max. absorbance (u.a.)	Average aggregates radius (nm)
Annealed at 550 °C for 1 h	429.6	140.3	1.48	0.97
Irradiated at 250 kGy and annealed at 550 °C for 1 h	421.4	94.0	2.99	1.40

the creation process of NBOHC centres by gamma irradiation, in silver exchanged samples, was purely extrinsic.

5.3.4 Combined Effects of Gamma Irradiation and Thermal Annealing

5.3.4.1 Thermal Annealing of Irradiated Exchanged Glasses

The only effect of thermal annealing at 550 °C for 1 h and the combined effects of gamma irradiation (at 250 kGy) and thermal annealing (at 550 °C for 1 h) on exchanged glass samples (with 1% AgNO$_3$) are shown in Fig. 5.11. We observed in the spectra a new band at 430 nm. As discussed in a preceding paragraph, this band was ascribed to Surface Plasmon Resonance (SPR) of nanosized silver particles. The diffusion and accumulation of Ag^0 atoms in glass surface during the irradiation by gamma rays and/or thermal annealing (Reaction 5.8) [14] may explain the formation of these nanosized particles.

$$nAg^0 \rightarrow Ag_n \tag{5.8}$$

From Fig. 5.11, it is clear that the FWHM for the spectrum of the nonirradiated glass is much greater than that for the spectrum of the irradiated one. The peak maxima of absorbance were increased significantly and the peak position exhibited the blue-shift from 430 nm to about 420 nm. The average radius R of the nanosized particles calculated for the two samples using (5.3) was found to increase considerably (by 50%) in the irradiated glass (Table 5.3). The increase of the radius of the particle for the irradiated glass may be due to the diffusion of silver in the glass when the ion-exchanged glass was exposed to radiation before thermal annealing.

5.3.4.2   Isochronal Annealing: Observation of the First Step of Silver Precipitation

Figure 5.12 illustrates the optical spectra of 5% $AgNO_3$ exchanged glasses, irradiated at 250 kGy and subjected to isochronal annealing (20 min) for temperatures from 100 to 600 °C. The evolution of different defects concentration and silver species as a function of the annealing temperature is shown in Fig. 5.13. The concentration of all radiation-induced defects, as well as to Ag^0, decreased with increasing temperature up to 200 °C. Trapped holes, as well as electrons, recombine according to reactions 5.9 and 5.10 [13]:

$$NBOHC + e^- \rightarrow NBO \tag{5.9}$$

$$Ag^0 + NBOHC \rightarrow Ag^+ + NBO \tag{5.10}$$

In between 200 and 400 °C, all NBOHC holes were converted to NBOs and therefore the Ag^0 concentration became practically stable.
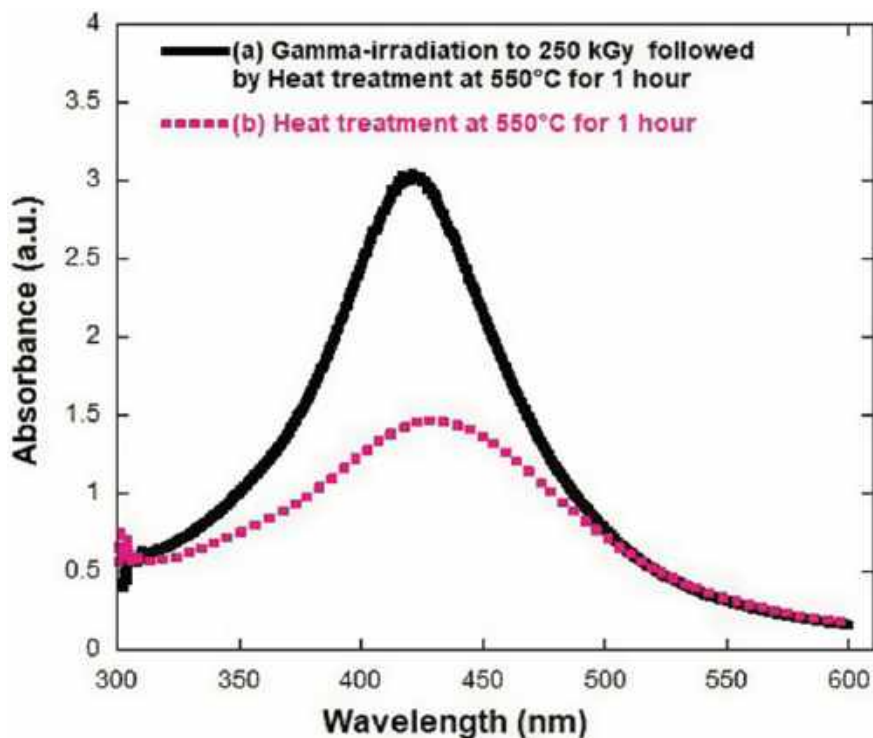
Fig. 5.11   Absorption spectra of ion-exchanged silicate glass, under the following conditions: **a** irradiated at 250 kGy and annealed at 550 °C for 1 h: **b** annealed at 550 °C for 1 h
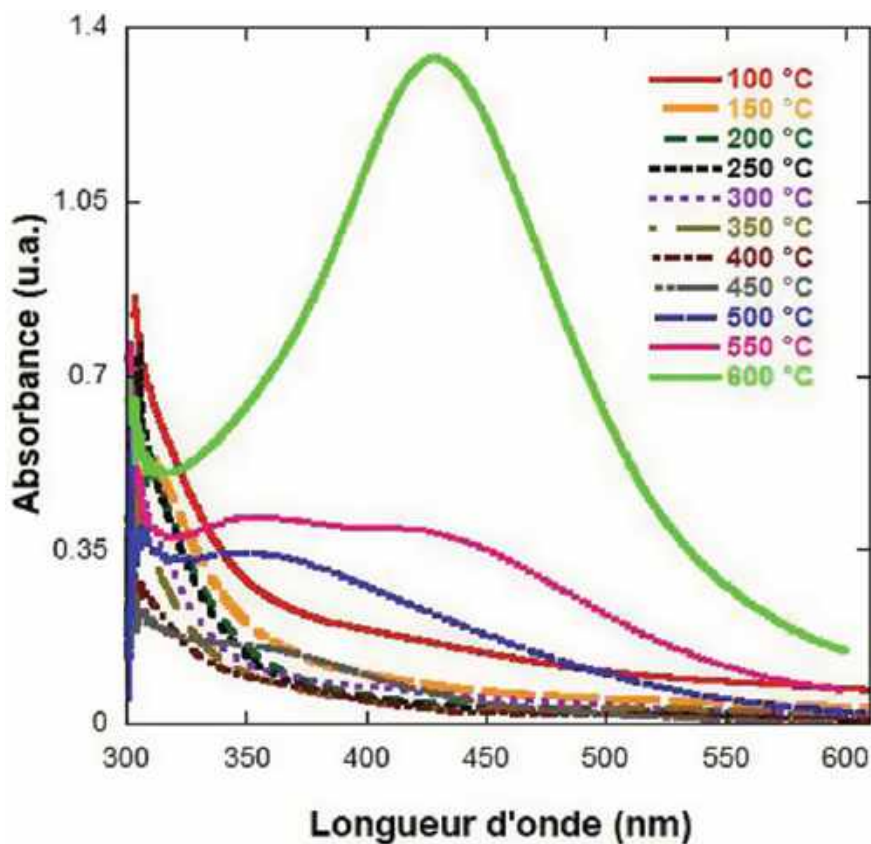
Fig. 5.12 Absorption spectra of samples glass samples exchanged at 5% AgNO₃, irradiated at 250 kGy by gamma rays and subjected to isochronal annealing (20 min) for temperatures ranging from 100 to 600 °C

Between 400 and 550 °C, an increase in Ag^0 concentration was observed which is assumed due to electron trapping according to (5.5). At 550 °C, a low-intensity new peak around 440 nm appeared which was due to the Surface Plasmon Resonance (SPR) of silver nanosized particles. When the annealing temperature increases up to 600 °C, the maximum absorbance of the new band at 440 nm increased by a factor of 4. A blue-shift of the peak position to 425 nm was also observed. We observed the disappearance of the band attributed to Ag^0. The average radius R of the nanosized particles calculated using (5.3) was about 0.9 nm.
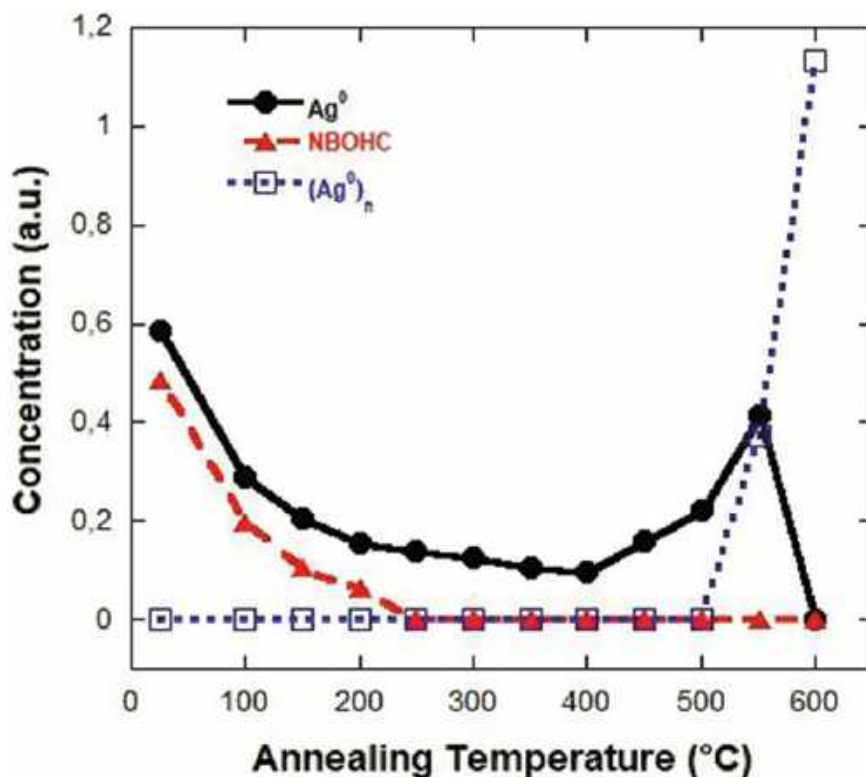
Fig. 5.13 The evolution of the concentration of different defects and silver species plotted as a function of the annealing temperature

5.3.4.3   Isothermal Annealing at 550 °C: Observation of the Precipitation of Silver Aggregates

The ion-exchanged glass sample (10% $AgNO_3$) was gamma irradiated at 250 kGy and then annealed at 550 °C for different time periods from 10 to 492 min. The results of isothermal annealing are presented in the Fig. 5.14.

Table 5.4 exhibits the characteristics variation of the band at 439 nm, calculated by a Lorentzian form of fitting, with the increase of heat treatment time. Substantial increase of the area under the peak by the increasing of heat treatment time and a significant blue-shift of the peak position from 439 to 419 nm were noticed. Concurrently, the band became sharper and the FWHM decreased from 159 to 97 nm. The number of Ag^0 atoms increased with increasing of heat treatment time. Consequently, the number and the dimensions of the nanosized silver particles increased. The gradual blue-shift of the peak position with increasing annealing time indicated the shape of the nanoparticles that progressively changed to more spherical. From
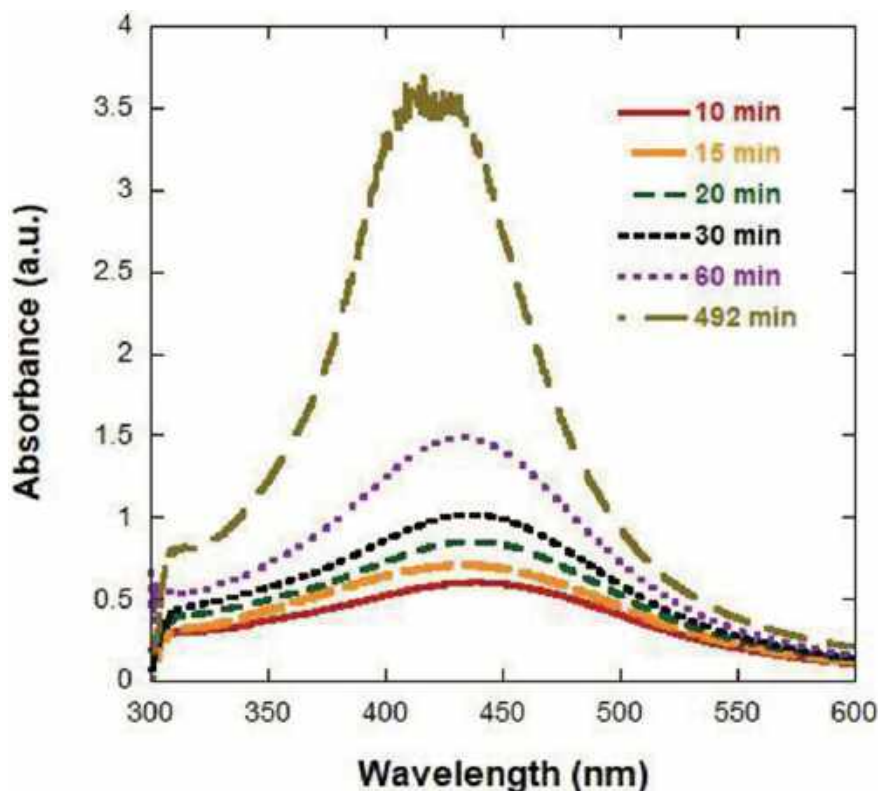
Fig. 5.14 Absorption spectra of ion-exchanged silicate glass at 10% AgNO$_3$, irradiated with γ rays at 250 kGy and annealed at 550 °C for the indicated times

Table 5.4 it is also evident that the average radius of the nanoparticles increased from 0.9 to 1.35 nm when the annealing time increased from 10 to 492 min.

5.3.4.4 Effect of Absorbed Dose Variation

In order to study the evolution of the nanoparticles characteristics when glass samples will be exposed to incremental gamma doses, samples exchanged at 10% AgNO$_3$ were irradiated between 1 and 100 kGy and then heat-treated at 550 °C for 1 h. For an absorbed dose of 1 kGy, the recorded broad spectrum (Fig. 5.15) is due to the superposition of two independent bands (350 and 450 nm). The band at 350 nm completely disappeared when the dose was higher than 1 kGy, and band at 450 nm became well resolved. The main characteristics of this band with incremental gamma doses, calculated by multi-Lorentzian functions are listed in Table 5.5. For doses between 5 and 20 kGy, the peak position shifted from 448 to 428 nm. A significant

Table 5.4 Characteristics of the plasmon resonance band as a function of annealing time at 550 °C, obtained by Lorentzian fitting, of glass samples exchanged to 10% $AgNO_3$ and irradiated to 250 kGy

Annealing time (min)	Peak position (nm)	FWHM (nm)	R^a(nm)	Area under band (a.u.)
10	439	159	0.89	154.78
15	435	158	0.89	179.12
20	438	146	0.97	200.88
30	437	140	1.01	229.09
60	433	126	1.10	300.61
492	419	97	1.34	562.30

[a]The average aggregate radius R

increase in the maximum of absorbance and a reduction of the FWHM from 172 to 135 nm for doses below 10 kGy were observed. These modifications induced by the increase of the gamma doses can be related to the increase of the average radius of the nanoparticles as it was found previously. Likewise, doses greater than 5 kGy have no effect on the shape of the nanoparticles since no significant shift in the absorption peak has been detected beyond this limit.

As pointed out in the literature [8, 41], the nanoparticles shape depends mainly on the position of the peak, while the nanoparticles size depends on the FWHM values. Therefore, perfect spherical nanoparticles could be radiation synthesized at a specific delivered absorbed dose.

A significant decrease in the maximum absorbance of the peak and a re-increase of the FWHM were observed when the samples were irradiated at doses above 10 kGy.

These results could be explained as follow, in a first step ($D < 10$ kGy), we observe the partial neutralization of Ag^+ in Ag^0 by gamma rays. In the next step ($D > 10$ kGy), we observe the first stage of silver aggregation (5.11) [13]:

Table 5.5 Characteristics of the plasmon resonance band as a function of gamma irradiation dose, obtained by Lorentzian fitting, of glass samples exchanged to 10% $AgNO_3$

Dose (kGy)	Peak position (nm)	FWHM (nm)	R^a(nm)	Max. absorbance (u.a.)
1	448	172	0.86	0.38
5	434	147	0.95	2.80
10	430	135	1.02	3.38
20	428	140	0.97	3.29
40	436	154	0.92	2.80
60	434	161	0.87	2.45
100	433	186	0.75	1.59

[a]The average aggregates radius
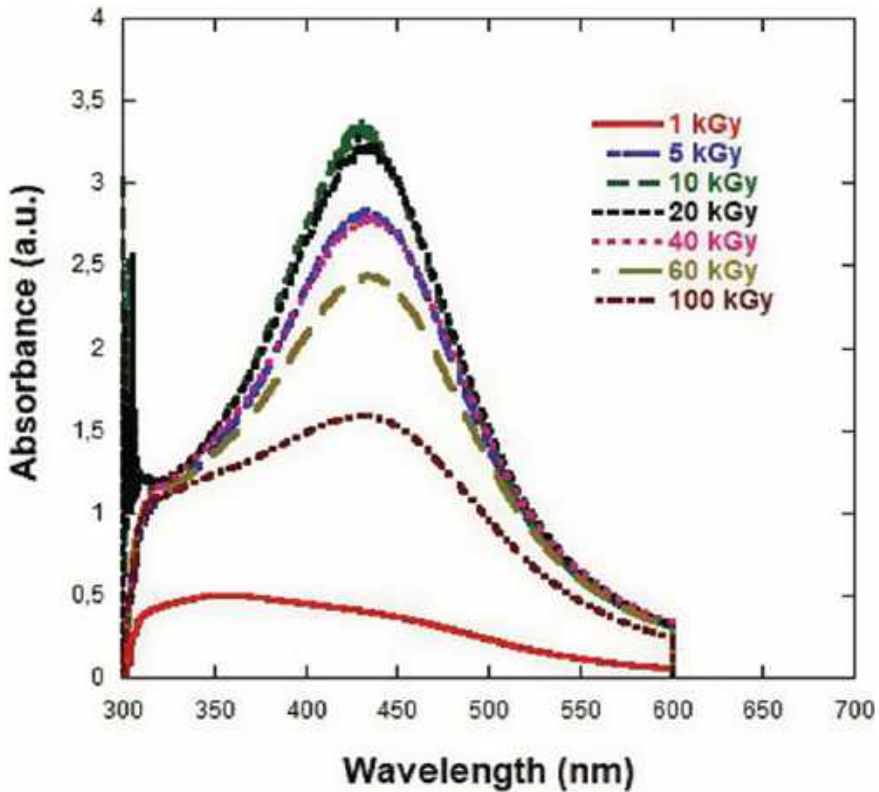
Fig. 5.15 Absorption spectra of ion-exchanged silicate glass 10% $AgNO_3$, irradiated with γ rays in the dose range of 1–100 kGy and annealed at 550 °C for 60 min

$$Ag^+ + Ag^0 \rightarrow Ag_2^+ \tag{5.11}$$

The decrease in Ag^0 concentration due to gamma irradiation is indicated both by the reduction of the area under the absorption band and the increase of its FWHM when the dose increases between 10 and 100 kGy. Since for doses $D > 10$ kGy, the formed Ag^0 atoms (by reduction Ag^+) were converted to Ag_2^+ ions (5.11). It seems that for dose lower than 10 kGy the quantity of the neural silver atoms Ag^0 was not enough to stimulate this reaction [37].

5.4   Conclusion

In the first part of this chapter, we had introduced silver ions in a commercial silicate glass surface by ion exchange technique at 320 °C under different conditions of silver

concentration and ion-exchange time. The ion-exchanged glasses were subjected to different heat treatments. The absorption spectra were recorded in the range of 200–700 nm and used to identify the various states of silver existing in these glasses, to determine the range of stability of each identified state and to determine the size of the formed silver aggregates. The results suggested that silver ions (Ag^+) exist in almost all conditions, neutral silver atoms (Ag^0) exist only in samples subjected to heat treatment in the range 250–450 °C and silver aggregates (Ag^0)$_n$ produced by thermal annealing at 550 °C are responsible for the absorption bands observed around 305, 350 and 450 nm, respectively.

In the second part of this chapter, we studied the synthesis and control of nanosized silver particles in the surface of ion-exchanged glass using combined techniques. Ion-exchanged glass samples were exposed to gamma rays at different doses between 1 and 100 kGy and then subjected to thermal treatment. Optical absorption spectra have been recorded. During the annealing at 550 °C of the irradiated samples, the silver atoms diffused and aggregated and nanosized particles were formed. The average radius of the nanoparticles depends on annealing time and gamma doses and found to be between 0.9 and 1.35 nm.

We have demonstrated that gamma rays increase considerably the diffusivity of neutral silver atoms in the glass surface and initiate the first stage of silver aggregation. As a result, the silver nanoparticles formation process can be improved if ion-exchanged glasses were exposed to gamma radiation before heat-treated.

References

1. Seward TP (1980) J Non-Cryst Solids 40:499
2. Rao KJ (2002) Structural chemistry of glasses. Elsevier Science, Amsterdam
3. Ageev LA, Miloslavskiĭ VK, Makovetskiĭ ED (2007) Opt Spectrosc 102:442
4. Bandyopadhyay AK (2008) Nano materiels. New Age International, Kolkata, India
5. Schulman JH, Ginther RJ, Klick CC, Alger RS, Levy RA (1951) J Appl Phys 22:1479
6. Bach H, Neuroth N (1998) The properties of optical glass. Springer, Berlin
7. Doremus RH (1964) J Chem Phys 40:2389
8. Doremus RH (1965) Physics 42:414
9. Manikandan D, Mohan S, Magudapathy P, Nair KGM (2003) Phys B 325:86
10. Ahmed AA, Abd-Allah EW (1995) J Am Ceram Soc 78:2777
11. Kowal TM et al (2000) Nucl Instr Meth B 166:490
12. Hofmeister H, Thiel S, Dubiel M, Schurig E (1997) Appl Phys Lett 70:1694
13. Espiau de Lamaestre R et al (2008) Phys Rev B 76:205431
14. Zhang J (2008) J Cryst Growth 310:234
15. Farah K et al (2002) Current topics in ionizing radiation research, In: ed. by M Nenoi (InTech Open Access Publisher, Croatia), p. 603
16. Farah K et al (2007) Fundamental and applied spectroscopy. In: Seddiki E, Telmini M (eds) Conference Proceedings, vol. 935. AIP, Melville, New York
17. Farah K et al (2006) Radiat Meas 41:201
18. Yamane M, Asahara Y (2004) Glasses for photonics. Cambridge University Press, Cambridge, UK
19. Ito T (1961) Bull Chem Soc Jpn 35:1312
20. Piquet JL, Shelby JE (1985) J Am Ceram Soc 68:450

21. Bach H, Baucke FGK, Duffy JA (1986) Chem Glasses 27:215
22. Shelby JE, Vitko J Jr, Non-Cryst J (1982) Solids 50:107
23. Spierings GACM, Non-Cryst J (1987) Solids 94:407
24. Paje SE, García MA, Llopis J, Villegas MA, Non-Cryst J (2003) Solids 318:239
25. Paje SE, Llopis J, Villegas MA, Fernández Navarro JM (1996) Appl Phys A 63:431
26. Villegas MA et al (2005) Mater Res Bull 40:1210
27. Shelby JE (2005) Introduction to glass science and technology. The Royal Society of Chemistry, Cambridge, UK
28. Chopinet MH, Lizarazu D, Rocanière C (2002) C R Chim 5:939
29. Kaganovskii Yu et al (2007) J Non-Cryst Solids 353:2263
30. García MA et al (2011) J Phys D: Appl Phys 32:975
31. Ahmed AA et al (1992) In: Proceeding of 16th international congress on glass, vol 4, Madrid, Spain, p 503
32. Paje SE et al (1998) Appl Phys A 67:429
33. Sarker S, Kumar J, Chakravorty D (1983) J Mater Sci 18:250
34. Schreurs JWH (1967) J Chem Phys 47(2):818
35. Battaglin G et al (1996) Nucl Instrum Methods B 116:527
36. Griscom DL (1984) J Non-Cryst Solids 64:229
37. Farah K et al (2014) Nucl Instr Meth B 323:36
38. Bellouni J, Mostafavi M (1999) Metal clusters in chemistryIn: Braunstein P, Oro LA, Raithby PR (eds) (Wiley-VCH Verlag GmbH, Weinheim, Germany 1999), p 1213
39. Galeneer FL et al (1993) Phys Rev B 47:7760
40. Farah K et al (2010) Nucl Instr Meth A 614:137
41. Mennig M, Berg KJ (1991) Mater Sci Eng B9:421

Chapter 6
Use of Ion-Exchange Resin in Reactive Separation

Neha Srivastava and Mohammed Kuddus

Abstract In the last few years, we have seen a dramatic increase in the application of reactive separation processes to various fields including pharmaceutical, chemical, biochemical, agrochemical, petrochemicals, fragrances, food and biotechnology industries. Reactive separation process synchronizes the reaction and separation processes in a single reactor. Usually, the separation processes were performed in different columns for reaction followed by separation. The key players of these reactive separation processes are heterogeneous catalysts, among which ion-exchange resins are most promising, efficient and economical. The use of ion-exchange resins not only overcome the problems associated with conventional separation technologies but also become an economical and flexible choice. This chapter introduces the conceptual understanding of reactive separation processes such as reactive distillation, reactive extraction, reactive chromatography and reactive absorption in different areas and the use of ion-exchange resin in these processes.

6.1 Introduction

In order to add flexibility and cost-effectiveness, numerous advancements are being employed in the processes that require chemical reaction followed by separation of products at the laboratory as well as industrial scale. Reactive separation is one among those advancements. The traditional process design was based on sequential reaction and separation processes, where a chemical reactor is attached with a downstream separator. In this type of system, the feed is converted into the product and separated by the separator. In order to increase the efficacy and productivity, unreacted output feed or intermediate products are again recycled to reactor or separator. In contrast, the most recent advanced systems such as reactive separation processes (reactive distillation, RD; reactive extraction, RE; reactive chromatography, RC and

N. Srivastava
Department of Biotechnology, CET-IILM, Greater Noida, India

M. Kuddus (✉)
Department of Biochemistry, University of Hail, Hail, Saudi Arabia
e-mail: mkuddus@gmail.com
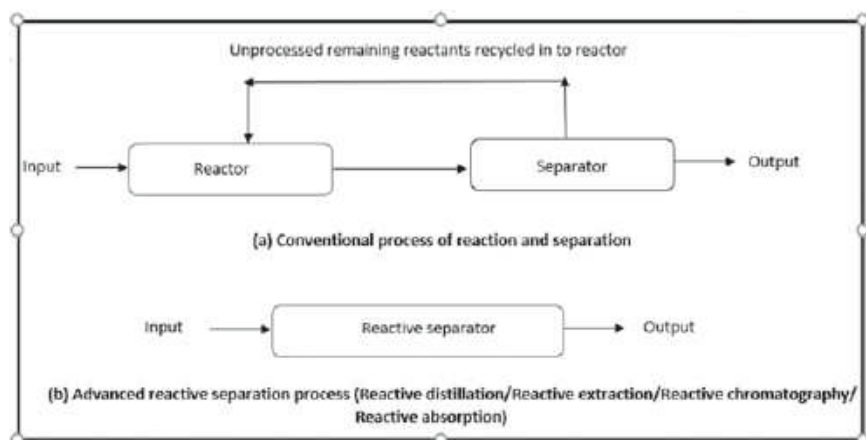
Fig. 6.1 Basic methodology of conventional (**a**) and advanced separation processes (**b**) [1]

reactive absorption, RA) incorporate the reaction and separation process into a single operational chamber (Fig. 6.1) [1].

In other words, reactive separations could be defined as a single operation that syndicate dual processes viz., the chemical reaction and physical separation into a single unit. It favours the simultaneous production as well as separation of products which contributes to the productivity, selectivity and high-efficiency with green engineering attributes. The other benefits also include the reduction in energy consumption and elimination of the solvents requirement [2]. However, as both reaction and separation operation occurs simultaneously in the same unit, there must be a proper overlapping between the operating conditions (e.g. temperatures and pressures) required for reaction and separation. If there is no significant match in the operating conditions of the processes required for reaction and separation, then the combination of reaction and separation, i.e. reactive separation process, is not possible. Reactive processes such as distillation, absorption, adsorption, extractions, etc. are the examples of separation that are widely used in various industries. Reactive separations typically included esterification, transesterification, etherification, hydrolysis and alkylation [3]. Recently, reactive separation processes (reactive distillation/absorption/extraction and membrane reactors) have been reviewed for the production of biodiesel, a biodegradable and renewable fuel, which is also emerging as a viable alternative to petroleum diesel. These techniques have been proven to overcome the problem associated with conventional biodiesel production such as the use of homogeneous catalysts and the limitations imposed by the chemical reaction equilibrium that charges penalties to the economy and environment [4]. This chapter covers an introductory description of different types of reactive separation processes, their advancements over conventional processes and applicability in different industrial processes. The main focus of this chapter is to review different types

of resins used in different reactive separation processes such as reactive distillation, chromatography, extraction and adsorption.

6.2   Use of Ion-Exchange Resin in Reactive Separation

In all reactive separation processes, commercially available ion-exchange resins are the prime players of the advanced technology. These ion-exchange resins are with strong acidic or basic groups, thus serve as an excellent source of acid or base which acts as a catalyst for many chemical reactions. For example, Amberlyst 15 ion-exchange resins attached with the strongly acidic sulphonic group (an excellent source of a strong acid) are used in various acid-catalyzed reactions. The ion-exchange resins being used frequently are mentioned in tabulated form along with their salient features (Table 6.1).

6.2.1   Reactive Distillation (RD)

Reactive distillation is a process in which distillation is coupled with an operating reaction simultaneously. A generalized configuration of RD includes the three following zones:

(1) Upper zone: A rectification section
(2) Middle zone: A reactive section
(3) Lower zone: A stripping section

The design required for conventional distillation has been modified to prepare RD reactors so that it would be favourable for both distillations as well as reactions. The catalyst can be homogenous or heterogeneous. In RD reactors, heterogeneous catalysts, are used which have several advantages over homogeneous catalysts such as elimination of separation and recycling of catalyst, corrosion-related issues, that accounts for the budget as well as flexibility and convenience. Cation exchangers, anion exchangers and zeolites, etc. are frequently used as heterogeneous catalysts in RD and are preferred over the homogeneous catalysts. The major challenge in this area is the development of a cost-effective catalyst which can be sustainable at both the required conditions for reaction as well as distillation. Among heterogeneous catalyst, ion-exchange resins are widely used for RD such as Amberlyst 15, Amberlite IR-120, Dowex 50W, Indion 130, etc. The general features of ion-exchange resins are tabulated in Table 6.1. The other table (Table 6.2) trotted out the chemical applications in which these resins have been used at commercial and industrial scale [5]. These applications include acetalization, aldol condensation, etherification, dehydration, esterification, trans-esterification and hydrolysis, etc. as listed in Table 6.2.

The reactive distillation column is also incorporated into the process of hydrolysis of methyl acetate for the recovery of acetic acid and methanol or methyl alcohol. The

Table 6.1 Resins used in reactive separation processes

Resin	Type	Base polymer	Functional group	Particle size	Max operating temp.	Total exchange capacity	References
Amberlyst® 15 in the hydrogen form	The strongly acidic cation-exchanger	styrene-divinylbenzene (macroreticular)	strongly acidic sulphonic group	<300 μm	120 °C	1.7 meq/mL by wetted bed volume 4.7 meq/g by dry weight	http://www.arkat-usa.org/get-file/44731
Amberlite IR120 Na	The strongly acidic cation-exchanger	styrene-divinylbenzene (gel)	sulphonic acid	620–830 μm	121 °C	1.8 meq/mL by wetted bed volume	https://www.sigmaaldrich.com/catalog/product/aldrich/224359?lang=en&region=IN
Dowex 50WX8 hydrogen form	The strongly acidic cation-exchanger	styrene-divinylbenzene (gel)	sulphonic acid functional group	200–400 mesh	150 °C	1.7 meq/mL by wetted bed volume	https://www.sigmaaldrich.com/catalog/sial/product/217514?lang=en&region=IN

Table 6.1 (continued)

Resin	Type	Base polymer	Functional group	Particle size	Max operating temp.	Total exchange capacity	References
INDION 130 resin	Acidic cation-exchanger	styrene-divinylbenzene copolymer	sulphonic acid	0.42–1.2	150 °C	4.8 meg/g	http://www.ionresins.com/pdf/pds/INDION_130_PDS_MSDS%20.pdf
Amberlyst36	Strongly Acidic exchanger	styrene-divinylbenzene	sulphonic acid	<0.425 mm (0.5% max)	150 °C	>1.95 eq/L exchange capacity; >5.40 meq/g exchange capacity	https://www.sigmaaldrich.com/catalog/product/aldrich/436712?lang=en&region=IN

Table 6.2 Heterogeneous catalysts (ion-exchange resin) in different reactive distillation process

Application	Catalyst	References
Esters synthesis		
Methyl acetate	Dowex 50WX-8	[6]
	Amberlyst-15	[5]
Methyl lactate	Dowex 50W	[7]
Ethyl acetate	Amberlyst-15	[5]
n-Butyl acetate	Cation-exchange resin (Indion 130, Amberlyst 15)	[5]
i-Propyl acetate	Amberlyst-15W	[8]
n-Propyl acetate	Amberlyst-15W	[9]
n-Propyl propionate	Amberlyst-46	[10]
n-Amyl acetate	Amberlyst-15	[5]
i-Amyl acetate	Cation-exchange resin (Indion 130, Amberlyst 15)	[5]
2-Ethylhexyl acetate	Amberlyst 15	[5]
2-Methyl propyl acetate	Ion-exchange resin	[5]
n-Hexyl acetate	Amberlyst CSP2	[5]
n-Butyl acetate	Ion-exchange resin	[11]
Cyclohexene esterification	Ion-exchange resin	[5]
Methyl dodecanoate	Amberlyst 15	[5]
Lactic acid	Amberlyst 15	[12]
Etherification		
Methyl tert-butyl ether (MTBE)	Amberlyst-15	[5]
Tert-amyl methyl ether (TAME)	Amberlyst XAD	[5]
Ethyl tert-butyl ether (ETBE)	Amberlyst-15	[5]
Di isopropyl ether (DIPE)	Amberlyst-36	[5]
2-Methoxy-2,4,4-trimethyl pantane	Amberlyst-35	[5]
Tert-amyl ethyl ether	Amberlyst-15	[13]
Methylal	Anion-exchange resin	[5]
Ethylal	Indion 130	[5]

Table 6.2 (continued)

Application	Catalyst	References
3-Methoxy-3-methylpentane	Cation-exchange resin	[5]
Isobutyl tert-butyl ether	Ion-exchange resin	[5]
Hydrolysis		
Furfural	Dowex	[14]
Methyl acetate	Ion-exchange resin	[5]
Methyl formate	Ion-exchange resin	[5]
Hydration/dehydration		
Ethylene oxide	Cation/anion exchange	[15]
Isobutene	Amberlyst-15	[5]
Acetalization		
1,1 Diethoxy butane	Amberlyst-47	[16]
Ethylene glycol	Amberite IR-120	[17]
Propylene glycol	Amberite IR-120	[17]
Trans-esterification		
Butyl acetate from methyl acetate	Amberlyst-15	[5]
Condensation		
Diacetone alcohol	Heterogenous catalyst	[18]
Dismutation		
Silane from trichlorosilane	Heterogenous catalyst	[19, 20]

advantages of the new process are the elimination of two columns in the conventional process and reduction of the heat requirement of the total process. The decrease in heat requirement is estimated to be about 50% that of the conventional process. In conventional reactive distillation process, a liquid catalyst such as sulphuric acid is used in the reaction zone, which is provided in a flash drum at the bottom of the reaction zone in order to separate the catalyst from the reaction mixture. In advanced reactive distillation process, solid catalyst packed in a reactive zone of the column replaces the need of flash drum for catalyst separation, and at the same time, it also replaces the need of expensive anti-corrosive material for the column. The complexed conventional process and advanced reactive distillation process are compared in Fig. (6.2), which demonstrates that advanced reactive distillation process eliminates the need of two towers viz., water wash tower for separation of methyl acetate (MeOAc) from methyl alcohol (MeOH) and methyl alcohol enriching tower for recovery of methyl alcohol from the water-diluted methyl alcohol that makes it easy to handle and cost-effective too [21].

(a)

(b)
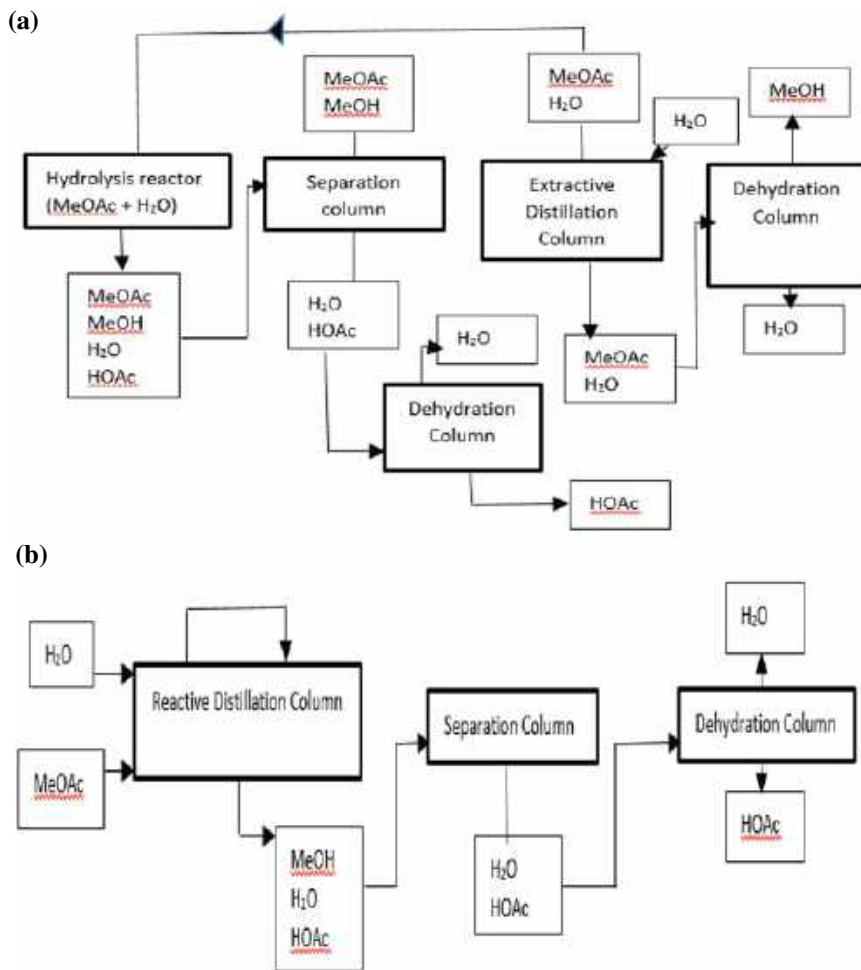
Fig. 6.2 Comparison of complexity between conventional distillation and reactive distillation process. **a** MeOAc hydrolysis by conventional distillation process; **b** MeOAc hydrolysis by advanced reactive distillation process [21]

Esterification of acetic acid with ethanol catalyzed by an acidic ion-exchange resin (Amberlyst 15) has been studied which includes reliable kinetic data, model covering a wide range of operating conditions, the interaction between the solid catalyst and the reactants. According to this study, a combination of an esterification reaction with distillation in a reactive distillation column either in batch or continuous mode led to a large increase in the purity of ethyl acetate in the distillate [22]. In another study, 1,1 diethoxy butane, was produced from renewable source using heterogeneous catalyst Amberlyst 47. Thermodynamics limitations associated with the production of 1,1 diethoxy butane by conventional processes could be overcome by reactive

distillation. It was concluded that the exchange resin has shown better performance than other catalysts (homogenous) by facilitating much faster equilibrium [23].

6.3   Reactive Chromatography (RC)

Just like reactive distillation, reactive chromatography is also a separation technique which combines reaction and chromatography in a single unit. This process is mainly designed for reversible and equilibrium limited reactions. Similar to other reactive separation processes, as described in previous sections, simultaneous removal of product facilitates equilibrium to move in the forward direction that results in the enhanced output from reversible reactions [24]. In this separation technique, the column is packed with a resin that functions both as a catalyst as well as an adsorbent. The product produced by the reaction is separated through the adsorption on the resin. It is used as an alternative when reactants or products have constrained related to temperature sensitivity and volatility. Such efficient processes enable high-throughput and low-desorbent consumption compared to conventional chromatography.

According to the principle of the adsorptive separation process, the components are to be separated on the basis of their different affinities towards the adsorbent. For simultaneous reaction and separation, the packing material must be a catalyst that has a different affinity towards the reactants and products. Two components (A and B) react inside the column with the catalyst and produce two products (C and D). Among the two products, weakly adsorbed component (C) moves faster (less elution time) in comparison to the strongly adsorbed component (D; more elution time). Based on the differential elution rates, the products are collected separately through fractionation. Many stationary phases are available and are used for reactive separation but ion-exchange resins are more in attention in RC due to their variable flexibility in distribution, nature and the number of functional groups in addition to the morphology of pellet, etc. These resins are being used as a catalyst and adsorbent which facilitate reaction as well as separation [25]. In recent work, Amberlyst-15 has been used as catalyst/adsorbent in fixed-bed chromatographic reactor (FBCR) for the synthesis of *n*-propyl acetate from *n*-propanol and acetic acid. The obtained results concluded that the synthesis of *n*-propyl acetate using RC may be advantageous over other conventional reactors [26]. In another work, 2-ethylhexyl acetate through esterification of acetic acid with 2-ethylhexanol was synthesized, with the application of RC using Amberlyst-15 catalyst/adsorbent in the stirred batch reactor. Several aspects related to reaction kinetics, multicomponent adsorption equilibria and reaction–separation study using fixed-bed chromatographic reactor were included in this study. Apart from that, the effects of various parameters such as speed of agitation, particle size, temperature, mole ratio of reactants and loading of catalyst have also been investigated [27]. Reactive chromatography using an anion-exchange resin has been used for esterification of propylene glycol methyl ether with ethyl acetate to produce propylene glycol methyl ether acetate (PMA) which is highly demanded active solvent for industrial paints and coating in the automotive industry. The pro-

duction of PMA using reactive chromatography makes it favourable in terms of energy efficiency, productivity and consumption. Another advantageous alternative for the production of PMA is transesterification reaction, in which PM and ethyl acetate is used as reactants and ethanol is produced as a by-product. It is advantageous because of easy and fast removal of ethanol from the column as it has low affinity for adsorbent (cation-exchange resin) in comparison to water by-product in esterification process which has a strong affinity for cation-exchange resin that results in long retention time and inefficient separation of product. In this study, several catalysts such as AMBERLYST 15, DOWEX MARATHON, AMBERLITE IRA904, AMBERLITE IRA900 and DIAJON PA316 have been compared on the basis of swelling ratio of the catalyst at different solvent and conversion of reaction. After screening, AMBERLITE^{TM} IRA904 OH$^-$ was found to be best for column packing which results in efficient production and separation between two products [28].

6.4   Reactive Extraction (RE)

Many industrially applicable biochemicals or raw materials in chemical industries face the limitation of ineffective separation that limits their industrial utility. One example of such chemical is 2,3-butanediol, a renewable material with the potential to be used as an alternative fuel. Many processes have been reported for separation such as steam stripping, liquid–liquid extraction, aqueous two-phase extraction and the reaction-separation processes. However, these separation processes were found economically unaccepted at industrial scale. Finally, reactive extraction process was employed to separate 2,3-butanediol. Acetaldehyde and cyclohexane were chosen as the reactant and extractant, respectively. Ion-exchange resin HZ732 was used as a catalyst. Results of the study supported the efficient separation of 2,3-butanediol as compared to traditional processes [29].

The reactive extraction process was also used for the downstream separation of 1,3-propanediol (1,3-PD) from dilute aqueous solution. This chemical used in organic synthesis as well as a monomer for the production of biodegradable polymers. A process combining reversible reaction of 1,3-PD with acetaldehyde to 2-methyl-1,3-dioxane and a simultaneous extraction of the product by organic solvent appears to be technically feasible and attractive. Due to low volatility and hydrophilic properties of 1,3-PD, the recovery from the complex and dilute fermentation broths is critical for conventional separation techniques such as distillation. Under these circumstances, extraction strategies may significantly reduce the cost of the product separation. Since experimental studies revealed that the distribution of 1,3-PD into organic solvents is not good enough to make simple extraction efficient. Thus, 1,3-PD is converted into a substance without hydroxyl groups and then recovered by means of liquid extraction. This was achieved by an acid catalyzed, the reversible reaction of 1,3-PD with acetaldehyde, leading to 2-methyl-1,3-dioxane (2MD). The reaction was catalyzed by a Dowex or Amberlite ion-exchange resin. Through this reactive

extraction approach, 98% conversion of 1,3-propanediol, 75% recovery of dioxane into the organic extractants and 91–92% of yield was reported [30].

6.5   Reactive Absorption (RA)

One of the common examples of reactive separation just like reactive distillation is reactive absorption or chemical absorption in which chemical reaction and absorption process is synchronized in a single operational unit. It basically involves a reaction between the substance being absorbed and the bulk liquid or solvent. Just like other reactive separation processes, it also has advantages over conventional strategies for separation. It also proceeds through tray or packed column as stated for reactive distillation but unlike reactive distillation, it does not require boiler or condenser. The most common application of reactive absorption is a purification of the gas mixture, fatty acid manufacturing and biodiesel production using solid catalyst [31]. Polymeric ion-exchange resins are widely used in important industrial processes for reactive absorption applications. Its particular cross-linked structure supports a swelling phenomenon when contacted with polar solvents like methanol or water. The retention of high liquid volume and the selectivity for the absorption of particular substances can lead to a significant alteration of the liquid reactive mixture composition when polymeric resins are used as catalysts. In a recent research work, Amberlyst 15 and Relite CFS (Styrene-DVB porous matrix), two sulphonic ion-exchange resins, typically used as esterification catalysts for esterification reaction of free fatty acids (FFAs) that is a suitable pretreatment of cheap feedstock for biodiesel production [32]. Anion-exchange resins have also been used as an effective sorbent for removal of environmental pollutants such as acids and direct dyes from textile wastewaters [33]. A study on strongly basic anion-exchange resins containing quaternary ammonium functionality and fluoride or acetate anion has been performed for removal of carbon dioxide and hydrogen sulphide from gas streams. It was concluded that the fluoride and acetate containing resins F^- Amberlyst® A-26 were effective for removal of CO_2 and H_2S from gas mixtures [34].

6.6   Conclusion

The novel strategies of separation such as reactive distillation/absorption/extraction have been developed which have overcome the limitations associated with traditional conventional processes of separation. Nowadays, reactive separation processes have been used in many industrial fields related to pharmaceuticals, textiles, paints, herbicides, stabilizers and biodiesel production, etc. The basis of these advanced techniques is mainly conceptual design and use of a heterogeneous catalyst. The application of ion-exchange resins makes the process economical, flexible and convenient.

References

1. Leet WA, Kulprathipanja S (2002) Reactive separation processes. Taylor & Francis: New York, pp 1–10
2. Shah BH et al (2014) Recent trends in reactive separation technology. In: 10th Annual Session of Students' Chemical Engineering Congress (SCHEMCON–2014). https://doi.org/10.13140/2.1.1957.7927
3. Kiss AA (2014) Process intensification technologies for biodiesel production: reactive separation processes. Springer Science & Business Media, pp 25–27
4. Kiss AA, Bildea CS (2012) A review of biodiesel production by integrated reactive separation technologies. J Chem Technol Biotechnol 87(7):861–879
5. Mahajani SM, Saha B (2015) Catalyst in multifunctional reactors. Walter de Gruyter GmbH & Co KG pp 1–10
6. Neumann Ronny, Sasson Yoel (1984) Recovery of dilute acetic acid by esterification in a packed chemorectification column. Ind Eng Chem Process Des Dev 23(4):654–659
7. Choi JI, Hong WH (1999) Recovery of lactic acid by batch distillation with chemical reactions using ion exchange resin. J Chem Eng Jpn 32(2):184–189
8. Gadewar Sagar B, Malone Michael F, Doherty Michael F (2002) Feasible region for a countercurrent cascade of vapor-liquid CSTRS. AIChE J 48(4):800–814
9. Brehelin M et al (2007) Production of n-propyl acetate by reactive distillation: experimental and theoretical study. Chem Eng Res Des 85(1):109–117
10. Xia H et al (2017) Design and control of entrainer-assisted reactive distillation for N-propyl propionate production. Comput Chem Eng 106, 559–571
11. Zeng KL, Kuo CL, Chien IL (2006) Design and control of butyl acrylate reactive distillation column system. Chem Eng Sci 61(13): 4417–4431
12. Okon E, Habiba S, Gobina E (2015) Batch process esterification of lactic acid catalysed by cation-exchange resins for the production of environmental-friendly solvent
13. Aiouache Farid, Goto Shigeo (2003) Reactive distillation–pervaporation hybrid column for tert-amyl alcohol etherification with ethanol. Chem Eng Sci 58(12):2465–2477
14. Metkar PS et al (2015) Reactive distillation process for the production of furfural using solid acid catalysts. Green Chem 17(3):1453–1466
15. Ciric Amy R, Miao Peizhi (1994) Steady state multiplicities in an ethylene glycol reactive distillation column. Ind Eng Chem Res 33(11):2738–2748
16. Agirre I et al (2011) Catalytic reactive distillation process development for 1,1 diethoxy butane production from renewable sources. Biores Technol 102(2):1289–1297
17. Dhale AD et al (2004) Propylene glycol and ethylene glycol recovery from aqueous solution via reactive distillation. Chem Eng Sci 59(14):2881–2890
18. Podrebarac GG, Ng FTT, Rempel GL (1998) The production of diacetone alcohol with catalytic distillation: part I: catalytic distillation experiments. Chem Eng Sci 53(5):1067–1075
19. Müller D, Schäfer JP, Leimkühler HJ (2001) The economic potential of reactive distillation processes exemplified by silane production. In: Proceedings of the GVC, DECHEMA and EFCE meeting on distillation, absorption and extraction, Bamberg, Germany, 2001
20. Li Xue-Gang, Huang Xun, Xiao Wen-De (2017) Reactive distillation-aided ultrapure silane production from trichlorosilane: process simulation and optimization. Ind Eng Chem Res 56(7):1731–1738
21. Fuchigami Yoshio (1990) Hydrolysis of methyl acetate in distillation column packed with reactive packing of ion exchange resin. J Chem Eng Jpn 23(3):354–359
22. Kirbaşlar Şİ, Baykal ZB, Dramur U (2001) Esterification of acetic acid with ethanol catalysed by an acidic ion-exchange resin. Turkish J Eng Environ Sci 25(6):569–578
23. Agirre I et al (2011) Catalytic reactive distillation process development for 1,1 diethoxy butane production from renewable sources. Biores Technol 102(2):1289–1297
24. Lode F et al (2001) Continuous reactive chromatography. Chem Eng Sci 56(2):269–291
25. Sundmacher K, Kienle A, Seidel-Morgenstern A (eds) (2006) Integrated chemical processes: synthesis, operation, analysis and control. Wiley, Weinheim, pp 183–185

26. Reddy Bhoja, Mahajani Sanjay (2014) Feasibility of reactive chromatography for the synthesis of n-propyl acetate. Ind Eng Chem Res 53(4):1395–1403
27. Gyani VC, Mahajani S (2008) Reactive chromatography for the synthesis of 2-ethylhexyl acetate. Sep Sci Technol 43(9–10):2245–2268
28. Oh J et al (2016) Transesterification of propylene glycol methyl ether in chromatographic reactors using anion exchange resin as a catalyst. J Chromatogr A1466 84–95
29. Li Y et al (2012) Separation of 2,3-butanediol from fermentation broth by reactive-extraction using acetaldehyde-cyclohexane system. Biotechnology and bioprocess engineering 17(2):337–345
30. Malinowski Janusz J (2000) Reactive extraction for downstream separation of 1, 3-propanediol. Biotechnol Prog 16(1):76–79
31. Ramaswamy S, Huang HJ, Ramarao BV (eds) (2013) Separation and purification technologies in biorefineries. Wiley, Chichester, pp 467–484
32. Tesser R et al (2010) Absorption of water/methanol binary system on ion-exchange resins. The Canadian Journal of Chemical Engineering 88(6):1044–1053
33. Wawrzkiewicz Monika, Hubicki Zbigniew (2015) Anion exchange resins as effective sorbents for removal of acid, reactive, and direct dyes from textile wastewaters. Ion Exchange-Studies and Applications, InTech
34. Quinn R (2003) Ion exchange resins as reversible acid gas absorbents. Sep Sci Technol 38(14):3385–3407

Chapter 7
Chromatographic Reactive Separations

Akash V. Shetty and Yogesh S. Mahajan

Abstract Ion-exchange resins (IERs) possess the capability of catalyzing several classes of reactions, apart from their ability to make separations. In fact, it is possible to synthesize tailor-made IERs for the reactive processes at hand. Use of IERs can fetch a number of advantages compared to those of homogeneous catalysts and other solid catalysts. Reactive separation (RS) is a relatively new process technology that has the potential to offer several advantages over the conventional approach of reaction followed by separation. Various separation steps can be coupled with the reaction, including: distillation, extraction, chromatography, crystallization and separation by membranes. This chapter reviews the salient features and industrial applications of reactive separations using IERs.

Abbreviations

A-15	Amberlyst 15
AEM	Anion-exchange membrane
CD	Catalytic distillation
CEM	Cation-exchange membrane
CSTR	Continuous stirred tank reactor
FBCR	Fixed bed chromatographic reactor
GCE	Green chemistry and engineering
IER	Ion-exchange resin
LAB sulphonate	Linear alkyl-benzene sulfonate
LPG	Liquefied petroleum gas
PI	Process intensification
RA	Reactive absorption
RC	Reactive chromatography
RCond	Reactive condensation

A. V. Shetty · Y. S. Mahajan (✉)
Chemical Engineering Department, Dr. Babasaheb Ambedkar Technological
University, Lonere, Mangaon, Raigad 402103, Maharashtra, India
e-mail: ysmahajan@dbatu.ac.in; yogesh_mahajan66@yahoo.com

RCr	Reactive crystallization
RD	Reactive distillation
RM	Reactive membrane
RPr	Reactive precipitation
RS	Reactive separation
RStr	Reactive stripping
SCMCR	Simulated counter current moving bed chromatographic reactor
SMBR	Simulated moving-bed reactor
UO	Unit operations
UP	Unit processes
VLE	Vapor–liquid equilibrium
VLLE	Vapor–liquid–liquid equilibrium

7.1 Introduction

The process industry typically employees the traditional approach of initially carrying out the reaction(s) and then effecting the separation. More generally, this approach is non-practical owing to several shortfalls that include: large waste formation, increased energy requirement and lesser production from the given equipment volume. Reactive separation (RS) is a relatively new alternative process that involves *in situ* separation of products and/or reactants, thereby improving the process structure. In the recent past, the chemical process industry has shown considerable interest in RS, due to the several possible advantages.

These advantages include an increase in conversion and/or selectivity, decrease or elimination of waste, less recycling, better atom economy and thus adherence to the principles of green chemistry and engineering (GCE), which may help the environment by reducing the pollution levels and can benefit the manufacturer by increasing the profit margins, primarily due to reduced production costs, better use of inventory and reduced volume of equipment. Many times, it may be possible to convert the batch operation into continuous or at least semi-batch type, with obvious advantages. It may be noted that RS may not always offer the above-stated advantages but due to the super-impose of reaction and separation, it may also create constraints/problems which were previously unimaginable. Thus, constraints like reduced window of operating parameters and problems like previously non-existent mass transfer limitations may arise. Nevertheless; a well-designed RS process can offer unimaginable and unparalleled advantages [1–3].

This multifunctional reactor concept (*i.e.* RS) has the capability of process intensification (PI). Different separation processes (unit operations, UO) can be combined with the reaction part (unit processes, UP) to constitute the RS unit. These include: distillation (reactive distillation, RD); liquid–liquid extraction (reactive extraction, RE); membrane separation (reactive membranes, RM); adsorption or chromatography (reactive chromatography, RC); gas–liquid absorption (reactive absorption,

RA) and crystallization (reactive crystallization, RCr). Sub-variants are also possible: reactive stripping (RStr), reactive precipitation (RPr), reactive condensation (RCond), etc. Each of these has its own areas of application and offers advantages or disadvantages depending upon factors that also include the synergy (or otherwise) between the reaction step and the separation step [4–6]. The reaction step can be one of the several: hydrolysis, esterification, transesterification, acetylation, etherification, hydration and dehydration.

Ion-exchange resins (IERs) have long been known for their ability to catalyze reactions. Their applications in the chemical process industry in the fixed bed reactor, fluidized bed reactor, batch, semi-batch reactor, etc., are well established. The advantages that these offer over homogeneous catalysts and other solid catalysts are many, such as reduced waste formation; possibility of an increase in conversion, selectivity and yield; ease of separation and possibility of impregnation, among others. It is possible to impart acidity or basicity to these. It is also possible to make these stronger or weaker as per requirement. In short, the synthesis of tailor-made catalysts is possible. However, these catalysts may also pose certain disadvantages which include: temperature delimit, loss of activity and cost considerations. Many reviews have been published in the past delineating several areas of research and development of IERs. The areas covered include origin, development, types, applications, anecdotes and future possibilities [7–9].

By a look at the plethora of applications that have been cited in the literature, it can be envisaged that for almost every application, there is an IER available, and vice versa. It becomes a challenge for the chemists, scientists and technologists to identify a suitable IER. Applications as diverse as separation/removal of ions and molecules, water and wastewater treatment, as well as nuclear applications, are also on the anvil [10, 11]. The sections below review the applications of IER in the different RS units. A few of the important instances are described. The reactions that are catalyzed in the particular RS unit are discussed below with details like IER used, process parameters, advantages and disadvantages and the constraints.

7.1.1 Reactive Distillation (RD)

The term reactive distillation (RD) implies a process in which reaction and distillation are performed in a single vessel. The *in situ* separation, simultaneous to the reaction, naturally involves interactions with phase equilibrium; mass transfer; diffusion and reaction kinetics. In principle, RD was used commercially as early as 1860 (Soda ash process by Solvay) and patented in 1920 [12]; but the real boost for research in this important synthesis alternative was due to the game-changing process of production of methyl acetate [13].

Although the concept of reaction and distillation occurring in one single vessel is called reactive distillation (RD), the term catalytic distillation (CD) is often employed to indicate the use of a heterogeneous catalyst. However, more generally, RD and

CD are used synonymously. Several pros and cons can be listed for RD [5, 6, 13, 14]:

- Going beyond equilibrium limitations: due to *in situ* removal, it is possible to increase conversion to the tune of the asymptotic approach to 100%. Further, *in situ* removal reduces the probability of side reactions; thereby helping to achieve better selectivity and hence yield.
- The possibility of better heat utilization: the exothermicity of reaction can be utilized so as to reduce reboiler duty.
- Overcoming thermodynamic constraints: it is possible to use the azeotrope(s) for better reaction and separation performance.
- Reduction in investment and an increase in capital saving: most generally, due to the synergy of the two steps, the separation train is drastically reduced, thereby reducing cost.
- Better catalyst conditions: due to continuous washing, the lifespan of heterogeneous catalysts goes up. Also, a less amount of catalyst is required for given conversion.

Disadvantages: As previously stated, there may be unforeseen, unprecedented disadvantages, a few of which are listed below [5, 6].

- Non-applicability of RD to a given reaction: due to the requirement of the much-needed overlap of operating conditions for reaction and separation, it may not be possible to apply RD to each and every reaction one may think of. Usually, equilibrium-limited reactions are considered as suitable candidates for RD, although a few applications to apparently irreversible reactions are also known [15, 16].
- Process conditions: faster reaction rates require comparatively larger concentration of reactants (for conversion to go up) and lower concentration of products (for selectivity to be enhanced). The volatility of the reagents may not always permit this.
- Reaction kinetics: if the reaction rate is too small then it may be needed that the reactants spend more time in the reactor. This may necessitate larger volumes thereby rendering RD non-profitable. In such and other cases, scale-up issues might arise. Till date, liquid phase reactions have been predominantly explored in RD.

The reactions that have been explored in RD environment till now, are mainly from one of the following categories:

1. Reactions which require no catalyst or are auto-catalyzed [15, 17].
2. Reactions which are homogenously catalyzed [13].
3. Reactions which are heterogeneously catalyzed [16, 18].

The processes that have been explored in RD are many. Reactions like esterification, transesterification, hydrolysis, etherification, hydrogenation and dehydrogenation, hydration and dehydration, alkylation, disproportionation and metathesis,

carbonylation, production of polymers, silanes and carbonates, etc., have been studied in detail in the past. Unit processes like chlorination and amination are also reported. One of the special applications of RS and especially RD and RC can be to effectively perform difficult separations. In some instances, it is possible to perform separations which are otherwise not possible at all. Another area which has gained immense importance in the recent past is the recovery of chemicals which is important from pollution/environment point of view and also for imparting better economy and sustainability to the process structure [19].

The various questions that need to be answered for process development in RD include: exploring the right candidate for RD, process synthesis and development and actual design including scale-up, equipment choice, and sizing. The hardware selection for RD column is based on different considerations, *e.g.* whether homogenously catalyzed or heterogeneously catalyzed and whether vapor–liquid–equilibrium (VLE) or vapor–liquid–liquid equilibrium (VLLE). Also, it is necessary to have a good control structure for the RD process. The main focus of this article is to throw light on various reactions that have been candidates for RD using IERs.

At this juncture, it is not possible to cover all aspects in detail. Hence, a few of the above-mentioned reactions/processes are mentioned in Table 7.1. In order to condense more useful information in smaller space, a tabular format is used. The table includes the type of reaction/process, the IER used, process parameters, speciality, advantages and/or disadvantages along with the reference cited.

7.1.2 Reactive Chromatography (RC)

As the name implies, reactive chromatography (RC) combines reaction and separation (adsorption–desorption, *i.e.* chromatographic separation) in one single vessel. Traditionally chromatographic separation is employed in fine chemical, pharmaceutical and food industries among others. When the reaction and separation favour each other, then several advantages can usually be enjoyed: higher purity of products, larger throughputs, lesser separation duties, etc. In contrast to RD, RC is much less heat intensive and thus it offers added economic benefits. Also, since boiling is not intended, less harsh, *i.e.* milder reaction conditions can be used. As a result, the catalyst life can be tremendously increased; thus facilitating additional economic benefits. Also, since the equipment can be made continuous, running costs can be reduced. Size of the equipment is generally reduced. A well-designed RC technology can provide an increase in conversion, selectivity and hence yield of the desired product [20–22].

For the fruitful implementation of RC technology, various "correct first choices" need to be made. These are:

- The correct choice of reaction candidates: Usually equilibrium-limited reactions or reactions for which inhibition/deactivation of the catalyst occurs due to some

Table 7.1 Few instances of use of IERs for RD

Reaction/Process	IER used, packing used	Process parameters	Remarks	References
Esterification of different acids with cyclohexene	Indion 130, A-15, Amberlyst IR-120	343–373 K, 1:4 mole ratio of cyclohexene to acrylic acid	• Higher yield (~87%) and selectivity (~78%) • Higher catalytic activity, catalyst reusability • Replacement of H_2SO_4 as a catalyst with IER	[35]
Acetalization of formaldehyde with methanol	Indion 130 with three different packings 1. Directly packed along with Raschig rings 2. In cloth bags 3. Silica-supported organic catalyst	Batch kinetics: Agitation speed 16.77 rpm, 333–346 K, Mole ratio 6:1 (Methanol: Formaldehyde) RD runs at reflux ratio 1–1.5, mole ratio 2.25:1	• High conversion (99%) of formaldehyde in RD • 81% conversion achieved in Batch • Operating reflux ratio 2 times minimum found to be useful	[36]
Hydration of isoamylene to *tert*-amyl alcohol (TAA)	A-15 with bale-type packings	RD runs at pressure 145 kPa and 241 kPa. Total reflux condition	• Higher yield achieved using RD (94.5%) than in a separate reactor (30%) • The high TAA yield is achieved at low space velocities • Hydration of isoamylene is facilitated using acetone as a solvent • Acetone found to increase the reaction rate and it also avoids the formation of two liquid phases	[37]

(continued)

Table 7.1 (continued)

Reaction/Process	IER used, packing used	Process parameters	Remarks	References
Ketalization of acetone with 1,4-butanediol, 1,2-propanediol, 1,2-ethanediol	Indion 130, Amberlyst IR-120, K 2411 with S.S. wire mesh packing	RD runs at 340 K and at pressure 710 mm Hg	• 92% conversion of 1,2-propanediol achieved in RD as against only 52.5% equilibrium conversion in batch mode	[38]
Esterification of acetic acid with butanol and *isoamyl* alcohol	Indion 130, packed 'tea-bags'	Flow rate—192 mL/h, Molar ratio—1:2	• Replacement of liquid catalyst by IER • The recovery of acetic acid enhanced from 30 to 57.6% using RD • Using RD conversion of acetic acid increased from 36 to 52.7%	[39]
Separation of isobutene from C₄ mixture by decomposing methyl *tert*-butyl ether (MTBE)	A-15 with Katapak-S and Multipak	RD runs at 9.3 bar and reflux ratio of 4.55 and 10.21. The height of packing is 11.2 m	• RD perfect candidate to achieve high separation (99.9%) • High purity of isobutene (99.9%) • High selectivity towards isobutene (97.51%) • Methanol is suitable as reactive entrainer to achieve better separation (99.9%)	[40]

(continued)

Table 7.1 (continued)

Reaction/Process	IER used, packing used	Process parameters	Remarks	References
Esterification of acetic acid with amyl alcohol	A-15 packed in tray column	RD runs under atmospheric pressure conditions	• Two design alternatives, coupled reactor/separator assembly and reactive distillation column have been studied • RD is the better for amyl acetate formation • RD is 4 times more efficient than coupled reactor/separator for this process	[41]
Esterification of decanoic acids	A-15 with Katapak-S and Katapak-SP	Batch Kinetics: Stirrer speed 100–800 rpm, temperature 338 K RD runs under atmospheric pressure	• Due to use of IER, location and size of the reactive section can be chosen without considering thermodynamic constraints • Use of IER results in a reduction of corrosion rate	[42]

(continued)

Table 7.1 (continued)

Reaction/Process	IER used, packing used	Process parameters	Remarks	References
Esterification of *n*-hexanol with acetic acid to *n*-hexyl acetate	Amberlyst-CSP2 packed in Sulzer-s Katapak and/or Montz Multipak Type-II	RD column (pilot scale) height 11.4 m, diameter 162 mm, the total number of stages 16, Top pressure 300–500 mbar,	• A large number of RD experiments were carried out • Various azeotropes exist in the system • Laboratory scale (packing height 3.5 m), as well as pilot scale (packing height 11.3 m), experiments carried out • Despite the large difference between boiling points of reactants, 84% conversion was possible	[43]
Transesterification of methyl acetate with *n*-butanol.	A-15 with Sulzer Katapak-S and Sulzer Katapak-SP	RD runs at atmospheric pressure with reflux ratio between 0.5 and 2	• RD when coupled with pervaporation, 100% conversion is obtained (Batch reactor conversion ~75%)	[44]
Production of *tert*-amyl ethyl ether and *tert*-amyl alcohol from isoamylene-ethanol-water	A-15	RD column operated under total reflux	• An increase in the temperature resulted in an increase in the total conversion; at 90 °C conversion 76.8% and at 124 °C, 99.6% conversion • High conversion (>99%) can be achieved • If water not removed, the parallel reaction occurs as a result of which *tert*-amyl alcohol is formed at expense of *tert*-amyl ethyl ether	[45]

(continued)

Table 7.1 (continued)

Reaction/Process	IER used, packing used	Process parameters	Remarks	References
Recovery of acetic acid from aqueous solution	Amberlyst-CSP2 in Sulzer Katapak-S	RD runs under atmospheric pressure	• Conversion (81.9%) of acetic acid was achieved by changing operating conditions • Recovery of acetic acid (42%) from its aqueous solution was achieved, which is otherwise difficult by normal distillation	[46]
Aldol condensation of acetone	A-15 packed in Sulzer Katapak-S	RD column operated under total reflux conditions	• Selectivity towards di-acetone alcohol can be improved using RD but the formation of mesityl oxide cannot be completely avoided • Water acts as a rate inhibitor but the use of water can improve selectivity towards di-acetone alcohol • Presence of excess water slows the reaction rate	[47]

Table 7.1 (continued)

Reaction/Process	IER used, packing used	Process parameters	Remarks	References
Esterification of lactic acid with *n*-butanol	A-15 packed in Sulzer Katapak-S	Batch kinetics: 318–369 K RD runs under atmospheric pressure conditions	• Increase in the conversion (92%) by using IER due to the separation of water (Batch conversion ~40%) • Due to use of IER, the process is economical	[48]
Recovery of trifluoroacetic acid from dilute aqueous solutions	T-63, Hyflux non-reactive packing	Boiling conditions	• There is no apparent advantage of using an IER due to the presence of a large amount of water • RD (~60% conversion) helps to improve conversion significantly over batch runs (~20%)	[15]
Esterification of propionic acid with propanol	Amberlyst 46 with Katapak SP-11	RD runs under atmospheric pressure conditions with reflux ratio 2.48, 4	• Large mole fraction (up to 60%) of propyl propionate is achieved at feed molar ratio 2 • The temperature of reactor zone was kept below 120 °C	[49]
Esterification of acetic acid with *n*-butanol and *n*-amyl alcohol	A-15 packed in tray column	RD runs under atmospheric pressure conditions	• RD is better from an economy point of view than the traditional method (Reaction followed by separation) • Use of RD reduces total annual cost by 22% compared with traditional method	[50]

Table 7.1 (continued)

Reaction/Process	IER used, packing used	Process parameters	Remarks	References
Esterification of propanol and propionic acid to propyl propionate	Amberlyst 46 with Katapak SP-11	RD runs with minimum reflux ratio of 2	• Using RD acid conversion of 94.5% was obtained	[51]
Esterification of acetic acid/succinic acid with ethanol	Amberlyst 70 with Katapak SP-11	RD runs at pressure 310 kPa with reflux ratio between 0.58 and 0.97	• 100% conversion of acids is realized in RD • 98% yield of diethyl succinate obtained using RD • Simultaneous esterification and separation were possible using RD	[52]
Etherification of glycerol with *tert*-butyl alcohol	Amberlyst 15 with Katapak SP-11	RD runs at atmospheric pressure conditions with reflux ratio 2	• Higher reflux ratio results in a higher amount of water in the reactive section, which inhibits the reaction • Minimum reflux ratio 2 is used in RD to achieve better conversion to 70% from ~55% in batch mode	[53]
Esterification of acrylic acid with *n*-butanol	Amberlyst 46 with Katapak SP-11	RD runs at reduced pressure 0.3–0.4 bar, reflux ratio 0.75–2	• Replacement of traditional methods: Two homogenously catalyzed reactors followed by three distillation columns by RD • Traditional methods are cost intensive and challenging due to polymerization • Compared to pilot-scale RD experiments and simulation, RD is a good alternative to the traditional methods	[54]

Table 7.1 (continued)

Reaction/Process	IER used, packing used	Process parameters	Remarks	References
Esterification of acetic acid with methanol	Indion-190 in a packed bed	339–349 K, Catalyst loading—110 gm, Molar ratio—1:2	• Replacement of strong acid catalyst by IER • Investigation of various process parameters	[55]
Cumene hydro-peroxide decomposition to phenol	A-35 (dry and wet) packed in 'tea-bags'	Batch kinetics at 298 K	• Acetone as a by-product • Replacement of H_2SO_4 by IER • Dry grade IER performed better • Minimization of energy needs, thus reduction in operational costs • Higher conversion (100%) observed over the conventional process	[56]
Esterification of acetic acid with methanol	D072 and NKC-9 with fix bed type packing	Batch kinetics: 318 K and molar ratio of 0.8:1 (acetic acid: methanol) RD runs at atmospheric pressure conditions with reflux ratio 1.3	• High conversion 99.5% (FBR conversion ~75%) • Side reaction elimination • Faster reaction rate	[57]
Dehydration of 1,4-butanediol to tetrahydrofuran	A-15 packed in Katapak S	Batch Kinetics: 343–363 K, Agitation speed 300, 600, 900 rpm RD runs under atmospheric pressure	• Increase in the conversion (45.78%) due to the use of IER as water is continuously removed (~5–20% conversion in batch) • As the reaction rate is low, use of IER found to be useful	[16]

Table 7.1 (continued)

Reaction/Process	IER used, packing used	Process parameters	Remarks	References
Synthesis of acrylic acid via transesterification methyl acrylate	NKC-9	Batch kinetics at 353 K, molar ratio—1:1, agitation speed—300 rpm.	• Conversion of methyl acrylate to acrylic acid in RD found to be 94.5% • Pure acrylic acid (98%) can be obtained using RD	[58]
Production of 2-methoxy-2-methyl-heptane by etherification of 2-methyl-1-heptane and methanol	A-35 (wet)	RD column 1 operated at 1.77 atm. column 2 at 10 atm. and column 3 at 0.1 atm	• Minimization of energy needs, thus reduction in operational costs • Total annual cost reduced by 10.8%	[59]
Esterification of glycerol with acetic acid	A-15 and A-35	RD runs at1 bar, 373 K, feed rate of 0.5 mL/min, acetic acid to glycerol mole ratio 7	• High selectivity (80%) and complete conversion of glycerol towards triacetin were achieved • High conversion of glycerol to monoacetin (97%) with higher selectivity (85%) • Complete conversion of glycerol to diacetin with 65% selectivity	[60]

reason are better candidates for RC. Also, reactions for which selectivity issues are critical can be suitable candidates.

- The selection of the correct eluent: It is necessary to choose an eluent so as to facilitate reaction and separation, specifically in that order. In a non-reactive chromatographic operation, generally, the eluent is inert. However, in RC, it becomes imperative that reactants have similar (preferably same) adsorptive properties. Otherwise, reactant concentrations on catalyst sites would differ and reaction rates would be reduced. In many instances of RC, this requirement is fulfilled by choosing one of the reactants as the eluent. As an example, in the case of esterification, the alcohol can be the eluting reactant. The choice is many times further facilitated by factors like ease of handling (density and viscosity), aesthetics (*e.g.* odour) and complexity (*e.g.* polymerization or other side reactions) [23].
- The choice of correct adsorbent: Several adsorbents are available like activated carbon, alumina, zeolites and IER. Since the adsorbent has also to act as a catalyst, it is important that enough catalytic activity be present. It may also be needed to look into some of the desirable properties like durability, size of solid particles, possibility of retaining shape and the resistance to erosion etc.

IERs often offer an excellent combination of adsorptive capacity supplemented by adequate catalytic activity which is further augmented by other properties like durability and hence a large number of applications of RC utilize IERs [24].

Table 7.2 presents details of several reactions that have been explored in RC with IERs till date.

7.1.3   Reactive Extraction (RE)

Extraction is a known separation method since long. In this unit operation, a solute is partitioned into two partially miscible/immiscible liquid phases. Generally, these phases possess a considerably large difference in density for ease of separation. As with other RS processes, several advantages are possible. It is possible to consider irreversible as well as reversible reactions as candidates for reactive extraction (RE). As the name suggests, reaction and separation by simultaneous extraction occur in a single vessel. Various industries including metallurgical, pharmaceutical, petrochemical industries make extensive use of RE to produce soaps, LAB sulphonates, resorcinol, LPG, polyurethanes, polyamides and polycarbonates. Usually, the introduction of the second liquid phase allows equilibrium to be surpassed in many instances [25].

In many RE processes, there are two distinct organic and aqueous phases. The species that react are generally present in these two distinct phases, coming in contact at the interphase or inside one of the phases, react and the formed products diffuse to and fro as per solubility. The efficiency of many organic/inorganic liquid phase reaction systems can be substantially increased by the use of RE. The pair of the phases facilitates the RE structure in many ways like maintaining a higher concentration of

Table 7.2 Few instances of use of IERs for RC

Reaction/Process	IER used, packing used	Process parameters	Remarks	References
Production of *bis*-phenol A	Amberlyst 15	Batch kinetics at 323–363 K, mole ratio (acetone to phenol)—1:12	• About 99.5% conversion obtained using simulated moving-bed reactor (SMBR) (Batch conversion 95%) • Using IER water is removed hence increase in conversion	[61]
Esterification of acetic acid with methanol	Sulfonated poly (styrene *di*-vinyl benzene) resin and Amberlyst 15	Feed mole ratio (acetic acid: methanol)—1:3, Feed flow rate 0.2–0.5 mL/min	• Complete conversion using SMBR (Batch ~80%). • Though the system is equilibrium-limited, complete conversion of the reactants can be achieved • Major advantages of SMBR are the low operating temperature and the adsorptive separation	[62]
Etherification of *tert*-butyl alcohol with methanol	Amberlyst 15	Simulated counter current moving bed chromatographic reactor (SCMCR) runs at 328 K	• 94.4% conversion achieved using SCMCR (fixed bed reactor conversion was 85.3%) • 95% yield of MTBE is achieved in SCMCR (yield in fixed bed reactor 76.1%) • 98% purity is obtained using SCMCR while in fixed bed reactor purity was 43.2%	[63]

Table 7.2 (continued)

Reaction/Process	IER used, packing used	Process parameters	Remarks	References
Esterification of propionic acid 2-ethyl-1,3-hexanediol	Dowex HCR-W2	SMBR runs at—298 K	• Around 88% conversion using SMBR (Batch conversion 79%) • SMBR allows continuous operation along with a reduction in desorbent consumption and improving conversion relative to conventionally fixed bed reactors	[64]
Esterification of acetic acid with methanol	The sulfonated ion-exchange resin	SMBR runs at room temperature, feed molar ratio: 1:1, column length 25 cm, number of columns: 10	• Approximately 98% conversion with 99.5% purity • Influence of various process parameters on the performance of the SMBR investigated	[23]
Esterification of glycerol with acetic acid	Amberlyst 15	Batch kinetics at 333–373 K, stirring speed: 300–600 rpm FBCR runs at 353 K, mole ratio of feed: 1:4.5 (glycerol: acetic acid)	• Even under unfavourable equilibrium conditions, high yield of *tri*acetine can be obtained • Highest purity (60%) and conversion of *tri*acetine using FBCR	[65]
Esterification of acetic acid with methanol	Amberlyst 15	SMBR runs at 318 K	• Complete conversion of acetic acid achieved using SMBR • High yield up to 98% achieved using SMBR	[66]

Table 7.2 (continued)

Reaction/Process	IER used, packing used	Process parameters	Remarks	References
Hydrolysis of methyl formate and methyl acetate	Dowex 50 W-X8 resin	SMBR runs at room temperature conditions	• Using SMBR, total conversion of ester and complete separation achieved	[67]
Synthesis of *di*-methoxy-ethane using acetaldehyde and methanol	Amberlyst 15	Fixed bed chromatographic reactor (FBCR) runs at 293 K and feed flow rate: 6 mL/min	• Replacement of homogeneous acid catalyst by IER • IER prevents the formation of coproduct by acting as a good adsorbent, hence separating water and primary product	[68]
Esterification of acrylic acid with methanol	Amberlyst 15	Feed temperature—333.15 K	• Conversion 98% of acrylic acid and complete separation of the reaction products at a relatively low operating temperature	[22]
Esterification of acetic acid with 2-ethylhexanol	Amberlyst 15	Batch kinetics at 348–373 K, agitation speed: 600–1100 rpm FBCR runs at 353 K, feed mole ratio: 1:1, feed flow rate: 2 mL/min	• Fractional conversion as high as 95% obtained using FBCR (Batch conversion ~60%) • Although the reaction is reversible, using IER in FBCR separation of product and water enhances the extent of reaction	[69]

Table 7.2 (continued)

Reaction/Process	IER used, packing used	Process parameters	Remarks	References
Acetalization reaction of methanol and acetaldehyde	Amberlyst 15 wet	SMBR runs at 293 K, feed flow rate of 3 mL/min, switch time 3 min	• Conversion (99.52%) obtained using SMBR	[70]
Esterification of lactic acid with ethanol	Amberlyst 15 wet	SMBR runs at 323 K, feed flow rate of 1.8 mL/min	• Conversion (99.96%) obtained using SMBR • Purity as high as 95% is achieved using SMBR • The higher rates of productivity obtained	[71]
The esterification of butyl cellosolve with acetic acid	Amberlyst 15 dry	Batch runs at 373 K, stirrer speed 1000 rpm FBCR runs at 333 K, feed flow rate 2–6 mL/min	• Conversion (~80%) can be achieved using FBCR (batch conversion 60%)	[72]
Production of biodiesel: Esterification of fatty acids with methanol	Silica-supported Nafion resin	SMBR runs at feed mole ratio: 5, switching time 900 s, column length: 0.25 m	• Conversion (90.95%) using SMBR (~80% continuous stirred tank reactor (CSTR) conversion) • Higher purity (80.89%) of the product using SMBR • Higher conversion due to the separation of water	[73]

Table 7.2 (continued)

Reaction/Process	IER used, packing used	Process parameters	Remarks	References
Esterification of acetic acid with n-hexanol	Purolite CT-124	BCRC runs at temperature 353 K, feed flow rate 0.2 mL/min, feed molar ratio 3:1	• Almost 100% conversion realized using batch chromatography reactor column (Batch ~75%) • Increase in temperature increased a desorption rate of the product • A number of parameters such as feed flow rate, feed mole ratio, desorbent flow rate and reaction time were studied to maximize the yield as well as to achieve complete conversion	[74]
Esterification of acetic acid with 2-ethyl-hexanol	Amberlyst 15	Feed ratio—1:1, Temperature—353 K	• Purity and conversions were close to 99%	[75]
Esterification of 1-methoxy 2-propanol with acetic acid	Amberlyst 15 swollen in acetic acid as a slurry	Feed flow rates—(0.2–1 mL/min), Injection volumes—(0.05, 0.5 mL), and Temperatures—(343–383 K). FBCR runs at room temperature	• Increase in the conversion up to 100% • Using FBCR ~100% conversion obtained (Batch conversion 70%) • Decreased productivity because of low flow rates	[21]
Esterification of acetic acid with n-propanol	Amberlyst 15	FBCR at temperature 348 K, feed composition: 4:1, feed flow rate: 1–1.5 mL/min	• Possible 95% conversion using FBCR though, the reaction is reversible • Amberlyst-15 successfully served the dual purpose as catalyst and adsorbent	[76]

Table 7.2 (continued)

Reaction/Process	IER used, packing used	Process parameters	Remarks	References
Esterification of acetic acid with 1-methoxy-2-propanol	Amberlyst 15	Reactor temperature: 383 K, feed composition 50%	• Increase in conversion by use of SMBR up to 95% (Batch conversion ~70%) • Using the SMBR production rate was increased by 12–36%	[77]
Esterification of acrylic acid with *n*-butanol	Amberlyst 15	SMBR runs at temperature: 363 K, feed molar ratio 1, feed flow rate of 6.5 mL/min.	• Product purity (99.9%) with the conversion of 98%	[78]
Transesterification of propylene glycol methyl ether with ethyl acetate	Amberlite IRA904, Amberlite IRA900 Dowex Marathon, Amberlyst 15, Diaion PA316	Batch kinetics at 313 K, equimolar feed	• Better conversion (83%) in the reactive chromatography column using Amberlyst 15 compared to batch conversion (27%)	[79]
Esterification reaction of 1-methoxy-2-propanol with acetic acid	Amberlyst 15	SMBR runs at a feed flow rate of 0.38 mL/min, recycle flow rate 0.2 mL/min, switch time 51.3 min	• Higher conversion (95%) obtained using SMBR (Batch conversion ~70%)	[80]

reactants; facilitating reaction by acting as a sink/source so as to lead the reaction to completion and effectively removing exothermic heat of reaction etc. [24, 26].

There are several advantages of RE [27]:

1. It can be effectively used in case of relatively immiscible reactants.
2. In addition to an increase in extraction efficiency, it is many times possible to improve the selectivity.
3. Heat transfer can be advantageously improved.
4. RE can also be effective when the reaction mixture and products are immiscible with each other.
5. It is easier to separate the products as well as catalyst due to favourable LLE.
6. It can be effectively used for the recovery of chemicals from dilute aqueous solutions for cases in which distillation becomes very costly.
7. Most generally, RE is advantageous over normal extraction because of low recirculation rates.

Table 7.3 provides instances of use of IERs for RE.

7.1.4 Reactive Membranes (RM)

Membrane separation processes are rate based (rather than equilibrium based) in that the separation is dependent on the differences in the rate of transport through a medium (membrane) under the influence of a driving force. The driving force is generally a result of the gradient in some variable like pressure, temperature or concentration. The different materials used for making membranes are as many as 100 or more [28]. However, three broad classes of materials can be easily seen: rubbery polymers, glossy polymers and ion-exchange membranes (these types are apart from ceramic or mineral membranes, *i.e.* inorganic membranes and natural membranes).

Ion-exchange membranes are in reality ion-exchange resins converted into the form of a membrane. These possess ionic charge throughout the polymer structure. Thus, when the membrane is negatively charged, it can permeate only cations and so it is termed as a cationic membrane. Other membranes are anionic in nature. In the membrane reactors, one of the components (product) is removed through a membrane which causes the equilibrium to shift to the right as per Le Chatelier's principle. In a wide variety of the types of membrane reactors, enzymatic reactors, bioreactors are well known.

Natural membranes suffer from problems like smaller temperature range (up to 100 °C) and not wider pH range, difficulties to clean up and susceptibility to natural attacks. The inorganic membranes can generally operate above 250 °C, where organic membranes can operate up to 300 °C [29]. Membranes can be supported with metals, thus offering many advantages. Membrane reactors can be made in different geometries, but, tubular and flat geometries are widely used.

Table 7.3 Few instances of use of IERs for RE

Reaction/Process	IER used, packing used	Process parameters	Remarks	References
Separation of 1,3-propanediol from dilute aqueous solution by synthesizing 2-methyl-1,3-dioxane	Dowex 50-WX4-200	RE runs at 323 K with equal volumes of reactants	• Conversion (98%) of 1,3-propanediol • The yield of dioxane (91–92%) • Recovery of dioxane (75%)	[81]
Extraction of penicillin G	Amberlite LA-2	RE runs at 298 K, extraction time 60 min	• About 90.7% extraction using Amberlite LA-2	[82]
Extraction of penicillin G	Amberlite LA-2	Batch runs at 298 K and stirring speed—250 rpm	• Amberlite LA-2 used as a carrier • Higher the Biot number higher is the extraction rate of penicillin G	[83]
Reactive extraction of nicotinic acid using vibratory mixing	Amberlite LA-2	RE runs at 298 K, extraction time of 1 min, vibration frequency 50 s^{-1}, the initial concentration of nicotinic acid is 12 g/L, Solvents used are n-heptane, n-butyl acetate and dichloromethane	• At 4 pH, using dichloromethane as a solvent and at high concentration of Amberlite LA-2, ~100% extraction of nicotinic acid • Highest extraction constant for Amberlite LA-2 by using dichloromethane as a solvent • High extraction efficiency with the use of Amberlite LA-2	[84]

(continued)

Table 7.3 (continued)

Reaction/Process	IER used, packing used	Process parameters	Remarks	References
Reactive extraction of levulinic acid	Amberlite LA-2	RE runs at 298 K using various solvents	• With Amberlite LA-2 and isoamyl alcohol as a solvent 98.55% extraction • Using hexane-1-ol as a solvent, 98.23% extraction • 98.02% extraction using MIBK as a solvent • The highest value of distribution coefficient (K_D-68.017) using Amberlite LA-2 and solvent isoamyl alcohol	[85]
Selective separation of vitamin C from 2-keto-gluconic acid	Amberlite LA-2	RE runs at 298 K, solvents used were n-heptane, n-butyl acetate and dichloromethane	• Distribution coefficient as high as 0.55 obtained at 3 pH	[86]
Selective separation of vitamin C from 2-keto-gluconic acid	Amberlite LA-2	RE runs at 298 K, solvents used were n-heptane, n-butyl acetate and dichloromethane	• By changing the pH of the aqueous phase, selective separation of vitamin C achieved • At pH 3 with dichloromethane as a solvent, ~17% of vitamin C was extracted • At 1 pH using the same solvent ~40% of vitamin C has been extracted • Higher selectivity of vitamin C at lower pH	[87]

(continued)

Table 7.3 (continued)

Reaction/Process	IER used, packing used	Process parameters	Remarks	References
Recovery of 2,3-butanediol from the fermentation broth	HZ732 resin	Room temperature conditions, volumetric feed ratio 0.1–0.2	• Yield (94%) of 2,3-butanediol obtained along with the 99% purity of the final product	[88]
Reactive extraction of rosmarinic acid with vibratory mixing	Amberlite LA-2	Reactive extraction runs at 298 K, extraction time 1-minute vibration frequency 50 s^{-1}, the initial concentration of rosmarinic acid is 10 g/L, solvents used are n-heptane, n-butyl acetate and dichloromethane	• At low pH (2) highest degree of extraction ($\sim$100%) observed using Amberlite LA-2 • Maximum efficiency of extraction found at 2 pH using Amberlite LA-2 with high extraction constant using n-heptane as a solvent	[89]
Reactive extraction of oxo-ethanoic acid	Amberlite LA-2	RE runs at 298 K using various solvents, stirring speed 40 rpm, total time 8 h	• The highest value of distribution coefficient (K_D-92) using hexane-2-one • Using Amberlite LA-2 and hexane-2-one as a solvent, 98.92% extraction achieved	[90]
Reactive extraction of glyoxylic acid	Amberlite LA-2	RE runs at 298 K using various solvents, stirring speed 40 rpm, total time of 8 h	• About 98.92% extraction obtained using Amberlite LA-2 and isoamyl alcohol as a solvent as opposed to 24% without using IER • The highest value of the distribution coefficient using Amberlite LA-2 and solvent isoamyl alcohol	[91]

(continued)

Table 7.3 (continued)

Reaction/Process	IER used, packing used	Process parameters	Remarks	References
Extraction of picric acid from wastewater using octan-1-ol as a solvent	Amberlite LA-2	RE runs at 293–313 K using various solvents, stirring speed 20–80 rpm, total time 4 h, the solvent used octan-1-ol	• Approximately 11.45% extraction without using IER Amberlite LA-2 as opposed to 98% using IER • Distribution coefficient increased from 5.71 to 70.51 in the presence of Amberlite LA-2	[92]
Extraction of picric acid from wastewater using ketones as a solvent	Amberlite LA-2	Reactive extraction runs at 293 K and 313 K using various solvents, stirring speed 50 rpm, total time 4 h, solvents used are—methyl ethyl ketone (MEK), methyl propyl ketone (MPK), heptanone and octanone	• The highest value of the distribution coefficient using Amberlite LA-2 and solvent MEK • As high as 98.36% extraction obtained using Amberlite LA-2 and MEK as a solvent	[93]

Table 7.4 illustrates the details of some instances, wherein IERs have been used in a membrane reactor (RM).

7.1.5 Reactive Crystallization (RCr)

Crystallization essentially works by cooling a saturated solution to precipitate one or more components as (solid) products, much purer than would have been otherwise obtained. The temperatures are set taking into account the change in solubilities of the components and the desired purity levels, among other factors. Crystallization is itself a very intensive mass transfer operation coupled with heat exchange. When the reaction is introduced (reactive crystallization, RCr), the system becomes much more complex. Due to inadequate rates of heat and mass transfer or due to an imbalance between rates of reaction and transport processes and also due to the stickiness of the solid to the surface of the equipment, fouling becomes one of the major issues that need to be addressed. Due to fouling, rates of heat and mass transfer are further reduced thus further disturbing the balance. In addition to heat transfer, mass transfer and reaction rates, the kinetics of crystallization itself has remained a major area of research. Various phase diagrams including solid–liquid, solid–solid involving various components superimposed by reaction(s) complicate the problem of design of RCr [24]. Ideally, it is possible to obtain the desired product range through good design. It is also necessary to look into the various mixing scales involved, ranging from micro to macromixing. Cooling of the mother liquor is a crucial step because it dictates both the quality as well as the number of crystals [30].

In many reactive crystallization operations, the mother liquor is recirculated and hence it is necessary that reaction mass and crystallization mass have identical nature. It is also necessary that the product must have a lesser solubility at a desired lower temperature for effective separation [31]. As discussed, because of the complexity of reactive crystallization (RCr) a lesser number of applications of RCr are cited in the literature. The following discussion pertains to the case studies where reactive crystallization has been studied. Not all of these refer to the application of IERs.

(a) Kwak et al. [30] and Kim et al. [32] investigated the dependency of crystallization of vancomycin from the reaction solution when IER was used. They concluded that the presence of IER during crystallization decreased the time needed for crystallization substantially. Cation-exchange resins Amberlite 200, Amberlite IR 120 (Na), Amberlite IRC 50 and Amberlite IR 120 (H) and anion-exchange resins Amberlite IRA 400 (Cl), Amberlite IRA (910) and Amberlite IRA 400 (OH) were used. Moderately acidic to near neutral pH was observed to favour crystal growth.

(b) Seidlitz et al. [33] reported the synthesis of p—acetamido—phenol by reacting acetic acid with p—aminophenol where water was produced as a by-product. The upper and lower temperatures were 100 and 30 °C, as the reaction and crystallization temperatures, respectively. In this process, the mother liquor was

Table 7.4 Few instances of use of IERs for RM

Reaction/Process	Membrane used	Process parameters	Remarks	References
Two-stage electrodialysis for lactic acid recovery via sodium lactate to lactic acid by water-splitting electrodialysis	Ralex ion-exchange membrane	Experiments at 298 K, effective membrane area—180 cm², current 3.9 A and voltage 12 V were applied	• High concentration of lactic acid achieved • More than 94% lactate present in fermentation broth was recovered • ~45% conversion achieved	[94]
Recovery of hydrochloric acid by reactive electrodialysis	Hydrodex HDX100 (cationic) membrane and Hydrodex HDX200 membrane (anionic)	Experiments at 293–313 K	• Evolution of harmful chlorine gas in the electrolyte treatment plant, reactive electrodialysis using an ion-exchange membrane provides additional advantages • Complete recovery of HCl • Cost effective process	[95]
Production of monosodium l-glutamate by metathesis reaction	Anion-exchange membranes (AEM) and cation-exchange membranes (CEM)	Mixed bed reactor, experiments at 298 K, effective membrane area—158 cm²	• 94.15% of l-glutamate recovered • Use of ion-exchange membrane reduced reaction time as well as energy consumption	[96]

(continued)

Table 7.4 (continued)

Reaction/Process	Membrane used	Process parameters	Remarks	References
Tartaric acid production by electrometathesis	AEM and CEM used	Experiments at 298 K, effective membrane area—25 cm^2	• >94% selectivity for AEM and >92% selectivity for CEM • Energy consumption decreased from the 21.92 kWh/kg before the resin addition to the 11.98 kWh/kg after the resin addition	[97]
Water desalination	Nitex 03-PA 6.6, Nitex 07-PET	Experiments at 313 K, the current density between −10 and −47.5 A/m^2	• Meshed membranes with 2% open area were more advantageous than homogeneous membranes • About 90% dilute yield obtained	[98]
Electrodialysis and separation of monovalent ions from a solution	SPES-PDA/PEI-2	Experiments at 298 K, effective membrane area—13.84 cm^2	• Permselectivity was 2.5 times higher than other membranes • Increase in PEI (polyethyleneimine) content, the water uptake of membranes increased	[99]
Phosphoric acid concentration and purification	Polysulfone (PSU) anion-exchange membrane	Experiments at room temperature, effective membrane area—20 cm^2, current density 40 mA/cm^2, total experiment time 360 min	• Approximately 100% concentrated phosphoric acid achieved • About 90% calcium, ~90% iron and 94% magnesium impurities were removed • Efficiency close to 100% till 50 min	[100]

constantly moved to and fro between crystallization and reaction section. In addition, the solubilities of product and reactants must be as desired [33].

(c) Reactive crystallization process, where Li_2CO_3 crystals were prepared by gas–liquid reaction between the CO_2 gas and LiOH solution, was developed by Sun et al. [34]. The higher conversion was obtained with the use of higher LiOH concentration at elevated temperature.

7.2   Concluding Remarks

In this chapter, instances of the use of ion-exchange resins (IERs) in reactive separation (RS) environment have been summarized. Out of the various separation processes that can be combined with the reaction step of RS, distillation (RD), chromatography (RC), extraction (RE), crystallization (RCr), and membrane separation (RM) have been discussed to the possible extent. The ion-exchange resins used, the reaction carried out, the process parameters used and the gist of the results obtained have been adequately discussed. This chapter will be useful to the readers who are interested in reactive separations with a special focus on ion-exchange resins. Tables that contain condensed yet exhaustive information would be useful to the readers.

References

1. Hans JG (2003) A general approach for the conceptual design of counter-current reactive separations. Chem Eng Sci 58:809–814. https://doi.org/10.1016/S0009-2509(02)00611-5
2. Schembecker G, Tlatlik S (2003) Process synthesis for reactive separations. Chem Eng Process 42:179–189. https://doi.org/10.1016/S0255-2701(02)00087-9
3. Stankiewicz A (2003) Reactive separations for process intensification: an industrial perspective. Chem Eng Process 42:137–144. https://doi.org/10.1016/S0255-2701(02)00084-3
4. Kloker M, KenigY E, Hoffmann A, Kreis P, Gorak A (2005) Rate-based modelling and simulation of reactive separations in gas/vapour—liquid systems. Chem Eng Process 44:617–629. https://doi.org/10.1016/j.cep.2003.12.011
5. Taylor R, Krishna R (2000) Modelling reactive distillation. Chem Eng Sci 55:5183–5229. https://doi.org/10.1016/S0009-2509(00)00120-2
6. Tuchlenski A, Beckmann A, Reusch D, Dussel R, Weidlich U, Janowsky R (2001) Reactive distillation—industrial applications, process design & scale-up. Chem Eng Sci 56:387–394. https://doi.org/10.1016/S0009-2509(00)00240-2
7. Chakrabarti A, Sharma MM (1993) Cationic ion exchange resins as catalyst. React Polym 20:1–45. https://doi.org/10.1016/0923-1137(93)90064-M
8. Sharma MM (1995) Some novel aspects of cationic ion-exchange resins as catalysts. React Funct Polym 26:3–23. https://doi.org/10.1016/1381-5148(95)00029-F
9. Irving AM, John MR (1997) A history of the origin and development of macroporous ion-exchange resins. React Funct Polym 35:7–22. https://doi.org/10.1016/S1381-5148(97)00058-8
10. Harmer A, Sun Q (2001) Solid acid catalysis using ion-exchange resins. Appl Catal 221:45–62. https://doi.org/10.1016/S0926-860X(01)00794-3

11. Spiro AD (2009) Ion-exchange resins: a retrospective from industrial and engineering chemistry research. Ind Eng Chem Res 48:388–398. https://doi.org/10.1021/ie801242v
12. Backhaus AA (1921) Continuous processes for the manufacture of esters. US patent 1400849
13. Sharma MM, Mahajani SM (2002) Industrial applications of reactive distillation. In: Kai S, Kienle A (ed) Reactive distillation status and future directions, Wiley, pp 3–29
14. Towler GP, Frey SJ (2002) Reactive distillation. In: Kulprathipanja (ed) Reactive separation processes, Taylor and Francis, New York, pp 18–50
15. Mahajan YS, Shah AK, Kamath RS, Salve Mahajani S M, Nandkumar B (2008) Recovery of trifluoroacetic acid from dilute aqueous solutions by reactive distillation. Sep Purif Technol 59:58–66. https://doi.org/10.1016/j.seppur.2007.05.027
16. Shinde VM, Patil GN, Katariya A, Mahajan YS (2015) Production of tetrahydrofuran by dehydration of 1,4-butanediol using Amberlyst-15: batch kinetics and batch reactive distillation. Chem Eng Process 95:241–248. https://doi.org/10.1016/j.cep.2015.06.016
17. Talnikar VD, Deorukhkar OA, Katariya A, Mahajan YS (2017) Value-added esterification for the recovery of trifluoroacetic acid: batch kinetics and reactive distillation studies. Chem Eng Commun 204:356–364. https://doi.org/10.1080/00986445.2016.1271795
18. Mahajan YS, Kamath RS, Kumbhar PS, Mahajani SM (2008) Self-condensation of cyclohexanone over ion exchange resin catalysts: kinetics and selectivity aspects. Ind Eng Chem Res 47:25–33. https://doi.org/10.1021/ie061275b
19. Popken T, Steinigeweg S, Gmehling J (2001) Synthesis and hydrolysis of methyl acetate by reactive distillation using structured catalytic packings: experiments and simulation. Ind Eng Chem Res 40:1566–1574. https://doi.org/10.1021/ie0007419
20. Carr RW, Dandekar HW (2002) Adsorption with reactionin. In: Kulprathipanja (ed) Reactive separation processes, Taylor and Francis, New York, pp 15–153
21. Oh J, Agrawal G, Sreedhar B, Donaldson EM, Schultz KA, Frank CT, Bommarius SA, Kawajiri Y (2014) Conversion improvement for catalytic synthesis of propylene glycol methyl ether acetate by reactive chromatography: experiments and parameter estimation. Chem Eng J 1360:196–208. https://doi.org/10.1016/j.cej.2014.08.008
22. Strohlein G, Assuncao Y, Dube N, Bardow A, Mazzotti M, Morbidelli M (2006) Esterification of acrylic acid with methanol by reactive chromatography: experiments and simulations. Chem Eng Sci 61:5296–5306. https://doi.org/10.1016/j.ces.2006.04.004
23. Lode F, Francesconi G, Mazzotti M, Morbidelli M (2003) Synthesis of methylacetate in a simulated moving-bed reactor: experiments and modeling. Am Inst Chem Eng J 49:1516–1524. https://doi.org/10.1002/aic.690490615
24. Krishna R (2002) Reactive separations: more ways to skin a cat. Chem Eng Sci 57:1491–1504. https://doi.org/10.1016/S0009-2509(02)00020-9
25. Wardell JM, King CJ (1978) Solvent equilibria for extraction of carboxylic acids from water. J Chem Eng Data 23:144–148. https://doi.org/10.1021/je60077a009
26. Wasewar KL, Pangarkar VG, Heesink ABM, Versteeg GF (2003) Intensification of enzymatic conversion of glucose to lactic acid by reactive extraction. Chem Eng Sci 58:3385–3393. https://doi.org/10.1016/S0009-2509(03)00221-5
27. Brunt VV, Kanel JS (2002) Extraction with reaction. In: Kulprathipanja (ed) Reactive separation processes. Taylor and Francis, New York, pp 51–90
28. Nath K (2012) Membrane separation processes. Prentice Hall of India, Eastern Economy Edition, New Delhi
29. Jaroszek H, Dydo P (2015) Ion-exchange membranes in chemical synthesis—a review. Open Chem 14:1–19. https://doi.org/10.1515/chem-2016-0002
30. Kwak E, Kim S, Kim J (2012) Effect of ion exchange resin on increased surface area crystallization process for purification of vancomycin. Korean J Chem Eng 29:1487–1492. https://doi.org/10.1007/s11814-012-0135-8
31. Kelkar VV, Samant KD, Ng KM (2002) Reactive crystallization. In: Kulprathipanja (ed) Reactive separation processes, Taylor and Francis, New York, pp 209–245
32. Kim S, Kim J (2015) Investigation on the role of ion exchange resin in the crystallization process for the purification of vancomycin. Korean J Chem Eng 32:465–470. https://doi.org/10.1007/s11814-014-0222-0

33. Seidlitz F, Mathieu C, Breysse J, Houzelot JL (2001) Simultaneous synthesis and separation of a product by cooling crystallization into a multifunctional reactor. In: 2nd international conference on multifunctional reactors, Nuremberg

34. Sun Y, Song X, Jin M, Jin W, Yu J (2013) Gas–liquid reactive crystallization of lithium carbonate by a falling film column. Ind Eng Chem Res 52:17598–17606. https://doi.org/10.1021/ie402698v

35. Saha B, Sharma MM (1996) Esterification of formic acid, acrylic acid and methacrylic acid with cyclohexene in batch and distillation column reactors: ion-exchange resins as catalysts. React Funct Polym 28:263–278. https://doi.org/10.1016/1381-5148(95)00092-5

36. Kolah AK, Mahajani SM, Sharma MM (1996) Acetalization of formaldehyde with methanol in batch and continuous reactive distillation columns. Ind Eng Chem Res 35:3707–3720. https://doi.org/10.1021/ie950563x

37. Gonzalez JC, Subawalla H, Fair JR (1997) Preparation of *tert*-amyl alcohol in a reactive distillation column. 2. Experimental demonstration and simulation of column characteristics. Ind Eng Chem Res 36:3845–3853. https://doi.org/10.1021/ie960808l

38. Chopade SP (1999) Ion-exchange resin-catalyzed ketalization of acetone with 1,4-and 1,2-diols: use of molecular sieve in reactive distillation. React Funct Polym 42:201–212. https://doi.org/10.1016/S1381-5148(98)00072-8

39. Saha B, Chopade SP, Mahajani SM (2000) Recovery of dilute acetic acid through esterification in a reactive distillation column. Catal Today 60:147–157. https://doi.org/10.1016/S0920-5861(00)00326-6

40. Qi Z, Sundmacher K, Stein E, Kienle A, Kolah A (2002) Reactive separation of isobutene from C_4 crack fractions by catalytic distillation processes. Sep Purif Technol 26:147–163. https://doi.org/10.1016/S1383-5866(01)00156-3

41. Chiang S, Kuo C, Yu C, Wong D (2002) Design alternatives for the amyl acetate process: coupled reactor/column and reactive distillation. Ind Eng Chem Res 41:3233–3246. https://doi.org/10.1021/ie010358j

42. Steinigeweg S, Gmehling J (2003) Esterification of a fatty acid by reactive distillation. Ind Eng Chem Res 42:3612–3619. https://doi.org/10.1021/ie020925i

43. Schmitt M, Hasse H, Althaus K, Schoenmakers H, Gotze L, Moritz P (2004) Synthesis of *n*-hexyl acetate by reactive distillation. Chem Eng Process 43:397–409. https://doi.org/10.1016/S0255-2701(03)00124-7

44. Steinigeweg S, Gmehling J (2004) Transesterification processes by combination of reactive distillation and pervaporation. Chem Eng Process 43:447–456. https://doi.org/10.1016/S0255-2701(03)00129-6

45. Varisli D, Dogu T (2005) Simultaneous production of *tert*-amyl ethyl ether and *tert*-amyl alcohol from *iso*—amylene—ethanol—water mixtures in a batch-reactive distillation column. Ind Eng Chem Res 44:5227–5232. https://doi.org/10.1021/ie049241w

46. Singh A, Tiwari A, Mahajani SM, Gudi RD (2006) Recovery of acetic acid from aqueous solutions by reactive distillation. Ind Eng Chem Res 45:2017–2025. https://doi.org/10.1021/ie0505514

47. Thotla S, Agarwal V, Mahajani SM (2007) Aldol condensation of acetone with reactive distillation using water as a selectivity enhancer. Ind Eng Chem Res 46:8371–8379. https://doi.org/10.1021/ie061658

48. Kumar R, Mahajani SM (2007) Esterification of lactic acid with *n*-butanol by reactive distillation. Ind Eng Chem Res 46:6873–6882. https://doi.org/10.1021/ie061274j

49. Kotora M, Buchaly C, Kreis P, Gorak A, Markos J (2008) Reactive distillation—experimental data for propyl propionate synthesis. Chem Pap 62:65–69. https://doi.org/10.2478/s11696-007-0080

50. Lee H-Y, Yen L-T, Chien I-L, Huang H-P (2009) Reactive distillation for esterification of an alcohol mixture containing *n*-butanol and *n*-amyl alcohol. Ind Eng Chem Res 48:7186–7204. https://doi.org/10.1021/ie801891q

51. Altmana E, Kreis P, Gerven VT, Stefanidis GD, Stankiewicz A, Gorak A (2010) Pilot plant synthesis of n-propyl propionate via reactive distillation with decanter separator for reactant recovery. Experimental model validation and simulation studies. Chem Eng Process 49:965–972. https://doi.org/10.1016/j.cep.2010.04.008

52. Orjuela A, Kolah A, Lira CT, Miller DJ (2011) Mixed succinic acid/acetic acid esterification with ethanol by reactive distillation. Ind Eng Chem Res 50:9209–9220. https://doi.org/10.1021/ie200133w

53. Kiatkittipong W, Intaracharoen P, Laosiripojana N, Chaisuk C, Praserthdam P, Assabumrungrat S (2011) Glycerol ethers synthesis from glycerol etherification with *tert*-butyl alcohol in reactive distillation. Comput Chem Eng 35:2034–2043. https://doi.org/10.1016/j.compchemeng.2011.01.016

54. Niesbach A, Fuhrmeister R, Keller T, Lutze P, Gorak A (2012) Esterification of acrylic acid and *n*-butanol in a pilot-scale reactive distillation column—experimental investigation, model validation, and process analysis. Ind Eng Chem Res 51:16444–16456. https://doi.org/10.1021/ie301934w

55. Sandesh K, Babu J, Math S, Saidutta MB (2013) Reactive distillation using an ion-exchange catalyst: experimental and simulation studies for the production of methyl acetate. Ind Eng Chem Res 52:6984–6990. https://doi.org/10.1021/ie3029174

56. Ye J, Li J, Sha Y, Xu Y, Zhou D (2014) Novel reactive distillation process for phenol production with a dry cation exchange resin as the catalyst. Ind Eng Chem Res 53:12614–12621. https://doi.org/10.1021/ie500165m

57. Zuo C, Pan L, Cao S, Li C, Zhang S (2014) Catalysts, kinetics, and reactive distillation for methyl acetate synthesis. Ind Eng Chem Res 53:10540–10548. https://doi.org/10.1021/ie5

58. Zuo C, Ge T, Li C, Cao S, Zhang S (2016) Kinetic and reactive distillation for acrylic acid synthesis via transesterification. Ind Eng Chem Res 55:8281–8291. https://doi.org/10.1021/acs.iecr.6b01128

59. Hussain A, Minh LQ, Muhammad AQ, Lee M (2017) Design of an intensified reactive distillation configuration for 2-methoxy-2-methylheptane. Ind Eng Chem Res 57:316–328. https://doi.org/10.1021/acs.iecr.7b04624

60. Rastegari H, Ghaziaskar HS, Yalpani M, Shafiei A (2017) Development of a continuous system based on azeotropic reactive distillation to enhance triacetine selectivity in glycerol esterification with acetic acid. Energy Fuels 31:8256–8262. https://doi.org/10.1021/acs.energyfuels.7b01068

61. Kawase M, Inoue Y, Araki T, Hashimoto K (1999) The simulated moving-bed reactor for production of *bis*-phenol A. Catal Today 48:199–209. https://doi.org/10.1016/S0920-5861(98)00374-5

62. Lode F, Houmard M, Migliorini C, Mazzotti M, Morbidelli M (2001) Continuous reactive chromatography. Chem Eng Sci 56:269–291. https://doi.org/10.1016/S0009-2509(00)00229-3

63. Zhang Z, Hidajat K, Ray AK (2001) Application of simulated counter-current moving-bed chromatographic reactor for MTBE synthesis. Ind Eng Chem Res 40:5305–5316. https://doi.org/10.1021/ie001071

64. Meissner JP, Carta G (2002) Continuous regioselective enzymatic esterification in a simulated moving bed reactor. Ind Eng Chem Res 41:4722–4732. https://doi.org/10.1021/ie0202625

65. Gelosa D, Ramaioli M, Valente G (2003) Chromatographic reactors: esterification of glycerol with acetic acid using acidic polymeric resins. Ind Eng Chem Res 42:6536–6544. https://doi.org/10.1021/ie030292n

66. Yu W, Hidajat K, Ray AK (2003) Modelling simulation, and experimental study of a simulated moving bed reactor for the synthesis of methyl acetate ester. Ind Eng Chem Res 42:6743–6754. https://doi.org/10.1021/ie0302241

67. Vu D, Seidel-Morgenstern A, Gruner S, Kienle A (2005) Analysis of ester hydrolysis reactions in a chromatographic reactor using equilibrium theory and a rate model. Ind Eng Chem Res 44:9565–9574. https://doi.org/10.1021/ie050256j

68. Gandi GK, Silva V, Rodrigues AE (2006) Synthesis of 1,1-di-methoxy-ethane in a fixed bed adsorptive reactor. Ind Eng Chem Res 45:2032–2039. https://doi.org/10.1021/ie051096e

69. Gyani VC, Mahajani SM (2008) Reactive chromatography for the synthesis of 2-ethylhexyl acetate. Sep Sci Technol 43:2245–2268. https://doi.org/10.1080/01496390802118871

70. Pereira C, Gomes P, Gandi GK, Silva V, Rodrigues AE (2008) Multifunctional reactor for the synthesis of dimethyl-acetal. Ind Eng Chem Res 47:3515–3524. https://doi.org/10.1021/ie070889t

71. Pereira C, Zabka M, Silva V, Rodrigues AE (2009) A novel process for the ethyl lactate synthesis in a simulated moving bed reactor (SMBR). Chem Eng Sci 64:3301–3310. https://doi.org/10.1016/j.ces.2009.04.003

72. Deshmukh KS, Gyani VC, Mahajani SM (2009) Esterification of butyl cellosolve with acetic acid using ion exchange resin in fixed bed chromatographic reactors. Int J Chem Reactor Eng 2:1542–6580. https://doi.org/10.2202/1542-6580.1793

73. Kapil A, Bhat SA, Sadhukhan J (2010) Dynamic simulation of sorption enhanced reaction processes for biodiesel production. Ind Eng Chem Res 49:2326–2335. https://doi.org/10.1021/ie901225u

74. Patel D, Saha B (2012) Esterification of acetic acid with n-hexanol in batch and continuous chromatographic reactors using a gelular ion-exchange resin as a catalyst. Ind Eng Chem Res 51:11965–11974. https://doi.org/10.1021/ie3007424

75. Gyani VC, Reddy B, Rahul B, Mahajani SM (2014) Simulated moving bed reactor for the synthesis of 2-ethylhexyl acetate—Part I: Experiments and simulations. Ind Eng Chem Res 53:15811–15823. https://doi.org/10.1021/ie502090z

76. Reddy B, Mahajani S (2014) Feasibility of Reactive chromatography for the synthesis of *n*-propyl acetate. Ind Eng Chem Res 53:1395–1403. https://doi.org/10.1021/ie403533t

77. Agrawal G, Oh J, Sreedhar B, Tie S, Donaldson ME, Frank TC, Schultz AK, Bommarius AS, Kawajiri Y (2014) Optimization of reactive simulated moving bed systems with modulation of feed concentration for production of glycol ether ester. J Chromatogr A 1360:196–208. https://doi.org/10.1016/j.chroma.2014.07.0800021-9673

78. Constantino D, Pereira C, Faria R, Loureiro JM, Rodrigues AE (2015) Simulated moving bed reactor for butyl acrylate synthesis: from pilot to industrial scale. Chem Eng Process 55:10735–10743. https://doi.org/10.1016/j.cep.2015.08.003

79. Oh J, Agrawal G, Sreedhar B, Donaldson ME, Schultz AK, Frank TC, Bommarius AS, Kawajiri Y (2016) Transesterification of propylene glycol methyl ether in chromatographic reactors using anion exchange resin as a catalyst. J Chromatogr A 1466:84–95. https://doi.org/10.1016/j.chroma.2016.08.0720021-9673

80. Tie S, Sreedhar B, Agrawal G, Oh J, Donaldson M, Frank T, Bommarius A, Kawajiri Y (2016) Model-based design and experimental validation of simulated moving bed reactor for production of glycol ether ester. Chem Eng J 301:188–199. https://doi.org/10.1016/j.cej.2016.04.062

81. Malinowski J (2000) Reactive extraction for downstream separation of 1,3-propanediol. Biotechnol Prog 16:76–79. https://doi.org/10.1021/bp990140g

82. Lee S, Ahn B, Kim J (2002) Reaction equilibrium of penicillin G with Amberlite LA-2 in a nonpolar organic solvent. Biotechnol Prog 18:108–115. https://doi.org/10.1021/bp010145p

83. Lee S (2004) Kinetics of reactive extraction of penicillin G by Amberlite LA-2 in kerosene. Am Ins Chem Eng J 50:119–126. https://doi.org/10.1002/aic.10011

84. Cascaval D, Blaga A, Camaruţ M, Galaction A (2007) Comparative study on reactive extraction of nicotinic acid with Amberlite LA-2 and D2EHPA. Sep Sci Technol 42:389–401. https://doi.org/10.1080/01496390601069937

85. Uslu HS, Kırbaslar I, Wasewar K (2009) Reactive extraction of levulinic acid by Amberlite LA-2 extractant. J Chem Eng Data 54:712–718. https://doi.org/10.1021/je800261j

86. Blaga A, Galaction A, Cascaval D (2010) Reactive extraction of 2-keto-gluconic acid Mechanism and influencing factors. Rom Biotechnol Lett 15:5253–5259

87. Blaga A, Malutan T (2012) Selective separation of vitamin C by reactive extraction. J Chem Eng Data 57:431–435. https://doi.org/10.1021/je2010193

88. Li Y, Zhu J, Wu Y, Liu J (2013) Reactive extraction of 2,3-butanediol from fermentation broth. Korean J Chem Eng 30:154–159. https://doi.org/10.1007/s11814-012-0114-0
89. Kloetzer L, Postaru M, Galaction A, Blaga A, Cascaval D (2013) Comparative study on rosmarinic acid separation by reactive extraction with Amberlite LA-2 and D2EHPA 1. Interfacial reaction mechanism and influencing factors. Ind Eng Chem Res 52:13785–13794. https://doi.org/10.1021/ie4023513
90. Uslu H, Datta D, Kumar S (2014) Reactive extraction of oxoethanoic acid (glyoxylic acid) using Amberlite LA-2 in different diluents. J Chem Eng Data 59:2623–2629. https://doi.org/10.1021/je5003972
91. Uslu H, Datta D, Kumar S (2015) Investigations on the reactive extraction of glyoxylic acid by Amberlite LA-2 dissolved in alcoholic diluents. Sep Sci Technol 50:2658–2667. https://doi.org/10.1080/01496395.2015.1067229
92. Uslu H, Datta D, Bamufleh H (2016) Extraction of picric acid from wastewater by a secondary amine (Amberlite LA2) in 1-octanol: equilibrium, kinetics, thermodynamics and molecular dynamic simulation. Ind Eng Chem Res 55:3659–3667. https://doi.org/10.1021/acs.iecr.5b04750
93. Uslu H, Marti M (2017) Equilibrium data on the reactive extraction of picric acid from dilute aqueous solutions using Amberlite LA-2 in ketones. J Chem Eng Data 62:2132–2135. https://doi.org/10.1021/acs.jced.7b00226
94. Habova V, Melzoch K, Rychtera M, Pribyl L, Mejta V (2018) Application of electro—dialysis for lactic acid recovery. Czech J Food Sci 19:73–80. https://doi.org/10.17221/6579-CJFS
95. Cifuentes G, Guajardo N, Hernandez J (2015) Recovery of hydrochloric acid from ion exchange processes by reactive electro—dialysis. J Chil Chem Soc 60:2711–2715. https://doi.org/10.4067/S0717-97072015000400015
96. Chai P, Wang J, Lu H (2015) The cleaner production of monosodium l-glutamate by resin-filled electro-membrane reactor. J Membr Sci 493:549–556. https://doi.org/10.1016/j.memsci.2015.07.023
97. Zhang K, Wang M, Gao C (2011) Tartaric acid production by ion exchange resin-filling electrometathesis and its process economics. J Membr Sci 366:266–271. https://doi.org/10.1016/j.memsci.2010.10.013
98. Porada S, Egmond W, Post J, Saakes M, Hamelers H (2018) Tailoring ion exchange membranes to enable low osmotic water transport and energy efficient electrodialysis. J Membr Sci 552:22–30. https://doi.org/10.1016/j.memsci.2018.01.050
99. Li J, Yuan S, Wang J, Zhu J, Shen J, Bruggen B (2018) Mussel-inspired modification of ion exchange membrane for monovalent separation. J Membr Sci 553:139–150. https://doi.org/10.1016/j.memsci.2018.02.046
100. Duan X, Wang C, Wang T, Xie X, Zhou X, Ye Y (2018) A polysulfone-based anion exchange membrane for phosphoric acid concentration and purification by electro-electro—dialysis. J Membr Sci 552:86–94. https://doi.org/10.1016/j.memsci.2018.02.004

Chapter 8
Ion-Exchange Chromatography in Separation and Purification of Beverages

Muhammad Razeen Ahmad, Muhammad Rizwan Javed, Muhammad Ibrahim, Arfaa Sajid, Muhammad Riaz, Ijaz Rasul, Muhammad Hussnain Siddique, Saima Muzammil, Muhammad Amjad Ali and Habibullah Nadeem

Abstract Beverage industries including water treatment industry, employ ion-exchange chromatography in different forms in several processes to remove chemicals, ions, additives, colourants or harmful substances from drinks. The ion-exchange materials employed are nonreactive and physiochemically stable, and therefore, are a suitable choice for beverage treatment. The most widespread use of ion-exchange process is in the water treatment industry; seawater and brackish water desalination, water softening, removal of heavy metals, harmful ions and dissolved organic contaminants. The ion-exchange chromatography used in these industrial processes is the courtesy of the processes: electrodialysis and electrodeionization, both of which use ion-exchange membranes and the latter use ion-exchange resins also. Exces-

M. R. Ahmad · M. R. Javed · I. Rasul · M. H. Siddique · H. Nadeem (✉)
Department of Bioinformatics and Biotechnology, Government College University, Faisalabad, Pakistan
e-mail: habibullah@gcuf.edu.pk

M. Ibrahim
Department of Applied Chemistry, Government College University, Faisalabad, Pakistan

A. Sajid
Department of Chemistry, University of Lahore, Lahore, Pakistan

M. Riaz
Department of Food Sciences,
University College of Agriculture, BahauddinZakariya University, Multan, Pakistan

S. Muzammil
Department of Microbiology, Government College University, Faisalabad, Pakistan

M. A. Ali
Department of Plant Pathology, Center of Agricultural Biochemistry
and Biotechnology (CABB), University of Agriculture, Faisalabad, Pakistan

sive organic acids are removed from acidic fruit juices and wine using the same ion-exchange techniques. Electrodialysis and electrodeionization, along with their modifications and combination with other membrane filtration techniques, prove to be the most efficient in beverage treatment for best quality control.

8.1   Introduction

The word beverage is used to refer to 'bottled or canned drinks' that include bottled drinking water, carbonated/soft drinks, fruit juices, energy drinks, tea, coffee and alcoholic drinks. So, beverages are drinkable liquids that come in many forms, including drinking water. The beverage industry is one of the major industries in the world.

Drinking water is usually obtained after several treatments like chlorination and desalting of brackish and seawater. The major things to be checked for water quality are its total dissolved solids (TDS) that include dissolved ions, organic and inorganic matter particles and microbes. Water is thus easily processed by filtration and its ion content is efficiently controllable through ion-exchange-based techniques. Water treatment is by far the most widespread application of ion exchange in beverage industries worldwide. Unlike water, soft drinks are carbonated, and thus contain high concentrations of carbonate ions, organic acids (citric acid) and sweeteners. Fruit juices like orange, lemon, pineapple, apple and passion fruit juices, contain a high concentration of organic acids, sugars, minerals and other particles like pulp. Energy drinks also contain sugars, vitamins and necessary minerals. In such types of drinks where the ions are to be retained in the final beverage product, either ion exchange is very carefully employed to selectively remove excess ions or other filtration/separation techniques be used. Therefore, ion exchange has minor applications in soft drinks, energy drinks and coffee industry. Among alcoholic drinks, wine or other drinks may be treated for excess ion and alcohol removal.

The importance of ion exchange in any process is its efficient and high-specificity application that reduces the overall energy consumption and cost of the process. Other separation/purification techniques for beverage production include physical processes like centrifugation, filtration and membrane processes (reverse osmosis, dialysis, etc.) and chemical processes like precipitation of a specific component by adding chemicals. Membrane processes have proven to be the most efficient in the separation of solutes from beverages, and ion-exchange materials have been used to develop membranes for highly efficient separation/purification. Combinations of ion-exchange materials and resins have been a popular choice for efficient water treatment. This chapter discusses the major applications of ion exchange in water treatment by membrane and resins, and minor applications of ion exchange in other beverage industries like fruit juice, nonalcoholic and alcoholic drinks.

8.2 Ion-Exchange Resins

Ion-exchange chromatography has been used to separate and purify specific components with high efficiency. Today, the biggest consumer of ion-exchange resins is the water treatment industry. Ion-exchange resins are currently available in many different forms, shapes and chemical natures but are intrinsically the same in having polar ends attached to polymeric or crystalline matrix beads. These polar heads, either cationic (positively charged) or anionic (negatively charged), play their role in the separation of charged components needed to be separated out from a given solution.

8.2.1 Properties of Ion-Exchange Resins Used for Industrial Applications

The major advantages of ion-exchange resins, which make them suitable for beverage industry are

(1) Ion-exchange materials have high physical and chemical stabilities which ensure no contamination of the fluid/solution under treatment.
(2) Ion-exchange chromatography works best when a dilute component needs to be purged from the whole solution. In many types of beverages, this is the case and is described in the chapter in detail.
(3) Parameters like flow rate, the concentration of the solution etc., do not have any adverse effect on these materials.
(4) The target substances removed from a solution are removed with high efficiency, e.g. in water purification, few or none microbes are left when passed through an exchanger (see the removal of NOM from water).

8.2.2 Applications in Drinking Water Treatment

Drinking water is one of the major sources of diseases around the world. In many areas, adequate quality of drinking water from ground or other sources is not available and people are compelled to drink contaminated water, such as in deserts, mountainous plateaus and terrains away from water bodies (e.g. Africa). The treatment of drinking water on an industrial level is always required. As the afore-mentioned properties of ion exchangers are ideal for such contaminated water treatment, these are employed in various ways to remove contaminants like excess salts, harmful ions (Fe^{2+}, Cd^{2+}, Cr^{2+}, Hg^{2+}, Mn^{2+}, etc.), colourants and dissolved organic matter [1].

8.2.3 Major Ion-Exchange Processes in Water Treatment

Depending upon the composition of water and the chemical nature of the contaminants to be removed, there are several applications of ion-exchange chromatography as mentioned below:

- Water desalination
- Water softening
- Removal of harmful ions
- Removal of organic contaminants.

8.2.3.1 Water Desalination

The increase in demand for freshwater for drinking and domestic purposes, removal of salts (desalination) from seawater and brackish water is a necessity to fulfil our needs. About 97% of the world's water is stored in the oceans; it can be reused if we remove salts to safe levels and hugely benefit from this global resource. Total dissolved solids (TDS) are the measure of how many inorganic salts and organic matter particles are present in water. TDS majorly includes dissolved ions like Na^+, K^+, Ca^{2+}, Mg^{2+}, CO_3^{2-}, HCO_3^-, Cl^-, SO_4^{-2} and NO_3^-. The brackish water [1–10 g/L TDS] and seawater [30–60 g/L TDS] are brought to freshwater level [≤500 mg/L TDS] by removing salts through pressure-driven techniques like reverse osmosis (RO), multi-effect distillation (MED), adsorption distillation (AD), membrane distillation (MD), electricity-driven electrodialysis (ED) and electrodeionization (EDI) [2–4]. RO and MD are very efficient and widely used in desalination but far from being energy efficient. ED and EDI use ion-exchange materials and this enhances the energy conservation, making them the most energy-efficient techniques [2, 5, 6].

Electrodialysis (ED)

Electrodialysis is a process in which ions can be selectively separated from a solution using electrochemical potential and ion-exchange membranes. The conventional electrodialysis cell consists of a series of alternating anion-exchange membranes (AEM) and cation-exchange membranes (CEM), stacked between two electrodes, as illustrated in Fig. 8.1.

The anion- and cation-exchange membranes are separated by a spacer, forming individual cells. When brackish/saline water is passed through the cells, the electric potential of the surrounding plates causes the movement of ions. Alternating cells with very high and very low concentration of ions so-called as 'concentrate' and 'diluate' cells are present. Each concentrate and adjacent diluate cell forms a cell pair. In industrial settings, the electrodialysis stack consists of 100–200 cell pairs between the electrodes. Depending upon the required efficiency, the solution–membrane contact area can be increased by different arrangements of the spacers and
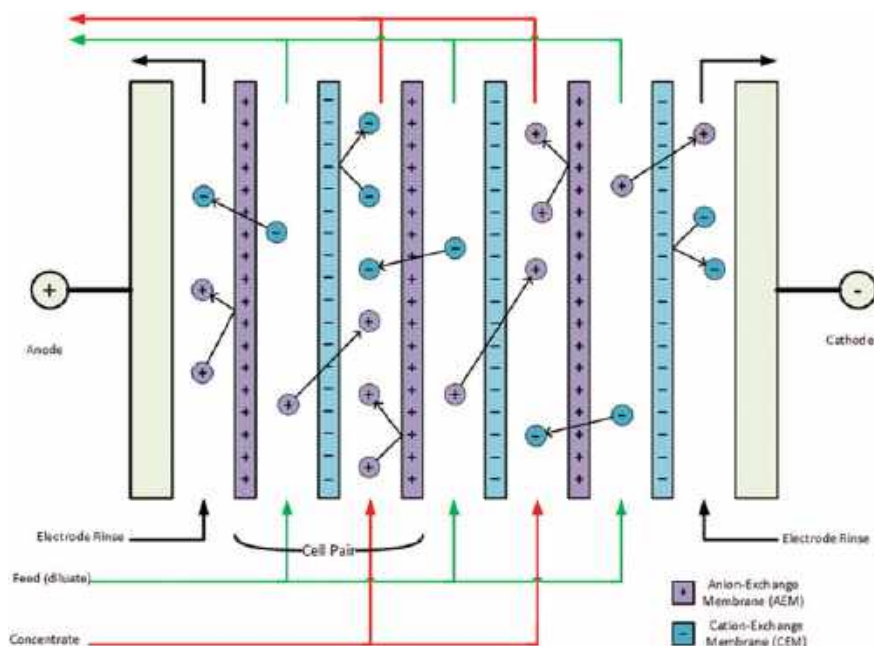
Fig. 8.1   Schematic representation of electrodialysis technique

ion-exchange membranes. There are two important arrangements: (i) sheet flow and (ii) tortuous path flow.

In the sheet-flow arrangement, ion-exchange membranes are vertically stacked as in Fig. 8.1. On the contrary, in a tortuous path flow, the membranes are horizontally stacked in a serpentine arrangement, which provides a long narrow path with lots of surface area for ion exchange. In sheet flow, the process path is shorter and renders lesser pressure loss [flow speed = 2–4 cm/s; pressure loss = 0.2–0.4 bar]. In tortuous path flow, the narrow path between membranes allows higher speed [6–12 cm/s] but the serpentine path results in higher pressure loss [1–2 bar]. Practically in industrial applications, this adds up to a lot of difference in the yield. Since the direction of inflow of concentrate and feed is the same, the feed outflow has ~50% fewer salts than the input (recovery rate). The outflow feed and concentrate thus can be passed again through the cell repeatedly, until the desired concentration of the diluent is obtained [5, 7], Na_2SO_4 is commonly used to rinse the electrode.

As it can be seen in the operation of electrodialysis, ions accumulate on the electrodes with the passage of time, as well as charged organic particles also accumulate on the surface of electrodes and membranes forming a 'fouling layer'. This can decrease the efficiency of the desalination. Reversing the electric field in a run causes reversal of the ion flow and the accumulated particles are removed. This type of 'self-cleaning' is widely used in water desalination industries. Electrodialysis is a very efficient method for brackish water with 1–5 g/L TDS. However, a major

problem of ED is its inability to filter/remove uncharged organic and toxic particles including viruses and bacteria. A conventional electrodialysis, such as described above can have very high costs. To manage cost-effectiveness in water desalination, other modifications of this process are used.

Electrodeionization (EDI)

Electrodialysis comes up with a big problem of high cost because of 'concentration polarization', which is the resistance developed by the concentrate cell. When a certain limit of the concentration is crossed in the concentrate cell, the electroneutrality of the membrane surfaces is changed due to the concentration gradient across the membrane. This leads to accumulation and subsequent precipitation of ions at the membrane surface facing the concentrate cell. As a result, the movement of ions in the given energy (electric field) is decreased and the overall efficiency of the ED cell is decreased.

To solve concentration polarization, solid ion-exchange (IEX) resin is introduced in the space of diluate cell, which acts as a conductor and ions can easily move through this bridge from one IEX membrane to another (illustrated in Fig. 8.2). Such a combination of IEX membranes and IEX resin is called 'electrodeionization' (EDI). As in this case, the diluate compartment is filled with IEX bed and this combination is also called continuous electrodeionization (CEDI) [4, 8]. The filling of IEX resin in the diluate compartments maintains neutrality across all cells of the stack. In the resin bed, water molecules dissociate as a result of the electric field, which continuously regenerates ion-exchange resin and lowers the salt stress in concentration polarization.

The ion-exchange membranes and resins used in ED and EDI are mostly synthetic, which are strong-acid-cation resins and strong-basic-anion resins. The matrix of strong-cation resins is mostly made up of styrene, divinylbenzene and sulphonic/poly-sulphonic acids. The strong anion exchangers are made up of polymeric materials with methyl, ethanol or amine functional groups [9]. For given membrane types, the thickness of the membrane plays an important role. Thick membranes offer higher resistivity and decrease the conductivity of product water by blocking the diffusion of H^+ ions, which restore the resin electrochemical properties. The diffusion of protons across thinner membranes is easier and results in higher conductivity of product water (in diluate compartments) [10].

Resin-Wafer EDI (RW-EDI)

The canonical EDI and CEDI are efficient but their matrices contain loose beads of resin. Such loose beads may form channels in the matrix and consequently results in a decline in ion removal efficiency. To overcome this, the IEX resin is first molded into a solid cast, with IEX beads fixed on a solid matrix, creating a porous and consistent sheet/ bed of resin matrix. RO is good for seawater reclamation (65% energy effi-
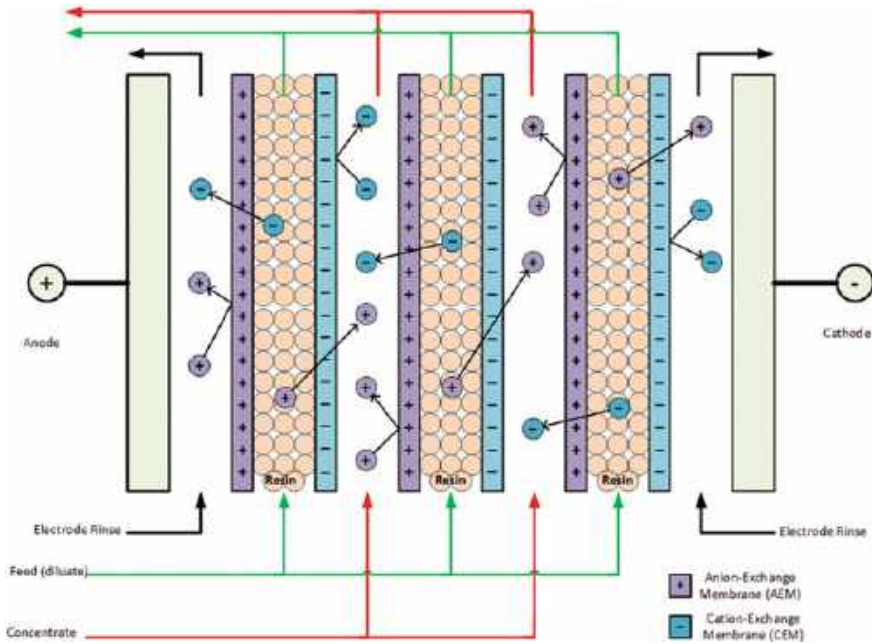
Fig. 8.2   Schematic representation of electrodeionization

ciency) but not so efficient for lower concentrations like that of brackish water (11%
energy efficient). Due to its less energy consumption [~0.35–0.66 kWh/m^3], with a
productivity of 20.1–44.7 L h^{-1} m^{-2}, it is the best for brackish water desalination at
about 35% more energy efficient than RO technology [11, 12].

8.2.3.2   Water Softening

It is evident from the electrodeionization process that the majority of ions can be
removed by this technology. There are many of its modifications to selectively remove
ions from the feed water. The usual ions that account for the majority of the dissolved
salts (TDS) in the freshwater and brackish/seawater are Na^+, K^+, Ca^{2+}, Mg^{2+}, CO_3^{2-},
HCO_3^-, Cl^-, SO_4^{-2} and NO_3^-. In chlorinated water for domestic use, chlorine ions are
in large quantities and need to be removed. Apart from these, there are other ions in
small quantities, which can be hazardous if their concentration is higher than a certain
limit. These include heavy metal ions like iron (Fe^{2+}), zinc (Zn^{2+}), nickel (Ni^{2+}),
lead (Pb^{2+}), chromium (Cr^{6+}, CrO_4^{2-}), copper (Cu^{2+}) and cadmium (Cd^{2+}). Other
ions include boron [$B_3O_3(OH)_4^{-1}$, $B_4O_5(OH)_4^{-1}$, and $B_5O_6(OH)_4^{-1}$] and ammonium
(NH_4^+) [4, 13]. These ions can have detrimental effects on body health if their level
in the drinking water is not safe. Therefore, WHO has specified safe levels of these
ions and it is crucial that drinking water treatment facilities manage to lower down

the levels of hazardous ions below the safe limit. The majority of the world's drinking water plants use reverse osmosis technology. RO and other similar technologies are efficient for high concentration salt removal but fall short at lower concentrations. Multiple passes through RO may remove most of the ions but the energy consumed is very high, which renders the process inefficient. Therefore, many electricity-based technologies like CDI, ED, EDI, and their combinations with other technologies (like RO) are used for best results.

Removal of Mg^{2+} and Ca^{2+} Ions

Hard water is the water containing sparingly soluble cations, i.e. magnesium (Mg^{2+}) and calcium (Ca^{2+}). The hardness of water influences the properties of water and produces undesirable effects. Hard water is also not suitable for drinking because of the high level of calcium, which poses a higher risk of calcium-based kidney stones (calcium nephrolithiasis) [14]. Common water softening methods include precipitation of Mg^{2+} and Ca^{2+} ions in the form of their carbonates. Chemical precipitation includes the addition of bicarbonates and alkaline chemicals, which cause the formation of $MgCO_3$ and $CaCO_3$ precipitates. Physical methods include boiling of hard water which is highly energy-exhaustive and cost-ineffective. Moreover, these carbonates are partially soluble in water and cannot be completely removed from the drinking water using such methods [15].

Ion-exchange process involves the use of cation and anion-exchange resins. Cation- and anion exchangers can be separately used to selectively remove divalent cations (Mg^{2+} and Ca^{2+}) and anions like sulphate and dissolved organic matter (DOM). In strong-basic-anion exchangers, ammonium ions are fixed with the matrix polymer and exchangeable anions are bound to them. The anion exchangers are capable for selective removal of unwanted anions such as SO_4^{-2} and dissolved organic particles from the drinking water. Strong acidic cation exchangers have fixed functional groups of sulphonic acid (fixed negative charge) and exchangeable cations are attached to these. Such a cation exchanger has a high affinity for divalent cations like calcium and magnesium ions, which are readily removed from the feed water [16]. Electrodialysis, electrode ionization and capacitive deionization (CDI) are better techniques for water softening. CDI is an older technique than EDI and does not use any expensive equipment like IEX membranes and high-pressure pumps. It uses high capacity porous carbon electrodes; when the voltage is applied, cations are adsorbed on the cathode and anions are adsorbed on the anode. The main advantages of CDI are its low-cost and small energy requirements. CDI can easily remove ~80% of Mg^{2+} and Ca^{2+} from a solution [17]. CDI stacks can also be made using alternate stacking of electrodes, just like IEX membranes in ED and EDI to increase treatment capacity.

As compared to calcium, magnesium is abundant in seawater and constitutes about 83% of total hardness (TH) of seawater. Mg^{2+} is present in the freshwater and required for normal life. Its deficiency can lead to hypomagnesemia and cardiovascular diseases [18]. Mg^{2+} ions can be supplemented in the drinking water

in chloride/sulphate form but the process is expensive. An alternative and efficient approach is selective desalination of seawater to enrich Mg^{2+} in the drinking water. For this purpose, a combination of ion exchange and filtration-based approaches are used. Tang et al. [19] used a combination of ion exchange and nanofiltration (NF; filtration of water through a nanometer pore size membrane) to selectively separate Mg^{2+} and SO_4^{-2} from seawater. They first used cation exchanger to remove salts and then used NF, to obtain $MgSO_4$-rich concentrate solution produced at ~\$1.6 per kg of Mg^{2+} separated. Enterazi et al. [20] showed that a combination of ultrasound and ion exchange increased the efficiency of removal of Mg^{2+} and Ca^{2+}.

Water softening using zeolites is cost-effective and efficient. Zeolites are natural ion exchangers; formed of silica and alumina joined in tetrahedral geometry by oxygen links. The exchangeable ions in zeolites are silicon (Si^{4+}) and aluminium (Al^{3+}). The most commonly used types of zeolites in water softening are Linde Type A (LTA) and NaA zeolites. These have a very high efficiency to remove Mg^{2+} and Ca^{2+} simultaneously [21].

8.2.3.3   Removal of Harmful Ions

The heavy metals are released into the environment by wastewater from anthropogenic activities like mining, electroplating, nuclear facilities and various other industries. The harmful ions include silver (Ag^+), iron (Fe^{2+}), cobalt (Co^{2+}), lead (Pb^{2+}), cadmium (Cd^{2+}), copper (Cu^{2+}), zinc (Zn^{2+}), nickel (Ni^{2+}), chromium (Cr^{6+}) and arsenic (As^{3+}). These ions in industrial effluents have been studied thoroughly to be removed by ion-exchange techniques like ED and EDI. In cities with industries, the levels of these toxic ions may rise in the groundwater, if untreated or improperly treated industrial wastewater is released into the environment. In such cases, it is further required to monitor their levels in the drinking water and these are adjusted below safe limits by EDI.

Chromium and Arsenic

Chromium and arsenic are released during mining processes like smelting of ores in metallurgical industries. Both are highly carcinogenic for humans. Chromium in wastewater is found in the hexavalent form as chromate ion (CrO_4^{-2}). Chromium in such form is readily taken up by body cells because of its similarity with SO_4^{-2} and PO_4^{-3} groups. Once inside the cell, it is reduced to Cr(III). Such a trivalent Cr formed by the reduction of Cr(VI) can cause heavy DNA damage, which induces apoptosis. It also causes many types of cancers including lung, skin, stomach, renal, bladder, genital, prostate, and brain cancers. The safe limit of Cr in drinking water is 50 parts per billion (ppb) [22]. As ED and EDI efficiently remove ions from water, their use for chromium removal has been well studied and established. Alvarado et al. demonstrated the removal of Cr(VI) from water with >98.5% efficiency using

continuous EDI [23]. Similarly, in another study, mixed resin bed EDI removed 99.8% of Cr(VI) from water [24].

Arsenic can cause skin, kidney, bladder, lung and liver cancer, depending upon the route of uptake. Arsenic exists as As(III) and As(V) forms and their safe levels in drinking water are 50 and 10 μg/L, respectively [25]. The removal of arsenic using electrodialysis and electrodeionization has been described and EDI followed by electrocoagulation (EC; coagulation of arsenic in the form of iron arsenate) showed maximum removal efficiency (As levels below detectable limit) [26].

Divalent Heavy Metals

Heavy metals as Zn^{2+}, Cu^{2+}, Fe^{2+}, etc. are essential for life but in trace quantities. Their levels in the drinking water higher than the safe limit are toxic to human. Electrodeionization is the best technique to be used for the removal of small quantities of such ions from water. More than 99% Co^{2+}, Cr^{3+}, Ag^+ and Fe^{2+} ions are removed by using continuous electrodeionization (CEDI) method [27]. Similarly, Souilah et al. described the removal of Zn^{2+}, Cu^{2+}, Cd^{2+} and Pb^{2+} by ED and EDI, and showed that maximum removal was obtained using IEX resins in EDI [28].

In another study, divalent ions like Pb^{2+}, Cd^{2+}, Cu^{2+} and Zn^{2+} were separated from diluted solutions using CEDI and their separation efficiencies were in the order: $Pb^{2+} \gg Cd^{2+} > Cu^{2+} \geq Zn^{2+}$. The high removal of Pb^{2+} was due to its high affinity with the IEX membranes and resin [29]. Ni^{2+} was removed with an efficiency of 99.8% by a combination of EDI and electrocoagulation [30]. In another study, nickel levels were reduced from 100 mg/L to <0.1 mg/L by EDI with IEX resin [31]. In an EDI without IEX membranes, porous ion-conducting polymer sheets have been proven to carry out EDI efficiently. This process was used to remove Co^{2+} from a water sample containing 300 mg/L Co^{2+}, to a concentration of <0.1 mg/L [32].

Removal of Other Ions

Ammonium ions (NH_4^+) present in natural groundwater have been removed by EDI to very low concentrations (1 ppm after treatment of 200 ppm solution) [33]. Boron is also an essential nutrient for our body but its safe limit is 2.4 mg/L, beyond this limit, it is toxic [34]. Boron is present in the form of boric acid (H_3BO_3) which forms borate ions ($B(OH)_4^-$) in solution. Boron is in high concentration in seawater and is efficiently removed from all types of feed water using EDI and CEDI. The use of ion exchange in combination with an RO system for efficient removal of boron has been described and successfully implemented on an industrial scale [13]. In addition, EDI was also used for boron and silicon removal from ultrapure water [35]. Nitrate is present in high amount in many water samples. Its safe level in drinking water is 50 mg/L. El Midaoui et al. optimized IEX membranes and ED conditions for nitrate removal. Their selected anion-exchange membrane removed anions in the order: $NO_3^- > Cl^- > HCO_3^- > SO_4^{-2}$[36].

8.2.3.4   Removal of Organic Contaminants

In surface and ground waters, biological activities combined with weathering and geological activity, give rise to a complex matrix of organic substances (macro- or micromolecules) in the water, which is called natural organic matter (NOM). NOM has soluble and insoluble substances called particulate (suspended) organic matter and dissolved organic matter (DOM). NOM is removed from drinking water because of its bad odour, taste and colour. Particulate NOM is easy to remove by distillation, coagulation, etc. DOM cannot be efficiently removed by membrane distillation techniques like RO, NF etc., because it causes fouling of membranes and can also react with other chemicals used during chemical treatment of water [37, 38].

DOM is separable from water using an anion exchanger because most of the DOM components are organic acids and peptides, which are negatively charged in solution form. Due to the high constituent organic carbon molecules, it is sometimes referred to as dissolved organic carbon (DOC). Research has indicated that the removal of DOM is the same in anion exchange and combined anion/cation-exchange treatment of DOM [16]. However, combined techniques are beneficial in the removal of multiple substances in a single run. Therefore, a combined magnetic and ion-exchange treatment is used for maximum removal of DOM and hardness, which are the two main parameters of drinking water to be maintained. For this purpose, magnetic ion-exchange resin MIEX® is used, which is a strong anion-exchange resin supplemented with magnetic iron oxide particles that are present in its core. These magnetic particles enable fast and efficient separation and recycling in a continuous run. Using MIEX in a combined ion-exchange treatment to impair water (containing DOM and hardness), 70% DOM (as DOC) was removed along with >55% hardness (as total hardness/TH) [39]. In another study, combined MIEX and cation-exchange treatment provided 76% DOC removal and 97% TH removal from groundwater samples [40]. This shows the potential application of combined MIEX treatment before membrane distillation processes such RO, NF etc., because DOM and hardness cations are the main reason of membrane fouling and subsequent efficiency downfall of these techniques.

8.2.4   Applications in Nonalcoholic Beverages

In nonalcoholic beverages such as fruit juices and soft drinks, ion exchange has a major role in pH control by deacidification (removal of acid). Fruit juices mainly consist of small molecules like sugars, organic acids, salts, vitamins and large molecules like cellulose and pectin. The large molecules are removed for clarification of juice by enzyme treatment and filtration. However, the small molecules like acids cannot be controlled easily by microfiltration or ultrafiltration. The acid content of the juice affects its pH and consequently its aroma and flavour. Ion-exchange membranes provide an easy solution for the removal of acids by electrodialytic techniques. Ion-exchange resins, on the other hand, are not suitable because the matrix of resin

Table 8.1 Applications of IEX in beverages

Beverage industry	Application	Major ions to be removed	Technology used
Water	Water desalination	Na^+, K^+, Ca^{2+}, Mg^{2+}, CO_3^{2-}, HCO_3^-, Cl^-, SO_4^{-2}, NO_3^-	CDI, ED, EDI, CEDI, RO + EDI, EDI + NF
	Removal of heavy metals	silver (Ag^+), iron (Fe^{2+}), cobalt (Co^{2+}), lead (Pb^{2+}), cadmium (Cd^{2+}), copper (Cu^{2+}), zinc (Zn^{2+}), nickel (Ni^{2+}), chromium (Cr^{6+}), arsenic (As)	ED, EDI, CEDI, EDI + Electrocoagulation (EC)
	Removal of other ions	$B(OH)_4^-$, NH_4^+, NO_3^-	EDI
	Removal of dissolved organic matter (DOM)	Organic acids, peptides, sugars	CEDI, MIEX
Fruit juice	Deacidification of fruit juice	Organic acids	ED, EDBM, ED + UF
Winery	Adsorption of wine proteins	Proteins	IEX resin
	Deacidification	Organic acids, tartrate	ED, IEX resin
	Removal of ions	Fe^{3+}, Cu^{2+}, Zn^{2+}	ED, IEX resin

can trap all types of particles in the juice, causing adverse effects on juice quality (Table 8.1).

8.2.4.1   Deacidification of Fruit Juices

Many fruit juices like pineapple, apple and passion fruit are acidic and cause a bitter or sour taste not appropriate for ready consumption. Juices of orange, lemon and pineapple are highly acidic. The sour or sweet taste in the juice comes from the acids and sugars, measured as the ratio of soluble sugars to acids called as Brix/acid ratio. A high Brix/acid ratio is desirable in the industrial production of the juice, which means the acid and the sourness of the juice are less [41]. The acidity of juices is because of organic acids like citric, malic and tartaric acids.

Conventional electrodialysis with a cation and anion-exchange membranes has been proven to be successful in lowering the acidity of many fruit juices. Vera et al. [42, 43] demonstrated the deacidification of four tropical fruit juices (passion fruit, castilla mulberry, najanrilla and araza) using ED. They also used ED configurations

with bipolar membranes (BM) efficiently deacidify fruit juices. In a separate study, orange juice was demonstrated to be 60–70% deacidified by ED combined with ultrafiltration (UF). It was also shown that other important nutrients like vitamin C, flavonoids and free sugar were minimally changed [44].

Bipolar membranes (BMs) are two homopolar (cation- and anion exchange) membranes joined together to form a single membrane. BMs allow only the passage of H^+ and OH^- ions while retaining all other ions in their compartments. This allows the flow of these ions to the concentrate cells. Hence, the fruit juice in the diluate cell gets lower acidity. The use of BMs allows the acids to be produced, which are removed from the juice. This process is used in the production of organic acids.

Vera et al. have studied various ED configurations for deacidification of passion fruit juice. They concluded that ED with bipolar membranes (EDBM) was better because of its simultaneous production of organic acids. EDBM was also beneficial because of its continuous running without reagent addition. The pH of passion fruit was efficiently brought to 4.5 [45–47]. Rozoy et al. used EDBM and deacidified cranberry juice by 22.84%. They also extracted organic acids (citric, malic and quinic acid) up to 25%. This efficiency can be increased by increasing the number of membrane stacks in the cell [48]. Similarly, Serre et al. studied various modifications of ED and found the best results from bipolar and anion-exchange membranes (ED2BM). ED2BM gave 40% deacidification with the recovery of pure and mixed acids [49]. The major benefit of this technique is its sustainability and no waste generation because the separated organic acids were used for other applications.

8.2.5   Applications in Alcoholic Beverages

Alcoholic beverages are all products of fermentation and contain alcohols along with some organic acids and phenols. All of these forming ions in the aqueous solution can be subjected to ion exchange. In alcoholic beverages, IEX materials are applied to remove ions for pH, taste and colour control. Although the application of ion exchange is dependent upon the type of alcoholic drink, the fundamental principle of ion exchange is the same.

8.2.5.1   Beverage de-Alcoholization

Recently, there has been a rise in the global demand for alcohol-free drinks that still have the same flavour and aroma, following better lifestyle to avoid the side effects of alcohol. For this purpose, beer or wine are subjected to the removal of alcohol to get an alcohol-free beer (0.05–1.2% alcohol) or wine (7%). In de-alcoholization, membrane-based technologies like reverse osmosis (RO), nanofiltration (NF), dialysis, etc. are used. The choice of the membrane for a given process is situational. Cellulose acetate membranes have been mostly used in RO for beer de-alcoholization and polyamide membranes were mostly used in NF [50].

8.2.5.2 Ion Removal and deacidification

Wine contains many salts, out of which tartrate/tartaric acid is an important one. Tartrate ions exist in the wine in their potassium and calcium salts; if untreated, these form precipitates in wine bottles. There are many preventive strategies for this; electrodialysis and ion-exchange resins are used for the removal of tartrate. Both cation-exchange and anion-exchange resins are employed at controlled pH for the removal of these ions. This has also been referred to as deacidification of wine, as the process removes most of the acid ions [51, 52].

An important aspect of wine stabilization is that it can suffer from oxidative degradation over time. As a result, continuous browning, condensation of polyphenols and loss of aromatic freshness occur. This is due to substances that can oxidize others, most importantly iron (Fe^{3+}) and copper (Cu^{2+}). Ion-exchange resins were used to treat wine to chelate such metallic ions. One chelating resin for this purpose is FEC-1, which has high selectivity for iron removal [53].

8.2.5.3 Adsorption of Wine Proteins

The production of quality product in the young white and rose wine production requires removal of proteins. Ion-exchange resins have been successfully applied to remove proteins from wine by using macroporous resins Macro-Prep™ 50S and Streamline® SP as adsorbing agents [54].

8.3 Conclusions

- One of the major industries in the world is the beverage industry because of the high consumption of canned and bottled beverages including bottled drinking water, alcoholic drinks, fruit juices and energy drinks. In all of these beverage industries, ion exchange plays a crucial role at some point in their processing line.
- Water treatment is the most widespread industrial application of ion-exchange chromatography. Water is subjected to an ion-exchange process to remove excess salts and harmful ions by ion-exchange membranes and resins.
- Ion-exchange membranes are stacked in an electrolytic cell, parallel to electrode plates in electrodialysis (ED). Electrodialysis efficiently desalinates brackish water.
- Ion-exchange resin is filled between the anion and cation-exchange membranes, in diluate compartment of ED to perform electrodeionization (EDI), which is more efficient for ion removal than conventional ED. Several modifications of EDI have been proposed in several beverage industries like continuous electrodeionization (CEDI) and resin-wafer electrode ionization (RW-EDI).

- Combinations of ED/EDI with membrane-based filtration technologies like reverse osmosis (RO) and nanofiltration (NF) have proved to be efficient in seawater desalination.
- Fruit juices and soft drinks have been treated with electrodialysis to remove excess acids like citric acid in lemon/orange juice and malic acid in apple juice.
- Alcoholic drinks like wine have been de-alcoholized by ion-exchange resins to produce 'nonalcoholic' or 'de-alcoholized' drinks. Wine contains excess tartaric acid, which hasbeen removed by ion exchange. Excess wine proteins have also removable by using ion-exchange resins.

References

1. Zagorodni AA (2006) Ion exchange materials: properties and applications. Elsevier, Amsterdam
2. Ghaffour N, Bundschuh J, Mahmoudi H, Goosen MF (2015) Renewable energy-driven desalination technologies: a comprehensive review on challenges and potential applications of integrated systems. Desalination 356:94–114
3. Zheng X-Y, Pan S-Y, Tseng P-C, Zheng H-L, Chiang P-C (2018) Optimization of resin wafer electrodeionization for brackish water desalination. Sep Purif Technol 194:346–354
4. Alvarado L, Chen A (2014) Electrodeionization: principles, strategies and applications. Electrochim Acta 132:583–597
5. Lopez AM, Williams M, Paiva M, Demydov D, Do TD, Fairey JL, Lin YJ, Hestekin JA (2017) Potential of electrodialytic techniques in brackish desalination and recovery of industrial process water for reuse. Desalination 409:108–114
6. Voutchkov N (2018) Energy use for membrane seawater desalination—current status and trends. Desalination 431:2–14
7. Strathmann H (2010) Electrodialysis, a mature technology with a multitude of new applications. Desalination 264(3):268–288
8. Singh R, Hankins N (2016) Emerging membrane technology for sustainable water treatment. Elsevier, Amsterdam
9. Etzel JE, Wachinski (1997) AM environmental ion exchange: principles and design. In: IWA leading-edge conference on water and wastewater treatment technologies. CRC Press LLC, Boca Raton, Florida
10. Arar Ö, Yüksel Ü, Kabay N, Yüksel M (2014) Demineralization of geothermal water reverse osmosis (RO) permeate by electrodeionization (EDI) with mixed bed configuration. Desalination 342:23–28
11. Pan S-Y, Snyder SW, Ma H-W, Lin YJ, Chiang P-C (2017) Development of a resin wafer electrodeionization process for impaired water desalination with high energy efficiency and productivity. ACS Sustain Chem Eng 5(4):2942–2948
12. Pan S-Y, Snyder SW, Ma H-W, Lin YJ, Chiang P-C (2018) Energy-efficient resin wafer electrodeionization for impaired water reclamation. J Clean Prod 174:1464–1474
13. Jacob C (2007) Seawater desalination: boron removal by ion exchange technology. Desalination 205(1–3):47–52
14. Bellizzi V, DeNicola L, Minutolo R, Russo D, Cianciaruso B, Andreucci M, Conte G, Andreucci V (1999) Effects of water hardness on urinary risk factors for kidney stones in patients with idiopathic nephrolithiasis. Nephron 81(Suppl. 1):66–70
15. Yildiz E, Nuhoglu A, Keskinler B, Akay G, Farizoglu B (2003) Water softening in a crossflow membrane reactor. Desalination 159(2):139–152
16. Indarawis KA, Boyer TH (2013) Superposition of anion and cation exchange for removal of natural water ions. Sep Purif Technol 118:112–119

17. Seo S-J, Jeon H, Lee JK, Kim G-Y, Park D, Nojima H, Lee J, Moon S-H (2010) Investigation on removal of hardness ions by capacitive deionization (CDI) for water softening applications. Water Res 44(7):2267–2275

18. Del Gobbo LC, Imamura F, Wu JH, de Oliveira Otto MC, Chiuve SE, Mozaffarian D (2013) Circulating and dietary magnesium and risk of cardiovascular disease: a systematic review and meta-analysis of prospective studies–. Am J Clin Nutr 98(1):160–173

19. Tang SC, Birnhack L, Cohen Y, Lahav O (2018) Selective separation of divalent ions from seawater using an integrated ion-exchange/nanofiltration approach. Chem Eng Processing Process

20. Entezari MH, Tahmasbi M (2009) Water softening by combination of ultrasound and ion exchange. Ultrason Sonochem 16(3):356–360

21. Xue Z, Li Z, Ma J, Bai X, Kang Y, Hao W, Li R (2014) Effective removal of Mg^{2+} and Ca^{2+} ions by mesoporous LTA zeolite. Desalination 341:10–18

22. Costa M, Klein CB (2006) Toxicity and carcinogenicity of chromium compounds in humans. Crit Rev Toxicol 36(2):155–163

23. Alvarado L, Ramírez A, Rodríguez-Torres I (2009) Cr (VI) removal by continuous electrodeionization: study of its basic technologies. Desalination 249(1):423–428

24. Alvarado L, Torres IR, Chen A (2013) Integration of ion exchange and electrodeionization as a new approach for the continuous treatment of hexavalent chromium wastewater. Sep Purif Technol 105:55–62

25. Morales KH, Ryan L, Kuo T-L, Wu M-M, Chen C-J (2000) Risk of internal cancers from arsenic in drinking water. Environ Health Perspect 108(7):655

26. Basha CA, Selvi SJ, Ramasamy E, Chellammal S (2008) Removal of arsenic and sulphate from the copper smelting industrial effluent. Chem Eng J 141(1–3):89–98

27. Yeon K-H, Song J-H, Moon S-H (2004) A study on stack configuration of continuous electrodeionization for removal of heavy metal ions from the primary coolant of a nuclear power plant. Water Res 38(7):1911–1921

28. Souilah O, Akretche D, Amara M (2004) Water reuse of an industrial effluent by means of electrodeionisation. Desalination 167:49–54

29. Smara A, Delimi R, Chainet E, Sandeaux J (2007) Removal of heavy metals from diluted mixtures by a hybrid ion-exchange/electrodialysis process. Sep Purif Technol 57(1):103–110

30. Dermentzis K, Christoforidis A, Valsamidou E (2011) Removal of nickel, copper, zinc and chromium from synthetic and industrial wastewater by electrocoagulation. Int J Environ Sci 1(5):697

31. Dermentzis K (2010) Removal of nickel from electroplating rinse waters using electrostatic shielding electrodialysis/electrodeionization. J Hazard Mater 173(1–3):647–652

32. Dermentzis K, Davidis A, Dermentzi A, Chatzichristou C (2010) An electrostatic shielding-based coupled electrodialysis/electrodeionization process for removal of cobalt ions from aqueous solutions. Water Sci Technol 62(8):1947–1953

33. Spiegel E, Thompson P, Helden D, Doan H, Gaspar D, Zanapalidou H (1999) Investigation of an electrodeionization system for the removal of low concentrations of ammonium ions. Desalination 123(1):85–92

34. Alharati A, Swesi Y, Fiaty K, Charcosset C (2017) Boron removal in water using a hybrid membrane process of ion exchange resin and microfiltration without continuous resin addition. J Water Process Eng 17:32–39

35. Wen R, Deng S, Zhang Y (2005) The removal of silicon and boron from ultra-pure water by electrodeionization. Desalination 181(1–3):153–159

36. El Midaoui A, Elhannouni F, Taky M, Chay L, Sahli MAM, Echihabi L, Hafsi M (2002) Optimization of nitrate removal operation from ground water by electrodialysis. Sep Purif Technol 29(3):235–244

37. Sillanpää M, Ncibi MC, Matilainen A, Vepsäläinen M (2018) Removal of natural organic matter in drinking water treatment by coagulation: a comprehensive review. Chemosphere 190:54–71

38. Levchuk I, Márquez JJR, Sillanpää M (2017) Removal of natural organic matter (NOM) from water by ion exchange—a review. Chemosphere

39. Apell JN, Boyer TH (2010) Combined ion exchange treatment for removal of dissolved organic matter and hardness. Water Res 44(8):2419–2430
40. Comstock SE, Boyer TH (2014) Combined magnetic ion exchange and cation exchange for removal of DOC and hardness. Chem Eng J 241:366–375
41. Bhattacharjee C, Saxena V, Dutta S (2017) Fruit juice processing using membrane technology: a review. Innovative Food Sci Emerg Technol 43:136–153
42. Vera E, Sandeaux J, Persin F, Pourcelly G, Dornier M, Ruales J (2007) Deacidification of clarified tropical fruit juices by electrodialysis. Part I. Influence of operating conditions on the process performances. J Food Eng 78(4):1427–1438
43. Vera E, Sandeaux J, Persin F, Pourcelly G, Dornier M, Piombo G, Ruales J (2007) Deacidification of clarified tropical fruit juices by electrodialysis. Part II. Characteristics of the deacidified juices. J Food Eng 78(4):1439–1445
44. Kang YJ, Rhee KC (2002) Deacidification of mandarin orange juice by electrodialysis combined with ultrafiltration. Nutraceuticals Food 7(4):411–416
45. Vera E, Ruales J, Dornier M, Sandeaux J, Persin F, Pourcelly G, Vaillant F, Reynes M (2003) Comparison of different methods for deacidification of clarified passion fruit juice. J Food Eng 59(4):361–367
46. Vera E, Ruales J, Dornier M, Sandeaux J, Sandeaux R, Pourcelly G (2003) Deacidification of clarified passion fruit juice using different configurations of electrodialysis. J Chem Technol Biotechnol 78(8):918–925
47. Vera E, Sandeaux J, Persin F, Pourcelly G, Dornier M, Ruales J (2009) Deacidification of passion fruit juice by electrodialysis with bipolar membrane after different pretreatments. J Food Eng 90(1):67–73
48. Rozoy E, Boudesocque L, Bazinet L (2015) Deacidification of cranberry juice by electrodialysis with bipolar membranes. J Agric Food Chem 63(2):642–651
49. Serre E, Rozoy E, Pedneault K, Lacour S, Bazinet L (2016) Deacidification of cranberry juice by electrodialysis: impact of membrane types and configurations on acid migration and juice physicochemical characteristics. Sep Purif Technol 163:228–237
50. Mangindaan D, Khoiruddin K, Wenten I (2017) Beverage dealcoholization processes: past, present, and future. Trends Food Sci Technol
51. Ibeas V, Correia AC, Jordão AM (2015) Wine tartrate stabilization by different levels of cation exchange resin treatments: impact on chemical composition, phenolic profile and organoleptic properties of red wines. Food Res Int 69:364–372
52. Lasanta C, Caro I, Pérez L (2013) The influence of cation exchange treatment on the final characteristics of red wines. Food Chem 138(2–3):1072–1078
53. Palacios V, Caro I, Pérez L (2001) Application of ion exchange techniques to industrial process of metal ions removal from wine. Adsorption 7(2):131–138
54. Sarmento M, Oliveira J, Slatner M, Boulton R (1999) Kinetics of the adsorption of bovine serum albumin contained in a model wine solution by non-swelling ion-exchange resins. J Food Eng 39(1):65–71

Chapter 9
Ion Exchange Resin Technology in Recovery of Precious and Noble Metals

A. Mohebbi, A. Abolghasemi Mahani and A. Izadi

Abstract Ion exchange technology has received outstanding attention in a wide variety of industries, including water treatment, pharmaceuticals, petrochemicals and hydrometallurgy due to its fast and high-efficiency operations. In hydrometallurgical applications, ion exchange resins have been used increasingly for the recovery and purification of metal pregnant solutions or for effluent treatment. This chapter devoted to an integrated evaluation of the present uses and future developments of the ion exchange resins in extraction and recovery of precious and noble metals including gold, silver, copper, uranium and iron. A detailed discussion about the recent advances of the ion exchange technique in metal recovery from their pregnant solutions is also presented from the aspects of anion metal adsorption on the resins and metal-loaded resin elution. Besides comprehensive overview about the effectiveness of surface modified resins, the major limitations of the resin adsorption techniques are pointed out.

Abbreviation

1EDA	1-ethylenediamine
aAEP	1-(2-aminoethyl) piperazine
BV	Bed volume
CMP	Chemical and mechanical polishing
CPU	Central processing units
DMA	Dimethylamine
DVB	Divinylbenzene
EPA	U.S. Environmental Protection Agency

A. Mohebbi (✉) · A. Izadi
Department of Chemical Engineering, Faculty of Engineering, Shahid Bahonar University of Kerman, Kerman, Iran
e-mail: amohebbi@uk.ac.ir

A. Abolghasemi Mahani
Faculty of Engineering, School of Chemical Engineering, University of Tehran, P. O. Box: 11365/4563, Tehran, Iran

EW   Electrowinning
IEX   Ion exchange
IEXRs   Ion exchange resins
MAs   Mixed amines
PAGs   Polyamine groups
PIN   Pin contact elements
PMLS   Precious metals
QA   Quaternary ammonium
QABs   Quaternary amino groups
QAGs   Quaternary amine groups
RIP   Resin in pulp
RIS   Resin in solution
SAGs   Secondary amino groups
st-DVB Polystyrene crosslinked with divinylbenzene
SX-EW   Solvent extraction-Electrowinning
TAGs   Tertiary amino groups
TEPA   Tetraethylenepentamine
VBC   Vinylbenzylchloride
WB   Weak base resin
WEEE   Wasted electronics and electronic equipment

9.1 Introduction

During the last century with the evolutional development of human society and technology, precious metals (PMLs) gradually received special attention in engineering areas outside of their traditional applications due to their excellent physical, chemical and mechanical properties. Hence, increasing demand of PMLs (i.e. Au, Ag, U, Cu and Fe) in special areas such as catalyst, electronics, pharmaceutical as well as their value has led to an increased interest in development of cost-effective processes of their refining (extraction from ores), separation and purifications [1–3]. Solvent (chemical) extraction technique is a general method for extraction of PMLs from their ores and electronic wastes. This method of extraction is no longer considered as an efficient way in terms of the operation time, the degree of separation and the yields, since PMLs naturally exist only in small amounts in the ores and these should be recovered effectively from their natural and secondary resources. In this regard, to overcome the aforementioned disadvantages, special efforts have been made to replace traditional refining methods with an advanced technique [4–7].

Adsorption in porous systems is an efficient physical method for extraction and removal of PMLs from minerals and waste solutions. Ion exchange resins (IEXRs), as well as activated carbon, are two classes of porous media that are currently used in separation industries. Higher metal ion loading capacity, elimination of thermal regeneration, less prone to fouling by organic materials and higher loading rates are

Table 9.1 The ion exchange resin operation conditions for different pulp/liquors systems [8]

Category	Operation condition
The resin in solution (RIS)	Fixed bed contactor: solutions containing solids of less than 50 mg/L Fluidized bed contactor: solutions containing solids less than 1000 mg/L (i.e. dirty solutions)
Resin in pulp (RIP)	Continuous contactor: solutions containing 30–50% solids (i.e. dirty solutions)

some noticeable advantages of IEXRs over the activated carbon [8]. IEXRs are composed of the polymeric matrix as an inert backbone and selective functional groups. The resins backbone can be either of gel or a macroporous-type structure. Functional groups that are attached to the backbone and located throughout the resin bead interact with ions in solution. This type of material is widely used in hydrometallurgy, especially for the separation of PMLs and noble metal ions from various solutions. The porous nature of the resin results in improved adsorption rates due to the enhanced diffusivity of ions. In total, macroporous resins have lower capacities than gel resins but this type of resins are more commonly used in hydrometallurgical applications, due to their improved resistance to mechanical and osmotic shock, although gel resins can be used for niche applications [9–13]. IEXRs can be employed to recover metal from liquors or pulps with a wide range of solids content. As presented in Table 9.1, the solid content of the resultant pulp/liquor indicates the choice of ion exchange operation conditions (Table 9.1) [8].

Resin in solution (RIS) process, production of a clear solution with low suspended solids is essential when employing fixed bed contactors. In such operational conditions, a bed of resin acts as an efficient filter resulting in accumulation of any presented solids in the feed and formation of a thick layer of solids on top of it, which this layer of solids results in increased pressure drop across the bed, making it difficult to pump the solution through it. Alternatively, the valuable metal can be recovered directly from leach pulp, via a so-called process of resin in pulp (RIP). This type of operation is advantageous in case of low-grade ores, which are economically very sensitive, or in cases where liquid–solid separation is difficult and costly. In this manner, resin and pulp are contacted counter-currently in a series of agitated contactors. The loaded resin is separated from the pulp over screens, washed and transferred to the elution section. Finally, the eluted resin is returned to the adsorption circuit [14, 15]. High capacity, fast reaction kinetics, efficient elution and service life durability are some important criteria for choosing the best resin for a specific application. The efficiency of the removal process is also strongly dependent on the process (i.e. pH of the solution, ion concentration and contact time) and the ion exchange/coordination resin properties (i.e. swelling, crosslinking degree, type and structure of the ligand) [16–19].

In this chapter, recent advances in the recovery of precious and frequently used noble metals including gold, silver, copper, uranium and iron by ion exchange (IEX)

technique from their ores and their corresponding leach solutions are presented in detail. The advantages and disadvantages of IEXRs in adsorption and the elution principles of metal-loaded resins are indicated. At the end, a relatively comprehensive summary of the existing problems of the resin adsorption technique is outlined.

9.2 Recovery of Metals from Their Pregnant Solutions

9.2.1 Gold

Over the last several years, development of advanced techniques for cost-effective recovery of gold has been the topic of concentration in many studies. The demand for industrial use of gold has increased (around 350–400 tonnes in recent years) in ornaments, medicine, aerospace and electronic (as gold plated circuit boards) due to its excellent electrical conductivity and high chemical stability [20–23]. Under ordinary conditions, gold is inactive to the oxidation reactions and classified as a noble metal. Although gold as the noble metal is available in its native state (free milling), complex ores such as sulfide and carbonaceous refractory ores as well as electronic waste recycle materials are the main natural and secondary sources of this noble metal, respectively [24–26]. Precipitation, ion exchange, solvent extraction and flotation are some known general methods for recovery and extraction of gold. These methods of recovery are associated with some advantages and disadvantage and choosing an appropriate method as optimal technique usually depends on stone cutie, the presence of foreign metal ions and type of ores [27–31].

From the literature, it can be understood that compared with the above-mentioned techniques, resin adsorption stands out as the most promising technique in gold recovery owing to its fast adsorption, high loading capacity, simultaneous elution and regeneration and an ambient temperature operation [32, 33]. It is well known that gold recovery efficiency is strongly dependent on physical and chemical properties of the resins. The degree of crosslinking and swelling, type and structure of introduced functional groups as well as sorption conditions (i.e. pH of the solution, contact time, the quantity of the resin and type and concentration of blast and metal ions) are the main features influencing the adsorption ability of gold from its pregnant solutions [17, 33, 34]. The ion exchange resin can be used to recover gold from its pregnant solutions through the reversible ion exchange reactions between the counter ions in the resins and gold complex in the solutions. Depending on the gold pregnant solution, gold exists predominantly in two different oxidation states (anion forms) of $[Au]^-$ and $[Au]^{3-}$ and the resins used in gold recovery are all weak, medium and strong base anion exchange resins [28, 32, 35].

Cyanidation is the most commonly used method for the recovery of gold from its ores. Generally, the dissolution of gold is carried out in a solution containing 0.03–0.1% $(CN)^-$ with a pH greater than 10 and aeration to keep the solution saturated with oxygen [36]. Gold extraction efficiency in cyanidation technique is typically

90%, even in ores containing low gold contents (2 ppm). From a thermodynamic point of view, in the gold–water–cyanide–oxygen system, the $[Au(CN_2)]^-$ complex is the equilibrium form of gold in cyanide system and can be stable in a wide range of pH values varying from 2 to 12. The overall reaction for gold dissolution in aqueous alkaline cyanide solution and the formation of gold (I) complex is proposed by Elsner equation and presented as follows (9.1) [37]:

$$4Au + 8CN^- + O_2 + 2H_2O = 4[Au(CN)_2]^- + 4OH^- \tag{9.1}$$

where oxygen and cyanide ion act as oxidant and ligand, respectively.

More recent progress in the development of gold extraction from cyanide solution indicates that compared with the traditional techniques, ion exchange method is a promising alternative to efficient recovery of this valuable metal. The permanent positive charge of quaternary functional group in strong base IEXRs poses to extract cyanide anions by an ion exchange reaction (9.2) [37].

$$\left|-^+NR_3X^- + Au(CN)_2^- \rightleftharpoons\right| - {}^+NR_3Au(CN)_2^- + X^- \tag{9.2}$$

The complex metal cyanide on the resin can be eluted by either conversion of the metal ions to cationic complex (by using thiourea) or by ion exchange method to force movement of equilibrium, depicted in (9.2), to the left-hand side by an increase in the concentration of X^-. On the contrary, in weak base resins, which contain primary, secondary, or ternary amine function, ion exchange properties are governed by pH value and adsorption of aurocyanide is favourable to be processed under acidic condition. On the other hand, loading capacity of weak base resins is strongly pH dependent and increases with increasing the acidity of the solution. In fact in acidic solution, weak base resins are protonated and behave like strong base resins. Mechanisms of protonation and recovery of gold from acidic cyanide pregnant solution are presented in (9.3) and (9.4), respectively [37].

$$\left|-NR_2 + HX \rightleftharpoons\right| - {}^+NR_2HX^- \tag{9.3}$$

$$\left|-^+NR_2HX^- + Au(CN)_2^- \rightleftharpoons\right| -^+ NR_2HAu(CN)_2^- + X^- \tag{9.4}$$

In an experimental design by Cromberge et al. [38], the effectiveness of both strong and weak base resins in the gold recovery of Grootvlei and Durban Roodepoort deep gold mines (a gold mine (Gauteng) in South Africa) was investigated. The results showed that rate loading of metal cyanide in both strong and weak base resins is first-order kinetic and film diffusion control mechanism of gold recovery from cyanide pregnant solution. In such operations, agitation offered a crucial effect on the rate of gold extraction and improved mixing causes to the easy recovery of metal cyanide by resins. The stability of the gold cyanide complex presents the possibility to improve gold loading uptake ability of resins by selective precipitation of base metals from gold pregnant solution. The stability order of metals cyanide complexes, which are
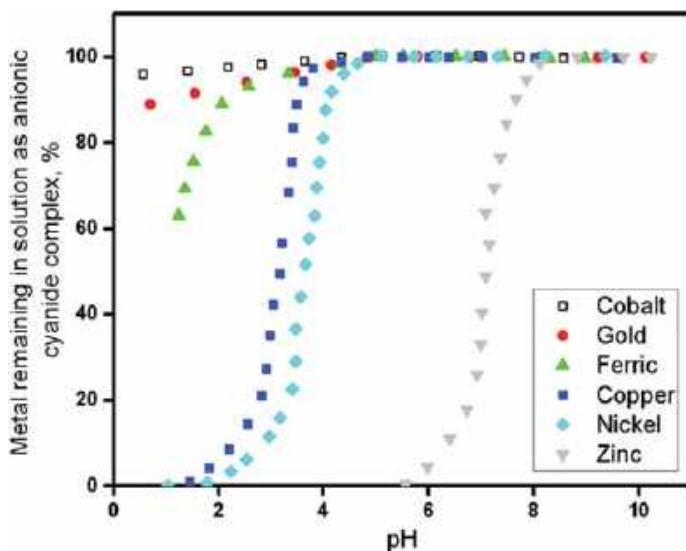
Fig. 9.1 Effect of solution pH on stability of various anion metal cyanide complexes in an aqueous solution [38]

commonly found in gold pregnant solution and compete with gold cyanide was $Co(CN)_6^{3-} > Au(CN)_2^- > Fe(CN)_6^{3-} > Ni(CN)_4^{2-} > Cu(CN)_4^{3-} > Zn(CN)_4^{2-}$. As shown in Fig. 9.1, at pH value ranges of 3–6, the zinc, nickel and copper cyanide complexes break down to form insoluble neutral cyanide species, which can improve resin selectivity in the gold recovery process.

It was also found that in the same conditions of the experiment, the maximum loading capacity of weak base resins was about a quarter of the maximum loading capacity of strong base resins (Fig. 9.2).

Depending on structural and surface functionality of weak base resins, solution pH plays a key role in ion exchange property of these types of resins. It seems that the presence of the strong base functionality within a weak base resin structure can influence exchange properties and improve its recovery performance, as happened in the case of functional groups in a strong base resin. Figure 9.3 shows the effect of strong base functionality on the equilibrium loading of aurocyanide in some commercial weak base resins. As revealed in Fig. 9.3, gold uptake capacity of resins containing strong base functionality (i.e. IRA 93, A378 and A 365) is independent of solution pH.

Table 9.2 provides the details about structural characteristics of commercially available weak-based IEXRs applied in the recovery of gold cyanide complex.

It is well known that compared with weak base resins, strong base resins have higher gold capacity in cyanide leach and are also less expensive but in the case of weak base resins, the loaded gold is eluted more rapidly and efficiently. Generally, loading capacities of weak base resins are significantly lower than those of strong
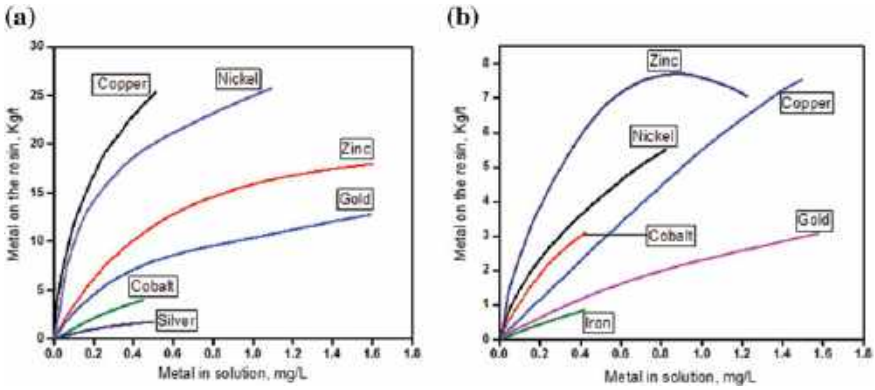
Fig. 9.2   Equilibrium loading of various metal cyanide complexes onto the strong (**a**) and weak (**b**) base resins [38]

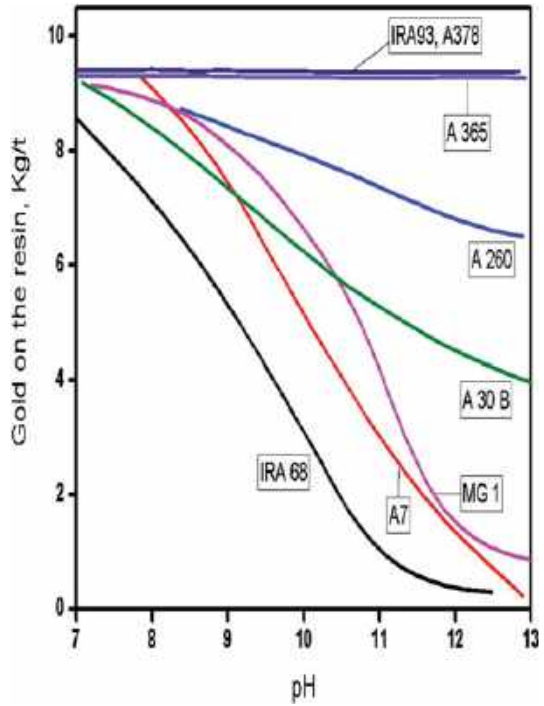**Fig. 9.3**   Effect of solution pH on the equilibrium loading of aurocyanide on various weak base ion exchange resins [38]

Table 9.2 Details of various weak base resins used in this study

Resin	Functional group	Matrix	Weak base capacity (eq/L)	Strong base capacity (eq/L)
A 365	Quaternary amine	Polystyrene	N.A	N.A
IRA93	Tertiary amine	Polystyrene-DVB	1.3	0.080
A 378	Tertiary amine	Polystyrene-DVB	1.24	0.245
A 30 B	Tertiary amine	Epoxy polyamine	1.99	0.343
IRA 68	Tertiary amine	Acrylic amine	1.57	0.038
A7	Secondary amine	Phenol formaldehyde	1.91	0.012
A260	Polyamine[a]	Aliphatic amine	2.61	0.080
MG 1	Polyamine	Acrylic-DVB	2.45	0.098

[a]A mixture of primary, secondary, tertiary and in some cases containing quaternary amine groups
N.A. Not analysis

base resins but elution process was carried out efficiently by increasing the pH of the solution. Elution ability and selective recovery of metals are highly dependent on charge density and strong base capacity of resins. In total, univalent charge stripping agents (less hydration ability) can be used to elute a large variety of metal cyanides simultaneously as one-step stripping process [18, 39, 40]. On the contrary, complexes with higher multivalent characteristic can be used for the selective recovery of metals from metal-loaded resins. In the case of two-step stripping process, strong base resins with short alkyl chain functionality are more favourable for selective elution of metals in multivalent eluent solution. As an example, trimethylamine functionalized resins have less hydrophobicity and are more favourable to hydrated divalent zinc-cyanide complex [8]. Comparing zinc-cyanide eluent with other known eluent agents (i.e. KSCN), extracted foreign metals such as iron, copper and nickel cyanides eluted faster in two-step stripping process due to the divalent charge of zinc-cyanide. The experimental results showed that the density of functional groups, as well as surface functionality, have a high impact on gold selectivity and uptake ability of weak base resins. Harris et al. [41] investigated the effect of density of functional groups on the gold sorption ability of the surface modified styrene-divinylbenzene copolymer resin with dimethylamine (DMA) as strong amino function. As evident from Fig. 9.4, in weak base copolymer resin with low content of salt splitting group (containing less than 1% DMA as a quaternary amine), gold uptake ability is strongly pH dependent and almost all gold in leach was removed from the solution with pH < 7, while above pH 7, the loading capacity of resins decreases dramatically. In a solution with pH of 10, only 20% of gold from pregnant leach was removed and at a pH of 12, the gold was readily eluted from resin. On the contrary, a weak base resin containing 16% of quaternary amine groups (resin with the high salt splitting group) behaves like
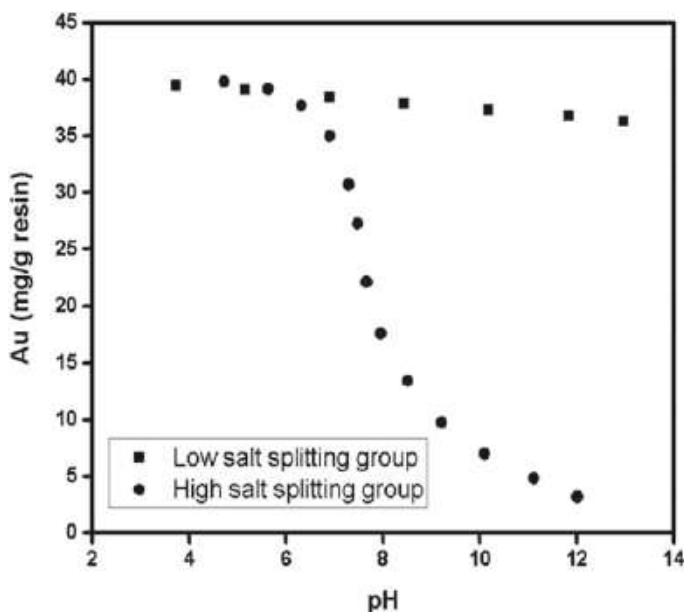
Fig. 9.4 Effect of solution pH on Au loading ability of DMA functionalized resin [41]

strong base resins. Gold uptake ability became evident over the entire pH range from 6 to 12 and elution at higher pH did not occur. At pH levels of 10–11, weak base groups are in form of none reactive free base and the presented strong base groups prefer monovalent aurocyanide groups over the multivalent base metal cyanide. In such resin structures, elution of gold cyanide was carried out efficiently with caustic soda upon increasing solution pH from 10 to 13.

Besides gold uptake ability of resin at the desired operating pH, resin selectivity for aurocyanide is another issue to be kept in mind. The competition experiments showed that (Fig. 9.5) compared with a resin containing a low content of quaternary amine, high level of salt splitting groups (i.e. 16% DMA) showed high affinity to the selective recovery of gold. For the purpose of comparison, the selectivity of activated carbon was also examined under the same condition with DMA based resin. It was found that metal uptake ability of activated carbon was about twice that of resin.

For more than a century, cyanide has been used to leach gold from ores; however, its extreme toxicity, the formation of HCN gas at low pH levels, high leaching period and inefficient leaching of refractory gold ores have been the main hindrance problems to the wide commercial application of cyanide leaching process [42, 43]. Therefore, considerable attention has been paid to the development and utilization of non-cyanide techniques. Thiosulfate leaching offered the advantages of non-toxicity, low reagent costs, fast leaching rate and high performance in treating certain refractory gold ores [44, 45]. It was found that the gold dissolution in thiosulfate was usually slow and needed to be catalyzed in the presence of Cu (II) and ammonia.
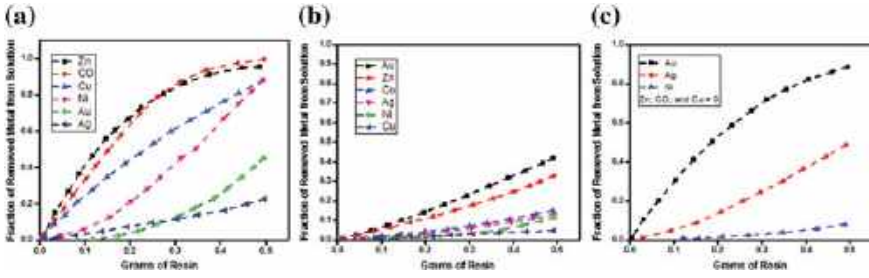
Fig. 9.5 Metal selectivity in the different adsorbents. DMA functionalized with low salt splitting group (**a**), high salt splitting group (**b**), activated carbon (**c**) [41]
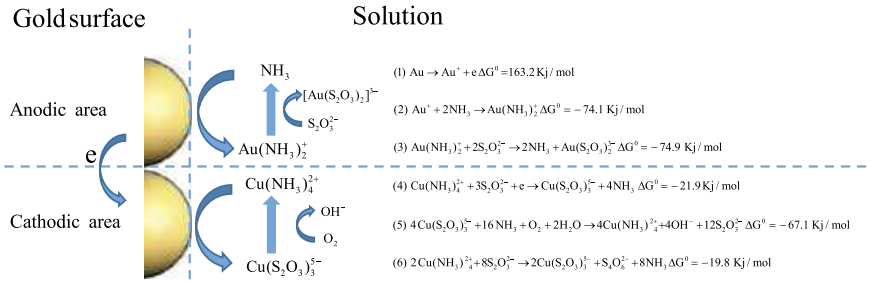

Fig. 9.6 The possible mechanism for the leaching reaction of gold in thiosulfate solution [40]

Figure 9.6 shows the possible mechanism for the leaching reaction of gold in thiosulfate solution and the formation of gold (I) thiosulfate. The principle leaching reaction is an electrochemical process involving gold oxidation and oxygen reduction at the anode and cathode, respectively [46, 47]. In the anode area, the complex is generated when NH_3 molecules move to the gold surface. NH_3 is then substituted by $S_2O_3{}^{2-}$ to form a more stable $[Au(S_2O_3)_2]^{3-}$ complex. In this situation (i.e. under alkaline condition) ammonia can not only catalyze the complex reaction between Au^+ and $S_2O_3{}^{2-}$ but also can stabilize Cu^{2+} by the generation of $[Cu(NH_3)_4]^{2+}$. In the cathodic area, the generated $[Cu(NH_3)_4]^{2+}$ complex is reduced to $[Cu(S_2O_3)_3]^{5-}$ (under dissolved oxygen) and then quickly oxidized to form $[Cu(NH_3)_4]^{2+}$. On the other hand, oxygen reduction is catalyzed by $[Cu(NH_3)_4]^{2+}$. It should be noted that although $[Cu(NH_3)_4]^{2+}$ complex acts as a catalyst to boost gold dissolution dramatically, over 18–20 times, it can also accelerate catalytic decomposition of thiosulfate due to strong oxidizing ability [40].

Weak and strong base resins are general types of IEXRs that are used in gold extraction from Thiosulfate leaching. Weak base resins are composed of primary, secondary or tertiary amine functional groups and their ion exchange properties are strongly related to the solution pH and need to be activated before using (9.5) [40].

$$-NR_2 + HX \Leftrightarrow -NR_2H^+X^- \qquad (9.5)$$

where R and X denote the amine functional group and counterions respectively that can be exchanged during activation (i.e. Cl or S elements). In weak base resins, the specific pKa for protonation is in the pH ranges of 6–8, and thus most of the weak base resins will not be protonated adequately in the common pH range of thiosulfate solutions (i.e. pH of 9–11) and also gold loading on weak base resins markedly decreases with the increase of solution pH from 8 to 11. On the other hand, adsorption of certain objective ions by strong base resins containing ammonium functional groups is not limited by protonation and it is applicable to gold recovery over a broad pH range with no need of activation. Therefore, they can be used directly to extract gold from thiosulfate leach. Equations (9.6) and (9.7) portray the adsorption mechanisms of gold (I) thiosulfate complex with weak and strong base resins, respectively [16, 40].

$$3[-NR_2H^+X^-] + [Au(S_2O_3)_2]^{3-} \Leftrightarrow [-NR_2H]_3^+[Au(S_2O_3)_2]^{3-} + 3X^- \qquad (9.6)$$

$$[-NR_3^+X^-] + [Au(S_2O_3)_2]^{3-} \Leftrightarrow [(-NR_3)_3^+[Au(S_2O_3)_2]^{3-} + 3X^- \qquad (9.7)$$

Zhang et al. [39] investigated comprehensively the gold uptake ability of a series of weak and strong base commercially available anion exchange resins. Experiments were conducted at ambient temperature with single and binary (i.e. gold and copper) solutions at pH 9. It was found that gold loading obeyed Freundlich adsorption model and the adsorption kinetics of strong base resins was fast and the equilibrium was reached within the first 5 h. The gold loading capacity of strong base resins varied from 10 to 25 kg/t (solution containing 1 ppm Au); whereas on weak base resins, it was less than 2.5 kg/t. The ion exchange ability of weak base resins was improved in solution with pH of lower than 7. Hence, these types of resins are not suitable for gold extraction from alkaline thiosulfate solutions. It seems that in strongly alkaline solutions, amino functional groups on polymer matrix tend to stay in the form of a free electron and thus their ion exchange ability is lost. Along with metal thiosulfate complexes, a range of other metal complexes including thionate and sulfur–oxygen anions may exist under industrial conditions of thiosulfate leaching. Metal anions can exert an important influence on gold adsorption ability of resins. Simultaneous adsorption of a considerable amount of foreign metal anions with gold has become a primary factor affecting gold recovery from thiosulfate solution. The affinity orders of the resin for these kinds of competitive anions solution were $[Au(S_2O_3)_2]^{3-} > S_3O_6^{2-}, S_4O_6^{2-} > SO_3^{2-} > S_2O_3^{2-}3 > SO_4^{2-}$, $[Au(S_2O_3)_2]^{3-} > [Pb(S_2O_3)_2]^{2-} \gg [Ag(S_2O_3)_2]^{3-} > [Cu(S_2O_3)_3]^{5-} \gg [Zn(S_2O_3)_2]^{2-}$ [48]. The presence of thionate complexes is also known as deleterious for gold adsorption capacity. Unfortunately, 0.01 M of tetrathionate $[S_4O_6^{2-}]$

Gold loaded resin

$A = [\ddot{R} - N^+(CH_3)_3 \, Y^- + [Au(S_2O_3)_2]^+$
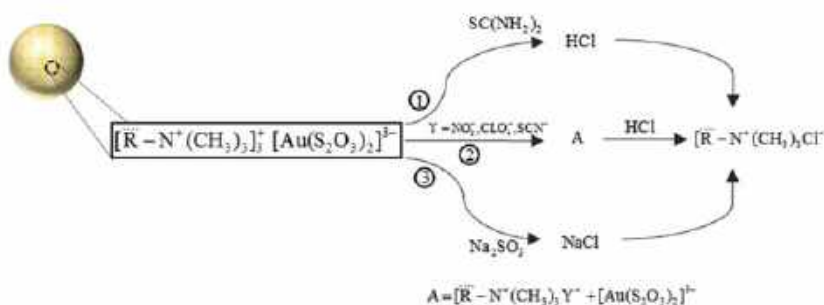
Fig. 9.7 The elution principles of gold thiosulfate loaded resins [40]

poisoned resins and occupied the most active sites of the resins, causing a drop in gold loading capacity by about 90% [39, 49]. In respect of amine functionality, a polymer matrix containing quaternary or polyfunctionality anion exchangers showed the highest gold capacity and the broadest effective applicable pH range. From the proposed studies that were conducted on the effects of activated carbon and IEXRs, it was found that the highest possible gold adsorption efficiency may reach up to 100% in polymers containing quaternary functionality [50, 51]. Table 9.3 compares total recovery efficiencies of gold from thiosulfate solution by commercially available IEXRs and activated carbon.
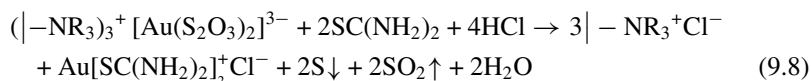
Elution process of gold loaded resins in thiosulfate leaching is somehow complex because of co-adsorption of copper and other foreign complexes by resin. Hence, depending on elution technique, copper (as major co-adsorbed metal) and gold can be eluted simultaneously or separately, which are known as one or two-step stripping processes, respectively. In one-step stripping, additional operations are necessary in order to obtain high purity gold metal. On the contrary, since affinity of IEXRs to Au (I) thiosulfate is higher than copper (I) thiosulfate, copper can be stripped during gold elution under pre-elution process using oxygenated ammonia, ammonium thiosulfate and ammonia–ammonium sulfate. The elution principles of $[Au(S_2O_3)_2]^{3-}$ loaded resins are briefly shown in Fig. 9.7.

Chemical reaction, displacement and synergistic ion exchange are three main principles in elution procedure of $[Au(S_2O_3)_2]^{3-}$ loaded resins, which are indicated as routes 1, 2 and 3, respectively (Fig. 9.7). In chemical reaction, elution (route 1) adsorbed $[Au(S_2O_3)_2]^{3-}$ anions are transferred into a stable cationic complex of gold. In this situation, resin affinity to a new generated cationic complex of gold reduces significantly and thus gold can be eluted readily from resin. Alternative ligands that can create cationic complex from gold (I) thiosulfate are limited and acidic thiourea is the only reported candidate ligand for $[Au(S_2O_3)_2]^{3-}$ elution by chemical reaction route. Equation (9.8) illustrates the proposed reaction pathway for elution of gold (I) thiosulfate by acidic thiourea [40].

Table 9.3 A comparison between the total gold recovery efficiency of the recently reported resins and activated carbons

Type of absorber	Type	pH	[Au] (ppm)	Au %	Contact time (h)	Reference
Resin						
Av-17-10P	QA	11	17.9	94.2	5	[52]
Amberlite IRA-400	QA	10	20	100	0.33	[53]
Amberlite IRA-400	QA	9	9.27	94.7	10	[54]
Purolite A500C	QA	8	1.8	99.45	6	[49]
Amberjet 4200	QA	9.5	10	99	–	[44]
Dowex 21 K	QA	11	20	100	24	[39]
Dowex 21 K	QA	9.5	100	95	3	[55]
Amberlite IRA-410	QA	11	8	>90	2	[56]
Purolite A530	QA	10	39.4	94	–	[43]
Dowex G51	QA	11.7	10	98	–	
Amberlite IRA-93	WB	8	10	94.3	2	
AN-85-10P	WB	11	17.9	51	5	[51]
AN-106-7P	WB	11		39		
AN-31	WB	11		37		
Activated Carbon	Cocoa stones	11	17.9	17.9	5	[51]
Activated Carbon	Charcoal			17.1		
Activated Carbon	Brown coal			16.8		
Activated Carbon	Anthracite			16.6		

QA Quaternary ammonium (strong base), *WB* weak base

$$\left(\left|-NR_3\right)_3{}^+ [Au(S_2O_3)_2]^{3-} + 2SC(NH_2)_2 + 4HCl \rightarrow 3\right| - NR_3{}^+Cl^-$$
$$+ Au[SC(NH_2)_2]_2^+Cl^- + 2S\downarrow + 2SO_2\uparrow + 2H_2O \tag{9.8}$$

Unlike chemical reaction route, the most commonly used method in gold elution is displacement principle, which is based on the application of an anion with higher affinity to resin compared with the adsorbed gold (I) thiosulfate. In fact, displacement method is based on shifting the adsorption equilibrium (9.7) to the left by increasing

Table 9.4 Elution effectiveness of perchlorates compared to the industrial Zadra process

Parameters	Perchlorate process	Zadra process
The gold capacity of resin (kg/t)	5	4–5
Elution time (h)	4	30–48
Temperature (K)	Ambient	363–373
Pressure (kPa)	Atmosphere	400–500
Flow rate (Bed volume number/h)	3	1–2
Maximum gold concentration (mg/L)	1250	1000
Average gold concentration (mg/L)	333	150–400
Gold recovery	>99.5%	96–98%
Gold loading capacity of stripped resin (kg/t)	<0.5	<0.15

the concentration of X^- anion. Thiocyanate, tetrathionate, nitrate and perchlorate are known anion stripping agents. Compared with different aforementioned elution agents, perchlorates have been found to be effective eluents compared to the industrial known Zadra process (Table 9.4). The feasibility of this method is demonstrated by a detailed comparison with elution efficiencies of the same resins with the different gold loaded capacities. It was found that ~100% gold can be eluted successfully by utilizing solution containing 2.5 molar perchlorate for resin with a gold loading capacity of 5 kg/t. However, the requirements of high concentrations of perchlorate and regeneration solutions are the only drawbacks of perchlorate technique in gold elution process.

As shown in Fig. 9.7, synergistic ion exchange is the third principle of gold (I) thiosulfate elution technique, which is known as two-step stripping process and is based on utilization of a mixture of a weak eluent and sulfite. The basic concept of using sulfite in elution system is that, in the presence of small amount of sulfite, $[Au(S_2O_3)_2]^{3-}$ converted to gold (I) thiosulfate-sulfite complex ($[Au(S_2O_3)(SO_3)]^{3-}$). The resin has a weak affinity to the newly generated $[Au(S_2O_3)(SO_3)]^{3-}$ ligand. Thus, it is able to efficiently strip gold from resin in the presence of the weak eluent. A summary of characteristics of single and two-stage elution techniques in stripping gold loaded $[Au(S_2O_3)_2]^{3-}$ resins is presented in Table 9.5.
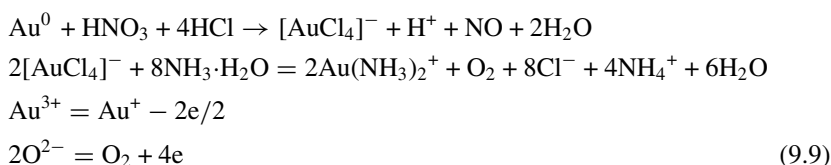
It can be concluded from the literature that weak and strong base anion resins have been very useful to recover gold from thiosulfate leach solutions. The weak resins exhibited a high selectivity of Au complexes but low uptake ability (less than 2 kg/t), thus, weak base resins were not an efficient and economical choice to recover gold from pregnant thiosulfate solutions. On the contrary, the loading capacity of the later

Table 9.5 A summary of advantages and disadvantages of single and two-stage elution techniques in gold (I) thiosulfate loaded resins

Elution process	Process characteristics		Reference
Single step	Thiocyanate	Fast elution, high reagent requirement and environmental hazard. Strong affinity to resin and regeneration content are required. Elution mechanism proposed	[49]
	Tetrathionate	Fast elution, high reagent concentration requirement, regeneration is required, metal sulfide precipitation can form for multi cyclic elution process. The high temperature is necessary. The elution mechanism proposed	[57]
	Nitrate	Weak affinity to the resin and slow elution process, a high concentration of eluent is necessary, no need of regeneration. Environmental friendly process. The elution mechanism proposed	[58]
	Perchlorate	Fast elution and high affinity to the resin, high reagent concentration and resin regeneration are the requirements. The elution mechanism proposed	[55]
Two-step	Thiourea + sulfuric acid/hydrochloric acid	No need of regeneration, sulfur precipitation from sulfur–oxygen anions decomposition. The high rate of resin losses due to the osmotic shock. The elution mechanism proposed	[51]
	Sodium chloride + sodium sulfite	Poisoning hazard of resin. Low concentration of eluent solution. The elution mechanism proposed	[59]

(strong base resins) usually was up to 10–25 kg/t, and was independent of solution pH. Although high capacities of the strong base resins make it possible to efficiently adsorb the extremely low concentration of aurothiosulfate complexes, the selectivity of these resins is poor and certain anions such as $[Cu(S_2O_3)_3]^{5-}$ and polythionate will co-adsorb with gold due to the strong competition with $[Au(S_2O_3)_2]^{3-}$. Finally, it can be concluded that thiosulfate leaching can be widely considered to be the most promising alternative method owing to its reduced environmental risk, high reaction selectivity, low corrosiveness of leach solution and cheap reagents.

Ammonia is another attractive alternative to a lixiviant for gold recovery. The main advantage of this alternative is easily regeneration, low cost of the primary medium and no need of pre-concentration. In this method, the gold solution in ammonium buffer was prepared by introducing aqua regia solution of gold into ammonium buffer solution under an oxygen atmosphere (10–15 atm and 120 °C). The preparation process of gold dissolution can be expressed as presented in (9.9) [37].

$$Au^0 + HNO_3 + 4HCl \rightarrow [AuCl_4]^- + H^+ + NO + 2H_2O$$
$$2[AuCl_4]^- + 8NH_3 \cdot H_2O = 2Au(NH_3)_2^+ + O_2 + 8Cl^- + 4NH_4^+ + 6H_2O$$
$$Au^{3+} = Au^+ - 2e/2$$
$$2O^{2-} = O_2 + 4e \tag{9.9}$$

Recent studies have proved that surface modification can improve gold recovery of the functionalized resins in terms of selectivity and loading capacity. In this regard, Trochimczuk et al. [60] employed microwave reaction method to surface modification of the synthesized resins with amino ligand functions and compared the gold extraction results with the synthesized resins under the conventional modification method. Synthesized resins were functionalized by different aliphatic and aromatic amino ligands and recovery experiments were performed under a single (Au or Cu) and binary (Au plus Cu) components in ammonium buffer. As presented in Table 9.6, it is clear that due to the different structures of the resultant resins, the synthesized adsorbents under microwave heating (i.e. 1-methylimidazole resin) show the highest sorption capacity (15.5 mg/g) towards gold. Beside structural characteristic, resins show preferential sorption of gold in the presence of copper. Soft donor atoms (i.e. N and S) in ligand structure have a high affinity toward Au, Ag and Pt as soft metals. On the other hand, compared to Cu complexes, ligands prefer smaller complexes.[1]

It was proved that resin structure and selective functional groups play a key role in an efficient recovery of gold from its leaches solutions. Pilsniak et al. [61] investigated the efficiency and selectivity of Au recovery from the single and the multicomponent solutions on a serious functionalized copolymer based resins with the different structures (i.e. expanded gel, gel and porous nature resins). The results showed that resin structure had a high impact on the grafting of functional groups. Comparison of various resin types indicated that expanded gels provided more sites to easy surface

---

[1]Ammine complex of gold, $Au(NH_3)_2^+$, displays linear structure, whereas $Cu(NH_3)_4^{2+}$ has tetrahedral structural characteristic.

Table 9.6 Effect of different surface functionalized groups on sorption ability of the resulted resins in a single and binary solution
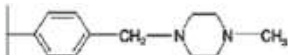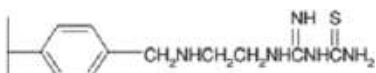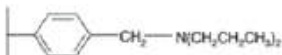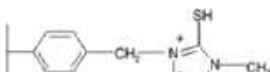
Resin structure	Sorption of Au in a single component (mg/g)	Log K_d	Sorption of Au in binary solution (mg/g)		Log K_d	
			Au	Cu	Au	Cu
1-methylpiperazine resin (Conventional Method)	1.37	1.84	1.84	0	1.98	–
guanylthiourea resin (Conventional Method)	12.5	3.03	7.7	0	2.82	0
dipropylamine resin (Conventional Method)	1.71	1.91	0	0	–	–
2-mercapto-1-methylimidazole resin (Microwave Method)	1.07	1.7	1.98	0	1.98	–
1-methylimidazole resin (Conventional Method)	15.5	2.94	12.9	0	2.84	–
2-mercapto-1-methylimidazole resin (Microwave Method)	7.12	2.68	13.6	0	2.89	–
1,2-dimethylimidazole resin (Microwave Method)	4.61	2.35	3.34	0	2.22	–
1-(3-aminopropyl)limidazole resin (Microwave Method)	3.08	2.17	2.74	0	2.13	–
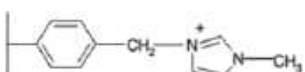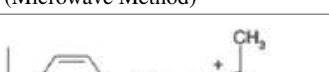
Table 9.7 Effect of resin morphology on Au sorption efficiency

Resin Type	Resin morphology	Ligand concentration (mmol/g)	Sorption of Au (mg/g)	Log K_d
1-Methylimidazole	Expanded gel	3.37	15.5	2.94
1-Methylimidazole	Gel	3.1	11.25	2.78
1-Methylimidazole	Porous	1.75	4.62	2.36

modification. According to this, the best results of the introduction of functional groups into the polymer matrix were obtained using an expanded gel type containing 2% of crosslinking agent [61]. Hence, ligand concentration and gold sorption on those resins are the highest (Table 9.7).

From sorption kinetic point of view, the authors investigated the effectiveness of three different guanylthiourea, 1-methylimidazole and 2-mercapto-1-methylimidazole ligands (Table 9.6). The maximum gold sorption (90 mg/g) was realized within 80 h on resins treated with 1-methylimidazole ligands (88%). It was also found that although immobilization of the functional groups improved the sorption kinetics, it had a negative influence on uptake ability of gold (I). Blocking of reactive sites in polymer resins as well as the repulsion of $Au(NH_3)_2^+$ are the main reasons for decreases of gold (I) sorption efficiency in resins containing hydrophilic ligand.

The recent studies revealed that piperazine surface modified resins exhibited strong affinity toward Au (III) complexes. Hydrochloric acid, cyanide and ammonium hydroxide were used as general pregnant systems for gold extraction by piperazine functionalized resins [62–65]. Cyganowski et al. [63] investigated the sorption affinity of three different piperazine surface functionalized resins in selective adsorption of Au (III), Pt (IV) and Pd (II) under bath and dynamic conditions. IEXRs were synthesized by functionalization of suspension derived vinylbenzylchloride (VBC) and divinylbenzene (DVB) copolymer with 1(2-aminoethyl) piperazine, 1-amino-4 methylpiperazine and 1-methylpiperazine (Fig. 9.8).

The sorption experiments were conducted in a solution containing multicomponent metal anion such as $AuCL_4^-$, $PtCl_6^{2-}$ and $PdCl_4^{2-}$ in the concentration range 10–919 mg/dm³. From the experimental results, it was found that the greatest total sorption capacities were determined as 331.7 mg/g Au for 1-amino-4 methylpiperazine resin. However, the 1(2-aminoethyl) piperazine resin showed the greatest affinity to platinum and palladium. As evident from Table 9.8, compared with an ammonium hydroxide pregnant solution, gold extraction by 1-methylpiperazine functionalized resins was better in the hydrochloric acid system. In case of Piperazine functionalized resins, high affinity toward gold complexes could be attributed to the presence of free electron pairs on the ligand (i.e. on nitrogen atoms) as well as high mobility of $AuCL_4^-$ through the resin 3D network. On the other hand, because of the smallest
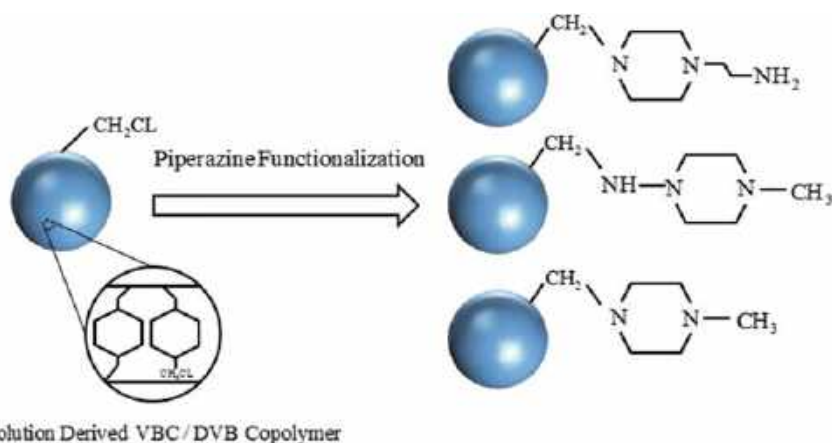
Fig. 9.8 Surface functionalized VBC/DVB copolymer with the different piperazine functions [63]

Table 9.8 Comparison of sorption capacity values for the different pregnant solutions and piperazine surface functional group

Functional group	Pregnant system	Total sorption capacity of Au (mmol/g)	References
1(2-aminoethyl)piperazine	Hydrochloric	5.38	[64]
1(2-hydroxyethyl)piperazine	Cyanide	0.76	[62]
1-methylpiperazine	Ammonium hydroxide	1.37	[60]
1(2-aminoethyl)piperazine	Hydrochloric	2.37	[63]
1-amino-4-methylpiperazine		2.89	
1-methylpiperazine		2.98	

charge density of Au (III), resin functional groups favoured interaction with Au (III) chloro-complex. On the contrary, the presence of excess ammonium cations (NH_4^+) in pregnant solution caused the formation of coordinate with 1-methylpiperazine VBC/DVB resin which hindered gold uptake ability of the resin.

Development of information technology has resulted in the production of great amounts of wasted electronics and electronic equipment (WEEE). From official statistics, the worldwide production of WEEE reached 50 million tonnes per year and this number increases annually by 5%. However, only 20% of this WEEE is globally recovered [66–68]. As presented in Table 9.9, despite environmental problems, wasted electronic is considered as a valuable resource of a lot of metals such as gold, copper, tin, nickel, lead, zinc and silver, some of which are considered as precious and essential for the development of industries and human society [19, 69].

The recovery of gold and other precious metals has attracted a great deal of attention. Complexity and variety of WEEE composition as well as ultralow content (~1

Table 9.9 Value versus weight distribution for typical electronic devices components

Weight share	Fe (%)	Al (%)	Cu (%)	Plastics (%)	Ag (ppm)	Au (ppm)	Pd (ppm)
Monitor board	30	15	10	28	280	20	10
PC-board	7	5	18	23	900	200	80
Mobile phone	7	3	13	43	3000	320	120
Portable audio	23	1	21	47	150	10	4
DVD player	62	2	5	24	115	15	4
Calculator	4	5	3	61	260	50	5
Value share	Fe (%)	Al (%)	Cu (%)	Sum PM (%)	Ag (%)	Au (%)	Pd (%)
Monitor board	4	14	35	47	7	33	7
PC-board	0	1	13	86	5	69	12
Mobile phone	0	0	6	93	11	71	11
Portable audio	3	1	73	21	4	16	3
DVD-player	15	3	30	52	5	42	5
Calculator	1	4	10	85	6	76	3

wt%) of precious metals have been the main challenges to development of technologies for effective recycling of the metals from electronic wastes (Table 9.9) [19, 70]. Cyanide, halide, thiourea and thiosulfate have been some general leachates that were investigated to extract gold from solutions. However, these mediums of extraction are reported to make a harmful impact on the environment while having poor efficiency. As reported, the most efficient extraction of gold from solid electronic elements was the appliance of HNO_3/HCl (i.e. aqua regia) [68, 71–73]. There are many examples indicating the 100% recovery of gold from scrap printed circuit boards using aqua regia [68, 74–77]. The schematic diagram of gold separation procedure from WEEE is illustrated in Fig. 9.9.

However, the process is still not effective as significant amounts of other metallic components are recovered and WEEE often contains ultra trace amounts of gold. According to Deventer [8], using ion exchange resin is the only economically viable method to concentrate and recover gold from such diluted media [19]. Although ion exchange polymers have established reliable applications in the separation of gold metal from its leach solution, degeneration of the functionalized agent in the presence of nitric acid (as strong oxidant) and structural blockage due to osmotic shocks can be accounted as their main drawbacks in gold recovery from aqua regia medium [18, 78]. For this reason, the development of an anion exchange resin with resistive characteristic to aqua regia solutions is necessary. In this regard, Cyganowski et al. [65] investigated the effectiveness of functionalized core–shell anion exchange resin using
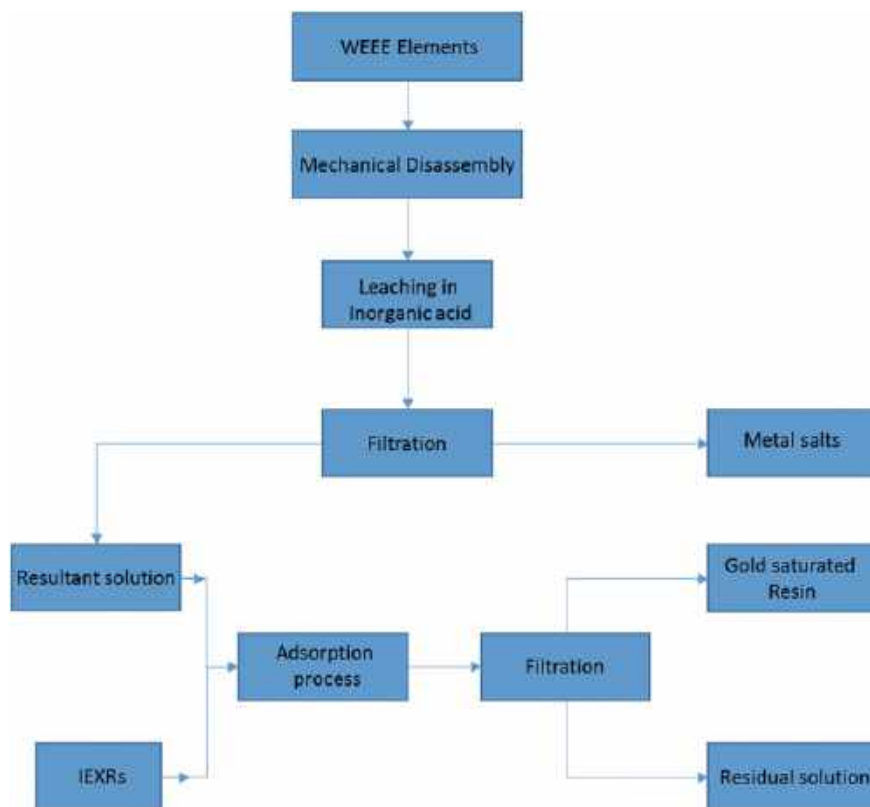
Fig. 9.9 The schematic diagram of gold separation procedure from WEEE [32]

1-ethylenediamine (1EDA) and 1-(2-aminoethyl) piperazine (aAEP) in the recovery of gold from aqua regia leach of electronic parts. Gold sources were obtained from leach solutions of central processing units (CPU) and pin contact elements (PIN), which can be classified as components with high (~1.5 wt%) and low amounts of (0.1 wt%) of gold, respectively. The study was conducted under the batch condition and the synthesized resins (0.05 g) were contacted in with 20 mL of either CPU or PIN solutions for 48 h at ambient temperature. Finally, the removal efficiency was calculated based on the concentration of the detected metals before and after the sorption processes and elution was proceeded using a solution of 5% thiourea in 0.1 M HCl. The experimental results showed (Fig. 9.10) that nickel and iron anions were competitive towards gold in recovery experiments using ethylenediamine-functionalized resin whereas the 1-(2-aminoethyl) piperazine functionalized resin revealed no affinity towards these competitive species. The affinity of IEXRs to gold was ten times more than the presented nickel in the solution and non-precious metals remained intact in solution. The recovery and elution efficiency of the adsorbed gold from the metal solution were 86 and 100%, respectively.
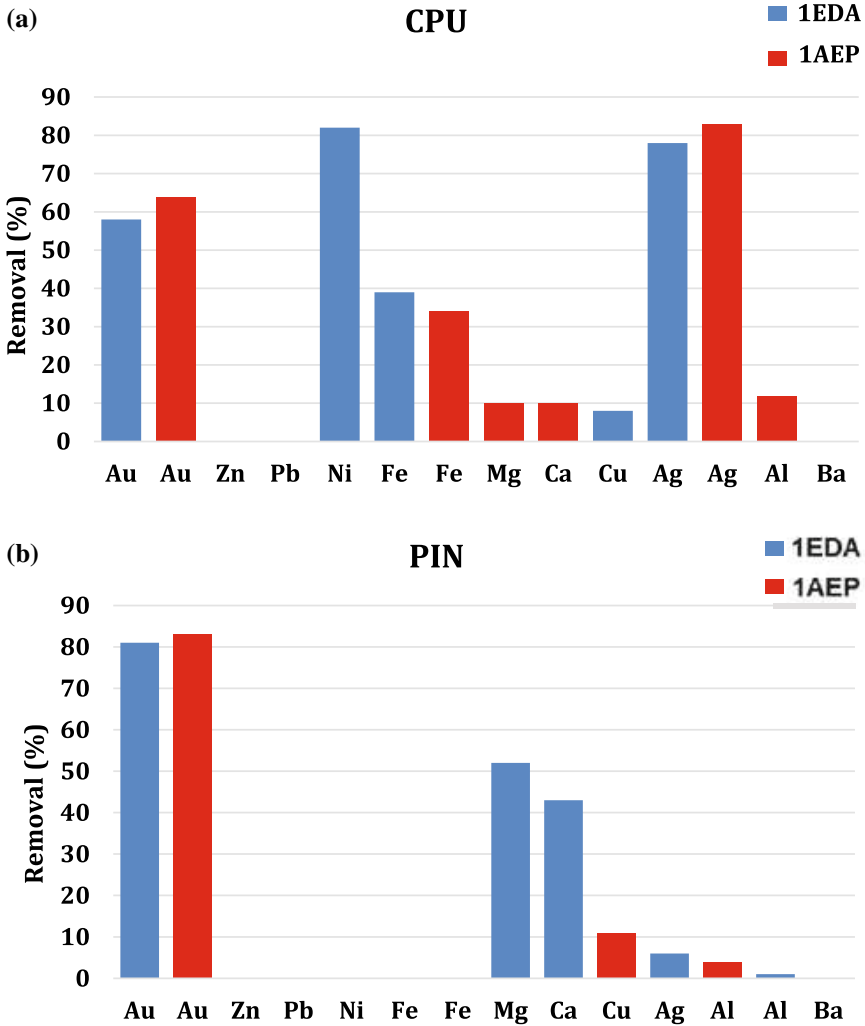
Fig. 9.10 Gold concentration from the leached CPU (**a**) and PINs (**b**) on the core–shell anion exchange resin [65]

Beside metal content of WEEE, processing condition also played a crucial role on extraction efficiency of the IEXRs. Alguacil et al. [79] investigated the process variables (i.e. temperature, hydrochloric acid and metal concentrations) on adsorption–elusion effectiveness of Lewatit MP-64 anionic IEXRs in gold (III)-hydrochloric acid solutions. Lewatit MP-64 resin is a polystyrene base matrix containing tertiary and quaternary ammonium groups (medium-basic anion exchange base). The details of investigation performed under the batch condition are presented in the following. As presented in Fig. 9.11, in batch experiments, (i) the initial rate of
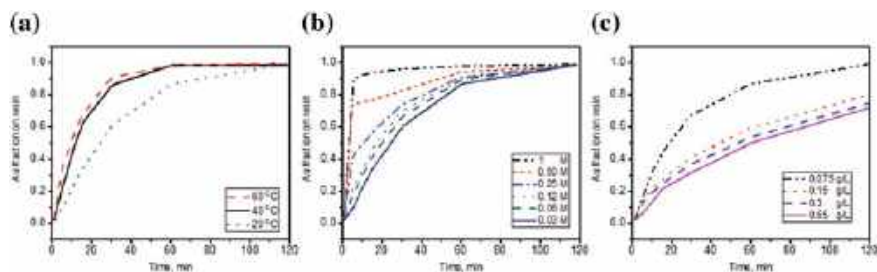
Fig. 9.11 Effects of temperature (**a**), HCl (**b**) and Au concentration (**c**) on adsorption efficiency of the synthesized resin [79]

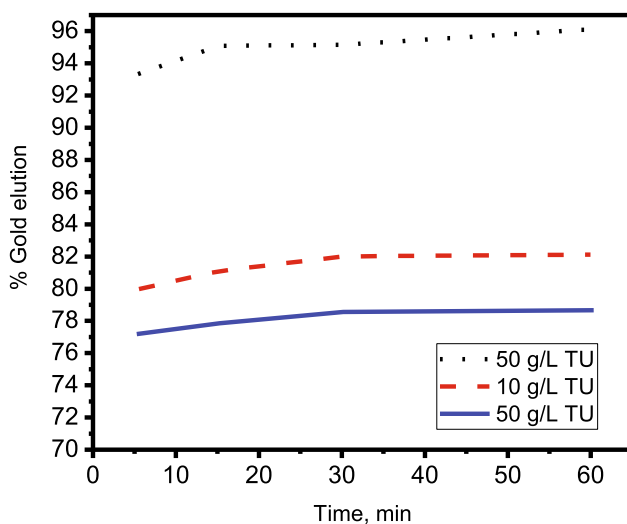**Fig. 9.12** Effect of thiourea concentration on elution effectiveness of resin (___) *solution/resin ratio 154, (……) solution/resin ratio 305* [79]

gold recovery was temperature dependent and the adsorption equilibrium reached to a constant value at 120 min. (ii) the increase of HCl concentration in aqueous phase increased the rate of metal adsorption up to 0.5 M. This may be attributed to the fact that, at higher acidity, resin swells more and so access to the pores becomes easier. (iii) about 85% of the gold was adsorbed during early 60 min of the experiment and loading approached a plateau after 120 min contact duration.

Finally, a resin containing 90 mg/g of gold was used in an acidic thiourea solution. As revealed in Fig. 9.12, it was found that although the increase in thiourea content led to increasing the percentage of metal desorption, it did not affect the kinetics of metal desorption.

9.2.2   Recovery and Removal of Silver from Aqueous Industrial Solutions by Ion Exchange Technology

Recently, an extensive degree of interest has been directed to investigating the recovery and removal of silver because of its increasing applications in industries and consequently environmental problems associated with it [80]. The main extraction route of silver in industries is hydrometallurgical process that includes leaching of silver by appropriate leaching agents and separating it from obtained solutions by techniques like chemical precipitation or ion exchange to concentrate the metal and finally treating the concentrated solutions by electrowinning or cementation. Some well-known silver leaching agents have been cyanide, thiocyanate, thiosulfate, chloride and nitric acid [80, 81]. In separating stage of silver through hydrometallurgical extraction, the application of sorption method by using ion exchange resins helps production of solutions with a high concentration of metals, whereas removal of silver ions from industries wastewater by ion exchangers efficiently reduces the amount of these ions in solution. However, in order to effectively use the ion exchangers in manufacturing schemes, the study of equilibria and essential properties of these sorbents is required to facilitate the choice of suitable sorbents, which possess sufficient and high affinity to extractable ions and selection of the optimal conditions to enhance their degree of recovery [81]. Table 9.10 presents some commercial and artificial IEXRs that can be used for recovery or removal of silver from various solutions. Researchers used these resins to investigate the sorption of silver from various leaching solutions. Some of the main results of these investigations are summarized as follows.

9.2.2.1   Chloride Solution

Resins in class A were investigated by Kononova et al. [82] for silver recovery from chloride solutions. They described the formation of silver ion $[AgCl_2]^-$ complexes in chloride solutions with 1–4 mol/L concentration and absorption spectra of the initial hydrochloric acid solution of silver confirmed this fact. Batch experiments were conducted by resins in class A to determine the ability of these resins for sorption of silver complexes from solutions containing various chloride concentrations. Results are provided in Table 9.11. According to this table, all resins adsorbed silver very well in 1 M chloride concentration especially the resins A500, A300 and S985. With increasing the chloride concentration in solution the sorption percentage decreased due to the competition between silver complexes and chloride ions that increased with increasing the chloride concentration; however, exceptionally the sorption percentage of Purogold A193 resin did not decrease even at 4 mol/L concentration of chloride ions.

Authors reported the anomalous isotherm curves that they found with equilibrium experiments on resins in silver chloride solution. Anomalous sorption isotherms were related to resins having several types of functional groups showing that the narrowing

Table 9.10 Some properties of ion exchange resins for recovery and removal of silver from aqueous industrial solutions

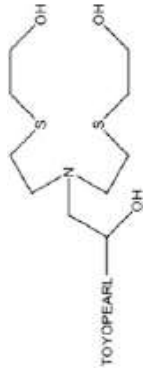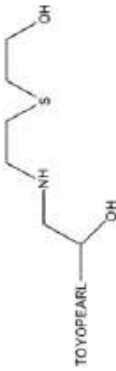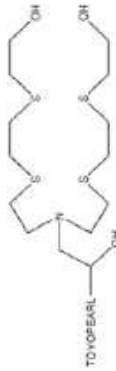| Class	Ion exchanger grade	Resin network	Functional groups/resin structure	Type	Physical structure	Exchange capacity in Cl^- form (mmol/g)	Solution
A, B	Purolite S985	st-DVB	PAGs $R–CH_2–NH_2$ $R–CH_2–CH=NH$ $R–CH_2–N(CH_3)_2$	Complexing ion exchanger	Macroporous	2.3	Thiosulfate Chloride
A	Purogold S992	st-DVB	MAs $R–CH_2–N^+(CH_3)_3$ $R–CH_2–N(CH_3)_2$	Weak base	Macroporous	4.4	Chloride
A	Purogold A193	st-DVB	QAB, TAGs $R–CH_2–N^+(CH_3)_3$ $R–CH_2–N(CH_3)_2$	Strong base	Macroporous	3.8	Chloride
A, B	Purolite A500	st-DVB	QAB, type (I) $R–CH_2–N^+(CH_3)_3$	Strong base	Macroporous	1.2	Chloride
A	Purolite A300	st-DVB	QAB, type (II) $R–CH_2–N^+(CH_3)_2(CH_2–CH_2–OH)$	Strong base	Gel	1.4	Chloride
A	Purolite A111	st-DVB	TAGs $R–CH_2–N(CH_3)_2$	Weak base	Macroporous	1.7	Chloride
B	Purolite A100	st-DVB	TAGs	Weak base	Macroporous	2.2	Thiosulfate
B	Purolite A530	st-DVB	QAB	Strong base	Macroporous	3.3	Thiosulfate
B	AM-2B	st-DVB	SAGs, TAGs	Weak base	Macroporous	2.3	Thiosulfate

(continued)

Table 9.10 (continued)

Class	Ion exchanger grade	Resin network	Functional groups/resin structure	Type	Physical structure	Exchange capacity in Cl⁻ form (mmol/g)	Solution
C	AV-17-10P	st-DVB	QAB	Strong base	Macroporous	4.4	Thiosulfate Thiocyanate
C	AV-85-10P	st-DVB	TAGs, SAGs	Weak base	Porous	6.2	Thiosulfate Thiocyanate
C	AN-25	st-DVB	TAGs	Weak base	Macroporous	5	Thiosulfate Thiocyanate
D	Duolite GT-73	st-DVB	– SH	Chelating	Macroporous	–	
D	Purolite Thiomethyl	st-DVB	– CH$_2$–SH	Chelating	Macroporous	–	
D	Spheron thiol	Glycol-methacrylate	– CH$_2$–CH(OH)–CH$_2$–SH	Chelating	Macroporous	–	
E	SP6cSN	Polystyrene		–	–	–	Nitrate 1,4-dioxane
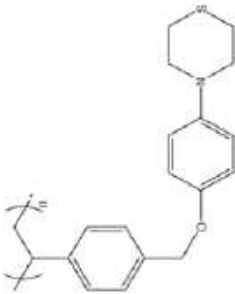
Table 9.10 (continued)

Class	Ion exchanger grade	Resin network	Functional groups/resin structure	Type	Physical structure	Exchange capacity in Cl⁻ form (mmol/g)	Solution
E	SP11AS2 N	Polystyrene		–	–	–	Nitrate 1,4-dioxane
E	SP17AS4 N	Polystyrene		–	–	–	Nitrate 1,4-dioxane

Table 9.10 (continued)

Class	Ion exchanger grade	Resin network	Functional groups/resin structure	Type	Physical structure	Exchange capacity in Cl⁻ form (mmol/g)	Solution
E	TY13AS2NO2	TOYOPEARL		–	–	–	Nitrate
E	TY7ASNO	TOYOPEARL		–	–	–	Nitrate
E	TY19AS4NO2	TOYOPEARL		–	–	–	Nitrate

(continued)

Table 9.10 (continued)

Class	Ion exchanger grade	Resin network	Functional groups/resin structure	Type	Physical structure	Exchange capacity in Cl⁻ form (mmol/g)	Solution
E	TY7ASN2	TOYOPEARL		–	–	–	Nitrate
E	TY6cSN	TOYOPEARL		–	–	–	Nitrate

Note st-DVB means polystyrene crosslinked with divinylbenzene, PAGs mean the polyamine groups, MAs mean mixed amines, QAB means quaternary amino groups, TAGs mean tertiary amino groups and SAGs mean secondary amino groups

Table 9.11 Silver sorption by class A resins at different chloride concentrations [82]

Exchanger resin	Silver sorption (%)		
	$[Cl^-] = 1$ M	$[Cl^-] = 2$ M	$[Cl^-] = 4$ M
Purolite S985	82.1	71.8	57.1
Purogold S992	55.8	–	7.7
Purogold A193	68.5	86.3	79.1
Purolite A500	84	84.8	75.2
Purolite A300	70.1	23	–
Purolite A111	55.8	–	50.7
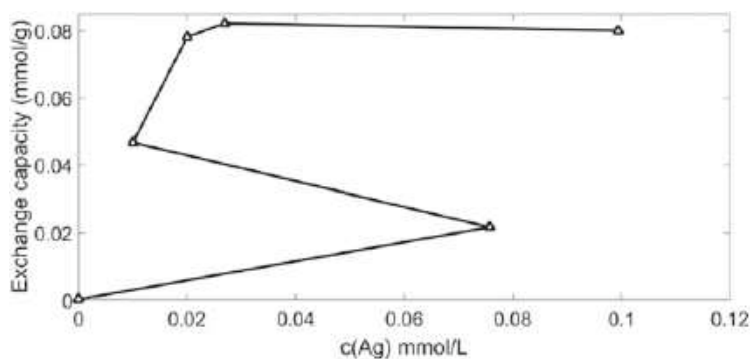
Fig. 9.13 Equilibrium isotherm curve for Purogold A193 resin [82]

of the sorbent pores happened during the ion exchange process. The results of Raman spectroscopic study of loaded S985 resin confirmed that the structure of polymer framework of resin changed and the stereochemical effects led to an anomalous sorption isotherm. Figure 9.13 shows the isotherm curve, which was obtained using Purogold A193 resin.

The regeneration of used resins was carried out with ammonia 1% solution. The choice of this elution was dictated by its interaction with silver ions to form ammonia complexes whose stability exceeded to that of silver chloride complexes by several orders of magnitude.

9.2.2.2 Thiosulfate and Thiocyanate Solutions

Resins in classes of B and C were surveyed by Kononova et al. [81, 83] with thiosulfate and thiocyanate solutions. They indicated that in thiosulfate solution, silver was in

Table 9.12 Silver sorption percentage of resins for classes of B and C in contact with thiosulfate and thiocyanate solutions [81, 83]

Exchanger	%R thiosulfate	%R thiocyanate
Purolite A100	41	–
Purolite A530	82	–
AM-2B	37	–
Purolite S985	45	–
Purolite A500	81	–
AV-17-10P	93	88
AV-85-10P	68	73
AN-25	69	78

Note R stands for recovery

the form of $[Ag(S_2O_3)_2]^{3-}$ complexes. Equation (9.10) shows the formation of these anions in a solution containing thiosulfate ions [81].

$$4Ag + 8S_2O_3{}^{2-} + O_2 \rightarrow 4[Ag(S_2O_3)_2]^{3-} + 4OH^- \tag{9.10}$$

Experiments showed that by adding sulfite ions to the solution, the formation of stable silver thiosulfate complexes facilitated because in the presence of sulfite ions, the oxidation of sulfide to thiosulfate ions occurred (9.11). On the other hand, the sulfite prevents the formation of tetrathionate ($S_4O_6{}^{2-}$) which in interaction with silver ions forms the precipitation of silver sulfide [81].

$$4SO_3{}^{2-} + 2S^{2-} + 6H^+ \rightarrow 3S_2O_3{}^{2-} + 3H_2O \tag{9.11}$$
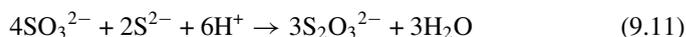
In thiocyanate solutions, silver thiocyanate complex $[Ag(SCN)_2]^-$ is formed and experiments showed that the maximum formation of silver thiocyanate complexes occurred at thiocyanate ions concentrations of 0.14–0.5 mol/L. If the SCN^- concentration is less than 0.14 mol/L, a precipitate of AgSCN is formed; while if the SCN^- concentration is more than 0.5 mol/L, the complex $[Ag(SCN)_3]^{2-}$ is formed. The reported findings indicated the optimum $[Ag(SCN)_2]^-$ formation concentration of 0.25 mol/L at a pH of 2.2. According to the results of sorption experiments on using resins of classes of B and C with different silver concentrations and pH values, all these resins adsorbed silver ions but their sorption efficiencies were obviously different. Table 9.12 shows the sorption percentages of resins in contact with about 0.2–0.3 mmol/L initial silver concentration of solution at pH = 2.2–10.

It seems that between the resins of classes of B and C, the sorption efficiencies of silver by strong base anion exchangers A500, A530 and AV-17-10P resins were better than others in thiosulfate and thiocyanate solutions. Authors [83] reported that with increasing the concentration of silver in thiosulfate solutions, the recovery of silver thiosulfate complexes enhanced at first and afterwards decreased, but rising the silver concentration did not significantly change the adsorption properties of AV-17-10P resin; however, by adding the sulfite anions to thiosulfate solution and
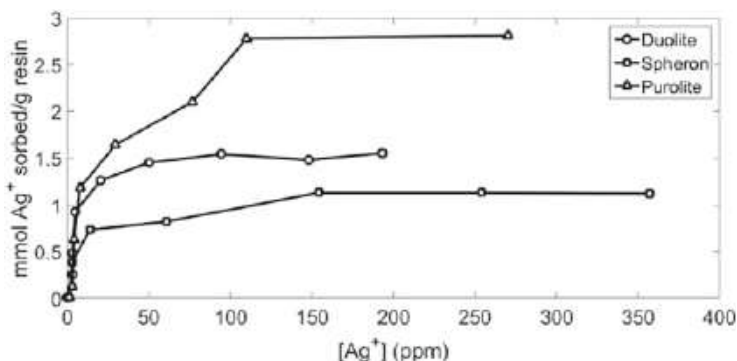
Fig. 9.14 Equilibrium isotherm curves of resins in class D [84]

increasing the concentration of these ions, the sorption of silver by AV-17-10P significantly improved. On the other hand, with increasing the concentration of silver in thiocyanate solutions, the sorption ability of all resins was enhanced and the silver sorption degree increased.

The experiment results of resins of class B showed strongly basic anion exchangers performance, not affected by pH of solutions but the sorption capacity of weakly basic anion exchangers obviously changed in various pHs, because of the degree of deprotonation of functional groups. The optimum pH and silver concentration found in different experiments were 10 and 0.5 mmol/L, respectively.

The comparison of the sorption in thiosulfate complexes of gold and silver in their joint presence on Purolite A530 showed the decrease in sorption recovery of both gold and silver compared to their recovery from the individual solutions due to mutual interference between gold and silver complexes. According to the results, the sorption capacity of gold in various ratios of silver and gold concentrations was about four times more than silver; therefore, the gold selectivity of this resin was higher than silver.

9.2.2.3 Nitrate Solution

Class D resins were investigated by Iglesias et al. [84] for sorption of the silver from its nitrate leaching solution. Equilibrium experiments with these resins indicated that all resins adsorbed silver ions; however, the silver sorption capacity of Purolite was significantly higher than Duolite and Spheron resins. They concluded that the silver was adsorbed by thiol groups in Purolite with 1:1 coordination reaction. Figure 9.14 shows the equilibrium data obtained in this investigation.

Moreover, Iglesias et al. [84] described both Purolite thiomethyl and Duolite GT-73 resins share the same polystyrene matrix and the same functional groups. Measurements of surface area and pore size distribution indicated a large volume of macropores within the polymer structure of both resins; however, according to
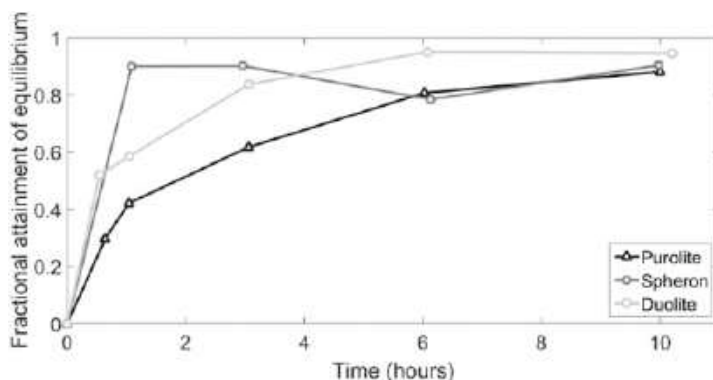
Fig. 9.15   Kinetics curves of class D resins [84]

the results, the capacity of Purolite was much greater than Duolite. The surface micrographs of these two resins confirmed that the surface of Purolite had a more homogeneous porous distribution.

Kinetics experiments of silver sorption on these resins showed that the sorption rate was much faster for Spheron than others. Figure 9.15 shows the experimental data [84]. Authors explained that the presence of numerous hydrophilic hydroxyl groups in the polymeric matrix of Spheron resin and the smaller particle size of this resin led to facilitate interaction of the resin with a solution and increase the sorption rate.

The elution experiments of class D resins showed that acidified thiourea solutions (thiourea 0.1 M, HNO_3 0.1 M) appeared to be the best stripping agents for regeneration of these resins. Results with this solution indicated that because of the stronger interaction between silver and thiol functional groups in Duolite and Purolite, the elution of these resins was not completed.

Resins of class E were manufactured and investigated by Sakamoto et al. [85] for sorption of silver from nitrate solutions. These resins have been divided into two categories as (a) the polystyrene-supported polythiazaalkane resins including SP6cSN, SP11AS2N and SP17AS4N and (b) the TOYOPEARL[2]-supported polythiazaalkane resins including TY19AS4NO2, TY13AS2NO2, TY6cSN, TY7ASNO and TY7ASN2. These two types of polymer matrices (polystyrene and TOYOPEARL) have been evaluated for the influence of their chemical properties on the sorption behaviour.

Both types of resins were capable of selectively recovering silver from nitrate solution and the uptake of silver from solutions containing various heavy metal ions like Mn^{2+}, Co^{2+}, Ni^{2+}, Cu^{2+} and Zn^{2+}. However, according to the results, the sorption rate of TOYOPEARL based resins was much higher than that of polystyrene-based ones. It happened because the polymer matrices of TOYOPEARL based resins made of polyvinyl alcohol were more hydrophilic than the polystyrene-based resins made

---

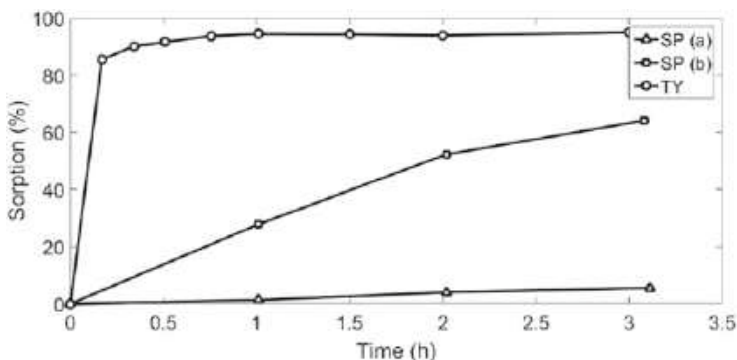[2]A kind of resin network which is composed of poly(vinyl alcohol).

Fig. 9.16 Silver sorption percentage by SP17AS4N without 1,4-dioxane (SP a), with 1,4-dioxane (SP b) and by TY19AS4NO2 (TY) resin [85]

of polystyrene. Experiments showed that the uptake rate of polystyrene-based resins increased by adding 1,4-dioxane into solutions. It seems that 1,4-dioxane reduced the hydrophobicity of these resins. Figure 9.16 shows the silver sorption percentage of TY19AS4 NO2 (TOYOPEARL based resin) and SP17AS4 N (polystyrene-based resin) under the same solution conditions to compare the resin performances; in addition, this figure illustrates the effect of 1,4-dioxane on SP17AS4N resin sorption.

Resins with limited complexation ability of their functional groups with silver ions were affected by pH changes because the protonation on the nitrogen atoms in polythiazaalkane derivatives functional groups at low pHs reduced the stability of complexes. For instance, each functional group in SP17AS4N has four sulfur atoms which are responsible for the high stability of formed complexes with silver ions. The protonation on the nitrogen atoms in resin functional groups does not prevent the complexation at low pHs, but functional groups of SP11AS2N have two sulfur atoms and hence the stability of their complexes with silver ions is less than SP17AS4N and the sorption ability of these resins decreased under highly acidic conditions.

9.2.3 Removal of Copper from Industrial Effluents by Ion Exchange Technology

Solutions including copper in high concentrations strongly damage the environment because this metal creates permanent toxicity and causes serious damage to human kidneys and livers [86]. Commonly the concentration of copper is high in untreated wastewaters of a lot of industries like iron and steel, leather tanning, metal plating, textile, battery and metal finishing industries and it is important to treat the wastewater of these industries. On the other hand, in some industrial processes due to product purity, the decrease of this metal concentration to very low levels is required [87]. To reduce and remove Cu, various methods and technologies like chemical

precipitation, membrane separation, solvent extraction and ion exchange have been adopted. Among these, the IEXRs have been frequently used by industries due to some appropriate features like the simplicity of equipment, reusability of resins and the fact that using this method does not lead to vast accumulations of sludge [86]. A lot of investigations were conducted to remove copper from various industrial solutions. In this section, some of these are briefly described and the main results, which were reported by researchers are presented. Table 9.13 lists useful information about some properties of used resins.

9.2.3.1   Cobalt Electrorefining

Due to the specifications of cobalt metal, it is necessary to purify cobalt electrolytes from metallic impurities prior to production of metal by electrowinning. Copper is one of the impurities that reduce the efficiency of the process. The typical concentrations of Cu in Co electrolytes have been found in the range with 0.5–2 g/L and the cobalt of about 50 g/L. It is important to reduce copper concentration without decreasing the cobalt amount of solution. Ion exchange technology can be used to achieve this goal [9, 10]. Wen et al. [88] investigated the removal of copper from cobalt sulfate electrolyte by a chelating cation ion exchange resin named as SP-C. Some characteristics of this resin are provided in Table 9.13. In this investigation, equilibrium and kinetics experiments were carried out at different temperatures to determine the performance of resin. According to the results, the Langmuir isotherm model was fitted very well by equilibrium data and the maximum capacity (q_m) calculated by this model was in the range 43.86–49.26 mg/g for the temperature ranges of 15–60 °C These findings indicated that with increasing the temperature, the capacity of resin slightly increased; therefore, the sorption process was endothermic. Continuous fixed bed experiments in a column at various temperatures were carried out and the results indicated [88] with increasing the temperature from 20 to 60 °C the saturated capacity of the resin increased from 43.3 to 48.8 mg/g. These results were in agreement with those obtained for the batch experiment. The kinetics experimental data were fitted to the pseudo-second-order model with high R-square values at different temperatures. Results showed that with increasing the temperature from 20 to 60 °C, the rate constant (that was calculated by pseudo-second-order model) increased from 0.0275 to 0.0818 min^{-1}, which implied the acceleration of adsorption rate at a higher temperature. From the comparison of IR spectra of loaded and unloaded resins, authors [88] concluded that the process of copper adsorbed onto SP-C resin could be considered as two steps, which can be described by (9.12) and (9.13).

Table 9.13 Some properties of ion exchange resins for the removal of copper

Ion exchanger grade	Resin network	Functional groups/resin structure	type	Physical structure	Exchange capacity (mmol/g)	Solution
SP-C	Silica-polyamine	Aminomethyl pyridine	Chelating	Macroporous	–	Cobalt electrolyte
Amberlite IRA 747	st-DVB	Aminomethylphosphonic acid	Chelating	Macroporous	2.3 in Na^+ form	Cobalt electrolyte
Purolite S950	st-DVB	Aminomethylphosphonic acid	Chelating	Macroporous	0.9 in Ca^+ form	Cobalt electrolyte
Lewatit TP260	Polystyrene	Aminomethylphosphonic acid	Chelating	Macroporous	3.2 in H^+ form	Cobalt electrolyte
717#(201 × 7)	st-DVB	QAGs, $-N^+(CH_3)_3$	Strong base	Gel	3.6 in Cl^- form	Nickel electrolyte
Lewatit MP500	Polystyrene	QAGs Type I	Strong base	Macroporous	1.72 in Cl^- form	Cyanide
Lewatit MP64	Polystyrene	TAGs QAGs	Weak base	Macroporous	2.1 in Cl^- form	Cyanide
Varion KCO	Polystyrene	Carboxyl (–COOH)	Weak base	Gel	–	Waste water
Varion KSM	–	Sulfonic acid ($-SO_3^-$)	Strong base	Porous	4.9 in H^+ form	Waste water
Ceralite IR120	st-DVB	Sulfonic acid ($-SO_3^-$)	Strong base	–	4.5 in H^+ form	Waste water
Amberlite IR 120	st-DVB	Sulfonic acid ($-SO_3^-$)	Strong base	Gel	2.4 in Na^+ form	Sulfate

Note st-DVB means polystyrene crosslinked with divinylbenzene, TAGs mean tertiary amino groups and QAGs mean quaternary amine groups

(9.12)

(9.13)
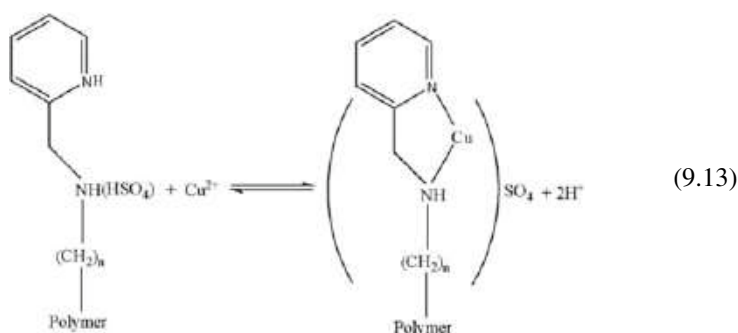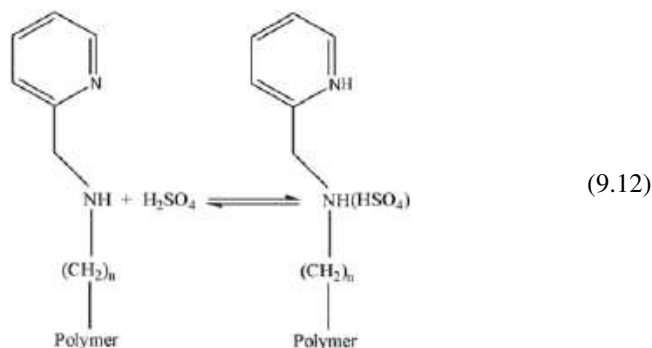
Fixed bed experiments at different pHs of the solution showed that with increasing the pH from 2 to 4, the saturation capacity of copper removal increased from 31.5 to 43.3 mg/g. It was due to the fact that at low pH values, hydrogen ions compete with copper ions leading to the reduction of copper sorption by resin. Also, by increasing the pH to a value of more than 4, because of copper hydroxide formation, the copper sorption significantly decreased by resin. In this investigation, the loaded resin was eluted completely with sulfuric acid with 2 mol/L concentration. Figure 9.17 shows the copper and cobalt concentrations measured in the outlet of eluent solution that regenerated resin in a fixed bed column. As one can see from this figure, the cobalt concentration of outlet eluent was extremely lower than copper, while the cobalt concentration in feed solution was about 50 times more than copper. This finding indicates that SP-C resin selectively removes copper ions from solution.

In another research [8] to reduce the concentration of copper from cobalt electrolyte, it was showed that the aminomethylphosphonic acid resins like Amberlite IRC 747, Purolite S950 and Lewatit TP260 were effective in removing copper selectively from this solution. The results indicated that resin loadings of 10–12 g/L copper were achieved while the cobalt co-loading amounted to 0.27% of total cobalt in the feed to the ion exchange unit; however, experiments showed that with the presence of the ferric ions in solution, these ions were very strongly extracted by resins and not
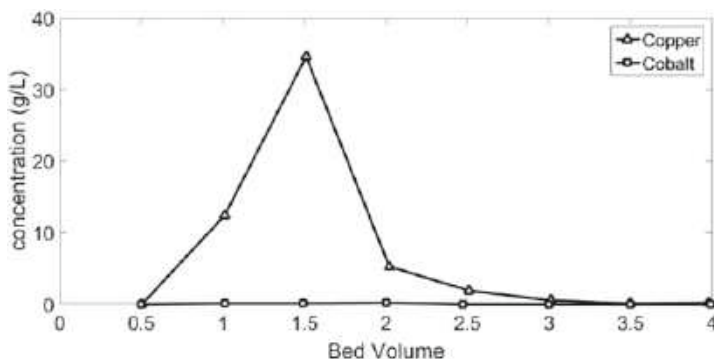
Fig. 9.17 Copper and cobalt concentration in eluent solution [88]

eluted by a standard sulfuric acid. Therefore, it is important that iron must be removed before the ion exchange operation unit by amino methyl phosphonic acid resins.

9.2.3.2 Nickel Electrorefining

The presence of a small amount of copper can significantly affect produced nickel properties because of the lower position of copper in the electric potential table than a nickel. On the other hand, copper is difficult to separate from the nickel solution due to the similar chemical properties of these two metals. Commonly, the copper concentration in nickel electrolytes is found in the range 0.4–1.2 g/L. To produce high purity nickel, the copper content in the solution should be reduced to less than 3 mg/L. One of the usual methods to decrease the concentration of this metal is ion exchange technology [89]. The sorption of copper from nickel electrolyte solution using ion exchange resin was investigated by Ai-Liang et al. [90]. The used solution had metal ions such as Ni^{2+}, Cu^{2+}, Cl^- and SO_4^{2-} with pH of about 4.5 and the 717[#] anion exchange resin was used to decrease the copper concentration. Cupric ions form $CuCl^+$ cation complexes in solutions containing Cl^- and these complexes are not adsorbed by anion exchange resins. However, cupric ions converted into cuprous ions by appropriate reducers like sulfite ions (SO_3^{2-}) which form anions such as $CuCl_2^-$ and $CuCl_3^{2-}$ that are adsorbed by some anion exchangers like 717[#] resin. The reaction of reduction of cupric into cuprous ions is illustrated by (9.14) [90].

$$2Cu^{2+} + SO_3^{2-} + H_2O \rightleftharpoons 2Cu^+ + SO_4^{2-} + 2H^+ \qquad (9.14)$$
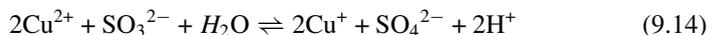
According to this investigation, with increasing the dosage of reductive agent (SO_3^{2-}) the sorption of copper increased, because it led to increasing the concentration of Cu^+ and consequently $CuCl_2^-$ and $CuCl_3^{2-}$ complexes in solution. The symbolic sorption reaction of copper anion complexes ($CuCl_2^-$ and $CuCl_3^{2-}$) with this resin is described by (9.15) [90].
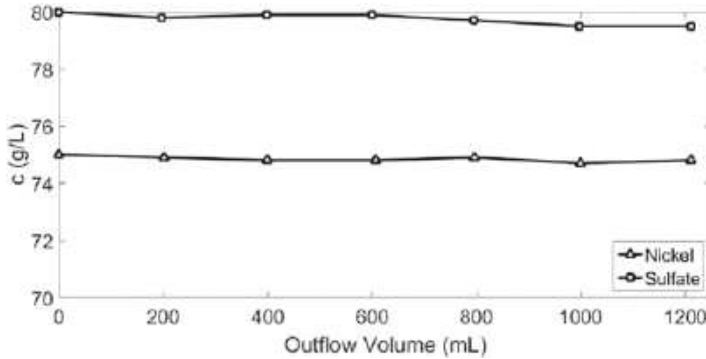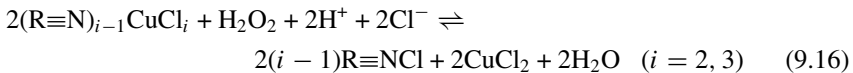
Fig. 9.18 Nickel and sulfate concentrations in outflow stream [90]

$$i\text{R}{\equiv}\text{NCl} + \text{CuCl}_i^{(i-1)-} \rightleftharpoons (\text{R}{\equiv}\text{N})_{i-1}\text{CuCl}_i + i\text{Cl}^- \quad (i = 2, 3) \tag{9.15}$$

Despite that the $717^{\#}$ resin is strong basic one, authors reported the copper was adsorbed by resin selectively and the concentration of nickel or sulfate ions did not obviously change in the solution. A fixed bed column experiment was conducted and the concentrations of nickel and sulfate ions in the outflow stream were measured. The results are shown in Fig. 9.18. As one can see, the value of these ions did not change in outflow stream; therefore, the resin did not adsorb other species in solution.

Copper desorption from the used resin was carried out perfectly by a solution containing sodium chloride (3M) and 4% H_2O_2 at pH about 4.5–5.5. The Cu^+ ions in resin were oxidized into Cu^{2+} by H_2O_2. The reaction of this process is described by (9.16) [90].

$$2(\text{R}{\equiv}\text{N})_{i-1}\text{CuCl}_i + \text{H}_2\text{O}_2 + 2\text{H}^+ + 2\text{Cl}^- \rightleftharpoons$$
$$2(i-1)\text{R}{\equiv}\text{NCl} + 2\text{CuCl}_2 + 2\text{H}_2\text{O} \quad (i = 2, 3) \tag{9.16}$$

9.2.3.3 Gold Extraction

The gold extraction process consists of several stages, gold concentrates produced in flotation are dissolved in some leaching agents like cyanide and the gold complexes are allowed to adsorb by ion exchange resin or activated carbon. Some metallic ions that are present in the gold ore, especially copper, form stable complexes with cyanide and consequently decrease the efficiency of the sorption process; therefore, the removal of these ions from leaching solution is important. Copper cyanide can be dissolved in aqueous solution in the presence of excess cyanide to form cyanocuprate complexes Cu(CN)_2^-, Cu(CN)_3^{2-} and Cu(CN)_4^{3-} [91]. Bachiller et al. [92] investigated the sorption of copper cyanide complexes from an industrial gold cyanide leaching solution by two commercial anion exchanger resins (Lewatit MP500 and
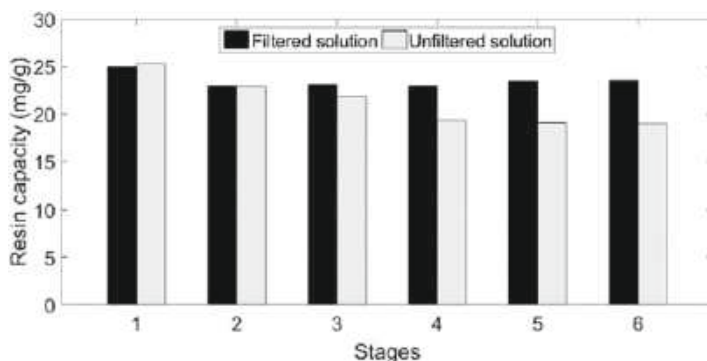
Fig. 9.19 The sorption capacity of MP500 in contact with filtered and unfiltered solution [92]

Lewatit MP64). In addition to gold, the solution has copper (580 ppm), cyanide (1300 ppm), chloride (300 ppm) and some other ions. The results of this study showed that both resins adsorbed copper complexes and the concentration of this metal significantly reduced in solutions but the sorption capacity of the strong base resin (MP500) was much more than that of the weak base resin (MP64). The sorption capacities of the resins, which were contacted with the same solution were reported as 7.41 and 25.7 mg/g for MP64 and MP500, respectively.

According to elution experiments, thiocyanate solution (NaSCN 1.25 M) was the best eluent among other solutions like sodium cyanide or sodium nitrate. The elution percentage of this solution was close to 100% and the capacity of resin did not significantly decrease during several consecutive stages of load and elution. Authors [92] indicated after elution stage, the recovery of loaded thiocyanate ions in the resin can be performed by a ferric sulfate solution to improve the efficiency of the process economically.

The mechanical resistance of resin is an important factor especially in the economic aspect of ion exchange operations. Experiments with filtered and unfiltered industrial gold cyanide solutions showed that the copper sorption capacity of resin was decreased during consecutive stages load/elution by unfiltered solution but this parameter was not significantly changed by the filtered solution. Figure 9.19 summarizes the results of the copper capacity of MP500 resin that was contacted with industrial filtered and unfiltered cyanide solutions in several stages of loading/elution.

Microphotographs of resin particles after runs demonstrated that the surface of particles, which were contacted with unfiltered solution was damaged and some of them were actually disintegrated. The presence of solid in the effluents poses attrition and breaking of the resin particles. Therefore, filtration of the effluents before ion exchange operation causes a significant increase in the sorption of ions by resin.
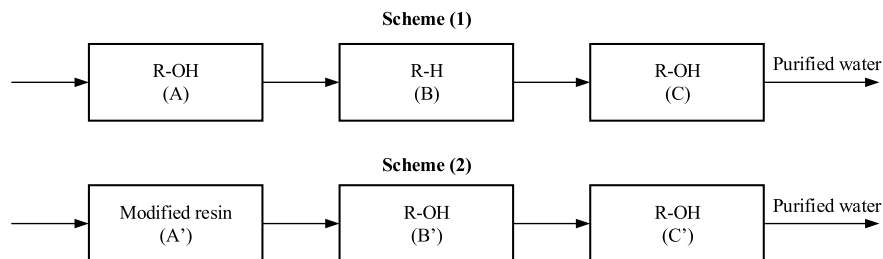
Scheme (1)

```
┌──────────┐   ┌──────────┐   ┌──────────┐  Purified water
│   R-OH   │   │   R-H    │   │   R-OH   │
│   (A)    │   │   (B)    │   │   (C)    │
└──────────┘   └──────────┘   └──────────┘
```

Scheme (2)

```
┌──────────────┐   ┌──────────┐   ┌──────────┐  Purified water
│ Modified resin│   │   R-OH   │   │   R-OH   │
│     (A')     │   │   (B')   │   │   (C')   │
└──────────────┘   └──────────┘   └──────────┘
```

Fig. 9.20 Schemes 1 and 2 used to purify rinse water [94]

9.2.3.4 Metal Finishing

Electroplating and electronic industries are the main culprits of copper pollution. The rinse water in electroplating process is usually used after plating and this stream including some heavy metal ions like copper, zinc and nickel, is known to be the major source for water pollution as well as the loss of useful metals [93]. Some investigations have focused on the purification of the copper from these streams by ion exchange technology. Dobrevsky et al. [94] studied the performance of two cation exchangers, a weak base resin (Varion KCO) and a modified resin (modified Varion KSM), to remove copper ions from the electroplating plants waste streams. They used two cation exchangers in H-form to purify copper from acidic solutions (pH < 4) in two technological schemes, which are illustrated in Fig. 9.20. Scheme (1) used a weak base anion resin (Varion ADAM) in OH-form (A), a weak base cation resin (Varion KCO) in H-form (B) and a strong anion resin (Varion ATM) in OH-form (C). The weak base anion exchanger (Varion ADAM) in the first stage was used to increase the pH of solution above 4.5 to improve the performance of weak acid cation exchanger (Varion KCO) because of the competition between hydrogen and copper ions in sorption at low pH values. Scheme (2) used a modified cation exchanger (Varion KSM that was modified by 5% thiocarbamide solution) in H-form (A′), a weak base anion exchanger in OH-form (B′) and a strong base anion exchanger in OH-form (C′).

In the scheme (1), the wastewater with a concentration of about 55–60 mg/L copper was purified up to 650–700 bed volume so that the copper concentration in outlet stream reduced below 10 mg/L. In the scheme (2) by using the modified cation exchanger, the purification of 780–830 bed volume was possible in the same condition of the inlet solutions. Authors [94] claimed that the useful capacities of unmodified and modified exchangers as calculated were about 1.38 and 1.8 eq/L, respectively; therefore, the capacity of the modified resin was improved about 30% without increasing pH of the solution. Figure 9.21 shows the breakthrough curves of copper removal in a fixed bed column for two schemes.

In another investigation, Revathi et al. [93] studied the removal and recovery of copper from rinse water in the electroplating process by using strong cation exchange resin Ceralite IR 120. They showed that the equilibrium data were fit-
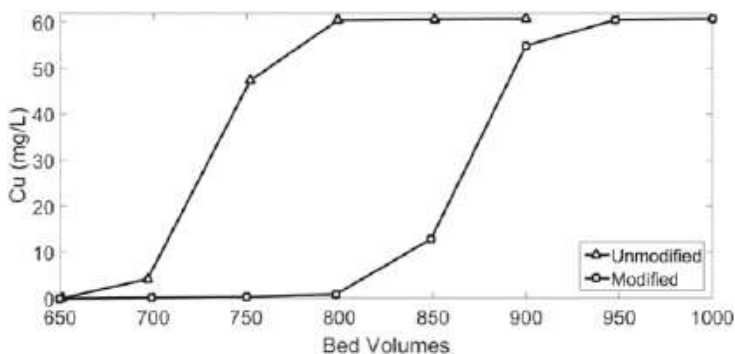
Fig. 9.21 The breakthrough curve of copper sorption by unmodified (scheme 1) and modified (scheme 2) resins [94]
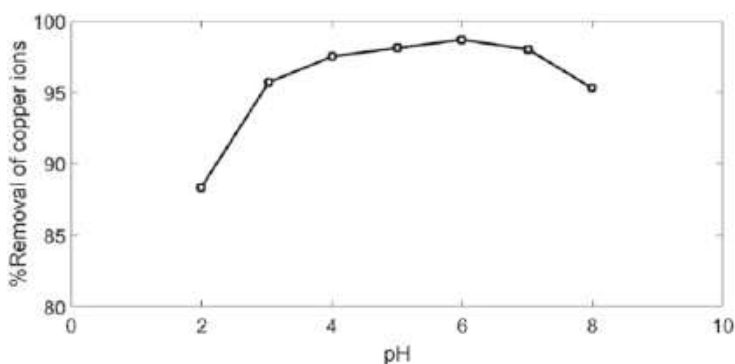

Fig. 9.22 Effect of pH on removal percentage of Ceralite IR120 resin [93]

ted by the Langmuir model and the maximum copper sorption by the resin was about 163.3 mg Cu (II)/g resin. This relatively high value indicates desirable affinity between the adsorbent and adsorbate molecules. On the other hand, authors reported that the pseudo-second-order kinetics model fitted kinetics data with a constant rate of 0.0072 g/mg.min very well. The effect of solution pH on the resin performance was also investigated and the results indicated that the removal percentage of copper increased with increasing the pH up to 6 and after that further increase in the pH results in the decrease of copper ion sorption. It seems that at low pH values, the hydrogen ions compete with copper ions, leading to the decrease in the sorption of copper. At high pHs, the hydroxide ions available in the solution react with copper to form copper hydroxide that gets precipitated in solution. Figure 9.22 shows the effect of pH on copper removal percentage by Ceralite IR120.

The effect of zinc and nickel ions on the removal efficiency of copper from wastewater was investigated. As Fig. 9.23 shows the zinc ions decreased the copper sorption significantly, but nickel ions did not affect on copper sorption noticeably, which is due to the more competing capacity of zinc metal than nickel and copper. According
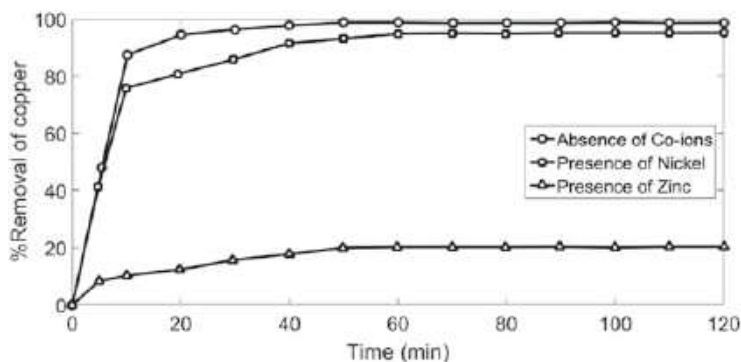
Fig. 9.23 The effect of nickel and zinc ions on copper sorption by Ceralite IR120 resin [93]
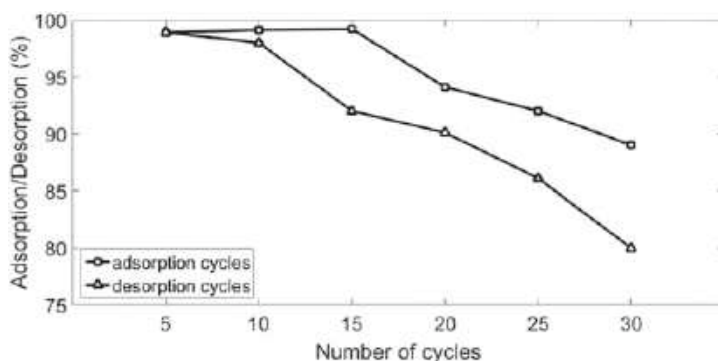

Fig. 9.24 The performance of Ceralite IR120 resin in several cycles of loading/elution [93]

to this result, it is important to remove zinc ions from solution before using resin to ensure acceptable performance of resin in copper removal.

According to the results of the resin elution, the used resins were regenerated almost perfectly by 2 M concentration of sulfuric acid. Figure 9.24 illustrates the adsorption/desorption percentage of the resin in several cycles. It seems that with 10 cycles of loading/elution, the efficiency of the resin did not change and with 15 cycles, the efficiency reduced by 3%. These results indicated that the regenerated resin can be used repeatedly for several cycles with negligible loss of efficiency.

9.2.3.5   Electronic Industries

In electronic industries, copper metal is widely used and consequently, a large amount of copper-bearing waste streams are produced. These streams are the major contributors to heavy metal pollution in surface water. Chemical and mechanical polishing (CMP) is one of the processes used by electronic industries to produce a very smooth

surface on each layer of a microchip. In this process, a large amount of copper-bearing sulfate waste effluent is generated, in which the concentration of copper in this effluent is up to 1000 mg/L, while the U.S. Environmental Protection Agency (EPA) has set the maximum contaminant level for copper at 1.3 mg/L in drinking water. One of the main methods to decrease the heavy metals concentration from industrial effluents involves the use of IEXRs. The application of resins for the removal and recovery of copper from CMP waste effluent was investigated by Kumar Jha et al. [95]. They used Amberlite IR 120 resin. According to this investigation equilibrium and kinetics, experimental data were fitted very well by Langmuir isotherm and pseudo-second-order models, respectively. The equilibrium sorption capacity and kinetics constant rate were reported as 107 mg/g and 0.022 g/mg min, which indicated the suitable performance of resin to sorption of copper from CMP solution. On the other hand, experiments with the resin in a fixed bed column to achieve the equilibrium indicated the maximum capacity of the resin as 115 mg/g in the column that was about 7.5% more than that value determined by Langmuir isotherm. It seems that partially multilayer adsorption happened which led to an increase in resin capacity in the column. The results of copper sorption by this resin in various pHs showed the maximum sorption of copper (97–99%) at pH around 2.5. At lower pH values, the sorption obviously decreased. It happens due to the competition between copper and hydrogen ions at lower pH values and because of high concentration and mobility of hydrogen, these ions are preferentially adsorbed by the resin. Elution of IR 120 resin was carried out by sulfuric acid and according to the results with increasing the concentration of acid, the elution percentage increased; for example, using 1 and 1.8 mol/L sulfuric acid concentration, the elution percentages were found to be 80 and 100%, respectively.

9.2.4 Uranium

With the rapid development of human society and considering the global climate change and a shortage of the fossil fuels, it is essential to find a sustainable energy supply with highly efficient and zero greenhouse emission characteristics. Nuclear power energy is regarded to be a promising alternative to the traditional energy sources, which is considered for the strong development of the uranium industry. Hence, efficient extraction of uranium from its natural resources has been always subjected to significant interest [96–98].

The uranium processing started in the late 1950s as the technology used in the Manhattan Project. However, until now especially during the past 5 decades, technologies for uranium processing did not change significantly [99, 100]. The general processing of uranium involves ore loading onto haul trucks, after ore mined blasting, and delivering to the primary crushers and reduce ore rocks to an average size of 16 cm. Milling and crushing stages continue to further reduce ore size. Depending on the method of extraction, uranium is dissolved in an appropriate leach solution and following subsequent recovery and precipitation steps ammonium diu-

ranate ($(NH_4)U_2O_7$), known as yellow cake is obtained. Finally, for the purpose of marketing, ammonium diuranate is then calcinated to produce triuranium octoxide (U_3O_8) or uranium dioxide (UO_2) as the final products [99, 101, 102]. Sulfuric acid and carbonate leaching have been two main approaches in uranium leach processing. In both processes, the aggressive leaching conditions (i.e. high temperature and high standard redox potentials) resulted in dissolving many other co-existing metals such as Mn, Fe, W, Sb and Mo as an impurity. Hence, concentration and purification of uranium mother liquor are essential in between uranium leaching and precipitation steps [33].

Ion exchange and solvent extraction methods are typical routes for concentration and purification of uranium from its primary solution. Both methods have their inherent advantages/disadvantages and choice of which is highly dependent on the mineralogy and presence of counter metal ions in the ores. Comparing to solvent extraction, uranium recovery by ion exchange method is preferred because the ion exchange process is safe due to the low toxicity of the media and negligible fire risk. Furthermore, ion exchange route can be used effectively for lower grade ores or systems with difficult liquid–solid separation characteristic [98]. IEXRs are applied to both acidic and carbonate leach slurries and can be used directly for efficient extraction of uranium. Strong base IEXRs containing quaternary ammonium surface functionality are the most general resins that are used for uranium recovery. Equations (9.17) and (9.18) described the reactions for the resin loading of uranyl anions in acidic or carbonate leach, respectively [98].

$$UO_2(SO_4)_3{}^{4-} + 4| - NR_3X \rightarrow (| - NR_3)_4UO_2(SO_4)_3 + 4X^- \qquad (9.17)$$

$$UO_2(CO_3)_3{}^{4-} + 4| - NR_3X \rightarrow (| - NR_3)_4UO_2(CO_3)_3 + 4X^- \qquad (9.18)$$

where R and X stand as grafted alkyl group on the resin backbone and quaternary amine counter ion, respectively. Ore mineralogy, as well as the presence of counter metals, are important parameters influencing uranium recovery from its ores. More than 185 uranium minerals are known. Uraninite (UO_2), coffinite ($U(SiO_4)_{1-x}(OH)_{4x}$) and utanothorite ($(U, Th)SiO_4$) are generally known as tetravalent uranium ores.

Carnotite ($K_2(UO_2)_2(VO_4)_2 \cdot 3H_2O$), autunite ($Ca(UO_2)_2(PO_4)_2 \cdot 10 - 12H_2O$) and uranophane ($Ca(UO_2)_2(HSiO_4)_2 \cdot 5H_2O$) are some other less known uranium ores with the hexavalent characteristic. In some cases, oxidation as additional processing is necessary for uranium extraction [99].

Uptake ability, as well as uranium selectivity of IEXRs, vary with the nature of the resin functionality, matrix of polymer and method of application. Pore characteristics of the prepared resins have a crucial effect on the adsorption properties of uranium. Kabay et al. [103] investigated the effect of the solvating diluent agent on structural and uranium uptake ability of lightly crosslinked poly acrylonitrile divinylbenzene resins. The results prove that the thermodynamic interactions between solvent and polymer affect the physical pore structure of the resin. As summarized in Table 9.14,

Table 9.14 Effect of the diluent agent on structural and uranium uptake ability of prepared acrylonitrile resin

Solvating agent	Solubility parameter $(cal/cm^3)^{0.5}$	Specific surface area (m^2/g)	Pore volume (cm^3/g)	Average pore radius (nm)	UO_2^{2+} uptake ability
Toluene	8.9	22.5	0.8	69	0.77
Dichloroethane	9.8	28.2	0.363	22	0.91
Tetrachloroethane	9.8	31.3	0.289	22.2	0.96
Chloroform	9.4	28.8	0.366	22.1	0.94
Methyl isobutyl ketone	8.4	22.4	0.789	59.3	0.81
O-Dichlorobenzen[a]	10	26.9	0.531	33.8	0.94

[a]1,2-Dichlorobenzene

the differences between solubility parameters of polymer and solvating agent can dictate the pore structure of the resulted resins. It was found that dichloroethane, tetrachloroethane and chloroform are responsible for the formation of porous polyacrylonitrile base resins with high specific surface area and low pore size, which improve uranium uptake ability.

Acidic leaching is more favourable to uranium recovery from its resources due to the lower temperature and decreased leaching time processing. In an experimental investigation [104], the optimum leach condition was identified to the recovery of uranium from acidic pregnant leach solution by synthesized strongly acidic IEXR (Dowex DVB gel type resin) with different degrees of crosslinking. The experimental results show an important fact that under the low concentration of sulfuric acid (0.1 mol/lit), $UO_2(SO_4)_3^{4-}$ is the predominant stable form of uranium sulfate and leach solution with the low concentration of sulfuric acid as an optimum leach condition of uranium. UO_2SO_4 and $UO_2(SO_4)_2^{2-}$ are also another stable sulfate forms of uranium (Fig. 9.25).

Resins with a higher degree of crosslinking also behave more efficiently in terms of uranium selectivity and uptake ability because of lower swelling and smaller water content. On the other hand, as revealed in Fig. 9.26, resins with higher crosslinking density show satisfied uranium selectivity.

The selectivity characteristic of IEXRs can be improved by tuning their structural properties. As an example, a higher percentage of the crosslinking agent in resins causes the increase in uranium loading capacity whereas the kinetics of adsorption decreases. The reason for such behaviour may be due to the fact that increase in the percentage of crosslinking agent results in an increase in the resin functional groups density but decrease in the interdiffusion coefficient of the exchange ions. Table 9.15 makes a comparison in uranium uptake capacity in resins with a similar backbone (styrene backbone) but different percentages of divinylbenzene (DVB) as a crosslinking agent [105].
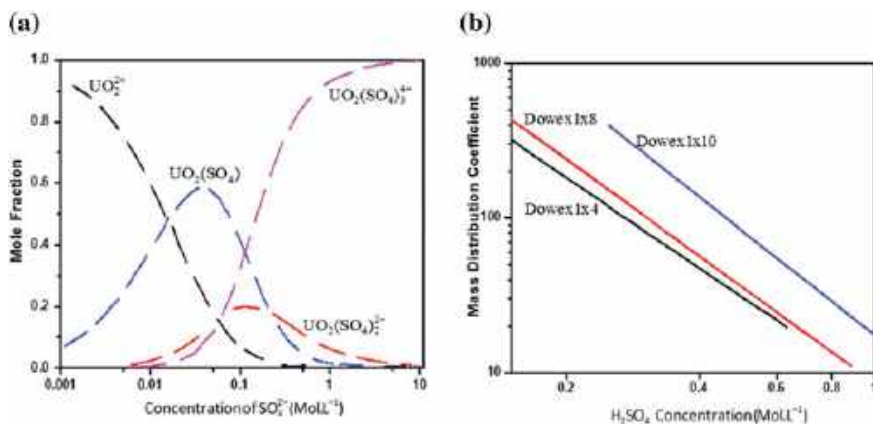
Fig. 9.25 Effect of SO_4^{2-} concentration on uranium sulfate mole fraction (**a**). Mass distribution coefficient of uranium as a function of H_2SO_4 concentration for ion exchange resins with the different degrees of crosslinking (**b**) [104]
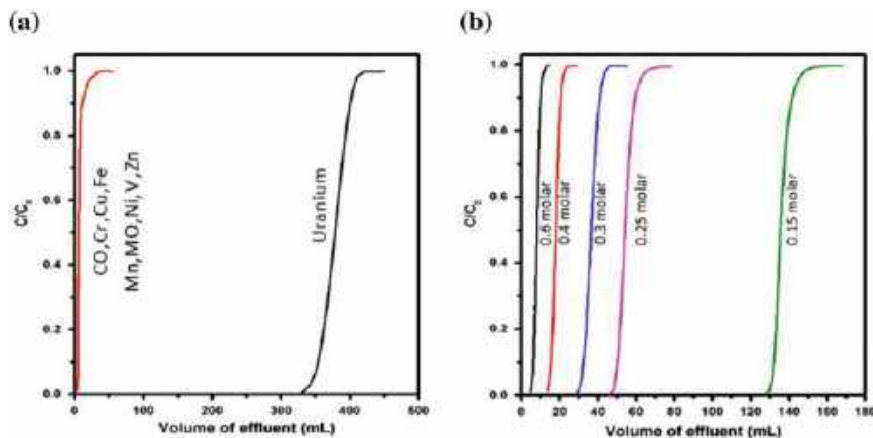

Fig. 9.26 Breakthrough and metal anion selectivity in Dowex1X10 ion exchange resin (**a**). Effect of H_2SO_4 concentration on uranyl anion breakthrough in Dowex1X10 ion exchange resin (**b**) [104]

Table 9.15 Effect of crosslinking content on uranium uptake capacity of styrene backbone resin

Percentage of crosslinking agent (%)	Uranium content at equilibrium (g/L)	The rate of approach to the equilibrium ($S^{-1} \times 10^6$)
2	15.7	437
4	27.6	176
8	42.9	79

Table 9.16 Effect of surface functional groups on uranium loading capacity of some commercial resins

Commercial resin	Resin structure	Uranium loading capacity (g/L)	Rate of approach to equilibrium $(S^{-1} \times 10^6)$
IRA400	Conventional strong base	45.8	43
BRS76	High-density strong base	45	56
XE299	Conventional weak base	23.8	31
WBR6	High-density weak base	30.7	33

Table 9.17 Effect of cobalt poisoning on uranium uptake ability of A101DU resin

Cobalt content on the resin (g/L)	Uranium loaded on resin (g/L)	The rate of approach to equilibrium[a] $(s^{-1} \times 10^6)$	Initial loading rate $(g/L^{-1} min^{-1})$
0	44	45.3	0.95
0.27	43	8.2	0.54
0.49	38	9.1	0.45
1.35	34	4.7	0.24
10.02	22.5	1.1	0.08

[a]The rate of approach to equilibrium refers to the term of $D\pi^2 r^{-2}$ in quadratic driving force equation of $Log\{[U]_e^2\} - [U]_t\} = D\pi^2 r^{2-}t + cons$ where D, r, U_e and U_t stand as average interdiffusion coefficient, the radius of resin beads, uranium concentration at equilibrium and relevant time

Compared to the weak base resins, strong base resins containing quaternary amine functional groups have greater attraction force for anionic uranium species. As shown in Table 9.16, the adsorption capacity and rate of extraction of uranium are better with strong base resins [105].

In some cases like South Africa gold mines, uranium is a by-product of the gold recovery process. In these mines, the presence of cobalt, pentacyanide $[CO(CN)_5]^{3-}$ and polythionate species in acidic media depress uranium extraction due to the resin poisoning. To overcome this drawback, acid leach of uranium is favoured before cyanidation of the residual for gold recovery. However, returning any solution from gold recovery circuit that still contains cobalt cyanide would cause a similar problem. The experimental results show that in fresh solutions, $[CO(CN)_5 \cdot H_2O]^{2-}$ will polymerize in the resin pores to form $[CO(CN)_6]^{3-}$ as its most stable form and poisoning the resin. As shown in Table 9.17, the results prove that cobalt poisoning ends in the decrease in uranium uptake capacity of the poisoned resins. Uranium loading capacity of the poisoned resins can reduce up to 50% [105].

It should be noted that polymerization kinetics of cobalt cyanide is slow, therefore, most of the $[CO(CN)_5 \cdot H_2O]^{2-}$ would be eluted before it has time to polymerize. However, once the resin is poisoned, it can be regenerated completely by treating resin with 20% ammonium thiocyanate solution followed by washing with strong acids (HCl or H_2SO_4).

Mining of uranium ores, hydrometallurgical processing as well as its industrial usages such as a power plant are potential sources of radioactive pollution. Since uranium ions often accumulate in the environment (because of long half-life), they create a serious long-term environmental hazard. So, it is necessary to find a viable solution for storing of industrial nuclear fuel cycle effluents. Recovery of wasted uranium from effluents and its recirculation into the industrial processes would be an effective alternative to solve problems related to storing of uranium effluent [15, 99, 106]. Seneda et al. [107] proposed a new mechanism to facilitate the recovery of the uranium contained in a residual stream of a nuclear research reactor. The mechanism involved the recovery of uranium fluoride by IEXRs and its exchange from fluoride $UO_2F_4{}^{2-}$ to well-retained uranium carbonate $UO_2(CO_3)_3{}^{4-}$ complex inside the resin. On the other hand, it is preferred to first separate uranium fluoride from effluent solution using ion exchange resin (in this study commercial type Rohm and Haas IRA-458 resin), after that elution and conversion of the adsorbed $UO_2F_4{}^{2-}$ ions to $UO_2(CO_3)_3^{4-}$ will be carried out simultaneously in diluted alkaline carbonate medium (0.2 M). This simultaneous elution and conversion of uranium can facilitate the decontamination of eluent and recovery of uranium into the fuel cycle. Uptake ability of uranium from ammonium fluoride solution is highly pH dependent and the recommended pH for recovery operation is in the range of 9.5–10 (~99.8% uranium was recovered). At pH values higher than 10, the possibility of uranium ions precipitation inside resin is high. Effective conversion and removal of uranium ions (99%) are also achievable by using approximately 4-bed volume (BV) of diluted sodium carbonate solution. From the literature, it can be understood that the selectivity sequence of presented anions for resins in a carbonate multicomplex anions solution is $[UO_2(CO_3)_3]^{4-} \gg NO_3{}^- \gg SO_4{}^{2-} \approx CO_3{}^{2-} > HCO_3{}^- > Cl^-$ and the optimum pH range in uranium selectivity and uptake ability is highly sensitive to the solution composition. In the nuclear fuel cycle, generation of an alkaline solution containing uranium with a concentration higher than 120 mg/L as effluent is common. Hence, recovery of uranium from its solution has the advantage of saving this valuable element and inhibiting environmental hazards. The alkaline effluent generally contains fluoride, carbonate and ammonia in high concentrations around 112, 55 and 80 g/L, respectively. The adsorption of the uranyl complex is strongly dependent on the percentage of other anions competing with uranium to occupy active sites of resins. In this regard, Ladeira et al. [108] assessed the uranium uptake ability of three commercial resins in an alkaline solution containing carbonate, fluoride and ammonia inions. Experimental trials were carried out under different solution pH values varying from 9.2 to 10.4 and initial uranium concentration of 100 mg/L. It was found that the presence of an excessive amount of carbonate and fluoride can inhibit uranium recovery effectiveness of resins. On the contrary, a high concentration of ammonia did not seem to affect the uranium uptake efficiency of the resin.
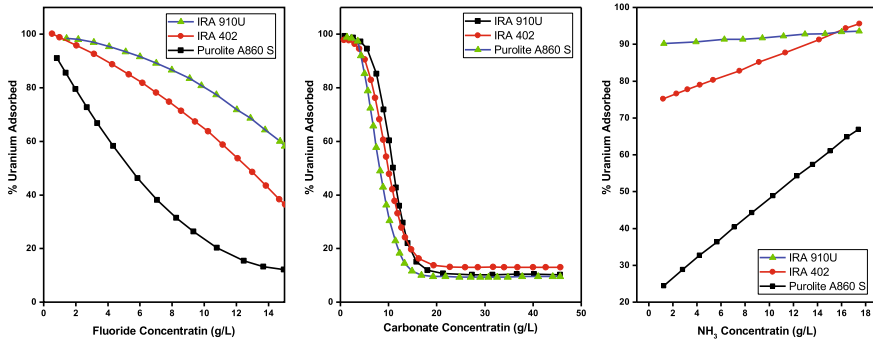
Fig. 9.27 Effect of different ion concentration on uranium uptake ability of commercial resins [108]

Figure 9.27 shows the effect of foreign ions on the percentage of uranium adsorption by resins. As an example, a high concentration of carbonates (usually present in the industrial effluent of nuclear cycles) leads to definite depletion of uranium extraction by resins. Hence, it is proposed that for efficient recovery of uranium, it is essential to keep the concentration of carbonate and fluoride as low as possible, which are considered as the main ions affecting uranium adsorption. The concentration limits of fluoride and carbonate ions to efficiently remove uranium from nuclear effluents have been proposed to be 2.5 and 5 g/L, respectively.

Acid mine drainage is the most serious problem of the uranium mining industry. Generally, during water and oxygen exposure, acid mine drainages oxidized to produce dissolved metals such as sulfates. The presence of a large number of dissolved metals has a high impact on uranium recovery efficiency and environmental contamination hazards. In order to recover uranium as a commercial product to minimize disposal of this element into the environment, Nascimento et al. [109] investigated the impact of process conditions on uranium recovery from Caldas uranium mining[3] acid effluent by weak base IEXRs (Amberlite IRA 93). The elemental analysis of typical raw mine water is presented in Table 9.18.

The experimental results showed that the presence of a large content of a foreign element (Iron sulfate in this study) has a crucial effect on occupancy of resin active sites and reducing the uranium uptake ability. The authors believed that in the case of multicomponent uranium solution, pretreatment of effluent is essential. Iron sulfate was precipitated by using lime solution in the pH range of 3.3–3.8 and then the final solution was subjected to the ion exchange extraction. The elemental analysis of resin loaded before and after iron exchange experiment showed that after iron sulfate precipitation, the uranium uptake ability of resins improved significantly and at a lower concentration of iron ions (8 mg/L) uranium loading capacity increased from 14.5 to 91%.

---

[3]In the southeast of Brazil.

Table 9.18 Chemical and radiochemical analysis of typical raw mine water

Element	Metal content (mg/L)
U	10
Fe	190
SO_4	1300
Ca	51
Al	90
Si	18
Mn	30
Zn	15
pH	2.6
E_H	678 mV

The vent gas from fluidized bed furnace, which is the final step in converting yellow cake to UO_2 usually contains uranium, ammonium and carbon dioxide and is another source of uranium emission into the environment. The furnace exhaust absorbed by water stream in a countercurrent contact tower generating an alkaline uranium-rich effluent. This alkaline effluent is then subjected to ion exchange extraction to readsorption and recovery of the valuable uranium metal. In alkaline solutions, uranium is present in the form of uranyl carbonate complexes ($[UO_2(CO_3)_2]^{2-}$ and $[UO_2(CO_3)_3]^{4-}$) and strong base anion exchangers are the most efficient resins for recovery of uranium. Ladeira et al. [97] investigated the influence of the difference in effluent flow rate on adsorption kinetics of uranium by a commercial IEXRs of Rohm and Hass IRA 910A. The trials were carried out with the different flow rates of 1, 2 and 5 mL/min and the results showed that resins with recommended operation flow rate of 2 mL/min (equal to 5 min retention time) indicated the highest breakthrough of 600 BV and uranium uptake capacity reached to 40 g/L. The shortest elution with the least possible volume of eluate was accomplished with carbonate solution containing CO_3^{2-} (3 molars) and retention time of 10 min. Effective uranium elution (about 99%) was accessible by using around 8 BV of carbonate solution. The maximum uranium concentration in the eluate was 2.7 g/L. In order to reduce chances of contacting with radioactive radiation and effective UO_2^{2+} removal from aqueous media, Guibal et al. [96] investigated the uranium (VI) sorption capacity of the amino magnetic chitosan resin modified with Tetraethylenepentamine (TEPA). The experimental examinations were performed at different initial pHs (from 1.1 to 5.7) to evaluate the effectiveness of solution pH on UO_2^{2+} adsorption. They found that the adsorption kinetics of UO_2^{2+} in TEPA modified chitosan resin had two phases. Initial rapid and slow phases were interpreted as external surface adsorption and intraparticle diffusion adsorption, respectively. It is well known that adsorption in solid media takes place through multistep mechanisms including; (i) external film diffusion, (ii) intraparticle diffusion and (iii) interaction between adsorbate and active sites. About 98% of the initial uranium in solution was removed within the first 30 min of contact and the adsorption kinetics of uranium in chitosan base resin obeyed the pseudo-

second-order rate equation and the authors believed that the chemical adsorption was the rate-determining step. Formation of protonated amine groups (NH_3^+) in strongly acidic media led to the reduction of binding sites for adsorption of UO_2^{2+} and uranium uptake ability of resins decreased in solution media with pH < 4. The maximum uptake ability of uranium was maximal at pH 4.1 due to the availability of both amino and free uranium anions. Further increase in solution pH (above 4.6) also caused precipitation of uranyl hydroxides (($UO_2)_3(OH)_5^{3+}$, $(UO_2)(OH)_2$) on resin pore surface.

In recent years, IEXRs have been used to recover and concentration of uranium from its dilute solution in the quadrivalent complex formed under the controlled pH range of 8–10 and significant advances have been made in improving extraction processes by using IEXRs. Resin technologies have challenges with the reducing of the operation cost, especially in RIP processing of uranium. Both solvent extraction and ion exchange methods have advantages and limitations in progress of uranium extraction. Solvent exchange can be employed in systems with less than 20 ppm suspended solids, while ion exchange is more efficient in systems with more solid content and enabling ion exchange to be used in operating systems with difficult liquid/solid separation characteristic. Using the IEX route alone is only possible if the uranium leach solution is relatively free of impurities. On the other hand, the advantage of the ion exchange method as economically and cost-effective route in uranium plans cannot be achievable unless the downstream solvent exchange circuit reduces significantly or it is eliminated completely. Hence, the sequential combination of ion exchange and solvent extraction offers greater selectivity and higher purity. The solvent exchange has been used to treat high grades of leach solutions (above 0.9 g/L U_3O_8) and required phase contact times of less than 30 s for reaching to equilibrium, while ion exchange kinetics are slow and require high resin inventory. Ion exchange method is also a costly route if it is necessary to neutralize all of the acids present in eluent solution before precipitation.

9.2.5 Removal of Iron and Sulfate Ions from Copper Streams by Ion Exchange Technology

9.2.5.1 Iron Removal

Nowadays Ion exchange technology has been employed widely in hydrometallurgical processes, especially in copper hydrometallurgical solvent extraction-electrowinning (SX-EW) extraction. This technology has been employed to remove impurities from electrolyte solutions and purification of wastewaters. In copper hydrometallurgical SX-EW extraction, a small amount of iron and other impurities are transferred to electrowinning solution and due to the existence of the circuit, these impurities are accumulated in this solution. Generally, low level of iron (about 1–2 g/L) is useful in electrolyte because it controls manganese species in electrowinning (EW) process,

Fig. 9.28 Sulfonated diphosphonic resin structure [110]
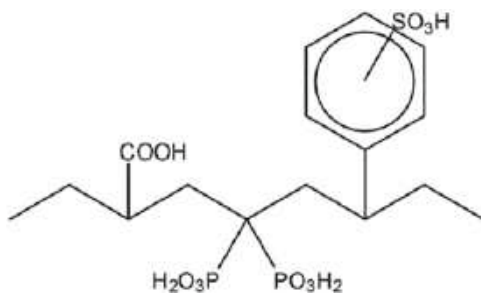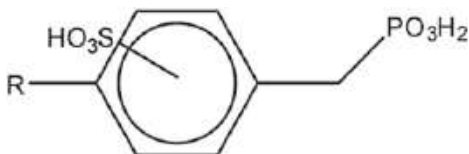

Fig. 9.29 Sulfonated monophosphonic resin structure [110]

but the high concentration of an iron ion in the electrolyte significantly decreases the current efficiency of EW process and affects the properties of produced copper. This is due to the oxidation and the reduction of ferrous and ferric ions present in solution at the EW process [110, 111]. Traditionally, decreasing the iron ion concentration is achieved by bleeding a portion of the EW solution that leads to waste some important species in a solution like cobalt, which is added to electrolyte solution to protect anode from corrosion. Nowadays, ion exchange technology applications to control the iron concentration are extended due to its advantages and simplicity. The removal of iron and sulfate ions from copper streams by various IEXRs has been investigated by several researchers. Table 9.19 presents some important properties of the resins used.

The iron removal from electrowinning electrolyte solution was investigated by McKevitt and Dreisinger [20, 21]. In this study, four chelating cation ion exchange resins, Eichrom Diphonix (sulfonateddiphosphonic), LanXess Lewatit MonoPlus TP-260 (aminophosphonic), Purolite S957 and Generic D416 (sulfonatedmonophosphonic) were used to reduce the iron concentration of solution, which included 30 g/L copper, 220 g/L sulfuric acid and 1.3–1.4 g/L iron in ferric state. Some investigations showed the adsorption of ferric ions by resins including some specific functional groups like iminodiacetic, picolylamine, sulfonateddiphosphonic, sulfonatedmonophosphonic and aminophosphonic groups. In solutions at low pH values, the resins with sulfonic and phosphonic groups were found suitable because sulfonic group preserved the performance of resin in solutions at low pH values, but this group did not adsorb selectively. On the other hand, phosphonic group selectively reacted with ions. The performance of the resin including phosphonic group decreased with decreasing the pH. Figures 9.28 and 9.29 illustrate the sulfonated di and monophosphonic resins structures. These types of resins include both sulfonic and phosphonic functional groups.

Table 9.19 Some properties of ion exchange resins for the removal of iron and sulfate ions

Ion exchanger grade	Resin network	Functional Groups	Type	Physical structure	Exchange capacity (mmol/g)	Solution
Eichrom Diphonix	–	Diphosphonic Sulfonic Carboxylic	Chelating	Gel	5.6 in H^+ form	Copper electrolyte
Lewatit TP-260	st-DVB	Aminomethylphosphonic	Chelating	Macroporous	3.6 in Na^+ form	Copper electrolyte
Purolite S957	st-DVB	Monophosphonic Sulfonic	Chelating	Macroporous	8 in H^+ form	Copper electrolyte
Generic D416	–	Monophosphonic Sulfonic	Chelating	Macroporous	–	Copper electrolyte
Lewatit K6362	st-DVB	Quaternary amine Type I	Strong base	Gel	1.7 in Cl^- form	Wastewater

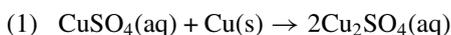*Note* st-DVB means polystyrene crosslinked with divinylbenzene
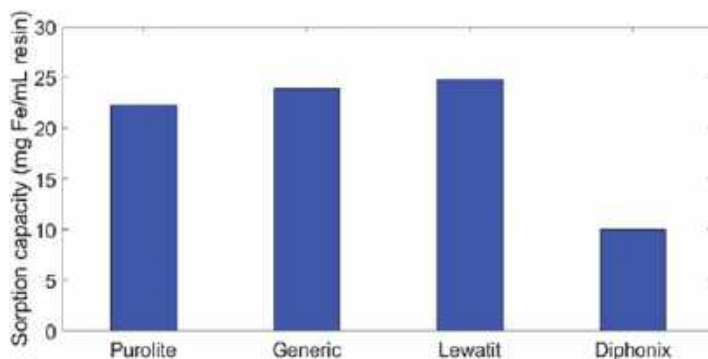
Fig. 9.30 Sorption capacities of various resins in contact with identical electrowinning solution [112]

According to the results of loading experiments in a fixed bed column, all used resins in this investigation were found suitable for adsorbing iron ions. However, the sorption capacities of Purolite, Generic and Lewatit (aminophosphonic and sulfonatedmonophosphonic resins) were significantly higher than Diphonix. Figure 9.30 exhibits the reported sorption capacities of different resins [112].

The elution from used resins was carried out with a process including reduction of adsorbed ferric ions to ferrous because of the fact that the affinity of ferrous ions to resin structure was very low. The elution process was completely done in two steps and the chemistry equations associated with each step can be described by (9.8) and (9.9). In the first step, cupric sulfate according to (9.8) was converted to cuprous sulfate by passing copper electrowinning electrolyte over a bed of copper cuttings and in the second step, loaded resins were eluted by cuprous sulfate according to (9.19) [20].

(1) $CuSO_4(aq) + Cu(s) \rightarrow 2Cu_2SO_4(aq)$

(2) $Cu_2SO_4(aq) + \overbrace{2Fe(Resin)_3(s)}^{\text{loaded resin}} + 3H_2SO_4(aq) \rightarrow 2CuSO_4(aq)$

$$+ \overbrace{6H\ Resin(s)}^{\text{eluted resin}} + 2FeSO_4(aq) \tag{9.19}$$
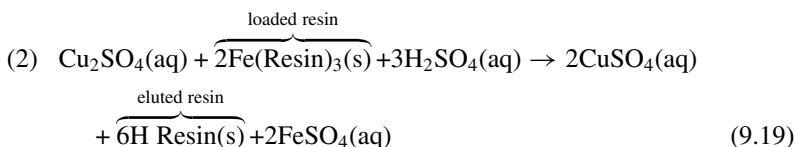
This elution method was used in FENIX Iron Control System at Mt. Gordon Operations in Queensland, Australia. This system significantly decreases reagent consumption like acid, cobalt and sulfate for electrowinning and lime for neutralization of the raffinate bleed [113]. In this investigation, the elution of loaded resins was carried out and according to the results Purolite, Generic and Diphonix resins (sulfonated mono and diphosponic resins) were eluted noticeably faster than Lewatit (aminophosphonic resin). Figure 9.31 shows the minimum time required to completely elute each resin.
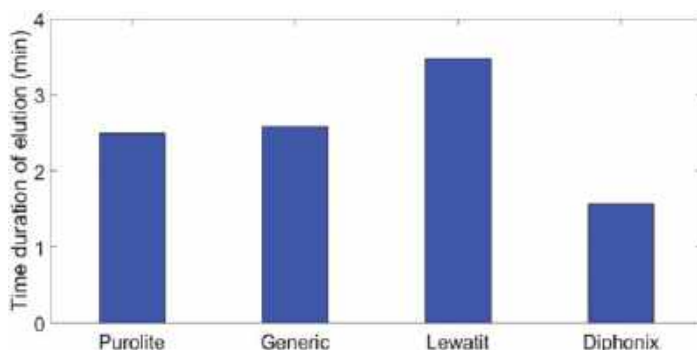
Fig. 9.31 Minimum time duration to achieve complete elution of various resins [112]

The effect of other metal impurities in electrowinning solution on sorption efficiency of these resins was investigated. The used solutions included copper (33–38.8 g/L), nickel (13.6–15.6 g/L), cobalt (10–12 g/L), iron (2–2.3 g/L), bismuth (0.29–0.44 g/L), antimony (0.12–0.29 g/L) and arsenic (2.6–2.9 g/L). Bath experiments in various volumes of solution to resin ratios were conducted. Figure 9.32 illustrates the results of sorption capacity of each resin for 100:1 ratio of volume solution to the resin. According to the results, Diphonix resin loaded the most copper, nickel and cobalt while the Lewatit resin loaded the least amount of these elements. It seems that sulfonic group in Purolite, Generic and Diphonix resins causes the non-selective sorption of various metal cations at low pH, while Lewatit is not included in this group and this leads to decrease the sorption of impurities by this resin; however, the sorption capacity of bismuth in this resin due to aminophosphonic groups in its structure [114] was higher than other resins. It seems that, despite high sorption capacity of Purolite resin, total impurities that were adsorbed by this resin were significantly lower than others. The iron sorption experiments by this resin with solutions including identical iron (2.1 g/L) and different antimony concentrations (0.01–0.25 g/L) showed that iron removal capacity of resin slightly decreased from 30.6 mg Fe/mL resin to 27.6 mg/mL (<10%). Thus, the presence of impurities slightly reduces the iron sorption capacity of the resin. According to the above description, authors concluded that the performance of resins that include sulfonatedmonophosphonic groups like Purolite S957 and Generic D416 in contact with a copper electrolyte solution at low pH is significantly better than other resins.

A complete investigation into iron removal from electrowinning solution by Purolite S957 resin was conducted by Izadi et al. [111]. The used solutions were from the electrowinning electrolyte solution supplied by Sarcheshmeh Copper Complex, Iran. The solutions contained various metal ions like copper, iron, cobalt and magnesium with concentration of about 33, 3, 0.1 and 1.68 g/L, respectively, and the pH value of the solution was about 1.2.

Equilibrium and kinetics experiments were carried out and the results indicated Sips isotherm and pseudo-second-order kinetics models were fitted by experimental
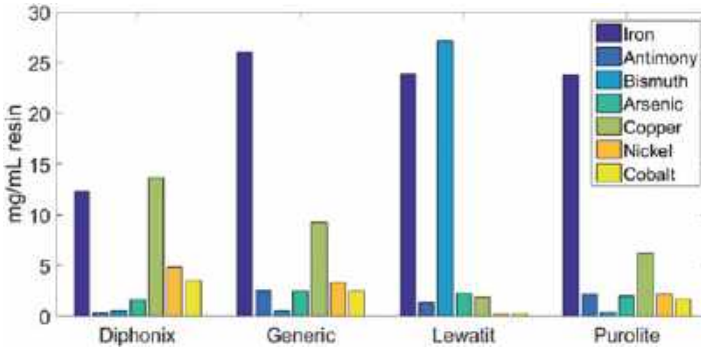
Fig. 9.32 Impurity sorption by various ion exchange resins [114]

data very well. It is important to note that Sips isotherm model, (20), is a com-
bined form of traditional Langmuir and Freundlich isotherms in which some main
limitations related to those isotherms were improved [115].

$$q_e = \frac{q_{ms}a_s c_e^{\beta}}{1 + a_s c_e^{\beta}} \tag{20}$$

In this equation, C_e, q_m and q_e are equilibrium concentration, equilibrium capac-
ity and maximum capacity of resin, respectively. The results showed that the max-
imum removal capacity of iron and the rate constant that was calculated by Sips
isotherm and pseudo-second-order kinetics models were about 42 mg Fe/g resin and
0.0408 g/mg min. On the other hand, the results of continuously fixed bed experi-
ments at various bed heights and flow rates indicated the iron and copper removal
capacities of resin in the column were found to be 26.5–37.5 mg Fe/g resin and
106–1.5 mg Cu/g resin. These findings confirmed that this resin is suitable to remove
iron selectively from copper electrowinning electrolyte solution.

The effect of pH on the performance of this resin was investigated and results
indicated that with increasing the pH from 0.5 to 1.3, the removal efficiency of
resin increased only 5%; therefore, authors concluded that the pH of solution does
not affect the capacity of this resin. Figure 9.33 shows the results of iron removal
efficiency by the resin at various pHs of the solution.

In this study, loaded resins were eluted with hydrochloric acid and according to
the results, the optimum concentration of the acid that eluted resins completely was
found to be 30% w/w. Figure 9.34 shows the iron removal efficiency of regenerated
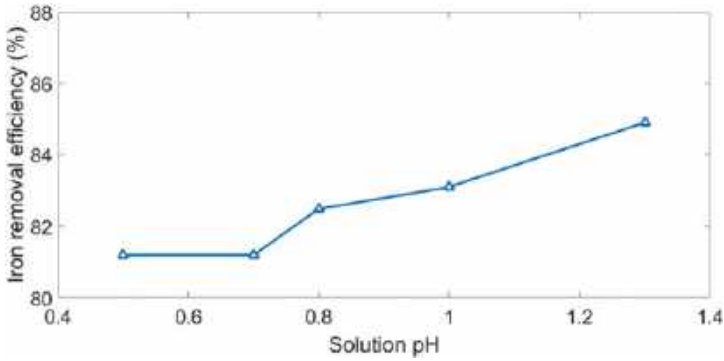resin, which was eluted with different concentrations of hydrochloric acid solutions.

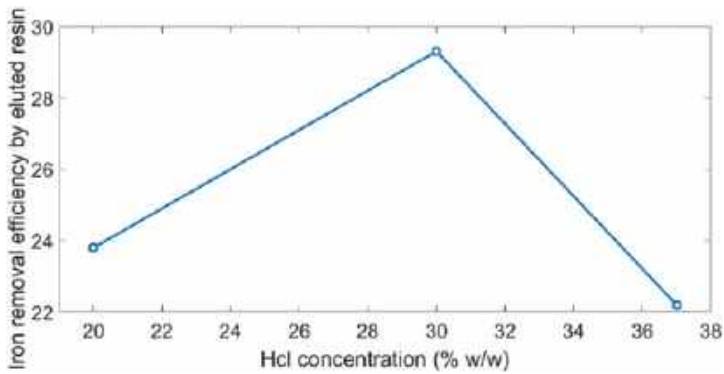**Fig. 9.33** The effect of pH on the performance of Purolite S957 resin [111]

Fig. 9.34 The effect of HCl concentration on the elution of Purolite S957 resin [111]

9.2.5.2 Sulfate Removal

One of the major pollutants existing in copper wastewater is sulfate ion. The removal of this ion was investigated by Haghsheno et al. [116]. They employed an anion exchange resin (Lewatit K6362) and used solutions which were prepared from several points of Sarcheshmeh copper complex wastewater lines. The solutions contained sulfate about 500–600 mg/L at a pH of 9. Equilibrium experiments were carried out and according to the results, isotherm data were fitted very well by both Langmuir and Freundlich models. The maximum sorption capacity, which was calculated by the Langmuir model was 166.67 mg/g. This finding indicated that the resin was suitable to remove sulfate ion from solution. The results of fixed bed column experiments at various bed heights, feed concentrations and inlet flow rates also confirmed the high performance of this resin. Figure 9.35 shows one of the breakthrough curves that were obtained in a fixed bed column with a feed solution containing 500 mg/L sulfate concentration.
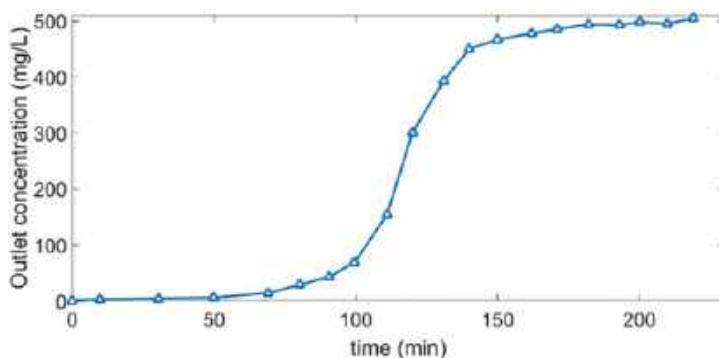
Fig. 9.35 The breakthrough curve of fixed bed column experiment [116]

A kinetic model based on the reversible process of ion exchange was fitted by time dependence data and according to the results, forward rate constant for the removal of sulfate ion was higher than the backward rate constant.

9.3   Conclusions

In the recent decade, considerable research has been aimed at processing of IEXRs in the recovery of metal ions from their pregnant solutions and the topics touched upon in the present study illustrate the wide range application of IEXRs in the hydromet-allurgical industry. These porous adsorbents can be used for the primary recovery of metals such as Au, Ag and U or selectively removal of low levels of impurities from concentrated solutions. A large variety of IEXRs are commercially available including weak, medium and strong base resins to be used efficiently in RIP and RIS solutions and the equipment design and processing incorporating IEXRs are varied and can be optimized depending on ore mineralogy.

Faster leaching kinetics, non-toxicity, easy elution and ambient temperature operation and regeneration are some advantages associated with using IEXRs in hydromet-allurgical industry. However, high-cost investment, poor selectivity, low mechanical stability and resin poisoning are some existed drawbacks of using IEXRs.

Resin functionalization, as well as its surface morphology, has been a key factor in improving the sorption kinetics and selectivity of the resulted adsorbents. Functionalized resin with sort alkyl chain results in the formation of resins with more hydrophilic characteristic, which leads to higher sorption kinetic but lower metal ion selectivity. Moreover, the complexation ability of resins is more important than ion exchangeability. In this regard, besides the nature of functionalized groups (soft or hard electron donor characteristic), the selectivity of IEXRs can be improved by increasing the degree of crosslinking and controlling the solution pH through pre-precipitation in two-step extraction. It was proved that increasing crosslinking has

a slight effect on sorption kinetic but plays a key role in the distribution of divalent and multivalent foreign metal ions such as Ni, Zn and Co especially when the pH solution is above 10 and the resin functional groups are not fully protonated. Recently, microwave-assisted surface functionalized resins have been found useful in case of selective sorption of metals. It seems that internal heating associated with microwave energy leads to the formation of porous resins with exceptional surface functionalized characteristics, which cannot be achievable under the conventional method. From an environmental point of view, IEXRs have played a crucial role in the reduction of contaminants in waste streams and also in the supply of water with suitable quality. Finally, it is concluded that in near future, the advances in IEXRs technology with specific lixiviant systems coupled with the development of more selective resins and appropriate leach systems will allow the processing of concentrated liquors or processing routes to successfully reject impurities .

References

1. Grumett P (2003) Precious metal recovery from spent catalysts. Platin Met Rev 47:163–166
2. Das N (2010) Recovery of precious metals through biosorption—a review. Hydrometallurgy 103:180–189. https://doi.org/10.1016/j.hydromet.2010.03.016
3. Maruyama T, Terashima Y, Takeda S, Okazaki F, Goto M (2014) Selective adsorption and recovery of precious metal ions using protein-rich biomass as efficient adsorbents. Process Biochem 49:850–857. https://doi.org/10.1016/j.procbio.2014.02.016
4. Slater MJ (2002) Ion exchange and solvent extraction: a series of advances volume 15. Hydrometallurgy 64:79–80. https://doi.org/10.1016/s0304-386x(02)00007-5
5. Verbych S, Hilal N, Sorokin G, Leaper M (2005) Ion exchange extraction of heavy metal ions from wastewater. Sep Sci Technol 39:2031–2040. https://doi.org/10.1081/ss-120039317
6. Williams A, Frasca V (1999) Ion-exchange chromatography. Curr Protoc Protein Sci 8.2.1–8.2.30. https://doi.org/10.1002/0471140864.ps0802s15
7. Tavlarides LL, Bae JH, Lee CK (1987) Solvent extraction, membranes, and ion exchange in hydrometallurgical dilute metals separation. Sep Sci Technol 22:581–617. https://doi.org/10.1080/01496398708068970
8. van Deventer J (2011) Selected Ion exchange applications in the hydrometallurgical industry. Solvent Extr Ion Exch 29:695–718. https://doi.org/10.1080/07366299.2011.595626
9. Kressman TRE (1950) Ion exchange membranes and resin-impregnated filter paper. Nature 165:568. https://doi.org/10.1038/165568a0
10. Hale DK (1957) Ion exchange technology. Nature 179:723. https://doi.org/10.1038/179723b0
11. De Dardel F (2011) Ion exchange resin properties. Exch Organ Behav Teach J 1–9. http://dardel.info/IX/resin_properties.html
12. Crittenden JC, Trussell RR, Hand DW, Howe KJ, Tchobanoglous G (2012) Ion exchange, in: MWH's water treatment. Princ Des Third Ed 1263–1334. https://doi.org/10.1002/9781118131473.ch16
13. Bhandari VM, Sorokhaibam LG, Ranade VV (2016) Ion exchange resin catalyzed reactions—an overview. Ind Catal Process Fine Spec Chem 393–426. https://doi.org/10.1016/b978-0-12-801457-8.00009-4
14. Van Tonder D, Van Hege B (n.d.) Uranium recovery from acid leach liquors: the optimization of RIP/SX based flowsheets. http://www.saimm.co.za/Conferences/BM2007/241-260_VTonder.pdf. Accessed 29 April 2018
15. Mikhaylenko M, van Deventer J (n.d.) Notes of practical application of ion exchange resins in uranium extractive metallurgy. https://www.purolite.com/dam/jcr:0a5722c6-bdc4-4f43-

b32c-c8df52164304/ScientificPaper_ResinsinUraniumExtractiveMeallurgy.pdf. Accessed 29 April 2018

16. Bernardis FL, Grant RA, Sherrington DC (2005) A review of methods of separation of the platinum-group metals through their chloro-complexes. React Funct Polym 65:205–217. https://doi.org/10.1016/j.reactfunctpolym.2005.05.011

17. Gupta C (2017) Hydrometallurgy in extraction processes, vol II. https://content.taylorfrancis.com/books/downloaddac=C2006-0-08509-X&isbn=9781351439619&format=googlePreview.Pdf. Accessed 27 April 2018

18. Dorfner K (ed) (1991) Ion exchangers. DE GRUYTER, Berlin. https://doi.org/10.1515/9783110862430

19. Syed S (2012) Recovery of gold from secondary sources—a review. Hydrometallurgy 115–116:30–51. https://doi.org/10.1016/j.hydromet.2011.12.012

20. Corti CW, Holliday RJ, Thompson DT (2002) Developing new industrial applications for gold: gold nanotechnology. Gold Bull. 35:111–117. https://doi.org/10.1007/bf03214852

21. Bond GC, Louis C, Thompson DT (2006) Catalysis by gold. Published by Imperial College Press and Distributed by World Scientific Publishing CO. https://doi.org/10.1142/p450

22. Louis C, Pluchery O (2012) Gold nanoparticles for physics, chemistry and biology. Imperial College Press. https://doi.org/10.1142/p815

23. Corti CW, Holliday RJ (2004) Commercial aspects of gold applications: from materials science to chemical science. Gold Bull. 37:20–26. https://doi.org/10.1007/bf03215513

24. Haque KE (1987) Gold leaching from refractory ores—literature survey. Miner Process Extr Metall Rev 2:235–253. https://doi.org/10.1080/08827508708952607

25. Afenya PM (1991) Treatment of carbonaceous refractory gold ores. Miner Eng 4:1043–1055. https://doi.org/10.1016/0892-6875(91)90082-7

26. Chancerel P, Meskers CEM, Hageluken C, Rotter VS (2009) Assessment of precious metal flows during preprocessing of waste electrical and electronic equipment. J Ind Ecol 13:791–810. https://doi.org/10.1111/j.1530-9290.2009.00171.x

27. Zhang T, Gregory K, Hammack RW, Vidic RD (2014) Co-precipitation of radium with barium and strontium sulfate and its impact on the fate of radium during treatment of produced water from unconventional gas extraction. Environ Sci Technol 48:4596–4603. https://doi.org/10.1021/es405168b

28. Awual MR, Ismael M (2014) Efficient gold(III) detection, separation and recovery from urban mining waste using a facial conjugate adsorbent. Sens Actuators B Chem 196:457–466. https://doi.org/10.1016/j.snb.2014.02.055

29. Behbahani M, Najafi F, Amini MM, Sadeghi O, Bagheri A, Hassanlou PG (2014) Solid phase extraction using nanoporous MCM-41 modified with 3,4-dihydroxybenzaldehyde for simultaneous preconcentration and removal of gold(III), palladium(II), copper(II) and silver(I). J Ind Eng Chem 20:2248–2255. https://doi.org/10.1016/j.jiec.2013.09.057

30. Jha MK, Gupta D, Lee J, Kumar V, Jeong J (2014) Solvent extraction of platinum using amine based extractants in different solutions: a review. Hydrometallurgy 142:60–69. https://doi.org/10.1016/j.hydromet.2013.11.009

31. Wilson AM, Bailey PJ, Tasker PA, Turkington JR, Grant RA, Love JB (2014) Solvent extraction: the coordination chemistry behind extractive metallurgy. Chem Soc Rev 43:123–134. https://doi.org/10.1039/c3cs60275c

32. Khaliq A, Rhamdhani M, Brooks G, Masood S (2014) Metal extraction processes for electronic waste and existing industrial routes: a review and Australian perspective. Resources 3:152–179. https://doi.org/10.3390/resources3010152

33. Calmon C (2018) Ion exchange pollution control. CRC Press, Boca Raton. https://doi.org/10.1201/9781351073868

34. Dwivedi AD, Dubey SP, Hokkanen S, Fallah RN, Sillanpää M (2014) Recovery of gold from aqueous solutions by taurine modified cellulose: an adsorptive–reduction pathway. Chem Eng J 255:97–106. https://doi.org/10.1016/j.cej.2014.06.017

35. Lampinen M, Laari A, Turunen I (2015) Ammoniacal thiosulfate leaching of pressure oxidized sulfide gold concentrate with low reagent consumption. Hydrometallurgy 151:1–9. https://doi.org/10.1016/j.hydromet.2014.10.014

36. Guo B, Peng Y, Espinosa-Gomez R (2014) Cyanide chemistry and its effect on mineral flotation. Miner Eng 66–68:25–32. https://doi.org/10.1016/j.mineng.2014.06.010

37. Sparrow GJ, Woodcock JT (1995) Cyanide and other lixiviant leaching systems for gold with some practical applications. Miner Process Extr Metall Rev 14:193–247. https://doi.org/10.1080/08827509508914125

38. Fleming CA, Cromberge CG (1956) South African Institute of Mining and Metallurgy. J S Afr Inst Min Metall. https://journals.co.za/content/saimm/84/5/AJA0038223X_1435. Accessed 27 April 2018

39. Zhang H, Dreisinger DB (2002) The adsorption of gold and copper onto ion-exchange resins from ammoniacal thiosulfate solutions. Hydrometallurgy 66:67–76. https://doi.org/10.1016/s0304-386x(02)00077-4

40. Xu B, Kong W, Li Q, Yang Y, Jiang T, Liu X (2017) A review of thiosulfate leaching of gold: focus on thiosulfate consumption and gold recovery from pregnant solution. Metals (Basel) 7:222. https://doi.org/10.3390/met7060222

41. Harris WI, Stahlbush JR, Pike WC, Stevens RR (1992) The extraction of gold from cyanide solutions using moderate base polyamine ion exchange resins. React Polym 17:21–27. https://doi.org/10.1016/0923-1137(92)90566-k

42. Atluri VP (1987) Recovery of gold and silver from ammoniacal thiosulfate solutions containing copper by resin ion exchange method. The University of Arizona. http://arizona.openrepository.com/arizona/handle/10150/276566. Accessed 1 April 2018

43. Zhang H (2003) 264 D Dreisinger. US Patent 6, 632, undefined 2003, Gold recovery from thiosulfate leaching, 6,632,264. https://patents.google.com/patent/US6632264B2/en. Accessed 1 April 1 2018

44. O'Malley G (n.d.) Recovery of gold from thiosulfate solutions and pulps with anion exchange resins. Murdoch University, Perth, Australia

45. Zhang H, Dreisinger DB (2002) The adsorption of gold and copper onto ion-exchange resins from ammoniacal thiosulfate solutions. Hydrometallurgy 66:67–76. https://doi.org/10.1016/s0304-386x(02)00077-4

46. Black SB (2006) The thermodynamic chemistry of the aqueous copper-ammonia thiosulfate system. Murdoch University. http://researchrepository.murdoch.edu.au/id/eprint/336/

47. K.A. Ter-Arakelyan, K.A. Bagdasaryan, A.G. Oganyan, R.T. Mkrtchyan, G.G. Babayan, On technological expediency of sodium thiosulphate usage for gold extraction from raw material, Izv VUZ Tsvetn Met. No 5 Pp 7276 1984. (1984)

48. O'Malley GP (2002) Recovery of gold from thiosulfate solutions and pulps with anion-exchange resins. http://researchrepository.murdoch.edu.au/id/eprint/3355/. Accessed 31 Mar 2018

49. Dong Z, Jiang T, Xu B (2017) Recovery of gold from pregnant thiosulfate solutions by the resin adsorption technique. Metals (Basel) 7:1–17. https://doi.org/10.3390/met7120555

50. Grosse AC, Dicinoski GW, Shaw MJ, Haddad PR (2003) Leaching and recovery of gold using ammoniacal thiosulfate leach liquors (a review). Hydrometallurgy 69:1–21. https://doi.org/10.1016/s0304-386x(02)00169-x

51. Kononova ON, Kholmogorov AG, Kononov YS, Pashkov GL, Kachin SV, Zotova SV (2001) Sorption recovery of gold from thiosulphate solutions after leaching of products of chemical preparation of hard concentrates. Hydrometallurgy 59:115–123. https://doi.org/10.1016/s0304-386x(00)00148-1

52. Vargas C, Navarro P, Araya E, Pavez F, Alguacil FJ (2006) Recovery of gold from solutions with ammonia and thiosulfate using activated carbon. Rev Metal 42. https://doi.org/10.3989/revmetalm.2006.v42.i3.22

53. Atluri VP (1987) Recovery of gold and silver from ammoniacal thiosulfate solutions containing copper by resin ion exchange method. The University of Arizona. http://webcache.googleusercontent.com/searchq=cache, http://arizona.openrepository.com/arizona/handle/10150/276566. Accessed 31 Mar 2018

54. Mohansingh R (n.d.) Adsorption of gold from gold copper ammonium thiosulfate complex onto activated carbon and ion exchange resins. University of Nevada, Reno, NV, USA

55. Arima H, Fujita T, Yen W-T (2003) Gold recovery from nickel catalyzed ammonium thiosulfate solution by strongly basic anion exchange resin. Mater Trans 44:2099–2107. https://doi.org/10.2320/matertrans.44.2099

56. Navarro P, Vargas C, Reveco V, Orellana J (2006) Recovery of gold from ammonia-thiosulfate media with amberlite IRA-410 ionic exchange resin. Rev Metal 42:354–366

57. Fleming CJ, McMullen J, Thomas KG (2003) Recent advances in the development of an alternative to the cyanidation process: thiosulfate leaching and resin in pulp. Miner Metall Process 20:1–9

58. Nicol MJ, O'Malley GP (2001) Recovery of gold from thiosulfate solutions and pulps with ion-exchange resins. Cyanide Soc Ind Econ Asp 469–483

59. Jeffrey MI, Hewitt DM, Dai X, Brunt SD (2010) Ion exchange adsorption and elution for recovering gold thiosulfate from leach solutions. Hydrometallurgy 100:136–143. https://doi.org/10.1016/j.hydromet.2009.11.003

60. Pilśniak M, Trochimczuk AW (2007) Synthesis and characterization of polymeric resins with aliphatic and aromatic amino ligands and their sorption behavior towards gold from ammonium hydroxide solutions. React Funct Polym 67:1570–1576. https://doi.org/10.1016/j.reactfunctpolym.2007.07.039

61. Pilśniak MR, Trochimczuk AW (2014) Selective recovery of gold on functionalized resins. Hydrometallurgy 146:111–118. https://doi.org/10.1016/j.hydromet.2014.03.016

62. Warshawsky A, Kahana N, Kampel V, Rogachev I, Meinhardt E, Kautzmann R, Cortina JL, Sampaio C (2000) Ion exchange resins for gold cyanide extraction containing a piperazine functionality. 1. Synthesis and physico-chemical properties. Macromol Mater Eng 283:103–114. https://doi.org/10.1002/1439-2054(20001101)283:1%3c103::aid-mame103%3e3.0.co;2-j

63. Cyganowski P, Jermakowicz-Bartkowiak D (2014) Piperazine functionalized resins for Au(III), Pt(IV), and Pd(II) sorption. Sep Sci Technol 49:1689–1699. https://doi.org/10.1080/01496395.2014.906460

64. Yi-Yong C, Xing-Zhong Y (1994) Synthesis and properties of 1-(2-aminoethyl) piperazine resin used in the sorption of the platinum group and gold ions. React Polym 23:165–172. https://doi.org/10.1016/0923-1137(94)90017-5

65. Cyganowski P, Garbera K, Leśniewicz A, Wolska J, Pohl P, Jermakowicz-Bartkowiak D (2017) The recovery of gold from the aqua regia leachate of electronic parts using a core–shell type anion exchange resin Recovery of gold from the aqua regia leachate of electronic parts. J Saudi Chem Soc 21:741–750. https://doi.org/10.1016/j.jscs.2017.03.007

66. He W, Li G, Ma X, Wang H, Huang J, Xu M, Huang C (2006) WEEE recovery strategies and the WEEE treatment status in China. J Hazard Mater 136:502–512. https://doi.org/10.1016/j.jhazmat.2006.04.060

67. Tuncuk A, Stazi V, Akcil A, Yazici EY, Deveci H (2012) Aqueous metal recovery techniques from e-scrap: hydrometallurgy in recycling. Miner Eng 25:28–37. https://doi.org/10.1016/j.mineng.2011.09.019

68. Hagelüken C, Corti CW (2010) Recycling of gold from electronics: cost-effective use through "Design for Recycling". Gold Bull 43:209–220. https://doi.org/10.1007/bf03214988

69. Sheng PP, Etsell TH (2007) Recovery of gold from computer circuit board scrap using aqua regia. Waste Manag. Res. 25:380–383. https://doi.org/10.1177/0734242x07076946

70. Hagelüken C, Corti CW (2010) Recycling of gold from electronics: cost-effective use through "design for recycling". Gold Bull. 43:209–220. https://doi.org/10.1007/bf03214988

71. Park YJ, Fray DJ (2009) Recovery of high purity precious metals from printed circuit boards. J Hazard Mater 164:1152–1158. https://doi.org/10.1016/j.jhazmat.2008.09.043

72. Bonggotgetsakul YYN, Cattrall RW, Kolev SD (2016) Recovery of gold from aqua regia digested electronic scrap using a poly(vinylidene fluoride-co-hexafluoropropene) (PVDF-HFP) based polymer inclusion membrane (PIM) containing Cyphos® IL 104. J Memb Sci 514:274–281. https://doi.org/10.1016/j.memsci.2016.05.002

73. Karamanoğlu P, Aydın S (2016) An economic analysis of the recovery of gold from CPU, boards, and connectors using aqua regia, Desalin. Water Treat 57:2570–2575. https://doi.org/10.1080/19443994.2015.1063086

74. Murakami H, Nishihama S, Yoshizuka K (2015) Separation and recovery of gold from waste LED using ion exchange method. Hydrometallurgy 157:194–198. https://doi.org/10.1016/j.hydromet.2015.08.014

75. Bonaccorso F, Calogero G, Di Marco G, Maragò OM, Gucciardi PG, Glorgianni U, Channon K, Sabatino G (2007) Fabrication of gold tips by chemical etching in aqua regia. Rev Sci Instrum 78. https://doi.org/10.1063/1.2782682

76. Parajuli D, Khunathai K, Adhikari CR, Inoue K, Ohto K, Kawakita H, Funaoka M, Hirota K (2009) Total recovery of gold, palladium, and platinum using lignophenol derivative. Miner Eng 22:1173–1178. https://doi.org/10.1016/j.mineng.2009.06.003

77. Fan R, Xie F, Guan X, Zhang Q, Luo Z (2014) Selective adsorption and recovery of Au(III) from three kinds of acidic systems by persimmon residual based bio-sorbent: a method for gold recycling from e-wastes. Bioresour Technol 163:167–171. https://doi.org/10.1016/j.biortech.2014.03.164

78. Cyganowski P, Jermakowicz-Bartkowiak D (2016) Synthesis and studies on core-shell type anion exchange resins based on a hybrid polymeric support. J Appl Polym Sci 133. https://doi.org/10.1002/app.43841

79. Alguacil FJ, Adeva P, Alonso M (2005) Processing of residual gold (III) solutions via ion exchange. Gold Bull 38:9–13. https://doi.org/10.1007/bf03215222

80. Syed S (2016) Silver recovery aqueous techniques from diverse sources: hydrometallurgy in recycling. Waste Manag 50:234–256. https://doi.org/10.1016/j.wasman.2016.02.006

81. Kononova ON, Shatnykh KA, Prikhod'ko KV, Kashirin DM (2009) Ion-exchange recovery of gold(I) and silver(I) from thiosulfate solutions, Russ J Phys Chem A 83:2340–2345. https://doi.org/10.1134/s0036024409130275

82. Kononova ON, Duba EV, Medovikov DV, Efimova AS, Ivanov AI, Krylov AS (2017) Ion-exchange sorption of silver(I) chloride complexes from aqueous HCl solutions. Russ J Phys Chem A 91. https://doi.org/10.1134/s0036024417120135

83. Kononova ON, Kholmogorov AG, Danilenko NV, Goryaeva NG, Shatnykh KA, Kachin SV (2007) Recovery of silver from thiosulfate and thiocyanate leach solutions by adsorption on anion exchange resins and activated carbon. Hydrometallurgy 88:189–195. https://doi.org/10.1016/j.hydromet.2007.03.012

84. Iglesias M, Anticó E, Salvadó V (2001) The characterisation of silver sorption by chelating resins containing thiol and amine groups. Solvent Extr Ion Exch 19:315–327. https://doi.org/10.1081/sei-100102698

85. Sakamoto H, Ishikawa J, Koike M, Doi K, Wada H (2003) Adsorption and concentration of silver ion with polymer-supported polythiazaalkane resins. React Funct Polym 55:299–310. https://doi.org/10.1016/s1381-5148(03)00021-x

86. Edebali S, Pehlivan E (2016) Evaluation of chelate and cation exchange resins to remove copper ions. Powder Technol 301:520–525. https://doi.org/10.1016/j.powtec.2016.06.011

87. Yalçin S, Apak R, Hizal J, Afşar H (2001) Recovery of copper (II) and chromium (III, VI) from electroplating-industry wastewater by ion exchange. Sep Sci Technol 36:2181–2196. https://doi.org/10.1081/ss-100105912

88. Wen JJ, Zhang QX, Zhang GQ, Cao ZY (2010) Deep removal of copper from cobalt sulfate electrolyte by ion-exchange. Trans Nonferrous Met Soc China 20:1534–1540. https://doi.org/10.1016/s1003-6326(09)60334-4

89. Li JT, Chen AL (2015) Deep removal of copper from nickel electrolyte using manganese sulfide. Trans Nonferrous Met Soc China 25:3802–3807. https://doi.org/10.1016/s1003-6326(15)64024-9

90. Chen A, Qiu G, Zhao Z, Sun P, Yu R (2009) Removal of copper from nickel anode electrolyte through ion exchange. Trans Nonferrous Met Soc China 19:253–258. https://doi.org/10.1016/s1003-6326(08)60261-7

91. Lu J, Dreisinger DB, Cooper WC (2002) Thermodynamics of the aqueous copper-cyanide system. Hydrometallurgy 66:23–36. https://doi.org/10.1016/s0304-386x(02)00081-6

92. Bachiller D, Torre M, Rendueles M, Díaz M (2004) Cyanide recovery by ion exchange from gold ore waste effluents containing copper. Miner Eng 17:767–774. https://doi.org/10.1016/j.mineng.2004.01.001

93. Revathi M, Saravanan M, Chiya AB, Velan M (2012) Removal of copper, nickel, and zinc ions from electroplating rinse water. Clean Soil Air Water 40:66–79. https://doi.org/10.1002/clen.201000477

94. Dobrevsky I, Dimova-Todorova M, Panayotova T (1997) Electroplating rinse waste water treatment by ion exchange. Desalination 108:277–280. https://doi.org/10.1016/s0011-9164(97)00036-2

95. Jha MK, Van Nguyen N, Lee J, Jeong J, Yoo JM (2009) Adsorption of copper from the sulphate solution of low copper contents using the cationic resin Amberlite IR 120. J Hazard Mater 164:948–953. https://doi.org/10.1016/j.jhazmat.2008.08.103

96. Elwakeel KZ, Atia AA, Guibal E (2014) Fast removal of uranium from aqueous solutions using tetraethylenepentamine modified magnetic chitosan resin. Bioresour Technol 160:107–114. https://doi.org/10.1016/j.biortech.2014.01.037

97. Ladeira ACQ, Morais CA (2005) Uranium recovery from industrial effluent by ion exchange—column experiments. Miner Eng 18:1337–1340. https://doi.org/10.1016/j.mineng.2005.06.012

98. International Atomic Energy Agency (1980) Significance of mineralogy in the development of flowsheets for processing uranium ores. International Atomic Energy Agency

99. Sole KC, Cole PM, Feather AM, Kotze MH (2011) Solvent extraction and ion exchange applications in Africa's Resurging Uranium Industry: a review. Solvent Extr Ion Exch 29:868–899. https://doi.org/10.1080/07366299.2011.581101

100. Seaborg G (1963) Man-made transuranium elements. Prentice-Hall, Englewood Cliffs. http://www.worldcat.org/title/man-made-transuranium-elements/oclc/546696. Accessed 5 April 2018

101. Safford HW, Kuebel A (1943) Preparations and properties of ammonium diuranate. J Chem Educ 20:88. https://doi.org/10.1021/ed020p88

102. Martin DS (1963) Man-made transuranium elements. Science 142:1288–1288. https://doi.org/10.1126/science.142.3597.1288-a

103. Egawa H, Kabay N, Shuto T, Jyo A (1992) Recovery of uranium from seawater. XII. Preparation and characterization of lightly crosslinked highly porous chelating resins containing amidoxime groups. J Appl Polym Sci 46:129–142. https://doi.org/10.1002/app.1992.070460113

104. Danko B, Dybczyński RS, Samczyński Z, Gajda D, Herdzik-Koniecko I, Zakrzewska-Kołtuniewicz G, Chajduk E, Kulisa K (2017) Ion exchange investigation for recovery of uranium from acidic pregnant leach solutions. Nukleonika 62:213–221. https://doi.org/10.1515/nuka-2017-0031

105. Fleming CA, Hancock RD (1979) The mechanism in the poisoning of anion- exchange resins by cobalt cyanide. J S Afr Inst Min Metall 79. https://www.saimm.co.za/Journal/v079n11p334.pdf. Accessed 6 April 2018

106. OECD Nuclear Energy Agency (2014) Uranium 2014: resources, production and demand (The Red Book). IAEA 488. https://doi.org/10.1787/uranium-2014-en

107. Seneda JA, Figueiredo FF, Abrão A, Carvalho FMS, Frajndlich EUC (2001) Recovery of uranium from the filtrate of "ammonium diuranate" prepared from uranium hexafluoride. J Alloys Compd 838–841. https://doi.org/10.1016/s0925-8388(01)01156-2

108. Ladeira ACQ, Morais CA (2005) Effect of ammonium, carbonate and fluoride concentration on the uranium recovery by resins. Radiochim Acta 93:207–209. https://doi.org/10.1524/ract.93.4.207.64073

109. Nascimento MRL, Fatibello-Filho O, Teixeira LA (2004) Recovery of uranium from acid mine drainage waters by ion exchange. Miner Process Extr Metall Rev 25:129–142. https://doi.org/10.1080/08827500490433197

110. Sole KC, Mooiman MB, Hardwick E (n.d.) Keynote address: present and future applications of ion exchange in hydrometallurgy: an overview. http://www.soleconsulting.co.za/IX1.pdf. Accessed 29 April 2018

111. Izadi A, Mohebbi A, Amiri M, Izadi N (2017) Removal of iron ions from industrial copper raffinate and electrowinning electrolyte solutions by chemical precipitation and ion exchange. Miner Eng 113:23–35. https://doi.org/10.1016/j.mineng.2017.07.018

112. McKevitt B, Dreisinger D (2009) A comparison of various ion exchange resins for the removal of ferric ions from copper electrowinning electrolyte solutions part I: Electrolytes containing no other impurities. Hydrometallurgy 98:116–121. https://doi.org/10.1016/j.hydromet.2009.04.008

113. Shaw DR, Dreisinger DB, Lancaster T, Richmond GD, Tomlinson M (2004) The commercialization of the FENIX Iron Control System for purifying copper electrowinning electrolytes. JOM 56:38–41. https://doi.org/10.1007/s11837-004-0090-x

114. McKevitt B, Dreisinger D (2009) A comparison of various ion exchange resins for the removal of ferric ions from copper electrowinning electrolyte solutions Part II: electrolytes containing antimony and bismuth. Hydrometallurgy 98:122–127. https://doi.org/10.1016/j.hydromet.2009.04.007

115. Foo KY, Hameed BH (2010) Insights into the modeling of adsorption isotherm systems. Chem Eng J 156:2–10. https://doi.org/10.1016/j.cej.2009.09.013

116. Haghsheno R, Mohebbi A, Hashemipour H, Sarrafi A (2009) Study of kinetic and fixed bed operation of removal of sulfate anions from an industrial wastewater by an anion exchange resin. J Hazard Mater 166:961–966. https://doi.org/10.1016/j.jhazmat.2008.12.009